

**Upon the characterization of destabilization and stabilization
phenomena in fine particulate systems – implications to
physicochemical removal of colour from effluents and colloidal
processing of ceramics**

Beitrag zur Charakterisierung von Destabilisierungs- und
Stabilisierungsphänomenen in Feinpartikelsystemen – die Relevanz zum
physiko-chemischen Farbstoffabbau und zum kolloidalen
Keramikformgebungsverfahren

Band I

Der Fakultät für Umweltwissenschaften und Verfahrenstechnik an der
Brandenburgischen Technischen Universität Cottbus vorgelegte
Habilitationsschrift zur Anerkennung der Befähigung für Forschung und Lehre für
das Fach Verfahrenstechnik

von

Dr.-Ing. Stoyan Gaydardzhiev

Tag der Eröffnung des Habilitationsverfahrens: 04. Oktober 2006

Tag der Zuerkennung der Lehrbefähigung: 04. Juli 2007

Gutachter: Prof. Dr. -Ing. habil. Peter Ay , BTU – Cottbus

Gutachter: Prof. Dr. –Ing. habil. Valko Mavrov, Universität des Saarlandes, Saarbrücken

Gutachter: PD Dr. rer. nat. habil. Siegfried Vieth, BTU – Cottbus

Gutachter: Prof. Dr Sc. Stoyan Groudev, Dept. of Engineering Geoecology, University of Mining
and Geology, Sofia, Bulgaria

CONTENTS

Introduction and work objectives	1
A Theoretical Part	4
A1 Upon the electrical properties at interfaces and charge generation in colloidal systems – short introduction	4
A.1.1 The concept of electrical double layer (EDL)	4
A.1.2 Electrokinetic phenomena inside the EDL - zeta and surface charge potentials	6
A.1.3 Surface interaction potential between particles	8
A.1.4 Description of colloidal stability	8
A.1.5 The electrochemical properties at the interface as a means to evaluate colloidal stability	9
A.1.6 Methods for registering electrokinetic phenomena in dispersed systems	12
A.1.7 Aggregation and stabilization of particulate systems: basic definitions	13
A2 Practical implications of the characterization and manipulation of colloidal dispersions - two exemplified systems	15
A.2.1 Dyes removal from effluents	15
A 2.1.1 Physicochemical methods in treatment of dye effluents: brief state-of-the-art	15
A 2.1.2 Views towards color removal mechanisms taking place during physicochemical treatment of dye effluents	16
A 2.1.3 Research incentives and needs	17
A.2.2 Colloidal processing of ceramics	18
A.2.2.1 Processing of ceramics: brief state-of-the-art	18
A.2.2.2 Methods for direct casting of ceramics	20
A.2.2.3 Gel-casting and its role within the novel near-net-shape forming methods	21
A.2.2.4 Stabilization mechanisms during gel-casting of oxide ceramics	22
A.2.2.5. Research incentives and needs	23
B Experimental Part	25
B1 Coagulation of dye bearing solutions	25
B.1.1 Materials	25
B1.1.1 Dyes	25
B1.1.2. Primary coagulants	25

B.1.2 Methods for coagulation and products characterization	26
B.1.3. Screening studies - dyes reactivity with primary coagulants	26
B1.3.1. Supporting examples of destabilization patterns	28
B.1.4 Conclusions	34
B2 Characterization of stability in aqueous alumina suspensions	36
B.2.1 Materials	36
B.2.1.1 Powders	36
B.2.1.2 Dispersants	38
B.2.2 Methods for evaluation dispersant efficiency	39
B.2.3 Powder suspensions in water: particle size distribution and surface charging	40
B.2.3.1 Nano-sized gama alumina (Aerosil - Alu-C)	40
B.2.3.2 Ultra fine alfa aluminas	45
B.2.3.2.1 CT3000SG	47
B.2.3.2.2 CR6 and AKP53	50
B.2.3.3 Hypothetical interaction patterns between the dispersants and the tested alfa aluminas	52
B.3 Development of dense and porous ceramic bodies by gel-casting	56
B.3.1 Gel-casting slurry formation and methods for bodies evaluation	56
B.3.2 Development of dense ceramics: parametric optimization	59
B.3.2.1 Conclusions	67
B.3.3 Possibilities for development of porous ceramics by use of fugitive pore developers	68
B.3.3.1 Characteristics of the fibres tested as pore developers	68
B.3.3.2 Measured and calculated effects of fibres addition on developed porosity	69
B3.3.3 Increasing the connected porosity by addition of foaming agent	74
B.3.3.4 Conclusions	75
Summary and directions for further work	76
References	79
List of related publications	89
Acknowledgment	90

Introduction and work objectives

The issue of particulate systems dispersibility and its characterization provides an important challenge for now-a-days-life: from stabilizing food products and designing of surfactants to the development of new materials. As a whole, particulate products make a significant contribution to the world economy generating in excess of ***one trillion dollars*** annually [94]. Some of the major industries impacted by particulate systems as a core technology are advanced materials, chemical, energy, environmental, mineral, agricultural, pharmaceutical, microelectronics, biotechnology, cosmetics, personal care and food processing. Regardless that many industries involve particulates, the applied processes rarely reach more than 60 percent of the design capacity due to the inadequate understanding of multiphase processing schemes and of the associated particle interactions effects. Hence, there is an urgent need to study the complex nature of the particles and to develop engineered products and processes with a fundamental understanding in particle science and technology. All applications involving colloidal particles have in common that the surface properties and interparticle interactions play a central role. Therefore, the control over particulate systems stabilization/de-stabilisation could be achieved by tailoring particle-particle interactions.

Main objective of the presented work is to demonstrate on the basis of ***two different colloidal systems*** (dye solutions and dispersions of fine ceramic powders) the importance of characterizing and understanding the inter-particle interactions as a key requirement for realising optimal process conditions.

The *first chosen system* is highly relevant to the general area of physico-chemical treatment of effluents, which often are involving colloidal sized contaminants. Here the need to design better performing and selectively acting chemical agents and to forecast the de-stabilization patterns during coagulation/flocculation of colloidal suspensions is an important issue.

Effluent treatment is a major focus in EU legislative policy illustrated by the fact that the recent EU Council Directive 96/61/EC stipulates that an urgent development of innovative or improving the existing treatment methods is needed, not ignoring the fact that the end-off-pipe technology is only part of the solution needed to combat the problem and in house prevention is necessary". For the dye effluents in particular, the selection of best polymers

is still accomplished empirically and no guidelines based on polymers physics and chemistry exist. This drawback reflects in inability to provide information about the predominant colour removal mechanisms and about process conditions leading to sludge with better water-draining properties,

The second studied system is relevant to the emerging area of colloidal processing of ceramics. Direct consolidation techniques (gel casting is one of them) claim to form complex near-net-shape bodies with consistent properties and minimal defects have been recently emerging, as alternative to the conventional processing routes such as Cold and Hot Isostatic Pressing (CIP/HIP). Most of them however, are considered immature and remain under development either in laboratories or in pilot plants of ceramic companies, with little small-scale production running for some complex-shaped parts. Principal commercialization barrier is the low production rate, which at present could not compete with dry pressing. Although the gel-casting properties of some systems are fairly well established, process break-through is not yet reached. Uncertainties remain about the nature of interactions between polymeric and colloidal phases and their interdependency. The majority of research efforts in suspension processing have been focused on the interactions between single organic components and particle surface. A key understanding is needed however, about the interaction between all phases and about the way to control over structural evolution to eliminate unwanted heterogeneities in development of near-net-shape bodies with consistent properties and minimal defects. From other side, the theoretical understanding of inter-particle forces is relatively matured, but there is a need for a systematic conduction of research about the interaction mechanisms between dispersants with various structures and ceramic powders having different particle and surface characteristics. Once this challenge is met, one could approach the ultimate goal to design tailored functional dispersants that bring the targeted colloidal stability of suspensions made from different powders, thus securing better foot fold for making end ceramic bodies with minimal defects at cost competitive way.

Worth mentioning is that, alone handling of colloidal and nano-particles, has practical significance for the field of process engineering, like for example finding a way to make granules of these powders, which can later be re-dispersed.

The **both** envisaged systems have in **common** the fact that surface and interfacial properties play a central role in reaching the particular technological objective. For the

chemical coagulation of dye effluents the ultimate goal is to remove/separate dye colorants by destabilizing the dye molecules or to capture them through sweep flocculation, while for the colloidal processing of ceramics the ultimate goal is to achieve stable suspension with maximum possible solids loading.

Thus the two key issues to be addressed by systematical investigation of the studied colloidal systems, is from one side the *interactions* between a macro colloidal systems in the face of textile dyes and the chemical additives like primary coagulants and from other side the *interactions* between a colloidal sized ceramic powders and the dispersants and other additives used in gel-casting process. For the *first system*, development of flocs with improved structure at optimized chemical dose is targeted, while for the *second system* manufacturing of ceramic bodies with improved properties is the principal aim.

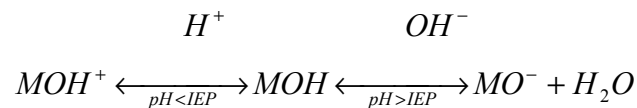
Other work objectives among all are:

- ✓ to yield a hypothetical model of dye destabilization/coagulation pattern for representative dye classes by examining the magnitude of surface charge density as expression of colloidal system destabilization;
- ✓ to answer which coagulation pattern under controlled application of shear, is leading to formation of sludge consisting from flocs with improved sedimentation and handling properties;
- ✓ to evaluate by comparative methods several commercially available dispersants towards stabilization of ultra fine alumina powders;
- ✓ to validate the optimal dispersant choice through development of complex shaped dense and porous ceramics by gel-casting.

A1 Upon the electrical properties at interfaces and charge generation in colloidal systems – short introduction

A.1.1 The concept of electrical double layer

Electrical interaction between colloidal particles is one of the most important factors that influence particle stability and aggregation. It is well known that immersing a ceramic powder in a polar liquid such as water creates a charge at the solid-liquid interface. The principal mechanism responsible to this effect is the surface groups ionization, e.g. by proton transfer reactions with the surface hydroxyl groups, or by adsorption of specifically adsorbed ions [13]. For amphoteric oxides this could be illustrated as:



where M stands for cations such as Al^{3+} , Zr^{4+} or Si^{4+} .

In such a powder suspension the point of zero charge (pzc) is the pH where the surface concentration of MO^- and MOH_2^+ are equal. The surface charge is negative at a $pH > pH_{pzc}$ and positive at $pH < pH_{pzc}$. Surface charging could be caused also by other possible mechanisms, like:

- ✓ differential solubility of ions (the ionic solids) when one or other constituent ions may have a greater tendency to dissolve;
- ✓ isomorphous replacement (lattice substitution);
- ✓ charged crystal surface fracturing;
- ✓ specific ions adsorption.

Whatever the surface charge origin is, it should be balanced by an equal and oppositely charges in solution. The balancing is realized by counter ions which are subject of two opposing influences: electrostatic attraction tending to localize them close to the particles and the tendency of ions to diffuse randomly throughout the solution, owing to their thermal energy. The like charge ions are repelled away from the surface. Thus the described arrangement leads to development of net electrical charge on one side of the

interface and a charge of opposite sign on the other side giving rise to an ***electrical double layer (EDL)***.

The theoretical and practical aspects of the EDL have been recognized and understood in modern colloidal and interface science and a major search has been placed for finding a means to predict and determine the exact distribution of electrical charges at or near the solid liquid interface. In practical sense the thickness of the electrical double layer is a very important parameter determining the range of the double layer repulsion. In such way the electric surface charge has been considered as the cause or the driving force in formation of the EDL since the creation of the classical Gouy-Chapman-Stern (GCS) model. This model represents successive evolution in the understanding of the DL model, firstly introduced by Helmholtz in 1879 as a “capacitor” model and further elaborated by Gouy (1910, 1917) and Chapman (1913) as “diffused layer” model. Lyklema has described in details many of the sometimes chemically complex ways that charge may appear at the interface [73]. Provided a more complex situation is excluded one could see that according to the Gouy-Chapman-Stern model, the double layer is a simple equilibrium structure resulting from the balance between electrostatic interactions (i.e. between the surface charge and bulk ions) on one hand and the thermal motion of the ions on the other.

The nowadays perception about the layers formation around a particle with negative surface charge dispersed in electrolyte containing water incorporates the further refinements suggested by Grahame (1947), who divided the Stern layer into two regions – inner layer occupied by specifically adsorbed, non-hydrated ions and a second layer where hydrated counter ions are located.

A.1.2 Electrokinetic phenomena inside the EDL - zeta and surface charge potentials

Elektrokinetic phenomena arise when a relative movement between a charged interface and the adjacent electrolyte solution exists, as result of which part of the double layer charge moves with the liquid. Fundamental to these phenomena is the concept of a plane of shear, separating the “fixed” from the “mobile” diffuse parts of the EDL.

The diffuse part of the EDL can be visualized as a charged atmosphere surrounding the particle, as shown at Figure A.1.1.

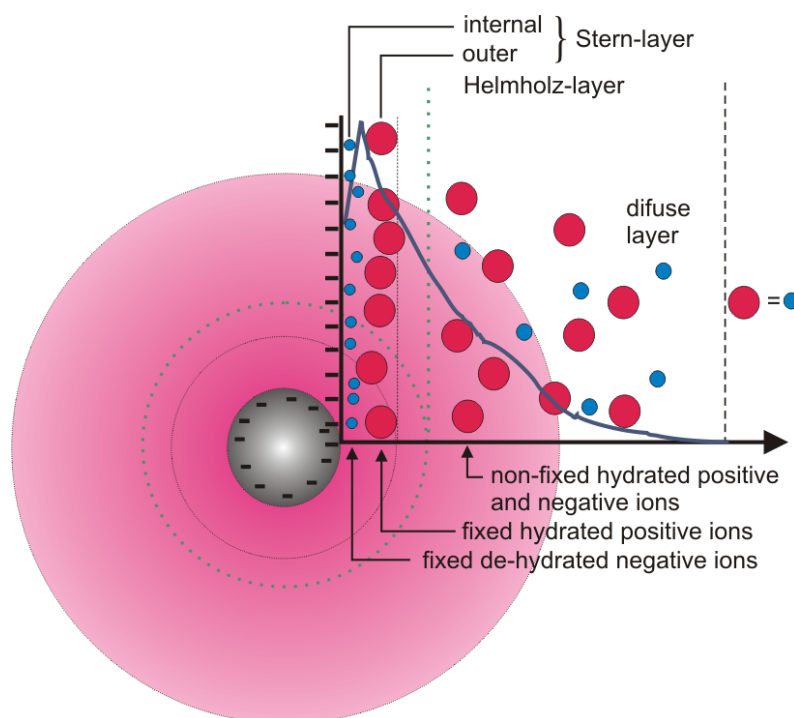


Figure A-1.1 Layers development around a negatively charged particle in electrolyte containing system (Stern-Grahame model) and surface potential diagram

The charge density at any distance from the surface is equal to the difference in concentration of positive and negative ions at that point. The drop in the potential apart from the surface is measurable and is expressed in voltage difference in order of millivolts. The interpretation of the potential curve has important practical implication since it is a measure of the strength of the electrical force between particles and the distance in which this force comes into play. Therefore, a detailed knowledge about the interfacial region (solid-liquid) is important in any attempt to secure optimal product characteristics.

It is believed, that the surface charge and the non-uniform distribution of counter ions near to the surface depend greatly on the nature and concentration of salts in solution, giving a relatively simple means of modifying colloidal interactions. Hence, according to the classical GCS theory the increase of the ionic strength should suppress the electrokinetic phenomena due to collapse of the double layer (DL). Thus it is believed that through changes in solution chemistry (i.e. ionic strength) reflecting in changing the electrical interactions, one could gain access on practical means of manipulating the stability of particulate systems. Following this logic the higher ionic strength could thin out the double layer to such an extent as to suppress electrochemical phenomena. However, like in some papers is reported, electrokinetic phenomena do exist also at high ionic strength,

for example zeta potential of 20-30 mV at 1 M ionic strength [52]. For explaining such findings the concept of the “zero surface charge DL” model has been introduced and for verifying the existence of this model and to study the DL structure, experiments have been performed in using non-ionic surfactant as a probe to modify the structure of the interfacial layer and to give light on the distribution of charge within it [30].

A1.3 Surface interaction potential between particles

The first step to understand colloidal system is to provide insight into particle interaction phenomena. A general consensus is that the DL electrostatic interaction occurs when two macroscopic charged bodies approach each other in electrolytic solution, since their diffuse double layers overlap and in case of similarly charged particles, *repulsion* is experienced between them. The precise way in which the double layers respond depends on a number of factors. It is generally accepted, that the double layer interaction depends on the potential at the Stern layer, which may respond quite differently to the approach of another surface. For practical implications, the energy of DL interaction is often calculated through approximation of particle interactions as plate-plate, sphere-sphere and plate-sphere. From other side, the existing of *attractive* forces between colloidal particles has long been recognized, but coherent understanding of these forces has been just recently emerging [47]. The force of attraction between two closely separated surfaces is generally called London-van der Waals (vdW). This force is electrodynamic in origin as it arises from the interactions between the oscillating or rotating dipoles within the media [13, 32]. The strength of the vdW force depends on the dielectric properties of the interacting colloidal particles [69] and for spherical particles of equal size, V_{vdW} is given by the known Hamaker expression

$$V_{vdW} = -\frac{A}{6} \left(\frac{2}{s^2 - 4} + \frac{2}{s^2} + \ln \frac{s^2 - 4}{s^2} \right)$$

where s is

$$s = \frac{2a + h}{a}$$

h is the minimum separation between the particle surfaces;

a is the particle radius;

A is the Hamaker constant, determined by spectral optical properties.

A1.4 Description of colloidal stability

By precise control of interparticle forces one could render colloidal particulate systems as dispersed, weakly or strongly flocculated. This idea is illustrated further at Figure A.1.5. Here more details will be given to the concept of total interparticle potential energy, V_{tot} in order to physically quantify colloidal dispersions stability:

$$V_{tot} = V_{vdW} + V_{elect} + V_{steric} + V_{structural} ,$$

where:

V_{vdW} - attractive potential energy due to long-range van der Waals interactions between the particles;

V_{elect} - repulsive potential energy resulting from electrostatic interactions between like-charged particle surfaces;

V_{steric} - repulsive potential energy resulting from steric interactions between particle surfaces coated with adsorbed polymeric species;

$V_{structural}$ - potential energy resulting from the presence of non-adsorbed species in solution that may either increase or decrease the suspension stability. Could be met as depletion forces.

For many years it has been believed that the balance between the two principal forces (first two terms of the equation) consisting the well-known DLVO theory developed independently by Derjaguin & Landau (1941), and Verwey & Overbeek (1948), could predict the stability of the colloidal particles suspended in polar liquids and as such was regarded as a milestone of modern colloidal science. Regardless of the wide acceptance of the DLVO theory however, there are certain phenomena, which could not be completely explained by this theory. This situation is additionally aggravated when concentrated suspensions were considered, in which cases no explanation about the effect of pH on viscosity was being possible by the classical DLVO theory [19]. The third and fourth components of the equation relate to the generic term of non-DLVO short-range forces,

which nowadays have been examined extensively and their consequences well documented. In case polyelectrolyte species are used as additives, they can impart both electrostatic and steric stabilization and accordingly the forces are referred as electrosteric.

A1.5 The electrochemical properties at the interface as a means to evaluate colloidal stability

An adequate characterization of disperse system is important if one needs to develop ways to predict its properties and relate them to product performance. A system of disperse particles might be characterized by properties of the disperse phase(s), continuous phase, interfacial properties and colloidal properties. The methods for characterizing the stability of concentrated dispersion have not been standardized and large variation in techniques and methodology exists in the literature. Table A.1.1 provides the parameters used for characterizing a system of dispersed particles.

Properties	Parameters
Disperse phase	Size distribution; Particle shape; Density; Surface energy; Homogeneity.
Several disperse phases	Solid particle or liquid droplets, each with properties listed above. Relative size of dispersed phase of different materials.
Continuous phase	Aqueous; Non-aqueous; Dissolved substances.
Interfacial	Electric double layer; Zeta potential. Adsorption density; Packing of molecules in the adsorbed layer; Thickness of adsorbed layer.
Colloid	Percent solids; Stability; Rheology; Light scattering.

Table A.1-1 Disperse system properties and parameters used for their characterization (after [19])

An easiest way to evaluate suspension stability is to follow the progression in particle size distribution over time. It is generally accepted that the dispersions is physically stable

when their particle size distributions do not change or change to a less extent within a given time frame. From other side, if the particle size distribution of a given dispersions increases within certain time frame, they are considered as physically unstable.

However, in order to manipulate system properties in view its aggregation/stabilization, a more fundamental characterization approach is required. It has been recognized that the phenomena taking place at the interface are of immense practical importance for colloid science since they provide information, which regardless is viewed as imperfect could not be obtained in any other way. The widely and most commonly accepted way to experimentally study the charging at particle surfaces, is the involvement of techniques based on registering electrokinetic phenomena caused by movements of charged particles relative to surrounding solution which yield either zeta or streaming current potentials. In very many cases there is a clear correlation for instance between zeta potential and colloid stability. The information however could be viewed rather as a descriptive one and any direct correlation between the measured zeta potential and the double layer structure is still not possible, since the shear plane can not be located with any certainty.

If a ***pure electrostatic DL stabilization*** is considered, its efficiency could be evaluated by the surface charge density (Nernst potential) and the thickness of the diffuse layer. Since the value of the measured zeta potential is function from the Nernst potential, the zeta potential could be viewed alone as a means to express the total particle charging and accordingly the correlated electrostatic attraction between the particles. Hence, by measuring the zeta potential, i.e. the active particle charging, it is possible to delineate the differences in surface charge density and in stability status of various particulate systems. As a general rule the higher the zeta potential, the higher the system stability. This rule could be explained through the theory of repulsion of similarly charged particles. Often when the zeta potential is used for evaluation the stability of colloidal dispersions a marginal value of +/- 30 mV is considered as an indication for an appreciable physical stability. Figure A.1.2 illustrates schematically the role of zeta potential as a means for evaluation the electrostatic stabilization of colloidal systems.

Electrostatic stabilization

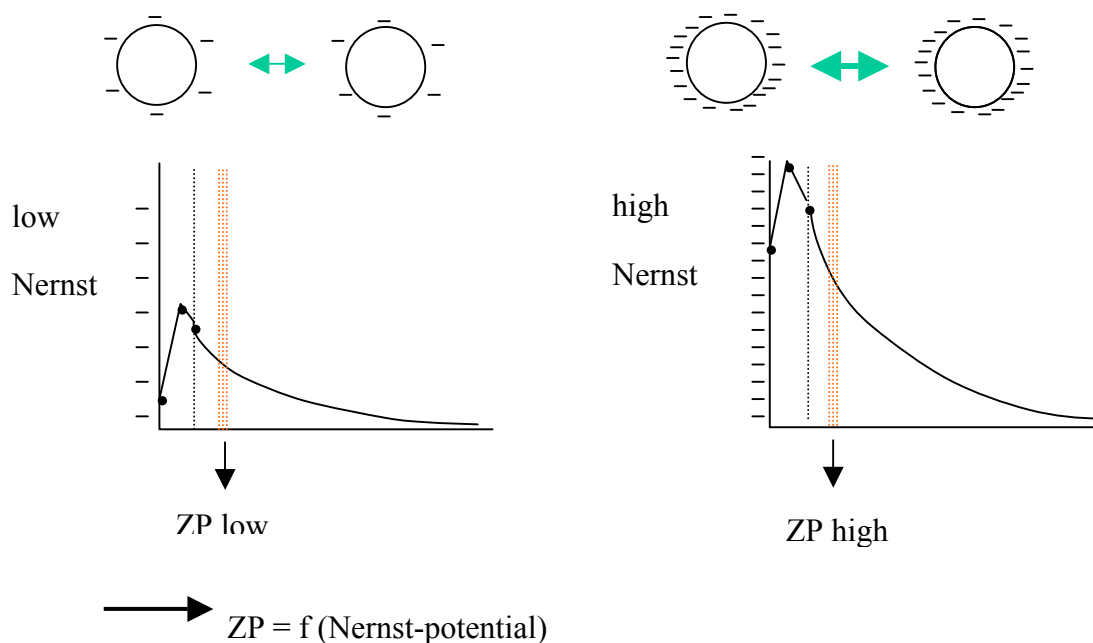


Figure A-1.2 Effect of zeta potential on colloidal systems stability (after [18])

The above considerations could be correctly interpreted however only, if the concentration of electrolyte is constant and is held at extremely lower level in the disperse system. This eliminates the need to consider the diffused double layer compression as a stability factor. This model, is based however on several assumptions, for example that the increase in surface charge density does not influence the adsorption in the internal and outer Helmholtz layer (the Stern layer).

In most practical cases it *is not possible* to stabilize particulate systems only by electrostatic DL forces, hence addition of suitable polyelectrolytes leading to *steric, electrosteric and depletion* mechanisms of stabilization is practiced. Steric stabilization is caused by macromolecules attached to the surface of the particles. It could be regarded as a loss of configuration entropy when polymer chains penetrate between two particles. Often it is possible to combine electrostatic and steric stabilization, what has been known as electrosteric stabilization. Electrosteric stabilization could be realized either through charged particles in combination with nonionic polymers or by polyelectrolytes attached to uncharged particles. Free macromolecules in solution that impart stabilization lead to

depletion mechanism. In cases of high concentration of free polymer in dispersion media it is also possible to have combination between depletion and steric stabilization. Figure A.1.3 provides a schematic view of the electrostatic (a), steric (b) and depletion (c) stabilization.

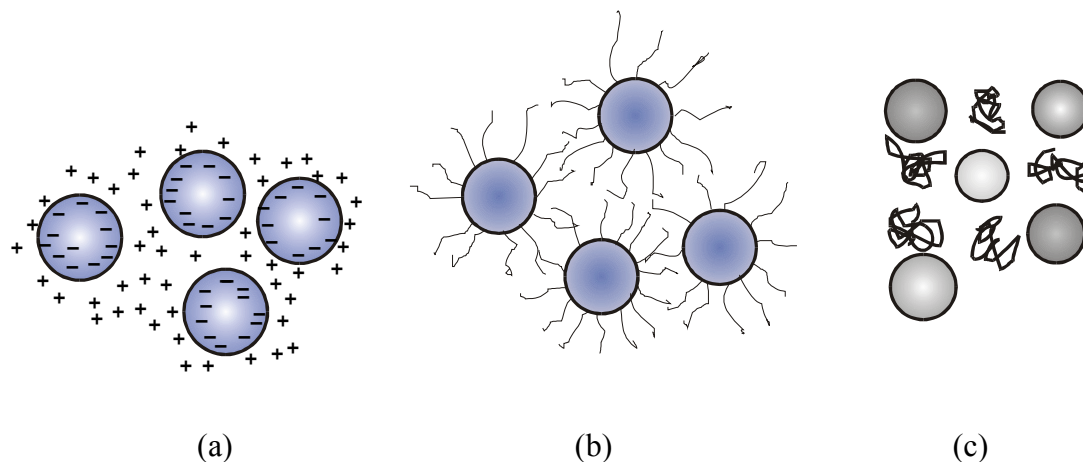


Figure A-1.3 Stabilization mechanisms

A1.6 Methods for registering electrokinetic phenomena in dispersed systems

The most commonly used practical methods for yielding electrokinetic signals and determining zeta potential are the streaming current, sedimentation potential, electroosmosis and particle electrophoresis. These methods however are mostly available to determine electrochemical properties under isolated conditions in relatively diluted suspensions. Additional difficulties arise for measurement in concentrated suspensions. As a consequence, in many industrial systems the state of aggregation of primary particles is most difficult to control and measure. Recently in attempt to overcome the problem of measurement in concentrated dispersions, devices based on the electroacoustical theory linking the dynamic electrophoretic mobility and electroacoustic parameters, such as colloid vibration current (CVI) and electrosonic amplitude (ESA) have been emerging. In the *present work*, zeta potential measurement instrument based on CVI and surface charge detector based on streaming potential, have been used. It is worth to note that in a study of ceramic powders in aqueous suspensions, a correlation between the zeta potential as derived from electrosonic amplitude (ESA) measurement and the streaming current measured by particle charge detector (PCD) has been established [118]. Moreover it has been demonstrated that the zeta potential is statistically identical with the streaming current. Both parameters are linked by a simple linear transformation function and both methods have been found equivalent with respect to determination of the $pH_{(iep)}$. The PCD

technique, however is known to suffer from a poor reproducibility [15] and alone the streaming current values does not deliver any quantitative information about system charging. Important information could be rather obtained by following the trend of the curves, their maximum, minimum and plateau regions as well as the iso electrical points [81].

A1.7 Aggregation and stabilization of particulate systems: basic definitions

Many properties of products developed on the basis of particulate systems depend apart from chemical compositions, also on dispersibility, colloidal stability and aggregation of the material. Therefore an extremely important aspect for studying their properties both in process industries and natural environment is the behaviour of dispersed particles which is determined directly or indirectly by the interaction forces between them, as postulated in the previous sections. The *dispersibility* could be regarded as the ease with which particles are distributed in a continuous phase, so that each one of them is completely surrounded by liquid phase and there is no permanent contact with any particles in such a way that they did not subsequently agglomerate. The dispersibility is characterized by size distribution, shape, morphology and interfacial properties of the particles and could be properly controlled by applying appropriate surfactants (steric, electrosteric, electrostatic) and additives (binders, thickeners, antifoamers).

A suspension in which the dispersed phase remains essentially as discrete, single particles on a long time scale (e.g. months or even years) is defined as a *stable* suspension. Such a suspension may be stable based on thermodynamic or kinetic reasons. In the latter case, typified by electrostatic stabilization, the system is said to be thermodynamically metastable. The dispersed particles of suspension can usually be induced to form doublets and higher multiplts by appropriately changing the system status. The process by which small particulate aggregates are formed is known under various terms depending on system type and specific conventions. These include coagulation, flocculation, agglomeration and agglutination. *Aggregation* (referred to either coagulation or flocculation) [31], depends essentially on two distinct influences:

- ✓ particles should move in such a way that collision should take place,

- ✓ interactions between colliding particles must be such that permanent contacts can be formed.

In most practical scenarios the two processes – transport and attachment, could be treated independently. The reason is that colloidal interactions are freely short ranged, much less than the particle size, so that particles have to approach very close to each other before any significant interaction being detected. The transport step has to bring particles together from a comparatively large distance where colloidal interactions play no role. In such way, through careful control of interparticle forces, colloidal suspensions can be prepared in dispersed, weakly flocculated or strongly flocculated state, as shown schematically at Figure A.1.4.

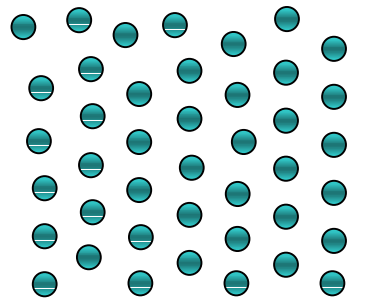
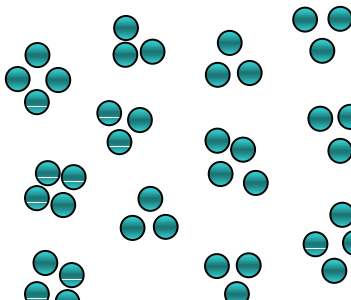
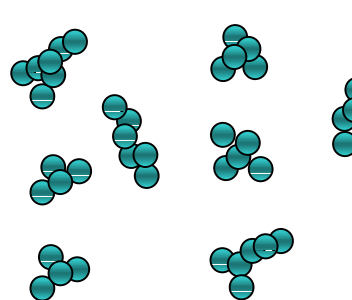
Repulsive interaction dominate	Attractive interaction dominate	
<i>Dispersed</i>	<i>Weakly flocculated</i>	<i>Strongly flocculated</i>
		

Figure A-1.4 State of colloidal system determined by the predominate forces

A2 Practical implications of the characterization and manipulation of colloidal dispersions - two exemplified systems

A.2.1 Dyes removal from effluents

A.2.1.1 Physicochemical methods in treatment of dye effluents: brief state-of-the-art

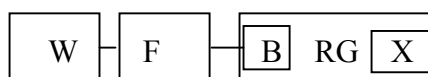
The published reviews on conventional and emerging technologies show that large spectra of techniques have been proposed and studied for colour removal, involving chemical (neutralization, oxidation), physical and physicochemical (sedimentation, flocculation, adsorption, ion exchange, membrane filtration) and biological processes. It is to be noted however that advances in *colour removal technologies* made during the last decades always make use of a *multi-stage treatment*. This is because, by far there is no single economically and technically attractive method to guarantee satisfactory colour removal and the effectiveness of a single used approach has never being proved on industrial scale [42, 92, 115]. When the hydrolyzed dyes in solution are subjected to different physical, chemical or biological impacts they undergo various transformations and under the broad definition of decolourization, there should be clear distinction among effluent decolourization only and degradation and mineralization (organic C to CO₂) of the dyes. For example, under oxidative and reductive conditions, cleavage of dye molecule takes place, in contrast, when a dye colloidal solution is subjected to coagulation, the dye molecule remains intact.

According to a recent literature review compiled within the EU Environment and Climate program [116], coagulation is envisaged intensively as pre-, main- or post treatment and its performance is regarded as case specific leading from full de-colorization in some instances to non-efficient at all in other cases. The plethora of studies however, does not add significantly to the current understanding of this important area and *break-through* is not reached. The fact that dye removal differs significantly within same dye class or hues groupings indicates that certain basic aspects like influence of chemical class and chemical constitution of dyestuffs and the criteria for selection of specific treatment chemicals and optimum system parameters need to be better understood.

A.2.1.2 Views towards colour removal mechanisms taking place during physicochemical treatment of dye effluents

Regardless the importance of physicochemical treatment of dye effluents, it is still an accepted view that coagulation and flocculation are currently practiced more like an art rather than like science and there are virtually no attempts to link the expected coagulation/destabilisation patterns and resulting floc properties. Moreover a fundamental understanding is needed about the role which dye molecular structure plays in its amenability to removal by chemical treatment and which predominant coagulation mechanism could be expected when various primary coagulants having different characteristics are used. In recognizing this, chemical companies are embarking on developing tailored coagulants selective towards colour removal especially for soluble reactive dyes and attempts are being made in this direction by grafting of synthetic polymers onto the backbone of natural ones. Dye molecules consist of chromagen, i.e. an aromatic structure adsorbing visible light, hydrophilic group and reactive group anchoring the dye onto or within the fibres. The dye structure must contain a chromophore, a chemical group that confers upon a substance the potential to becoming coloured, for example nitro, nitroso, azo and carboxyl groups. To become a useful dye, however, the molecule should contain other chemical groups such as amino, substituted amino, hydroxyl, sulphonic or carboxyl groups which are called auxochromes. These generally modify or intensify the colour, render the dye soluble in water and assist in conferring substantivity of the dye for the fiber. The size of the dye molecule is in the range of 1 nm [75]. There are more than 12 dye classes, but research on decolourization of textile waste waters, often focuses on reactive dyes.

A schematic illustration of a Reactive dye structure is shown below:



where:

W - hydrophile group; F – chromophor; B - bridge (-NH₂, -NHR, -OH, OCH₃); RG is the electrophile reactive group and X is the nucleophile group.

Based on their different chemical structures, dye molecules experience different response under action of coagulants. The established views about coagulation and flocculation patterns known from handling fine solids suspensions could be relevant to some extent in

the cases of colour removal from colloidal dye suspensions. Hence, a physico-chemical mechanism involving adsorption and charge neutralization, taking place in two successive steps could be considered, as shown below:

- ✓ reaction products from the primary coagulants hybridization (aquo species) are adsorbed onto dye colloid surfaces leading to *charge neutralization*;
- ✓ neutralized/destabilized dye colloids aggregate and form flocculated dye sludge.

Usually, the above mechanism is characterized by high dosages of coagulant and bulky non-well filterable flocs.

A *second*, distinctly different colour removal mechanism is also documented under the action of metal salts. It involves specific chemical interactions of the type coordination by rupturing covalent linkages or coordination with electron donating groups like $-NH_2$, $-N=N-$, $-COOH$ or at terminal functional groups, as well as chelation and complex formation. This mechanism is characterized by a low dose levels of coagulant, resulting in formation of a relatively small, strong and easily filterable flocs [54].

A.2.1.3 Research incentives and needs

For the both described removal mechanisms, it is conceivable that the micro interaction of individual dye colloidal components between themselves and with the chemicals in suspension is manifested by changes in the macroscopic properties of the system such as charge and potential. Hence, by considering the charge characteristics and the molecular weight of the polymer used as coagulant and by examining their association with the magnitude of surface charge density and zeta potential of the dye suspension, a hypothetical model about dye destabilization/coagulation pattern could be drawn. From other side, under constant shear conditions, the electrochemical environment and the charge characteristics under which the destabilised primary particles aggregate determine primary particles inter transport and hence the structure of resulting flocs. There are certain indications, that a sludge consisting mainly of self associated destabilized dye colloids in a polymer network-like aggregates would have better downstream separation

ability. Therefore the **objective of this part** of the work is to contribute towards outlining the role, which charge related effects play in the determining the predominant destabilization mechanisms and in development of flocs with specific structures.

A.2.2 Colloidal processing of ceramics

A.2.2.1 Processing of ceramics: brief state-of-the-art

With the necessity to manufacture most advanced ceramics from fine usually sub micrometer-sized powders, the handling of powder and the forming of green parts become a most important challenge [95]. Each defect having its origin in the powder processing steps will remain inevitably in the end product even an optimal sintering procedure is envisaged. At present there is a variety of methods for preparing **dense** ceramic green bodies possessing complex shapes. They are principally grouped into three major categories: dry shaping, wet shaping and plastic shaping, which are further divided upon dominating principles, and, where necessary, the specific chemistry and physics of the particular process – Figure A.2.1. However, the often controversially requirements for the complex processing scheme and the demand for low production cost have motivated an interest in new, innovative concepts of suspension handling and moulding of bodies.

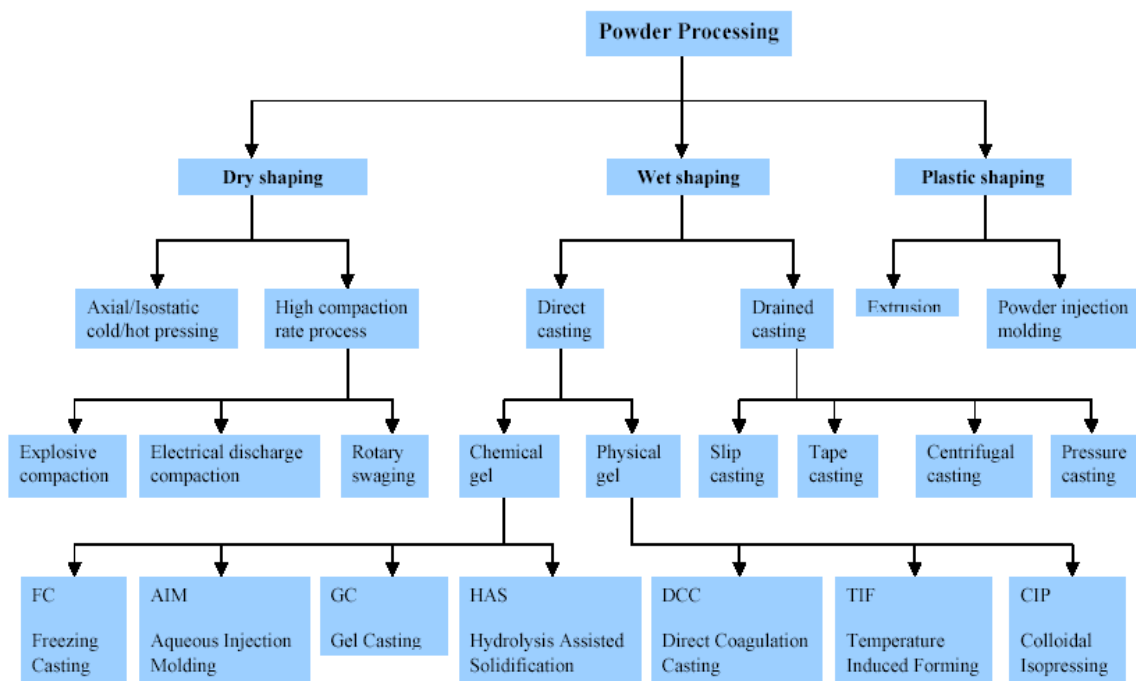


Figure A.2-1 Practice of current powder processing (after [71])

For all wet shape methods it is of particular importance to achieve homogeneous state of dense slurry with as much as possible high solids loading. Conventional wet shaping processes, such as slip casting, pressure casting and centrifugal casting, suffer from drawbacks associated with the solid-liquid separation before green body formation. The liquid vehicle should be either forced by an external pressure gradient flow (slip casting, pressure casting) or by centrifugal means (centrifugal casting). During removal of liquid its flow will affect suspension microstructure and will cause build-up and orientation of non spherical constituents leading to stress gradients, non-uniform densities and end body defects [95]. The direct casting methods, which together with injection moulding are regarded as a near-net-shape methods offer the possibilities for overcoming the above limitations by controlling the properties both of the material and the slurry. Thus they possess potential for lowering the production cost of complex near-net compounds [64]. The direct-casting methods use some of the inherent properties of dense suspensions to transform a fluid suspension to a stiff gel. Some of them use more than one physical or chemical principle for dispersion and gelling. Recent studies [96-98] indicate that engineered ceramics based on colloidal processing routes are more valuable for high temperature applications. Direct casting methods employing water as dispersing medium instead of organic solvents are gradually taking pace. This approach reduces the environmental problems and sinks the processing costs by eliminating the organic removal step. For example, in freeze casting (FC) the ceramic powders are dispersed in water, where the system is kept below water freezing point to maintain the shape. Aqueous injection moulding (AIM) uses cellulose derivatives (like starch) both like dispersant and gelling reagent in aqueous system. Gel-casting (GC) relies on in situ polymerization of organic binder. Hydrolysis assisted solidification (HAS), direct coagulation casting (DCC), temperature induced forming (TIF) and colloidal isopressing (CIP) also make use of water as main liquid vehicle. The use of water apart from its benefits, being a polar solvent, is leading to some technological drawbacks. As a rule for nitride powders it is very difficult to obtain a well-dispersed ceramic suspension using water as a dispersing medium. None of the methods mentioned above, is up to now commercialized under large-scale. Much work remains to be done to overcome existing limitations and to lower the productions costs and increase production rate.

The most of the efforts in development of *porous* ceramic materials have been focused towards the ceramic foams, where variety of techniques have been evolved. For

development of open cell ceramic foams, the most common method is the “replica technique”, i.e. impregnation of reticulated polyurethane sponge with ceramic slurry followed by removal of the excess slurry, burning out the polymer and end sintering. The developed material suffers however from low strength because of its hollow struts [113]. Added to this drawback is the gas build-up during polymer matrix pyrolysis leading to defects in the final structure. In the “direct” foaming techniques from other side, the slurry is foamed by using a blowing agent or a gas is produced by chemical reaction inside the slurry [20]. During ceramic foams development often the solidification of the foam is accomplished by gel-casting [27, 48]. Alternative methods for producing porous ceramics with various pores structures are continuously emerging, worth to mention among them are: the use of fugitives organics additives [113]; starch consolidation [25, 72]; the hetero-coagulation [108]; the freeze casting, [62, 88] and the dual phase mixing or “negative replica” [70]. Each of them has its advantages and potential uses. The control of processing and consequently, the ultimate material properties in term of pore dimensions and porosity structure remains a major challenge however.

A.2.2.2 Methods for direct casting of ceramics

The direct-casting methods are organized according to fundamental physical and chemical principles of their dispersing mechanism and gelling reaction. For all of them it is acknowledged fact that for ensuring high reliability and reproducibility of sintered parts, the dense slurries must be homogeneous with respect to the ceramic particles and organic processing additives. Therefore the solids loading should be maximized by tailoring the range and magnitude of the interparticle repulsion and optimizing the particle-size distribution. Gradients of any type should be avoided. The underlying mechanisms for most of the direct-casting methods are related to the formation of either physical or chemical bonds between either the particles or some species in the dispersion. The division between physical and chemical gels is somehow arbitrary, differing mainly in the strength of the green body; chemical gels are substantially stronger than physical gels.

Physical particle gels, sometimes referred to as a transient gels, rely on the formation of a physical bond between the particles in dense suspensions. This is mainly achieved by manipulating the interparticle forces to become attractive. In electrostatically stabilized slurries, this can be achieved by changing pH or increasing salt content, whereas sterically stabilized systems can be flocculated by changing the solvency of the adsorbed polymer

layers. At high solids loading, particle gels can develop sufficient strength to support their own weight and, thus, be handled without shape distortion. However, because no permanent bonds between the particles are formed, particles can rearrange because of thermal fluctuations or gravity and may undergo a slow densification with time. In contrast, the GC process uses a **chemical gelation** system leading to formation of strong gels by the formation of permanent chemical bonds between either the particles or some species in the dispersion. Figure A.2.2 illustrates the concept of local arrangement of particles and the microstructure of the dispersion by manipulation of interparticle potentials, showing in a sort of “phase” diagram the three regions with different structures.

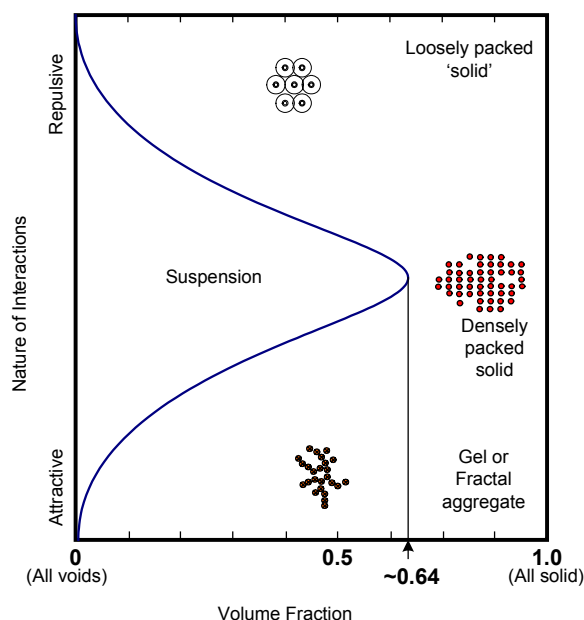


Figure A.2-2 Effects of solids loading and interparticle forces distribution on the microstructure transformation during suspension processing [45]

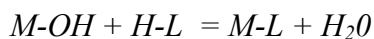
A.2.2.3 Gel-casting and its role within the novel near-net-shape forming methods

The application of the gel-casting in ceramics was pioneered by Omatete at the ORNL in 1991, as a promising technique for complex shaped structural ceramics. Although it represents a small departure from traditional slurry processing operations such as slip casting and spray drying it offers radical advantages. The principle of gel-casting consists of preparing concentrated slurry of ceramic powder in a solution of organic monomer and

dispersant which is poured into a mould and polymerised in-situ to form a green body having the mould shape. The advantage of the gel-casting concept is in retaining the homogeneous state of the dense slurry during green-body formation by minimizing slurry disturbance during gelation. Thus, introduction of larger heterogeneities can be avoided and density gradients minimized. In such a way it is possible to achieve very high packing densities at relatively lower sintering temperatures at shorter time, meaning less expensive densification and at the same time mechanical strengths higher than that achievable by classical processes like CIP and HIP [65]. By its virtue being a generic process, GC represents a small modification to existing ceramic slurry processing methods and retains many of their desirable attributes. The slurry can be processed in an entirely closed system. Mixing, filtration (to remove agglomerates or particulate impurities), de-airing (to eliminate bubbles), and mould filling can be accomplished without the danger of introducing contaminants or foreign material. The largest difference between gel-casting and the more traditional slurry processes is the solids loading. Gel-casting requires a higher solids loading (50 to 60 % V/V) as compared with that typically used in slip casting and spray drying (25 to 55 %V/V). The solids loading must be high in gel-casting since it determines the green density of the cast body. Like the most novel wet shaping methods however, gel-casting suffers still from lack of understanding about the relationships between the powder characteristics and the different constituents used in the process, thus process break-through is not yet reached.

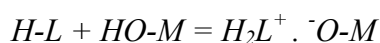
A.2.2.4 Stabilization mechanisms during gel-casting of oxide ceramics

For realizing a gel-casting process well-dispersed suspensions with high solids loading are needed. This requires achieving strong stabilisation of the suspension, governed predominantly apart from electrostatic also by steric or electrosteric mechanism. Various models of adsorption of polyelectrolytes with different molecular architecture on solid surfaces have been developed by use of techniques such as double layer capacitance, spin labelling, photon correlation spectroscopy and SALS [76]. For dilute suspensions of ceramic powders the models include the effects of variable ionic strengths, pH and double layer and make use of more advanced techniques such as Atomic Force Microscopy [36, 57]. In case of oxide ceramics (zirconia oxide) four principal mechanisms for dispersant adsorption have been recently postulated [124]. The first one is a ligand exchange, where the metal ion acts as a Lewis acid, which can exchange the coordinating hydroxyl group with the dispersant molecule, resulting in release of water molecule:

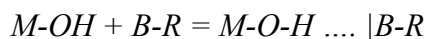


This mechanism is important in the presence of dispersant, which is able to form a chelate complex with the metal atom where two or more OH-groups are removed by one chelating molecule.

The second adsorption mechanism is ionic interaction under which the surface of the particle reacts with the dispersant, the charged dispersant molecule remains anchored to the particle surface by formation of an ionic bond:



The third way, is the molecule to adsorb by hydrogen bonding between the hydroxyl group of the particle surface and atoms of the dispersant molecule with non-bonding orbitals:



The last possibility to adsorb is through chemical adsorption. The dispersant reacts with the oxygen atom on the powder surface and forms a covalent bond while releasing a new molecule in solution.

A.2.2.5 Research incentives and needs

The majority of research efforts in colloidal processing of ceramic suspension have focused on the interactions between single organic components and particle surface. Since gel-casting is heterogeneous process, a main challenge remains in providing understanding about the interaction between *all phases* taking place in gel-casting and about the way to control over evolution of suspension structure during development of the near-net-shape bodies. Figure A.2.3 presents a conceptual view about the interactions met in colloidal and wet processing of particulate systems, which need to be considered. Especially the powder characteristics, like size, shape and surface modification and the role they play during powder dispersing aimed for subsequent gel-casting should be addressed as priority. There are indications that not the most fine-grained powder, rather the powder processing

approach, provides the best end body characteristics in terms of required microstructure [65].

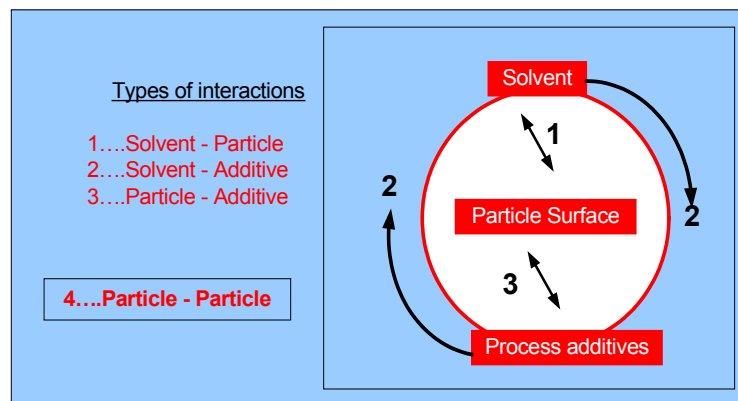


Figure A.2-3 Interactions in colloidal and powder wet processing

B1 Coagulation of dye bearing solutions

As noted in the introductory section, this part of the work is concerned with outlining the role of measuring charge related phenomena taking place during physico chemical treatment of dye effluents, as an indication for a particular destabilization mechanism. Therefore dyes with various molecular structures have been tested towards primary coagulants with different characteristics and their surface charge has been followed. Additionally, a contribution towards the role which the charge of coagulated dye sludge plays in determining flocs characteristics like size and shape has been aimed.

B.1.1 Materials

B1.1.1 Dyes

Due to their practical importance, anionic soluble dyes most of which demand pre-precipitation/coagulation were studied. Due to the large variety of dyes our choice was restricted on few types only owing to their industrial use and availability of comparative results regarding their removal ability by other competitive methods. Their characteristic properties are shown at Table B.1.1.

Chemical Index	Chromophore	Charge density, C/g	Wave length, nm, λ max
Reactive Black 5	Disazo	313	593
Reactive Red 2	Monoazo	84	536
Acid Black 1	Disazo	199	616
Acid Orange 7	Monoazo	186	481
Disperse Yellow 5	Monoazo	190	392
Direct Red 23	Disazo	130	501

Table B-1.1 Characteristics of the dyes used

B1.1.2. Primary coagulants

A series of Zetag polyelectrolyte coagulants, shown at Table B.1.2 claiming to be efficient for colour removal were tested on comparative basis.

Zetag	Chemical characteristic	Type	Activity, %	Charge density, C/g
7101	aqueous solution of cationic resin	Polyamine	50	494
7102	cationic polymer	Polyamine	55	577
7103	aqueous solution of	Polyamine	55	651

	cationic cross-linked condensation resin			
7197	aqueous solution of aliphatic resin	Polyamine	50	949
7125	aqueous solution of cationic homopolymer	Polydadmac	40	910

Table B-1.2 Characteristic features of Zetag cationic coagulants (supplied by Ciba, charge density measured by us using PCD instrument)

B1.2 Methods for coagulation and products characterization

Effluent resembling dye solutions with concentration of 100 mg/L prepared with the as received dye powder have been tested under the jar procedure pictured at Figure B1.1. The usual jar testing consists of short rapid mixing (1 – 2 min), followed by a prolonged slow mixing (10 – 20 min) to promote aggregation. Such jar tests are employed for coagulation of matured (clay-type) colloidal suspension found in water. However, dye solutions are micro, or even macro homogenous colloidal solutions often comprising ionogenic charges. Therefore, we have followed a shorter step of mixing of dye-coagulant solutions for 2 minutes at 200 rpm followed by further 5 minutes at 25 rpm, which resulted both in charge neutralization and aggregation into flocs. Since the used polyelectrolytes do not have acidic character, pH of the dye solution has not been adjusted and was kept in all tests in the range of 8 – 8.5. After coagulation elapsing samples have been collected for surface charge determination in the dye sludge (by streaming current) and floc characterization (median by laser diffraction and fractal dimension by Low Angle Light Scattering) [53]. Following solid-liquid separation by either centrifugation, plain sedimentation for 90 minutes or gravity filtration through paper micro-filter (pore openings 4 – 7 μm), analysis of residual colour concentration in the liquid phase has been done spectrophotometrically. For the Disperse dyes, the calculation of the colour removal has taken into account the degree of removal resulting from a “blank” experiment aiming determination of any colour removal by the presence of the micro-filter only.

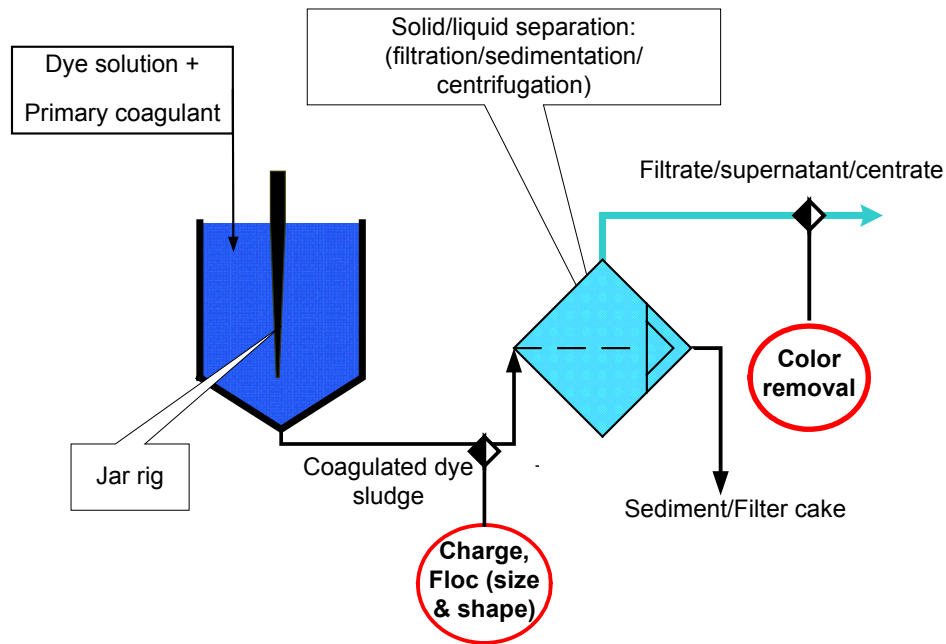


Figure B-1.1 Jar testing for dye coagulation and associated characterization sequences

B1.3 Screening studies - dyes reactivity with primary coagulants

The results from the initial screening tests summarized in Table B.1.3 confirmed that solutions from dyes belonging to six different chemical groups and application classes can be coagulated to a different extent by five cationic polyelectrolytes characterized by low molecular weight and high charge density.

Dye Coagulant	Reactive Black 5	Reactive Red 2	Acid Black 1	Acid Orange 7	Disperse Yellow 5	Direct Red 23
7101	++	++	++	++	++	++
7102	++	++	++	++	+ -	++
7103	++	++	++	++	++	++
7197	Nr	Nr	++	++	++	n.r.
7125	Nr	Nr	+ -	++	+ -	n.r.

++ - uniform charge neutralization pattern; + - "mosaic" charge neutralisation; n.r. - no reaction

Table B-1.3 Screening tests summary with hypothetical predominant mechanisms responsible for dye destabilisation (in yellow - the best performing coagulant)

In analyzing the behaviour of the dyes it is to be noted that the different dyes reacted in different extent with the studied polyelectrolytes and hence it was difficult to outline similarity in colour removal behaviour. This difference might be due to the intrinsic

structural arrangements of the dye molecules and the different chemistry of the cationic polyelectrolytes. The immediate impression was, that based on the pronounced correlation between coagulation ability and surface charge progression, ***charge neutralization pattern*** could be assumed as predominant mechanism of destabilization for the Direct and Reactive dyes. For these cases, it could be presumed that the active groups of the coagulants react with the dissolved anionic dyes, altering their surface charge to zero thus enabling the colloidal particles to subsequently aggregate and precipitate. In two cases, Disperse Yellow 5 and Acid Black 1 dyes, the so-called ***charge patch*** mechanism could be supposed. This mechanism is considered to be a specific kind of non-uniform charge neutralization pattern, where the polyelectrolyte active group creates a „mosaic” structure consisting from positive areas surrounded by a negative ones. The oppositely charged areas of the particles can then enter into contact forming larger aggregates through electrostatic way. For supporting the above postulated hypothetical mechanisms, three particular cases illustrating contrasting behaviour of dyes characterized by different chemical structures are presented below.

B.1.3.1 Supporting examples of destabilization patterns

The coagulation behaviour of the studied dyes with the optimally found polyelectrolytes is evaluated in terms of surface charge progression, colour removal and the characteristics of the flocs in dye sludge.

I: Complete charge neutralization pattern by chemical reaction

The optimal coagulant choice for the Reactive Black 5 dye was Zetag 7101. Accordingly, the influence of its addition on the progression of surface charge of dye sludge, the colour removal and the characteristics of the developed flocs is shown at Figure B.1.2.

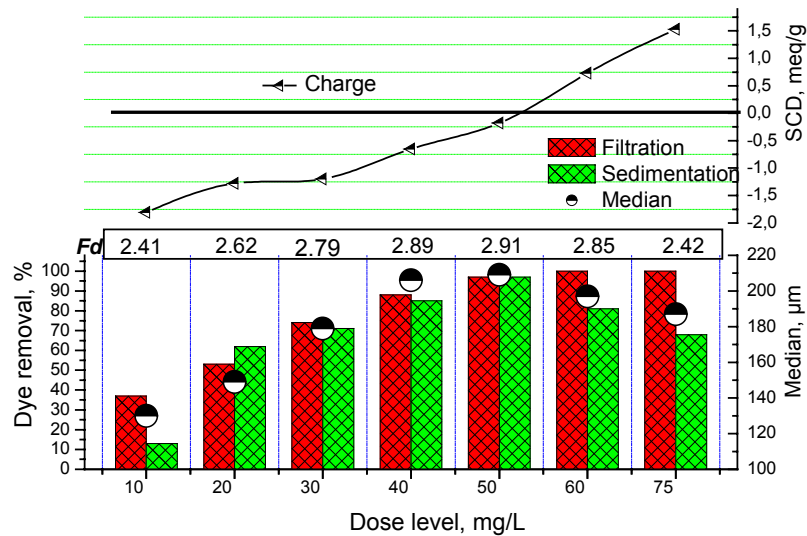


Figure B-1.2 Relationship between colour removal after filtration and sedimentation, surface charge density of dye sludge and floc features as a function of coagulant dosage (dye Reactive Black 5 – coagulant Zetag 7101)

Based on the quite good coincidence of PZC of the dye sludge with the maximum colour removal to be seen at Figure B.1.2., it could be suggested that the dose of 50 mg/L could be regarded as an optimal one. It could be assumed that the dye destabilization follows charge neutralization pattern, hence the hypothetical concept of dye reaction with Zetag 7101 could be illustrated like shown below (based on an approximately estimated chemical structure of the coagulant as $[R_2(NH_2)_2 \dots Cl_2]_n$)

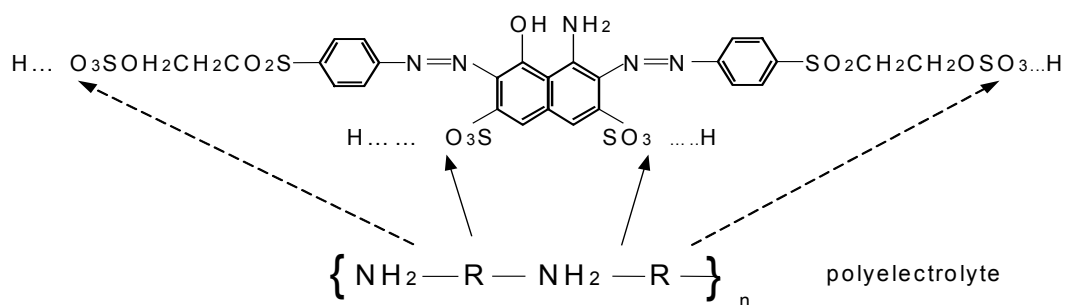
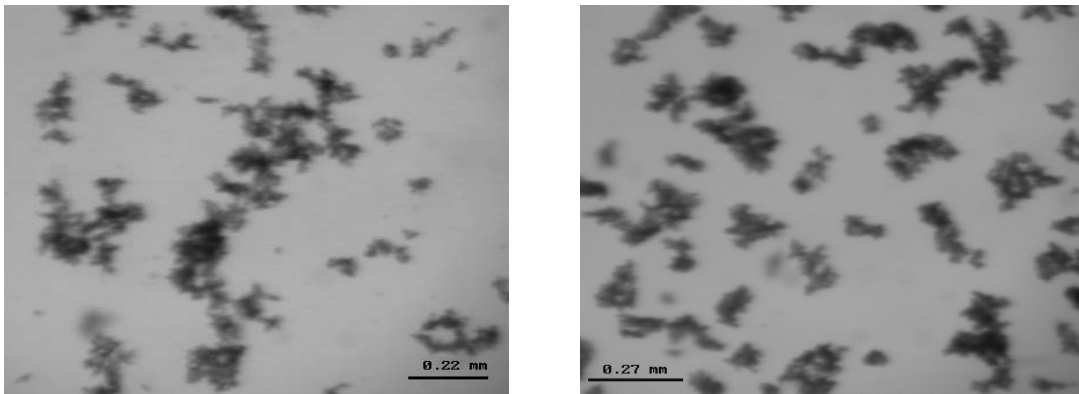


Figure B-1.3 Dye - coagulant interaction leading to coagulation via chemical reaction (Reactive Black 5 – Zetag 7101)



Picture B-1.1 Image analysis micrographs of characteristic dye aggregates (coagulant at 20 mg/L – left and 50 mg/L – right)

When comparing the results shown at Figure B.1.2 with the floc views at Picture B.1.1, the trend for developing more dense structures with increasing coagulant dose becomes obvious. As a rule, increasing the fractal dimension F_d denotes better settling of flocs. By rising the coagulant dosage above the optimal one, a re-stabilization perhaps occurs which reflects in reduced removal by sedimentation, corroborated by the fact that the sludge is characterized by a greater amount of fine sized flocs which settle slow. They however are well filtered which reflects in continuous total colour removal by filtration when the coagulant dosages are increased above 50 mg/L.

II: Complete charge neutralization pattern by adsorption and chemical reaction

The behaviour of the Acid Black 1 dye coagulated with Zetag 7103, which was the optimal coagulant type suggested by the screening studies, is illustrated at Figure B.1.4. The micro views of some characteristic floc samples from the dye sludge are shown at Picture B.1.2.

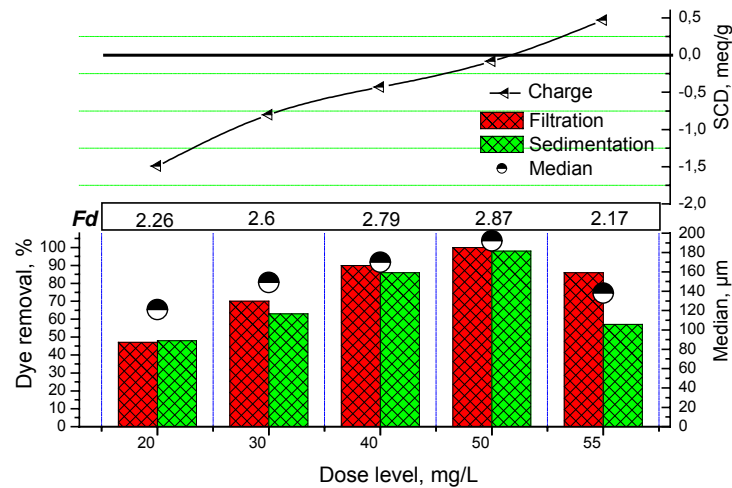
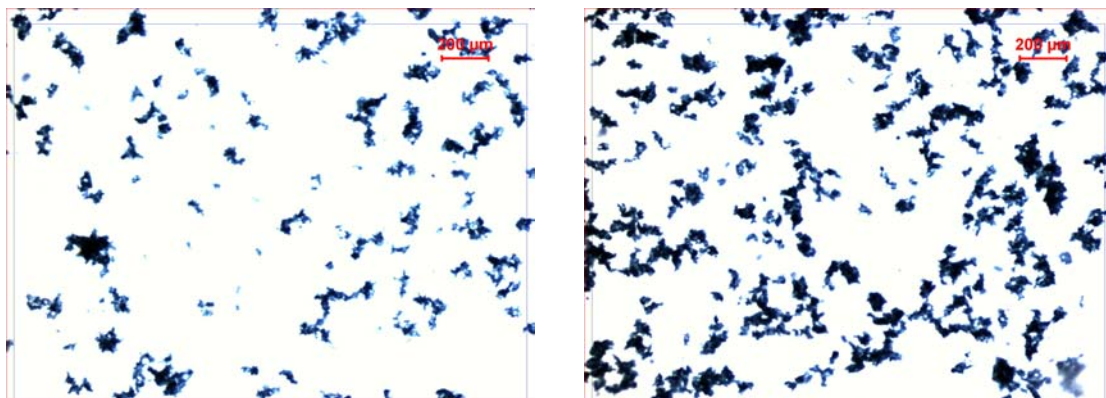


Figure B-1.4 Relationship between colour removal after filtration and sedimentation, surface charge density of dye sludge and floc features as function of coagulant dosage (Acid Black 1 – Zetag 7103)



Picture B-1.2 Image analysis micrographs of characteristic dye aggregates (coagulant at 20 mg/L – left and 50 mg/L – right)

A similarity in the behaviour of Acid Black 1 and Reactive Black 5 dyes could be noted. The flocs developed with Acid Black 1 at the optimal dose of 50 mg/L are characterized by dense structures and improved settling ability. The increase in coagulant dose is leading to reducing the negative surface charge density of the sludge rendering it close to zero at 50 mg/L. The further increase in dose level is leading to positive charging and eventual floc abrasion during sludge filtration, which effect finally results in reduced colour removal by filtration. Therefore it could be assumed that a kind of physical sorption is also operative in this case which is leading to weaker aggregation forces

between the destabilized primary dye colloidal particulates hence the formed aggregates are more abrasion prone.

Likewise to the case of the Reactive dye, the reaction between the Acid Black 1 dye and the coagulant could be illustrated as shown below:

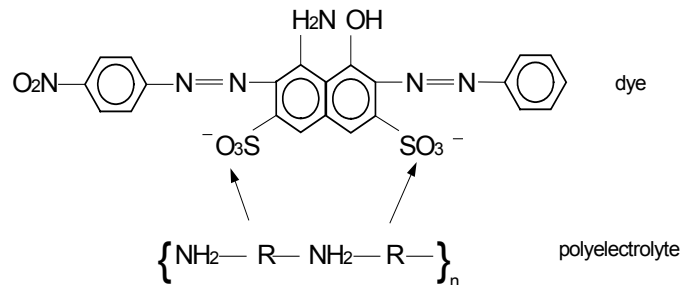


Figure B-1.5 Dye coagulant interaction leading to coagulation via adsorption and chemical reaction (dye Acid Black 1 – coagulant Zetag 7103)

III: Adsorption leading to “mosaic” charge neutralization

For the Disperse Yellow 5 dye, the best destabilization was achieved when a Zetag 7125, which is a low molecular weight Polydadmac (Poly-diallyl-dimethylammoniumchlorid) was applied. During the screening studies it has been found out that very negligible variation in coagulant dose level is leading to appreciable changes in surface charge density of dye solution. Therefore for this “dose sensitive” case, the effect of coagulant concentration on surface charge density, dye removal and floc features has been evaluated for three close to each other points - Figure B.1.6.

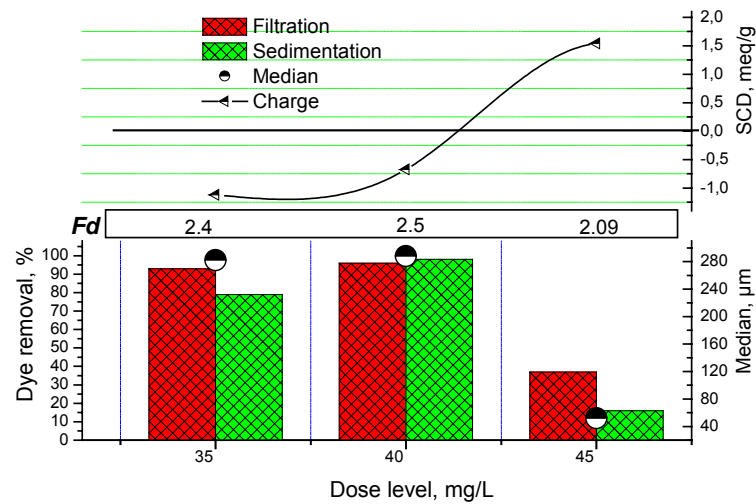
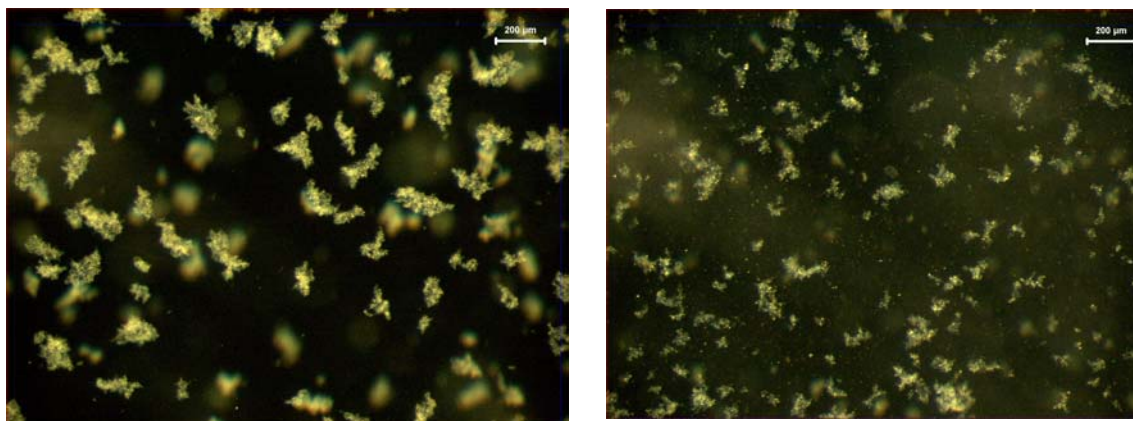


Figure B-1.6 Relationship between colour removal after filtration and sedimentation, surface charge density of dye sludge and floc features as function of coagulant dosage (dye Disperse Yellow 5 – coagulant Zetag 7125)

For the Disperse dye, which is not soluble, hence micro particles do exist, it could be assumed that the Zetag 7125 when supplied at its optimal concentration is adsorbed on the dye particle surface in patch like pattern. Well settling flocs are formed regardless that charge neutralization point has not been reached. The flocs developed both at 35 and 40 mg/L are quite similar in terms of size and shape. By further minute increase in dose level to only 45 mg/L, the polymer molecules perhaps tend to form double layer on the dye particle surface, which is leading to high positive charge with concomitant development of finer flocs which are both poorly settling and filtered. The obvious decrease in size between 40 and 45 mg/L could be seen at the image analysis views shown at Picture B.1.3.



Picture B-1.3 Image analysis micrographs of characteristic dye aggregates - (coagulant at 40 mg/L – left and 45 mg/L – right)

The hypothetical interaction of the Zetag 7125 with the surface of the dye, depicting a non-fully surface coverage is schematically illustrated at Figure B.1.7.

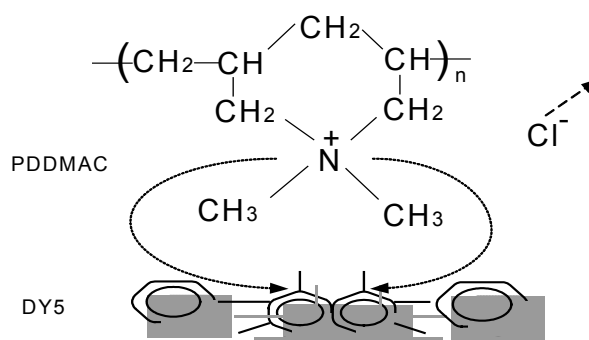


Figure B-1.7 Interaction pattern between Disperse Yellow 5 and Zetag 7125 leading to non-complete charge neutralization and “mosaic” type adsorption

B.1.4 Conclusions

The differences in the structural properties of the primary coagulants cannot explain the disparity in dyes removal, leading to the conclusion that the chemical structure of the dye plays a key role during the destabilization process. The mechanism of interaction between the dyes and the cationic polyelectrolyte could be hypothetically taking place as reaction between the dye molecule (free electrons present in the hydrophilic group of the aromatic ring) and the active group of the polymer. In case of the studied *Reactive* and *Acid* dyes, the polyamine type coagulant forms a complex with the dye leading to: (1) fully masking of the initial negative charge of the hydrolyzed dye and (2) its precipitation in form of

well settling flocs following *total charge neutralization*. In the case of the **Disperse** dye, the polyelectrolyte likely adsorbs on the dye surface creating a “mosaic” structure, with oppositely charged areas of the particles, which subsequently create larger aggregates at *not completely neutralized surface charge*.

By registering the generated streaming current of the dye sludge when placed inside the particle charge detector cell and by analyzing its progression due to addition of cationic polyelectrolyte, an indication about the predominant pattern of dye molecule destabilization could be figured out. However this signal could be viewed to a less extent as indication for the size and shape of the respective flocs, since dye aggregates with various sizes and shapes have been produced with same dye at constant shear, but by varying the charge density and molecular weight of the coagulant used. The schematic illustration of the operational principle of the PCD device is shown at Figure B.1.5. Due to piston movement up and forth, the coagulated dye species generate streaming current inside the PTFE cell, which is online registered.

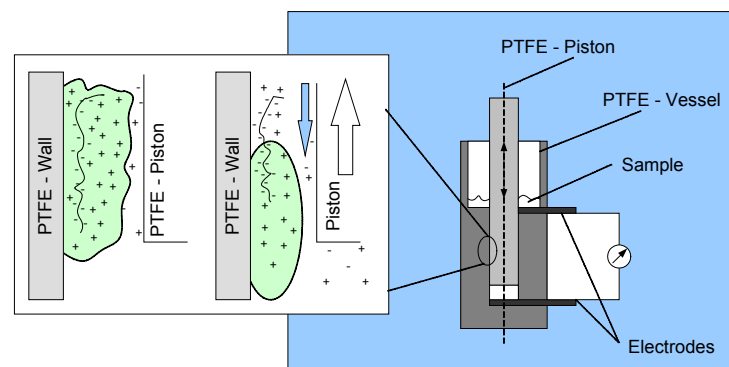


Figure B-1.5 Operational principle of a streaming current based particle charge detector. Magnified area (right) gives simplistic idea about the “shearing” due to piston movement of the diffuse layer of coagulated colloidal dye. In static position of the piston, the diffuse layer is intact (left).

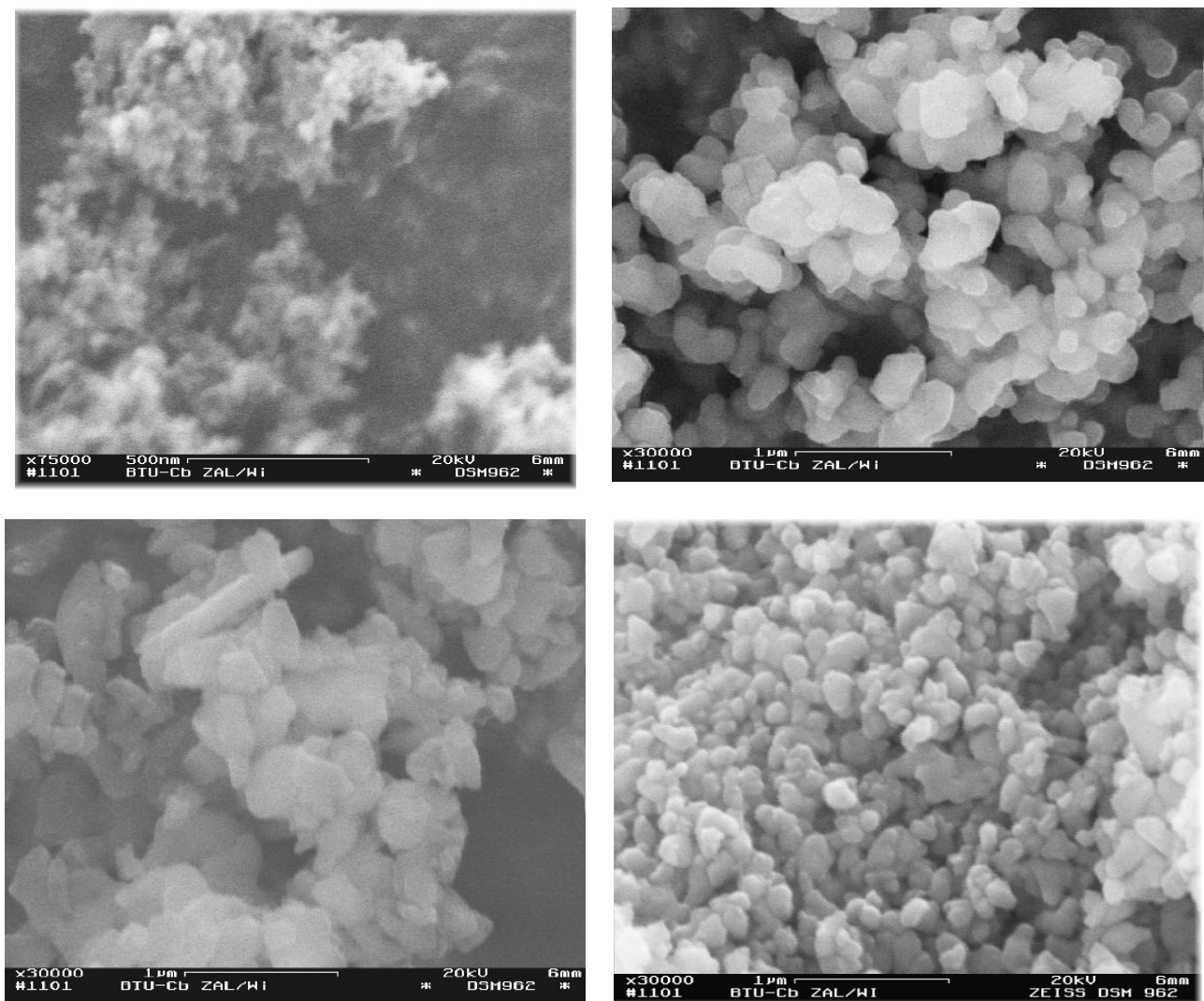
B2 Characterization of stability in aqueous alumina suspensions

B.2.1 Materials

B.2.1.1 Powders

In order to outline the effect of powder characteristics on their dispersive behaviour, our study has concentrated on different alumina powders – from nano to ultra fine sized. Their main properties as given by the manufacturers are summarized in Table B.2.1. As could be seen, apart from the three alfa alumina powders, a flame synthesized gamma alumina produced under the AEROSIL[®] process was tried. This gamma alumina powder has not been intended for gel casting, rather the aim was to deliver information about its stability behaviour with the tested dispersants. The AEROSIL[®] powders are designed for improving the flow ability of powder products (e.g. powdered lacquers), for thickening of liquids, for rheology maintaining and as antiblocking agent in PET films production. As a rule, most of the commercial products formulated on fumed oxides basis are used as aqueous suspensions, therefore their characterisation in terms of surface and interfacial properties, parallel to size, shape and morphology is mandatory. In order to characterize the shape and surface morphology of the powders, they were subjected to investigations by a Raster electronic microscope. Selected micrographs of the powders are shown at Picture B.2.1. What is to be noted is the difficulty in visualizing single particles owing to the natural tendency of the powders to agglomerate. This effect was particularly obvious in the case of Alu-C powder. It should be noted, that previous studies of fumed silica powder, have also reported that isolated primary particles did not exist [11]. For the alfa powders, the grain shapes vary from irregular (CR6), or nearly oval one (AKP 53) through lamella like one (CT3000SG), which inevitably will lead to quite different behaviour of these powders during the gel-casting process.

Granulometric analysis of the powder-water suspensions and their zeta potential estimation was performed by acoustic and electroacoustic spectrometer DT 1200. Before being transferred to the measuring chamber of the spectrometer, the suspensions were stirred for 2 minutes by magnetic stirrer and agitated 30 sec by ultra sonic disintegrator for de-agglomeration. The same procedure was followed before taking the capillary suction time (CST) measurement.



Picture B.2-1 REM micrographs of the powders under study

Alu-C	CR6
CT3000SG	AKP53

Producer Features	Degussa	Alcoa	Baikowski	Sumitomo
Trade name	AEROSIL [®] Alu-C	CT3000SG	CR6	AKP53
Crystal phase	gamma	alfa	alfa	alfa
Specific surface area (BET), m ² /g	100 ± 15	7	5.8	11.2
Primary particle size (PPS) as given by the producers (d ₁₀ ; d ₅₀ ; d ₉₀), μm	n.a.; 0.013; n.a.	n.a.; 0.8; 2.46	n.a.; 0.52; 1.4	n.a.; 0.30; n.a.
Measurement technique used for PPS	Microscopy	Laser	Sedigraph	n.a.
Fired density (approx. value), g/cm ³	2.9	3.92	3.9	3.9
pH of ca 4.8 % water suspension (measured)	4.5 – 5.5	8.5 – 8.6	7.5 – 8	4.5

Table B-2.1 Typical powder characteristics as given by the producers (n.a. – no data available)

B.2.1.2 Dispersants

In this work, four carboxylic acid based anionic (-COOH and -NH₄ functional groups) and one pseudo cationic polyelectrolytes were selected as dispersing agents, their principal characteristics being summarized in Table B.2.2. Most of the anionic dispersants used are described in the literature, for example Dolapix CE64 [4, 82, 111, 112], Darvan 7 [37] and Darvan C [8, 57, 79, 96, 113]. The exact mechanism of interaction/adsorption between the dispersants and the surface sites of the powder is still debatable. Being commercial products, little information about their precise chemical structure is provided by their producers. In an independent study aiming to reveal the chemical structure of Dolapix CE64, it has been found out that its average molecular mass is 320 g/mol and it represents an ethanolaminic salt of citric acid [22]. This finding leads to an assumption that the Dolapix CE64 is a short chain functional polymer belonging to the polyacrylic acid family similar to Darvan [4]. As carboxylic acid derivate, Dolapix CE64 possesses two carboxylic groups, the one left as active (anchor), while in the other the OH⁻ is replaced by

ONH_4^- , which is a better leaving nucleophilic group. The Darvan C is a homopolymer and with an average molecular weight between 8000 and 10000 g/mol. For long chain polyelectrolytes of carboxylic acid type, the degree of dissociation varies with pH and increases with increasing pH reaching full dissociation at pH of around 9 [17, 57].

Dispersant	Dolapix CE64*	Dolapix A88*	Dolapix PC75*	Darvan C**	Darvan 7**
Charge	Anionic	Pseudo cationic	Anionic	Anionic	Anionic
Type/active group	Carboxylic acid basis	Amino alcohol basis	Synthetic polyelectrolyte	Amonium polymethacrylate	Sodium polymethacrylate
Density, g/cm ³	1.2	0.95	1.1	1.11	1.16
Active substance, wt %	65	90	25	25	25

Table B-2.2 Principal characteristics of the dispersants used (produced by: *Zschimmer-Schwarz, Lahnstein, Germany; ** R.T. Vanderbilt Co., USA)

B.2.2 Methods for evaluation dispersants efficiency

The two principal methods used for evaluation the efficiency of dispersants towards keeping the particles in suspension, have been the zeta potential and the streaming current detection. It has been found out that a strong correlation between both parameters exists for ceramic powder suspensions and therefore the both techniques could be viewed as an identical ones regarding determination of optimal dispersant dose level [118]. The inflection point between the suspension potentials and dose level of dispersant (i.e. the curve flattening point) should be considered as an optimal dose level [36, 91, 99]. Any amount of dispersant supplied above that optimum will remain unbounded and could lead to unwanted increase in suspension viscosity. In all experimental investigations 4.76 % W of powder suspension in distilled and deionised water has been used. For selected powders, further verification of the chosen dispersant dose level has been carried out by sedimentation and capillary suction time (CST) measurements. The later technique yields information about suspension fluidity as well.

B.2.3 Powder suspensions in water: particle size distribution and surface charging

The most critical issue for the successful development of ceramics by colloidal processing is understanding the surface chemistry of the powders for producing flow able and stable slurries with as high as possible solids loading [16]. Therefore it was crucially important to fully characterize the studied powders in terms of surface charge of particles and their size distribution in suspension. The presented results are based on the mean data from minimum three independent measurements under same test conditions.

B.2.3.1. Nano-sized gamma alumina powder (Aerosil-Alu-C)

Owing to the indigenous characteristics of the fumed oxide, and to the fact that this powder is not intended to be used for gel casting, it was important to outline the powder behaviour towards two contrasting dispersants - a cationic and an anionic one.

Particle size distribution

A typical particle size distribution of the powder-water suspension is shown at Figure B.2.1. The median and mean diameters were determined respectively as 39 nm and 50 nm with standard deviation of 0.27. Since the producer specifies an average particle size for the dry powder about 13 nm – Table B.2.1, it could be presumed that regardless the ultrasonic impact, the powder is in agglomerated form when suspended in water. Additionally, it could be supposed that upon dispensing in water the powder reacts very strongly with it and produces $\text{Al}(\text{OH})_3$, which deposits on the particle surface and increases its size [38].

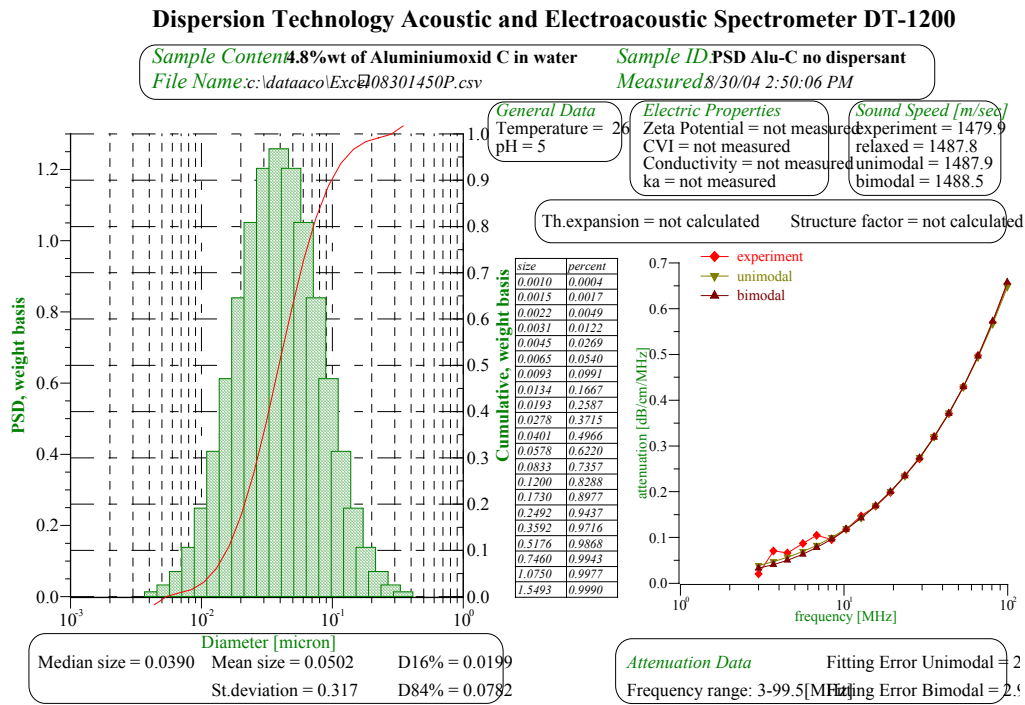


Figure B-2.1 Particle size distribution of Alu-C suspension at natural pH ($d_{10} = 0.017$; $d_{50} = 0.039$; $d_{90} = 0.082$)

Zeta potential and streaming current characteristics

The behaviour of the powder suspension under progressive supply of the tested dispersants in dose levels up to 27 mg/g has been studied by volumetric titration. The results obtained in this direction are shown at Figure B.2.2.

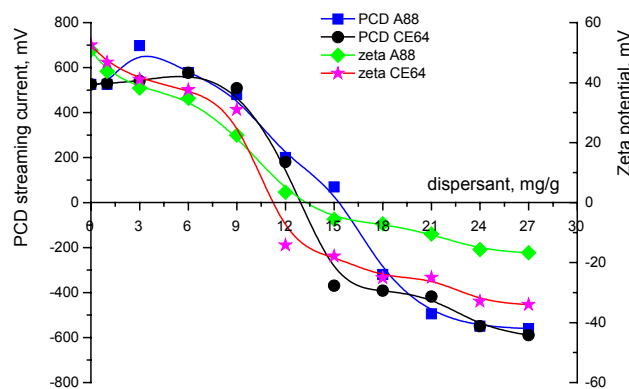
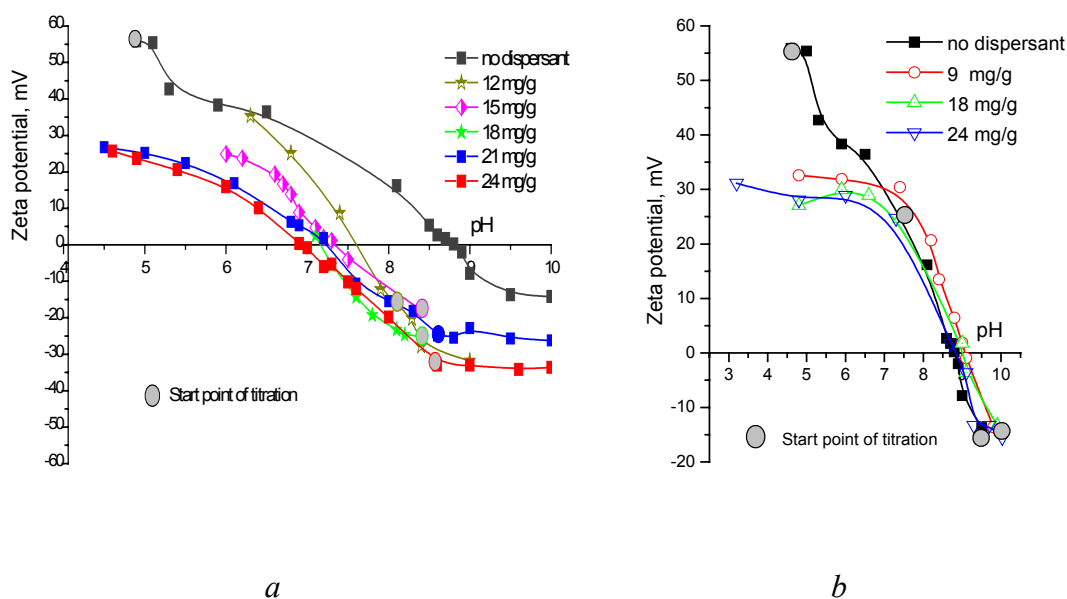


Figure B-2.2 Effect of dispersant concentration on zeta potential and streaming current

As could be seen from the figure, the four curves are characterized by a similar trend, they decrease monotonically parallel to dispersant addition. While the streaming current curves for the both dispersants nearly overlap, the zeta potential curves differ at higher dosages of dispersants. Both dispersants have completely neutralised the initial positive charge, but the Dolapix CE64 has provided higher charge loading compared to Dolapix A88. Without addition of dispersant, the suspension system acquires high positive charge, as result of surface hydroxyl groups, which dissociate in water or act as proton acceptors. Thus, although the absolute value of the zeta potential for the untreated powder is higher than the one treated with dispersants implying natural stabilisation, this could be entirely due to electrostatic repulsion forces, which are known as weak and short ranged ones, and as such could lead to less stable powder suspensions. Additionally, hydration forces could be suspected to exist. Their origin is debatable and for SiO_2 sols could be linked to hydration effects due to presence of silanol groups [39].

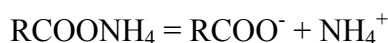
With the addition of dispersants, the positive zeta potential and the streaming current are reduced. At 15 mg/g, the suspension could be still partially stabilised by electrostatic and steric forces. At 18 and 21 mg/g dose levels, the zeta potential has almost approached -30 mV, a level considered as a minimum for full steric stabilisation. It has appeared from the CE64 curve (star symbols), that an inflection point is poor for description. Nevertheless, after 24 mg/g, a curve flattening could be distinguished, the potentials remaining almost constant thereafter. Therefore, a dose level of 24 mg/g could be considered as an optimal one for maximum powder suspension for the both dispersants.

Further it was important to follow the shift in the $\text{pH}_{(\text{i.e.p.})}$ for the powder stabilized with the optimal dispersant dose. Since during the volumetric titration, CE64 has shown better performance in comparison to A88, the effect of its addition has been studied within a broader dose level range, i.e. from 12 to 24 mg/g, while for A88 only three characteristic concentrations have been considered. The range for the CE64 has been intentionally chosen, since after 12 mg/g, a reversal in the zeta potential sign has been documented – Figure B.2.2. The results from the potentiometric titrations are depicted at Figure B.2.3.



FigureB-2.3 Zeta potential as function of suspension pH, without and with addition of dispersant at different concentrations - Dolapix CE64 (a) and Dolapix A88 (b)

Without dispersant, the $\text{pH}_{(i.e.p.)}$ of the suspension is around 8.9. For the same Aerosil powder there are different data reported in literature about the $\text{pH}_{(i.e.p.)}$. In a recent review by Kosmulski [63], a value of 8.3 is reported, however in another source the $\text{pH}_{(i.e.p.)}$ is given as 9.9 [38]. Upon addition of CE64 in concentration from 12 to 24 mg/g, the $\text{pH}_{(i.e.p.)}$ is shifted towards neutral region. From other side, the natural pH of the suspension is shifted from an acidic range of pH 4.9, towards an alkaline pH region of 8 - 8.5 where the dispersant should be nearly 100 % dissociated [91]:



In contrast to the CE64 case, the addition of A88 did not shift markedly the $\text{pH}_{(i.e.p.)}$.- Figure B.2.3-b. The nearly coincidence in the $\text{pH}_{i.e.p.}$, with and without dispersant could be due to the disruption of the shear plane because of presence of uncharged A88 chains at the solid-solution interface and therefore an indication that the interaction between the powder and the dispersant is a physical in nature. For the CE64 from other side, a chemical interaction could be presumed, an argument for a more detailed further evaluation of this dispersant. The pseudo cationic nature of the A88 dispersant (cationic amino groups) is manifested by the fact that when supplied at doses of 18 and 24 mg/g it

has provided negative charging of alumina surface and when supplied at 9 mg/g - a positive one.

Evaluation of suspension fluidity by CST

The rheological properties and fluidity of suspensions are affected by the surface structures of the particles, which often are determined by the powder manufacturing history. With view towards the practical use of the powder, it was important to find out, if a correlation between the suspension fluidity and the optimal level of dispersant determined by the volumetric titration exists. Figure B.2.4 displays the CST evolution for the suspension treated with increasing concentration of dispersant. The respective pH values are plotted as well. A perusal of the relationship shown at Figure B.2.4 indicates a pronounced maximum at 15 mg/g dispersant dose, after which point, the CST has dropped. At the optimum level of 24 mg/g suggested by the volumetric titration, the suspension is characterised by low CST and at the same time has been visually appearing quite fluid. Whilst the exact pore size of the CST filter paper is not known, it is for sure much larger than the primary particle size of the suspended powder. It could be presumed, that when the suspension has been treated with optimal dispersant dose, the suspended particles will go through the pores and the suspension will flow like water giving short suction time. On the other hand, at dose levels close to the I.E.P., particles agglomerate and tend to block the pores, thus yielding high CST values.

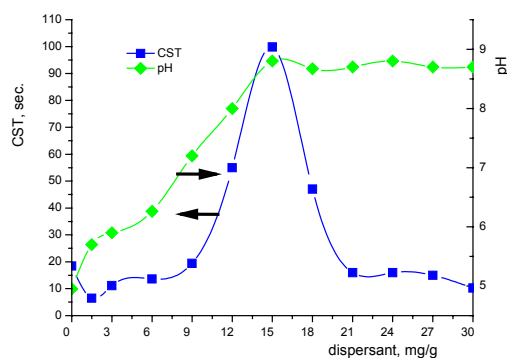


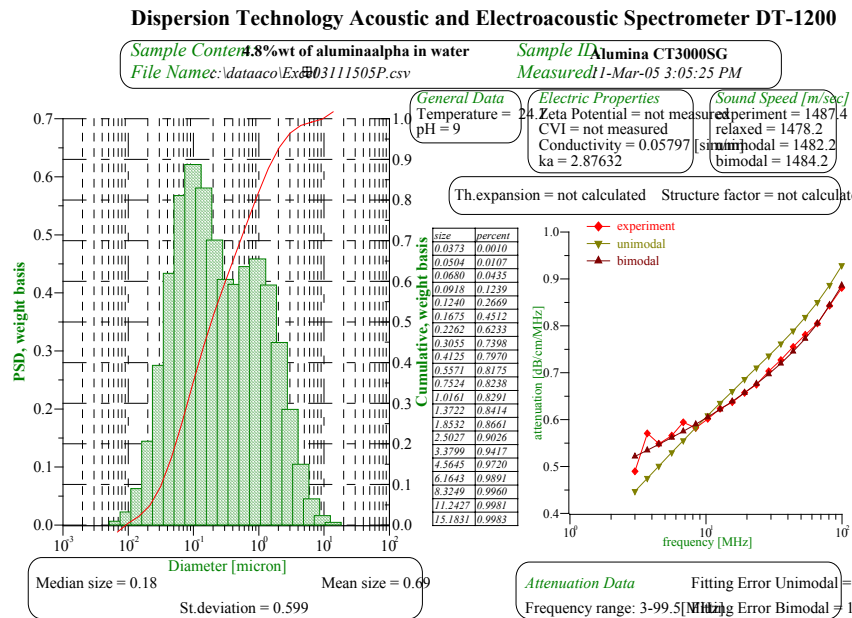
Figure B-2.4 CST and pH of suspension as function of Dolapix CE64 concentration

B.2.3.2 Ultra fine alfa aluminas

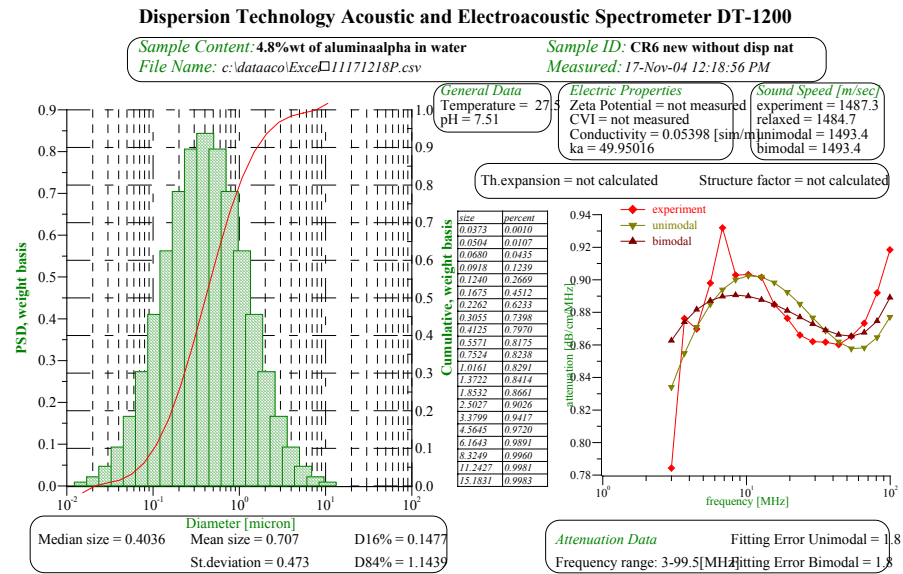
Since each of the three alfa alumina powders tested could be viewed as potential candidate for gel casting, it was important to evaluate the influence of particular powder characteristics (size, surface structure, level of surface modification) towards its dispersive behaviour within the range of studied dispersants. On a comparative cost basis, the CT3000SG has proved to be the best powder choice, therefore the screening of the four anionic dispersants has been studied more extensively with that powder.

Granulometric characteristics

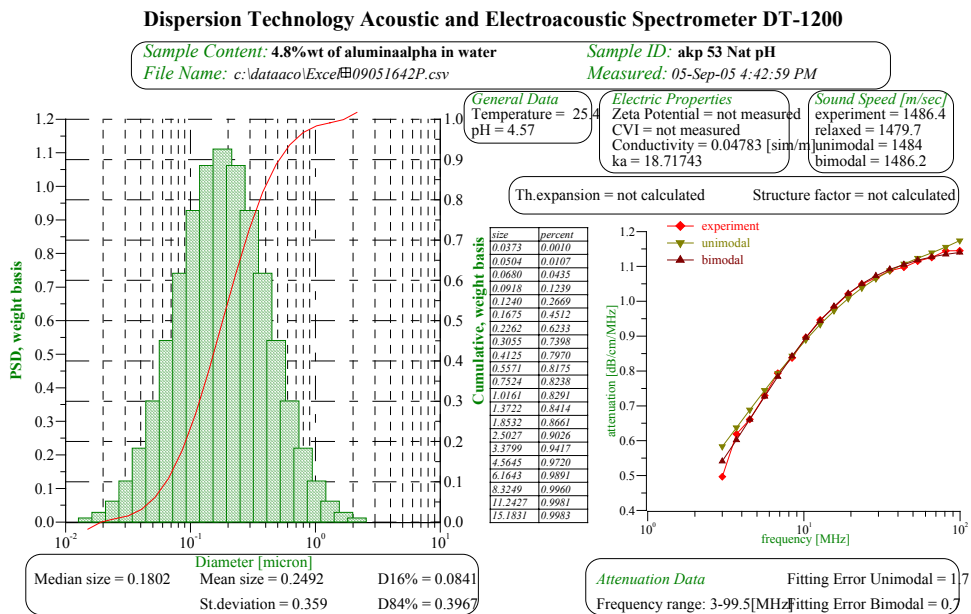
In order to secure sufficient statistical reliability of the determinations, several independent particle size distribution measurements have been performed for each powder, and satisfactory reproducibility has being found. The results from the particle size determinations for each of the suspensions of powders are shown at Figure B.2.5, respectively for CT3000SG (a), CR6 (b) and AKP53 (c).



(a): $d_{10} = 0.03$; $d_{50} = 0.18$; $d_{90} = 1.59$



(b): $d_{10} = 0.11$; $d_{50} = 0.4$; $d_{90} = 1.52$



(c): $d_{10} = 0.07$; $d_{50} = 0.18$; $d_{90} = 1.49$

Figure B-2.5 Granulometric analysis of powder suspensions with measured median, d_{10} and d_{90} diameters in μm . (a) - CT3000SG, (b) – CR6, (c) - AKP53.

It could be seen that the CT3000SG powder has a relatively broad bimodal size distribution with $d_{10}=0.03 \mu\text{m}$, $d_{50}=0.19 \mu\text{m}$ and $d_{90} = 1.59 \mu\text{m}$. The mean diameter is measured as 0.68 μm . The measured median (d_{50}) of 0.19 μm differs largely to that given

by the producer - 0.8 μm (Table B.2.1). The d_{90} diameter reported by the producer as 2.6 μm is also higher than the one measured by us – 1.5 μm . The reasons for this discrepancy could lie in the different measurement techniques (laser scattering vs. acoustics) and in the ultrasonic impact applied for de-agglomeration in our case. This powder is characterised by the highest amount of fines and large amount of relative coarse fractions. The later however possibly are resulting from agglomeration effects, since the REM micrograph does not indicate presence of single particles with such size. The CR6 powder from other side, has shown a unimodal distribution indicating $d_{10}=0.11 \mu\text{m}$, $d_{50}=0.4 \mu\text{m}$ and $d_{90}=1.52$. The producer reports for analysis carried out by Sedigraph, a median of 0.53 μm and $d_{90}=1.4 \mu\text{m}$, which lies in good agreement with our analysis. The granulometric analysis of the AKP53 powder suggests lack of agglomerated fraction and mono disperse characteristic in suspension - $d_{10}=0.07 \mu\text{m}$, $d_{50}=0.18 \mu\text{m}$ and $d_{90}=0.49$. This powder is characterized by highest surface area compared to the other two.

Surface charge characteristics

For finding out the optimal dispersant dose level leading to maximum particle charging and long-term suspension stability, a volumetric titration studies similar to the ones done for the Alu-C powder have been performed for the three alfa aluminas as well.

B.2.3.2.1 CT3000SG

The effect from the dispersant treatment on the streaming current and zeta potential of the powder suspension is shown at Figure B.2.6.

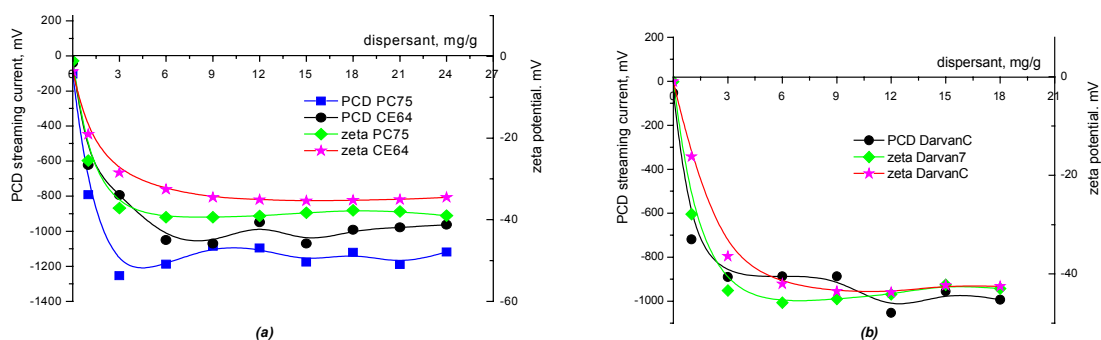


Figure B-2.6 Effect of dispersants concentration on zeta potential and streaming current of CT3000SG water suspension: (a) Dolapix CE64 and PC75 and (b) Darvan C and Darvan 7 (only zeta potential)

It should be noted that the Darvan 7 has been found unsuitable for studying under the streaming current instrument (PCD), since it was impossible to completely neutralize the charge till zero within the maximum allowable amount of counter electrolyte supply. The first observation, is that when suspended in water, the CT3000SG powder does not acquire charge, therefore it could be considered as naturally non stabilized. All the tested dispersants when supplied stepwise have rendered the zeta potential of the suspension towards relative close negative values of around - 40 mV. Based on the inflection points seen from both the zeta and streaming current curves, the dose levels shown at Table B.2.3 could be recommended as an optimal ones. It should be pointed out that the zeta potential curves have shown virtually no fluctuations in contrast to the streaming current. Since the studied dispersants possess different structures and their conformation changes with pH, of special importance was to follow also the pH evolution during the volumetric titration, therefore the suspension pH at optimal dispersant dose is also indicated.

Dispersant	CE64	PC75	D C	D 7
Opt. dose, mg/g	6.5	6	9	6
pH at opt. Dose	9.1	8.8	9.2	9.7

Table B-2.3 Optimal dispersant dose as estimated from the volumetric titrations and suspension pH at optimal dose (powder CT3000SG)

Using the estimated optimal dispersant concentrations, potentiometric titration tests have been performed in order to evaluate the level of interaction between each dispersant and the powder by analyzing the respective shift in $\text{pH}_{(i.e.p.)}$, the results of which are shown at Figure B.2.7. Since the PCD device has not been deemed suitable for this task, only the CVI instrument has been envisaged.

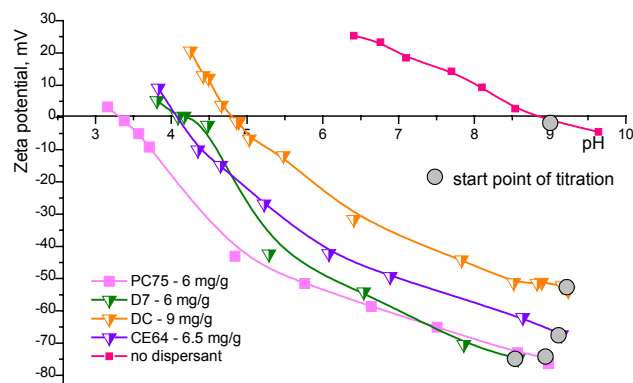


Figure B-2.7 Zeta potential of CT3000SG suspension as function of pH, without and with addition of dispersants at optimum concentration levels

When comparing the curves at Figure B.2.6 and B.2.7 one could notice a difference in the negative values of the zeta potentials at natural state, i.e. before starting the titration indicated with circles in Figure B.2.7, with that detected at the optimal dose levels during the volumetric titration – Figure B.2.6. The deviation could be attributed to the different mode of dispersant supply used in the both cases. During potentiometric titration, the dry powder was mixed directly with water containing the optimal dispersant dose, which could lead to better homogenization and higher degree of adsorption. In the case of volumetric titration however, the optimal dispersant dose was reached via stepwise dispersant addition in one and a same suspension.

For the Dolapix CE64 and Darvan C it could be supposed that they adsorb on the alumina surface predominately through H-bonds between the OH groups of the particle surface and the OH anchoring groups inherently present in the dispersants [111]. This adsorption is leading to increased powder dispersibility in water and low viscosity. For the both dispersants the slight increase in pH during adsorption of ammonium bearing dispersants could be due to acceptance of protons from water by the lone electronic pair of N atoms. The reaction results in change of the zeta potential of alumina to negative. Dolapix PC75 is a homopolymer polyelectrolyte and its molecular structure is not known, therefore its reaction pattern could not be outlined. It is however supposed that at alkaline pH a stretched conformation could be expected, while at acidic range it is slightly ionized and exists in coil/loop conformation [18, 90].

Since at its optimal dose the Darvan 7 has maintained very high pH, which could not be suitable for moulding (pH 9.7), this dispersant could not be considered as a suitable one. The relationships pH - zeta potentials presented in Figure B.2.7 indicate, that without addition of dispersant the pH of iso electric point is about 8.9. This value is in agreement with literature findings [51, 57, 98, 110]. Adding dispersants shifts the $\text{pH}_{(\text{i.e.p.})}$, suggesting that they interact with particle surface and alter it significantly through involvement of chemical sorption. However, different degree of shift in $\text{pH}_{(\text{i.e.p.})}$ could be observed, the dispersant with the larger shift being PC75 – shift to about pH 3.3 followed by the CE64 and Darvan 7 – shift to pH 4. Darvan C has provided the lowest shift in $\text{pH}_{(\text{i.e.p.})}$ – shift to pH 4.8. The observed deviation in the $\text{pH}_{(\text{i.e.p.})}$ shifts, most likely should be attributed to differences in the intrinsic chemical structure of the dispersants. The establishment of an anionic specific adsorption determines a shift of the $\text{pH}_{\text{i.e.p.}}$ towards acidic range, which for the case of CE64 could be due to the fact that the ammonia groups generated during dispersant dissociation in water consume the hydroxide ions during titrant (HCl) dissolution. In the case of Darvan C a similar pattern could be supposed, however it has been found that this electrosteric dispersant is strongly pH dependant. By AFM studies it was proved that at different pH, it stabilizes the system in various manner and only around neutral pH is physically adsorbed leading to sterical stabilization and good viscosity – result of combination of electrical double layer and steric interactions [57]. The large difference between the effective $\text{pH}_{\text{i.e.p.}}$ and suspension pH (i.e. the shift in $\text{pH}_{\text{i.e.p.}}$) for all the dispersants is an indication of existence of a strong chemical sorption and electrosteric stabilization effect [17, 90].

B.2.3.2.2 CR6 and AKP53

Since the Dolapix CE64 has provided virtually no shift in the pH for treated and non-treated (natural) suspensions (Table B.2.3) and during preliminary tests has maintained a maximum solids loading of the CT3000SG powder in comparison to the rest three dispersants, only this dispersant was selected for further investigation with the CR6 and AKP53 powders. A similar mode of volumetric titration in case of the CR6 and AKP53 powders has been followed for evaluation of dispersant performance, the results being graphically plotted at Figure B.2.9 and the estimated optimal dispersant dose and suspension pH shown in Table B.2.4.

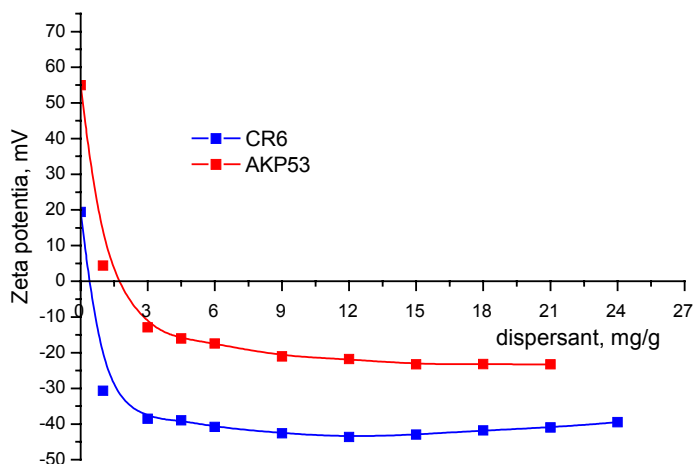


Figure B-2.9 Effect of CE64 concentration on the zeta potential of CR6 and AKP53 water suspensions

Powder	CR6	AKP53
Opt. dose, mg/g	6	9
<i>pH at opt. dose</i>	8.8	8.6

Table B-2.4 Optimal dose of Dolapix CE64 and suspension pH at optimal dispersant dose

The optimal dose of 6 mg/g for the CR6 powder has been additionally reconfirmed by CST and sedimentation experiments (please see article 7 in the attached publication list). In the course of several repetitive measurements, it was difficult to estimate an exact inflection point for the AKP53, however at 9 mg/g a slight curve flattening was always noted. The higher dose required for AKP53 is both due to the existence of natural charge for this powder and to its higher surface area. Similar to the experiments done with the CT3000SG powder, for evaluation the shift in $\text{pH}_{(\text{i.e.p.})}$ resulting from dispersant addition, potentiometric titration tests have been performed. For the CR6 powder this has been done only at its optimal dose of 6 mg/g, while for the AKP53 a two “neighbouring” dose levels were tested, i.e. at 6 and 12 mg/g. The results shown at Figure B.2.10 indicate that for the both powders there is a significant shift in $\text{pH}_{(\text{i.e.p.})}$ due to addition of CE64 at optimal dose. The nearly overlapping potentiometric curves for the AKP53 at 9 and 12 mg/g could

be an indication that at dose level above 9 mg/g, an added suspension stabilization could not be expected.

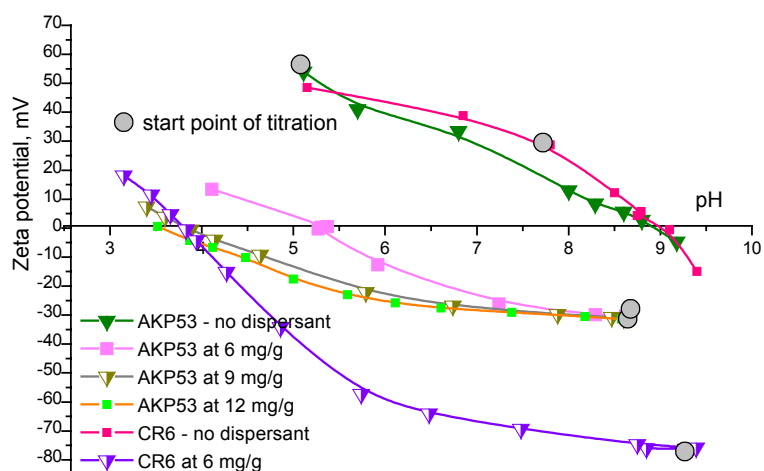


Figure B-2.10 Zeta potential of CR6 and AKP53 suspensions as function of pH, without and with addition of CE64 dispersant

B.2.3.3 Hypothetical interaction patterns between the dispersants and the tested alfa aluminas

When comparing the behaviour of the tested alfa alumina powders, it should be indicated that the natural pH for the AKP53 suspension lies in acidic range - pH 4.9, in contrast to the other alfa aluminas tested (CR6 and CT3000SG) having their natural pH in alkaline region. This fact could be due to surface modifications undertaken during powder manufacturing. From the three powders only AKP53 has shown a natural stabilization having absolute zeta potential above 30 mV. This stabilization is entirely of electrostatic origin, since during the volumetric titration it has been observed that only trace amount of added dispersant leading to incomplete adsorption (ca 1 mg/g) is masking this natural charge and is inducing flocculation, the AKP53 powder settling out of suspension. The CT3000SG powder from other side is naturally non-stabilized, since the charge at natural pH is near zero and as such it sediments immediately, which could explain its bi-modal size distribution - Figure B.2.5 (a). The CT3000SG powder belongs to a class of super ground powders, which for most practical applications are not calcined, rather organic additives are added [26].

It is known that dispersant adsorption is determined by a competitive affinity between adsorption on the surface and the solvent and the adsorption is strongly preferential when

the powder surface and the dispersant possess opposite charges. When the powder suspensions are treated with the tested anionic dispersants their surface charge is rendered negative and surface charging increase. However the absolute values of the zeta potential achieved with the different dispersants could not be necessarily viewed as an indication of good dispersion and improved slurry stability at high solids loading. [109]. Because each particle may have an interaction size of effective volume diameter that is approximately its real diameter (hard size) plus twice the range of interparticle forces, the larger effective volume diameter pertinent to a particle with higher zeta value may cause a high suspension viscosity. Therefore the intrinsic chemical structure of the dispersant should be considered with attention towards the level of electrostatic and steric component, which it brings in suspension stabilization. Generally steric stabilization requires adsorption of a reasonable dense polymer layer at each particle. The ideal case will be when for each powder and liquid vehicle, a unique functional dispersant with specific molecular architecture (anchoring group and hydrocarbon chain) providing maximum solids loading and low viscosity in slurry is identified and applied.

Theoretical studies about adsorption of polyelectrolytes [17] have postulated that the pH and respectively the degree of acid groups dissociation influences the amount of dispersant adsorption on the surface of ceramic particles. For anionic dispersants, the adsorbed amount increases with decrease in pH and in decrease in dissociation degree. At such condition the dispersant chains are uncharged and formation of compact coils is enhanced, thus the projected surface area per adsorbed chain is relatively small and more chains are required to build a saturated monolayer. On the other hand, at pH values higher or more alkaline than the I.E.P., polyelectrolytes with carboxylic acid groups are characterized by relatively large and open/expanded coils in solution. This is due to the electrostatic inter-segment repulsion between the negatively charged surface sites. In this situation they adsorbed in relatively flat conformation, with each chain covering more surface area. Therefore, regardless that we have not performed adsorption studies in this work, it could be presumed that for pH values near and more acidic than the IEP, the adsorption behaviour of the Dolapix CE64 is of the “high affinity type” [17]. The implications discussed above could be illustrated as shown at Figure B.2.11.

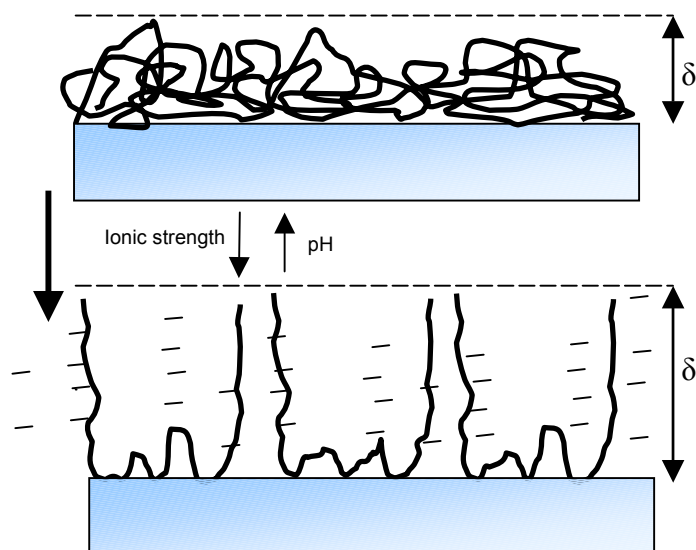


Figure B-2.11 Schematic illustration of configuration of adsorbed anionic polyelectrolyte species on alumina particle surface as a function of pH and ionic strength, δ - is the adlayer thickness (*adapted after* [69])

For all the studied powders the adsorption of the anionic dispersants most likely takes place by hydrogen bonding between surface OH^- sites and the carboxyl groups, which can act as proton donors or acceptors. An illustration of a hypothetical powder-dispersant interaction model for the case of CE64 is shown at Figure B.2.12. Since for all the powders, the adsorption of dispersant at its optimal dose is leading to alkaline pH where the dispersant is fully ionized, the steric interaction length determined by the adlayer thickness δ is increased. In a study concerning dispersant comparison it has been found that for dispersants with molecular weights similar to that of CE64, possess electrosteric characters and true steric stabilization of suspensions is reached only by dispersants with long chain providing separation distance of greater than 10 nm [124]. In contrast, at acidic or close to neutral pH regions, where the powder is positively charged and the polyelectrolyte non-fully ionized (i.e. partly negative) a favourable electrostatic interaction (i.e. physical sorption) is assumed and much more polyelectrolyte will be adsorbed onto the surface before the saturation limit is reached, leading to short length steric stabilization. In this case an added electrical double layer stabilization on adsorption could be presumed [17].

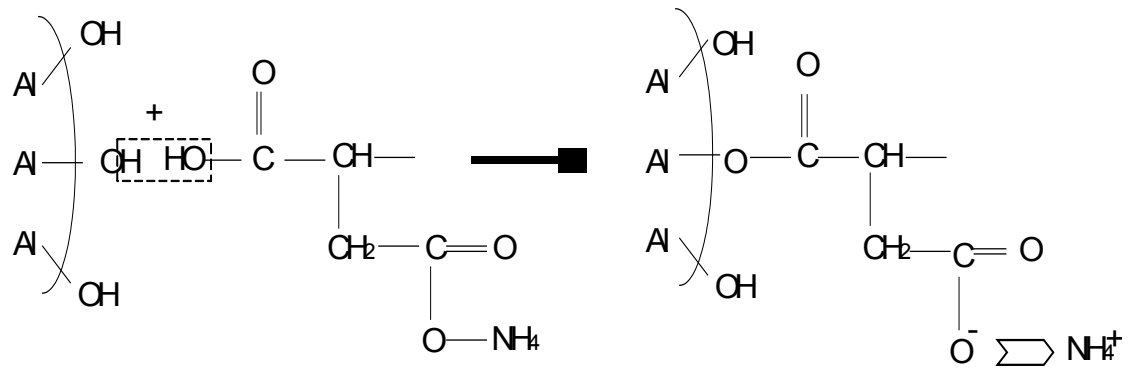


Figure B-2.12 Model of interaction of Dolapix CE64 with alumina surface

In summing, based on the performed volumetric titration, CST tests and according to the shift in the $\text{pH}_{\text{i.e.p.}}$, the Dolapix CE64 which is characterized by a relatively low MW in comparison to the rest dispersants, could be viewed as the one with the most favourable effect upon the stability of diluted water suspensions of the three alfa alumina powders tested. It should be proved whether this dispersant will likewise maintain stable and low viscous slurries at the much higher solids loading during the gel-casting process.

B3 Development of dense and porous ceramic bodies by gel-casting**B.3.1 Gel-casting slurry formation and methods for bodies evaluation**

Based on the findings discussed in Part B.2, slurries for gel-casting were prepared with the CT3000SG alumina using Dolapix CE64 for stabilization. A combination methacrylamide (MAM) : methylenebisacrylamide (MBAM) (monomer/cross linker) in ratio 6:1 was used as binder and an ammoniumpersulphate (APS) and tetramethyl-ethylenediamine (TEMED) as initiator and catalysts respectively. Their base dose levels and concentration were adapted from literature [34, 51]. For additional improvement of the dense structure and air elimination, an antifoam agent (Contraspum K1012, Zschimmer & Schwarz) has been occasionally used. The gel-casting tests for the dense and porous ceramics were carried out under the flow sheet presented at Figure B.3.1. The alumina powder was first added at 50 % mass into distilled and deionised water containing required concentration of gelling reagent and dispersant, followed by homogenization inside a planetary mill with ZrO₂ containers and balls. When porous ceramic was aimed, the pore developers have been introduced inside the slurry after the ceramic powder. The most critical aspects observed were the addition of the last batch of powder and keeping an optimal agitation speed. Air evacuation has been done for 1 min in exicator at vacuum of 900 mPa.

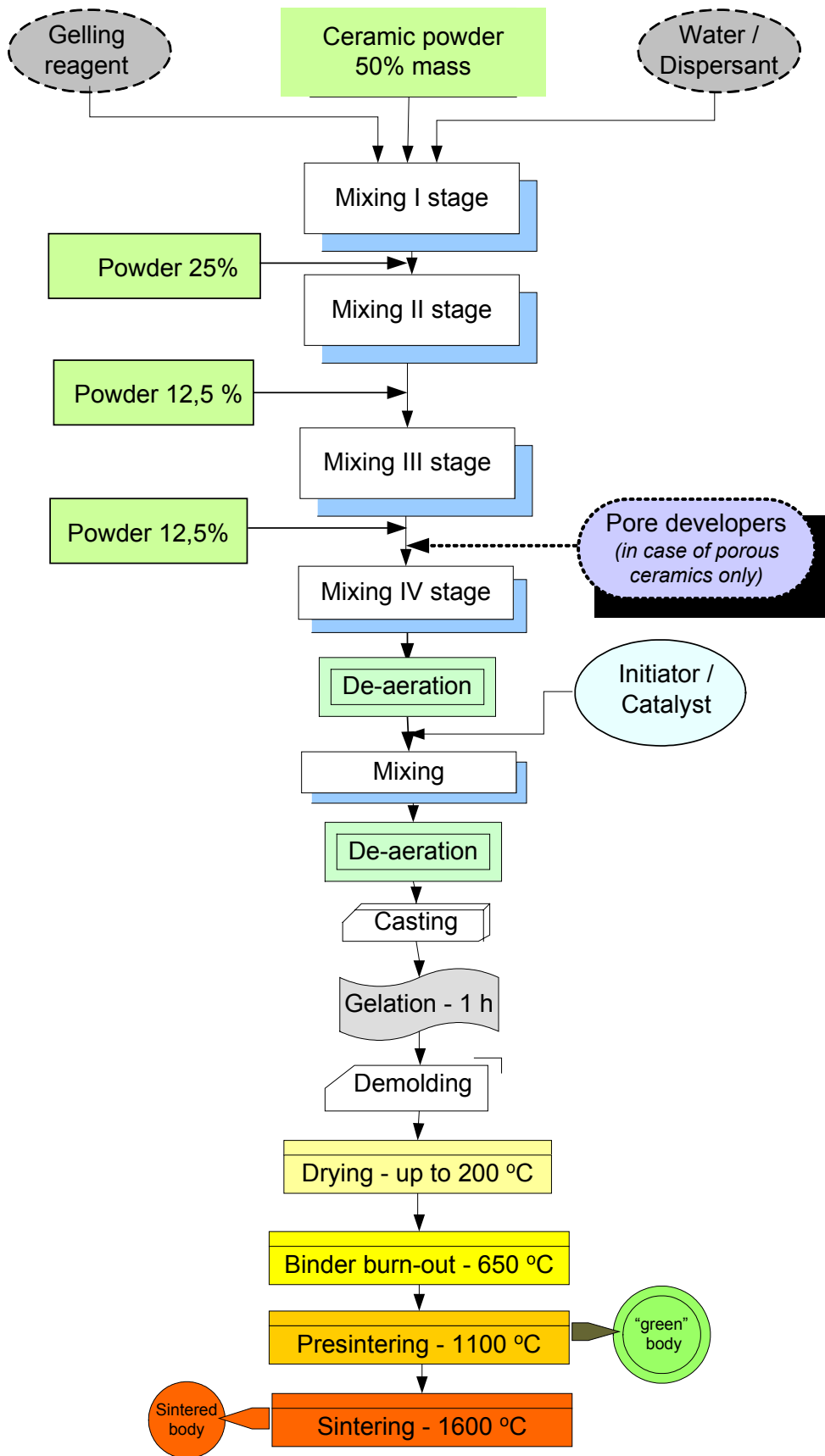
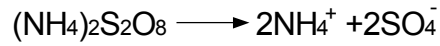
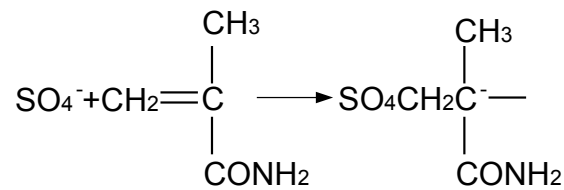


Figure B-3.1 Flow sheet used for development of ceramic bodies by gel-casting

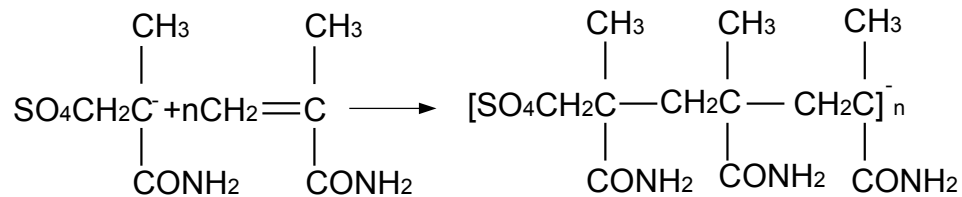
For the optimal design of the ceramic slurry, a sound knowledge about the reaction steps involved in slurry gelling is a prerequisite. The chemistry of free radical polymerization could be illustrated in the following step-sequences. Upon dissociation of ammonium persulphate (APS) according to the reaction:



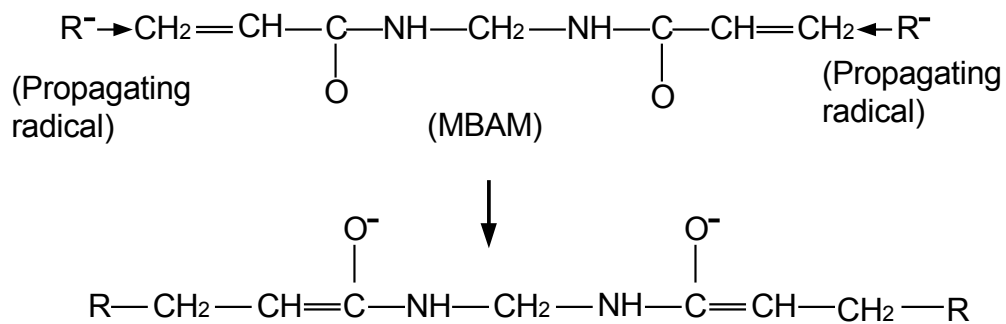
its initiating radical reacts with the monomer (MAM) similar to:



which from its side reacts the other monomer to form propagating radical (R^\cdot):



Finally, upon heating, the propagating radicals react with the cross linker (MBAM) to yield more stable polymer structure (chemical gel), in the following way:



After slurry casting and after elapsing of the indispensable time for slurry gelation, the developed wet bodies possess sufficient strength to be carefully removed from the moulds. After de-moulding, they have been subjected to thermo treatment encompassing the following stages: step wise drying (3 ramps) for 3 hours up to 200 °C in high humidity

ambient at heating rate of approx. 1 °C/min. This was followed by a step-wise (4 ramps) binder burnout and pre-sintering (up to 1100 °C) sequence as shown in Figure B.3.2.

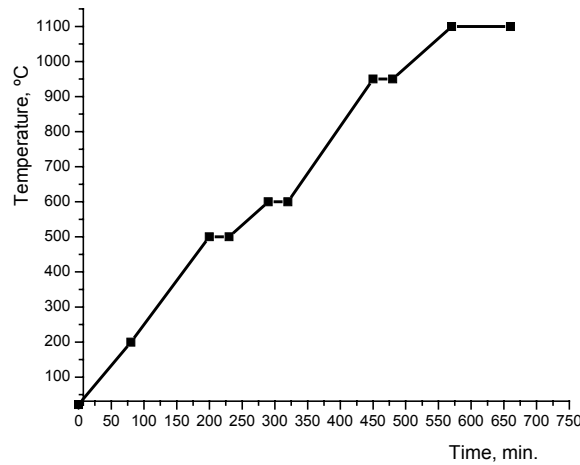


Figure B-3.2 Heating program of the high temperature oven used for binder burnout and pre-sintering

Because of their good machining ability, the “pre-sintered” bodies will be referred in our work upon convention as “green” bodies. The final sintering was done in high temperature oven, under air/nitrogen atmosphere for 30 min at 1600 °C with 10 K/min heating speed. Additionally, purposely casted small cylindrical test-bodies with $D = 0.6$ cm and $L = 2$ cm have been sintered inside a dilatometer system “NETZSCH 402” up to 1650 °C at a heating rate of 10 K/min. The screening of various mould materials and mould release agents had led to the conclusion that alumina moulds treated with XTEND 19MDR sealer and XTEND WS86 mould release agent (both manufactured by Axel Plastics Labs, USA) was the best choice for defect free de-moulding of green bodies having complex shapes.

For mechanical testing of the green bodies, 3-point bending strength measurements were performed under EU Norm EN 658-3:2002, using lamella-shaped specimens with the required size. Green density was calculated on geometric basis. For the porous bodies the density has been re-verified by Archimedes water displacement method.

B.3.2 Development of dense ceramics by gel-casting: parametric optimization

For the development of functional high-end dense ceramics by gel casting, parallel to the complex shape, a high strength and defect free green bodies should be an objective. Any density gradients inherent in the green bodies will lead to non-uniform sintering and will

not be eliminated. For a good gel-casting system to function, the gel-reagent (i.e. the binder) should not chemically react with the dispersant. Therefore of special importance was to carry out preliminary gel-casting tests for screening the three dispersants (Dolapix CE64, Darvan C and Dolapix PC75) at their optimal doses and at constant solids loading of CT3000SG powder of 50 % and gel reagent concentration of 5% on dry powder weight basis. The developed dense ceramic bodies were evaluated in terms of density, weight loss and shrinkage during “pre-sintering” and final firing, as well as visual inspection of slurry fluidity during powder mixing was done. The aim of these preliminary tests was to establish the role which dispersant type plays upon the characteristics of the slurry and its influence upon the properties of the bodies. The most important findings summarizing the properties of the bodies developed during the comparative tests are summarized in Table B.3.1. As a whole, it has been found that the largest part of the further weight loss of bodies (after their initial drying up to 200 °C) occurs during the pre-sintering (i.e. up to 1100 °C) stage. It is estimated that around 650 °C the polymer is 100 % ignited, hence within this temperature interval complete binder burnout should take place. At this temperature interval all the parts shrink parallel to weight loss, but at different rate determined by the dispersant type. It is accepted view that the weight loss during drying and de-binding is function primarily of water evaporation and gel burning, but our experiments indicate that the type of dispersant has also influence. From others side, the dimensional shrinkage during the pre-sintering has been found around 1 % with the largest part of it taking place during the final sintering (1100 – 1600 °C), where the full densification occurs. The weight losses during the full sintering were between 0.3 and 0.9 % (data not shown in Table B.3.1). The “pre-sintered” or “green” densities of the bodies have varied between 2.15 and 2.35 g/cm³, representing packing densities in the range of 55 to 58 %. The value of 2.26 g/cm³ given by the producer as green density of the powder lies between the calculated “pre-sintered” densities. It has been observed that during final sintering, the shrinkage for the large sized bodies was not homogenous and has occurred in anisotropic direction. This effect could be due to existing gradients during the densification in green state or to thermal gradients pertinent to their geometry or to differences in bodies positioning inside the sintering oven. Therefore it was difficult to calculate the fired density with sufficient precision and hence the values reported for “fired” density in Table B.3.1 should be used only for comparative purposes.

Dispersant/ Dose, mg/g	Temperature range: 200 – 1100 °C		“Pre-sintered” density, g/cm ³	Fired density (approx), g/cm ³
	Shrinkage, %	Weight loss, %		
DC / 9	1.3	4	2.3	2.87
PC75 / 6	0.84	5.13	2.15	2.7
CE64 / 6.5	1.1	3.37	2.35	3.07

Table B-3.1 Key data about dense ceramic bodies done from slurries with 50 % V solids loading stabilized with the three dispersants under study

The results from the dispersant comparative studies have suggested the CE64 supplied at its optimal dose of 6.5 mg/g as the optimal choice in terms ensuring slurry with the highest solids loading and the lowest viscosity. Therefore only this dispersant was considered and tested in more details further. The hypothetical mechanisms of adsorption and stabilization patterns pertinent to this dispersant were already discussed in Part B.2 and its better stabilization effect was attributed to the relatively moderate pH at optimal dose and the lower compared to the other dispersants “interaction” size of stabilized primary particles. At other process parameters (solids loading, mixing speed) being kept constant, these conditions are leading to development of slips with favourable viscosity at high solids loading.

It was important to study in more details, the degree of influence of the gelling reagent concentration (GR), solids loading (SL) and addition of antifoam agent (AF) and their possible interrelated effects on the bending strength and density of the green bodies. For this aim a full-factorial experimental design has been performed. Due to the preliminary character of the study no attempt was made for caring optimization of the variables, rather the aim was to outline the degree of their influence on the targeted parameter. For the three factors under study, the total number of experiments required to cover the investigated range was 11 (among them three at zero level). An Excel based software - “*Essential Regression*”, has been used for statistical analysis of the experimental data based on the least square method [2]. For outlining the main effects of the studied factors upon the dependent parameters, a multiple first order regression model with linear-linear

interaction effects was chosen. The test of model significance was performed by means of analysis of variance (ANOVA) and the significance of the individual regression coefficients, by F-test. The independent variables and their base levels and variation step are given in Table B.3.2 and the measured dependent parameters – in Table B.3.3. The presented green densities for each series are mean data from five cubic and five cylindrical (DLA) bodies. The 3-point bending strength is a mean value from 3 measurements.

Factor	Variable	Base level	Step	Units
X1	Solids loading	51	3	%, (V/V)
X2	Gel reagent	4.8	0.2	%, (dry powder mass)
X3	Antifoaming agent	0.05	0.015	%, (dry powder mass)

Table B-3.2 Investigated input variables and their base and variation level

Test N	Independent factors, X			Dependent parameters, Y	
	X1	X2	X3	Gr. density, g/cm ³	Bend. strength, MPa
1	54	5	0.075	2.28	22.11
2	48	5	0.075	2.55	21.14
3	54	4.6	0.075	2.29	38.29
4	48	4.6	0.075	2.14	25.3
5	54	5	0.025	2.26	24.08
6	48	5	0.025	2.15	20.45
7	54	4.6	0.025	2.31	32.12
8	48	4.6	0.025	2.26	13.6
8	51	4.8	0.05	2.25	21.37

10	51	4.8	0.05	2.17	19.34
11	51	4.8	0.05	2.16	22.13

Table B-3.3 Experimental results from factorial design

The regression model for the density of the green bodies has been calculated as:

$$Y = -13.60 + 0.362 X_1 + 3.267 X_2 - 66.52 X_3 - 0.075 X_1 X_2 + 14.15 X_2 X_3$$

The interaction term $X_1 X_3$ was eliminated because of low significance. The regression coefficient of the model is quite low 0.549. The signs before the coefficients indicate, that the green density is positively influenced by the solids loading and gelling reagent concentration and negatively influenced by the addition of antifoam agent. The analysis of variances (ANOVA) indicates that the model is significant only at 59 % error probability.

The regression model for the 3-point bending strength has been found respectively as:

$$Y = -1481.1 + 28.43 X_1 + 296.6 X_2 + 2383.3 X_3 - 5.61 X_1 X_2 - 479.25 X_2 X_3$$

The interaction $X_1 X_3$ was again deleted because of low significance level (high “t” value). According to the model, all the studied parameters have a positive influence upon the strength of the bodies, the factor with the strongest impact being the addition of antifoam agent and the factor of second significance being the concentration of gelling reagent. The model has correlation coefficient of $R^2 = 0.901$ and at critical significance level of 0.1 has low F_{sign} of 0.01, which means 99 % error probability.

A correct discussion of the parametric influences as suggested by the regression models is possible when the following conditional constraints are fulfilled:

- ✓ the binder does not react with the dispersant molecules;
- ✓ the binder activity is directed towards the liquid (water) phase only;
- ✓ during evaporation, moisture movement inside the bodies is uniformly restricted in vertical direction.

When comparing the both models, it is obvious that the regression model for the bending strength is characterized by much higher degree of correlation than the one for the green density. The later observation has its explanation in the fact that the green density of the bodies is basically function of water evaporation and compaction taking place during the

de-binding process, hence the less influence of the “chemical” component of the system (gel-reagent and antifoam agent concentration) upon the green density seems logical. It could be assumed that provided an optimal mixing leading to uniform distribution of alumina particles in the slip is guaranteed, the inter-particle voids of the “green” bodies will be also randomly distributed. After treatment of up to 1100 °C, they will contain only air, since the gel polymer is burnt out. This assumption is based on the drying sequences supposed to take place inside a gel casted body, schematically represented at Figure B.3.3. Here according to the level of water and organics release from the bodies, stages of wet (a), partially dried (b) and fully dried (c) gel-cast bodies could be distinguished. The progression of “free water” transportation by capillary forces towards the surface with time indicated as $l(t)$, could be seen during the stage of partial drying (b). During moisture release with time, the gel that coats the individual particle begins to shrink. During this shrinkage towards the particle surfaces, the gel matrix ruptures, which results in interconnected “voids”, which might be empty spaces but are more likely to contain “strands” of polymer gel. During the binder burnout stage, the dried gel rests are ultimately removed from the body.

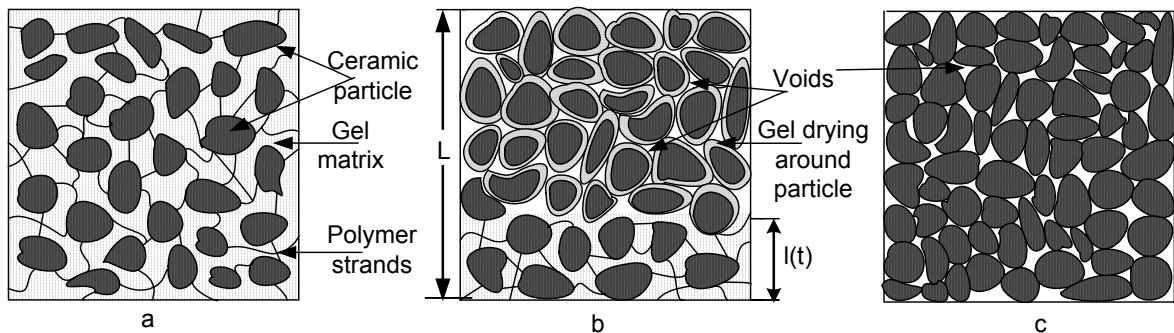


Figure B-3.3 Magnified cross section of gel cast body and associated drying and compaction phenomena taking place during drying, binder burn-out and pre-sintering (modified after [34])

From other side, the effect of pores elimination (function of the antifoaming agent) and gel-reagent concentration is more pronounced for the bending strength, hence the stronger correlation between the studied independent factors on the bending strength. The measured and predicted according to the model values for the green density and the 3-point bending strength are presented in Table B.3.4.

Dens.	Meas.	2.28	2.55	2.29	2.14	2.26	2.147	2.31	2.26	2.25	2.17	2.16
	g/cm ³ Prod.	2.35	2.43	2.24	2.13	2.14	2.22	2.312	2.21	2.25	2.25	2.26
B. S.	Meas.	22.1	21.14	38.29	25.3	24.08	20.45	32.12	13.59	21.37	19.34	22.13
	MPa Prod.	21.76	19.47	38.67	22.91	22.41	20.11	29.73	13.97	23.63	23.63	23.63

Table B-3.4 Density and 3-point bending strength of green bodies - measured and model predicted

The 11 pre-sintered cylindrical test bodies coming from the experimental planning were subjected to full sintering during dilatometric investigations, the results of which are presented at Figure B.3.4. For comparative purposes, the “green” (up to 1100 °C) shrinkage (a mean value from 5 cylinders) is also indicated in the Table inside.

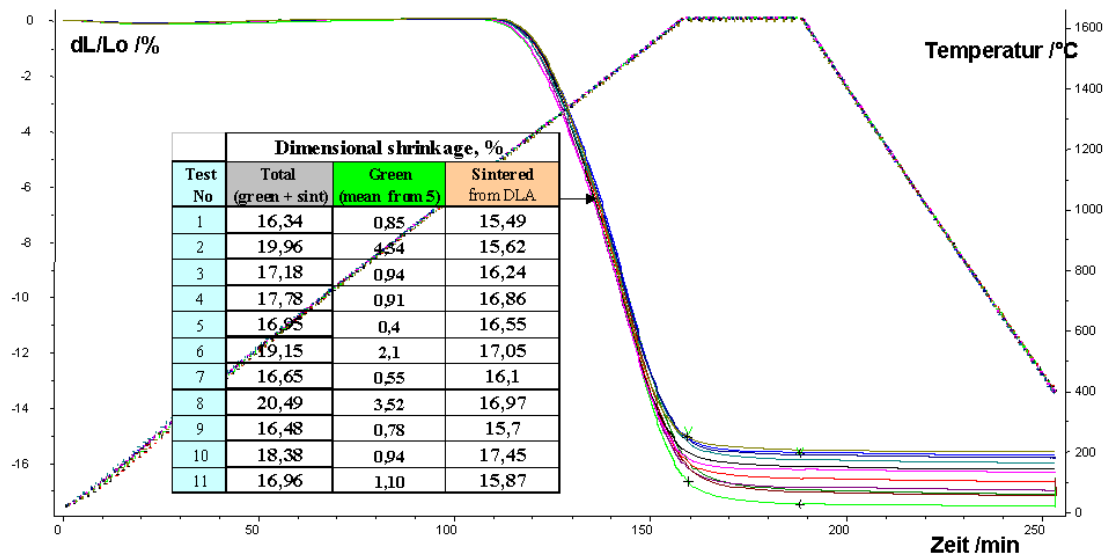


Figure B-3.4 Dimensional shrinkage from 11 statistically planned experiments: “green” (200 – 1100 °C), “sintered” (1100 – 1600 °C) and total shrinkage

The analysis of the DLA curves indicates that during the final firing, the shrinkage starts from around 1200 °C and lasts until 1600 °C. Further, it is to be noted that the investigated

variables do not show quite significant impact upon the dimensional shrinkage within this temperature range. A relationship between the “green” and the “fired” shrinkage is to be noted, which indicates that the densification process proceeds uniformly. It could be said that the total (green + fired) dimensional shrinkage lies in the range of 16.3 to 20.5 %, out of which more than 90 % is the “fired” shrinkage. In other words, the pre-sintering is leading mainly to drying and binder burnout, while the final pore elimination and densification occurs after 1100 °C during the final firing. Regardless that the drying and binder burn out stages contribute to less than 10 % of the total shrinkage, the proper conducting of the drying stage is a key for producing defect free bodies. The physical mechanism of drying can be classified into three stages in gel-casting and each of them should be well understood [34].

Choosing an optimal sintering regime is also an important factor in providing uniform densification leading to pore free and defect free ceramic parts. Therefore for further outlining the effect of heating rate on the sintering behaviour, a kinetic study was performed at three different rates – 1, 3 and 10 K/min and the results shown in Figure B.3.5. For these tests, the gel-casting slurries were prepared at solids loading of 51%, gel reagent of 4.8 % and without addition of foaming agent. The cylindrical bodies subjected to the DLA tests were characterized by nearly identical “green” shrinkage.

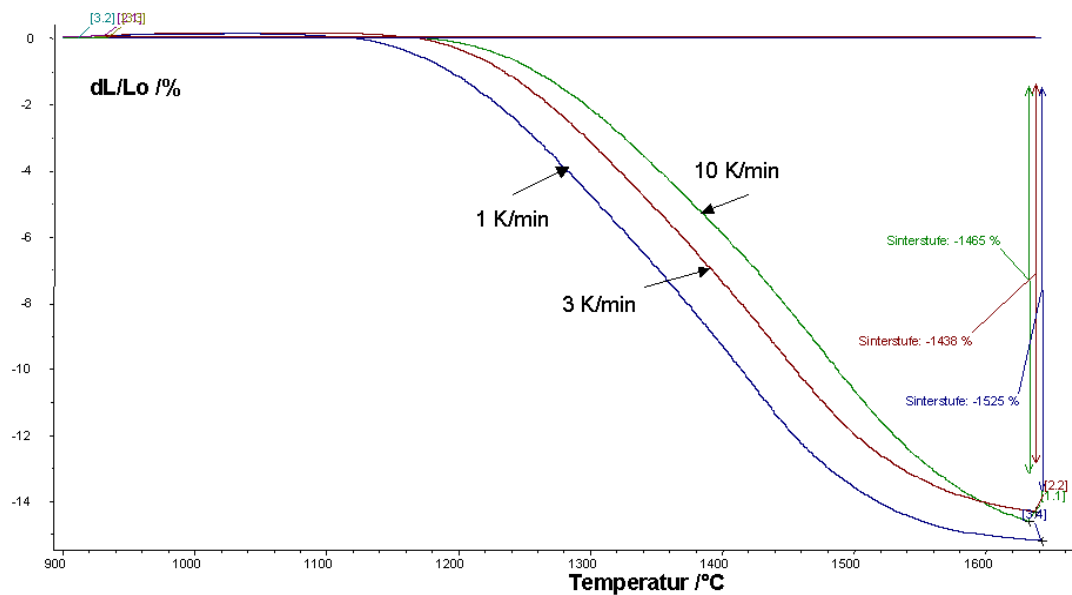


Figure B-3.5 DLA results of dimensional shrinkage at various heating rates (slurry characteristics: solids loading - 51 %, gel reagent 4.8 %, Dolapix CE64 - 6.5 mg/g)

The results shown at Figure B.3.5 are suggesting that both heating rates of 3 K/min and 10 K/min have provided virtually identical dimensional shrinkage of ca. 14.5 %. The heating rate of 1 K/min has led to the highest shrinkage - 15.25 %. Since the material transformation and the chemical reactions between the solid phases during the sintering process are accompanied by quite complex phenomena, a plausible conclusion is difficult to be presented from these preliminary results, rather further kinetic analysis should be considered.

B.3.2.1 Conclusions

The performed tests for development of dense ceramics by gel-casting have re-confirmed the fact that it is possible to achieve high solids loading of 54 % V in low viscosity ceramic slip containing ultra fine alfa alumina CT3000SG. The slip is permanently immobilized in the desired mould shape by polymerization of the polymer-water gel. In such a way complex shaped bodies are possible to be delivered, the photos of some of them being shown in the Annex.

The ultimate requirement for perfect ceramic phase homogenization in ceramic slurry is function both of the chemical environment and the type of mixing. For ensuring optimal physico chemical conditions leading to stable slurry at the high solids loading required, the choice of dispersant is a key issue. The relatively lower values of total shrinkage achieved within the tests performed however is not an indication and guarantee for complete pore elimination leading to the required high relative density, possibly > 99 %. Possibilities for further density increase definitely lie in the optimization of air evacuation cycle, as well as in the sintering stage (heating rate, sintering duration). For the green bodies characteristics a useful compromise between their relative density, shrinkage and bending strength should be agreed.

B.3.3 Possibilities for development of porous ceramics by use of fugitive pore developers

B.3.3.1 Characteristics of the fibres tested as pore developers

The chosen by us concept for manufacturing ceramic bodies with defined pore structures lies in the addition of fugitive fillers as pore developers inside a ceramic slip which subsequently is consolidated by usual gel-casting. Due to the intrinsic features of some natural fibres this approach has potential if a development of a pre-determined pore structure is an objective. It uses some of the features of the replica technique however instead of polymeric sponge, natural fillers are used. As was shortly commented in the literature review part, the approach of using burnable pore developers is not new, but the application of fibres as “pore developing” phase has not been studied. The most important advantages expected when natural fibres are used could be summarized as:

- ✓ fibres with required dimensions could be attainable by relatively simple mechanical processing;
- ✓ owing to their intrinsic shape and dimensions (high aspect ratio, i.e. length : thickness), it is possible to develop open porosity consisting from a channel or capillary like pore structures inside the ceramic bodies;
- ✓ their physical structure remains intact during mixing with the ceramic phase inside the slurry, thus porosity is controllable by using slurries with different concentrations of fibres;
- ✓ upon thermal decomposition, they virtually do not produce solid residues;
- ✓ they are amenable to surface modification (chemical or physical), which upon requirement could improve their mixing behaviour.

For improving the chances of application of natural fibres as pore developers in gel-casting of porous ceramics, the following challenges should be met:

- ✓ possibly narrow size distribution;
- ✓ reduced water uptake;
- ✓ restricted and predictable swelling;
- ✓ no “side” reactions with the liquid phase (dispersant and gelling reagent), leading to green bodies defects or to increased suspension viscosity and decrease in solids loading;

- ✓ fibres should maintain their physical structure until consolidation of suspension (i.e. transition gel-solid).

Resolving some of these problems requires a sound knowledge about the interaction between all the phases involved in development of porous ceramics by using fugitive fillers. Charge characteristics and water uptake behaviour of the fibres should play a decisive role for these interactions. For the development of porous ceramics by gel-casting we have adapted the optimally found process parameters from the dense ceramics gel-casting (powder, dispersant, mixing time etc.). The amount of added fibres has been always taken into consideration during the mass and volume balance calculation. To burn out or carbonize the fibres gradually in order to prevent the green bodies from cracking, a slower heating rates in comparison to those used for the dense ceramics, shown at Figure B.3.2 have been adopted. Sintering was performed however at the same heating rate of 10 K/min. The developed pore structures inside the bodies have been evaluated in terms of area, length and thickness by examination representative slices from the bodies.

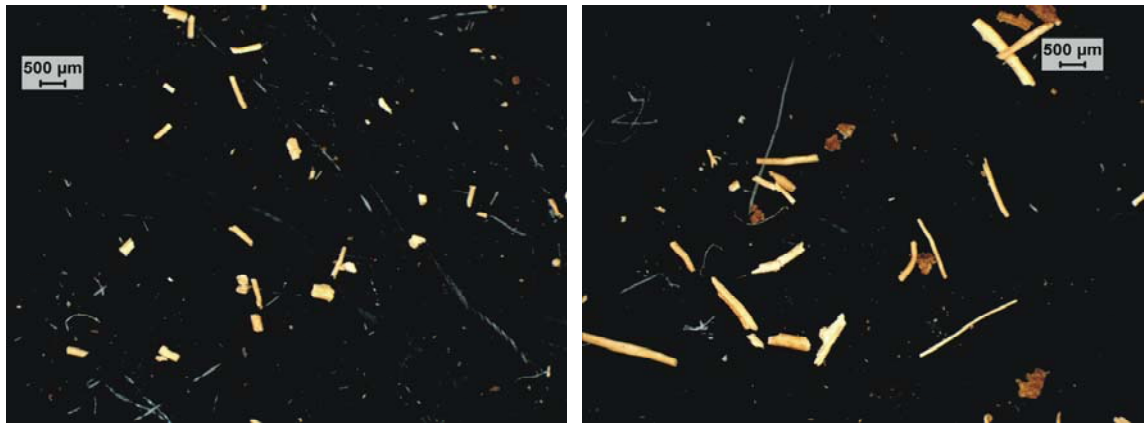
The following natural fibres have been envisaged as potential candidates for pore developing phase: flax, coco, bamboos, sisal and processed hemp. After appropriate size reduction by shredder, initial screening tests have been performed in direction of water uptake; density; swelling and zeta potential (based on electrophoresis). On comparative basis, the best behaviour in terms of water uptake (minimal) and surface charge (minimum negative), has been demonstrated by the coco fibres.

B.3.3.2 Measured and calculated effects of fibres addition on developed porosity

The experiments involved in this section have aimed to delineate any correlation between the dimensions of the added fibres and the resultant pores (size, shape, connectivity). The bodies were characterized also in terms of shrinkage during pre- and final sintering.

The analysis of fibres dimensions has revealed that they are characterised by a relatively constant thickness, with a mean value around 110 μm , their length however varying in the range from 70 to 1800 μm depending on the classification step undertaken after their size reduction in the shredder. Our studies have dealt with two classified size fractions from the fibres in terms of length, i.e. a “fine” class with mean length of ca 300 μm and a “coarse” one with mean length of 1200 μm .

A micrograph view of the both type fractionated coco fibres is presented at Picture B.3.2



Picture B-3.2 Image analysis view of dry coco fibres used as pore developers (left “fine”, right – “coarse” fractionated)

For evaluation the feasibility of the approach of using fibres as pore developers, gel-casting of ceramic slurries with constant solids loading of 32 % V on powder basis has been done. A predetermined amount from the “fine” fraction of the coco fibres was added inside the slurry in amounts up to 0.4 vol. fraction and the slurries were processed following the flow sheet shown at Figure B.3.1. The fibre-containing slips were casted in cubic shaped moulds and further treated in a way similar to that followed for the dense ceramic bodies. During casting, the influence on fibres amount upon the fluidity of the slip was of special importance. Specimens containing no porosity (dense bodies) were also developed for calculating the volume fraction of pores X_{st} in the “green” ceramic matrix according to:

$$X_{st} = \frac{V_F \cdot \rho_m}{1 - V_F + V_F \cdot \rho_m},$$

where: ρ_m is the relative packing density of the matrix studied and V_f is the volume of fibres added in the slurry [102]. In this work ρ_m was taken as 0.65 - which is the ratio between the density of a body without fibres and the fired density of alumina (3.92 g/cm^3). Image analysis was used for characterisation of the developed pores and for calculation of the surface porosity in cut and polished sections.

Developed porosity

During the casting of the ceramics slips it has been observed that fibres in amount up to 0.25 volume fraction readily disperse into the ceramic slurry, without increasing its viscosity. Figure B.3.6 shows the results coming from evaluation of the most important characteristics of the developed green porous bodies.

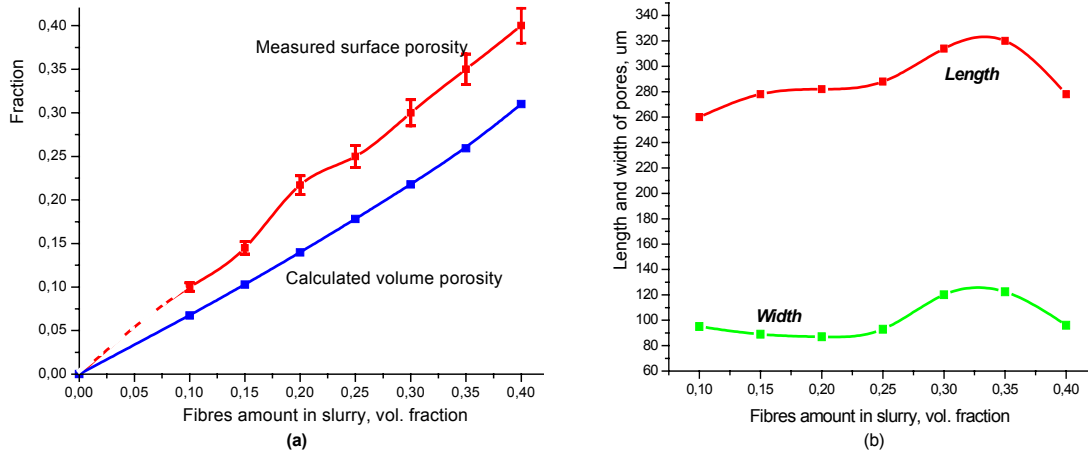


Figure B-3.6 Measured surface and calculated volume fraction porosity X_{st} (a) and thickness and length of pores (b) in thin sections from “green” bodies versus the amount of added “fine” fibres in slurry.

The measured by Image analysis surface porosity (the red line) is in quite good correlation with the added amount of fibres (i.e. the theoretical porosity) - Figure B.3.6-a. It is higher than the calculated volume one (the blue line), which is perhaps due to the two-dimensional image analysis method used for calculation the surface area. For selected bodies the calculated volume porosity – X_{st} , has been compared to the total porosity, as measured by the “Archimedes” water displacement method and a quite good data correspondence was observed.

The perusal of the results shown at Figure B.3.6-b, indicates that the length and width of introduced fibres does not correspond directly to the length and width of individual developed pores captured by the image. Although slightly, the length of pores has varied with the amount of fibres added into the slurry. With increase in amount of added fibres from 0.1 to 0.25 fraction volume, the length of the developed pores inside the green bodies is increasing – Figure B.3.6-b. Their thickness however does not rise significantly, meaning that the aspect ratio of pores increases and they acquire more elongated shape. The relatively steady increase in pore length up to 0.25 fraction could be explained by the fact that by increasing the fibres amount in slurry the possibilities for fibre particles touching each other increases, regardless the restrictions posed by the limited space available due to increasing total solids loading (fibres plus powder) [72]. At fibres fraction content of 0.30 and 0.35 however, the pore length increases sharply, suggesting that above a critical fraction of 0.25, connected channels are starting to appear, which finally results in open porosity. The drop in length of pores at 0.4 fraction of fibres could be attributed to the measurement mode chosen for pore length evaluation. The image analysis system was used in interactive “distance” measurement mode, which allows connected pores ordered as straight line to be considered only, and possibly the pores connectivity at 0.4 fraction was characterized by increasing amount of “curved” pore structure, which could not be detected in distance measuring mode.

Shrinkage during sintering

During the stages of binder burnout and pre-sintering (up 1100 °C), where the fibres are ignited as well, the shrinkage of the bodies has been found negligible, which agrees with published results about porous ceramics produced by addition of burnable pore developers [72]. The linear shrinkage of the bodies during sintering was found comparable to that for the dense ceramic bodies. This is in line with other studies indicating that the pores are too large to contribute to shrinkage [25, ref. 11]. The relationship between the dimensional shrinkage of bodies and length of pores and the amount of added fibres is shown at Figure B.3.7. The results are quite intriguing and the drop in linear shrinkage of the bodies at 0.3 fibres fraction (Figure B.3.7-a) could be linked to the emergence of connected porosity from this point on. This assumption corroborates with findings reported by other authors where appearance of connected porosity above 30 % starch inclusions in silicon nitride materials was observed [25].

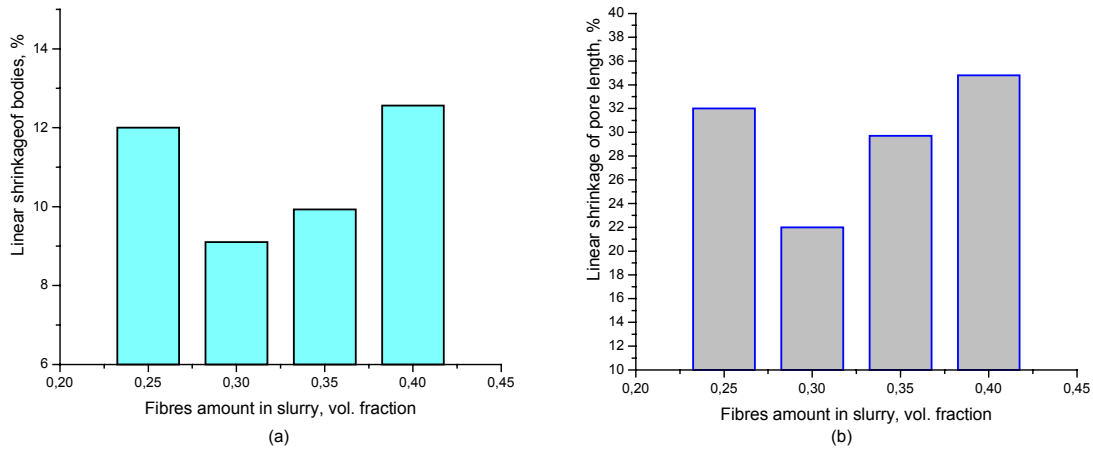


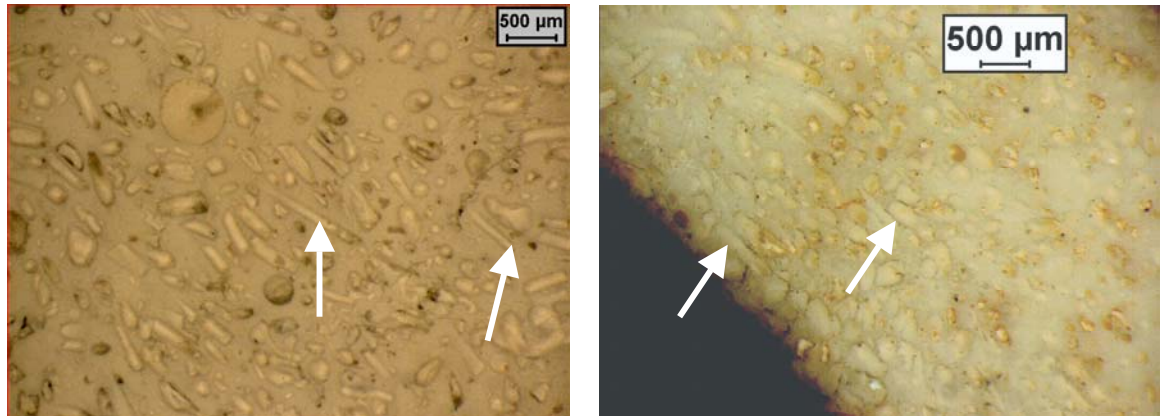
Figure B-3.7 Linear shrinkage for the bodies (a) and for the length of pores (b) during sintering (1100 – 1600 °C) as function of fibres amount in slurry

The closer examination of the results shown in Figure B.3.7 and of the image analysis pictures from the polished sections of green and sintered bodies indicates that the pores have shrank considerably when compared to the bodies structures. The decrease in length of pores in the sintered bodies in comparison to that in the green ones was found in the range from 22 to 35 % - Figure B.3.7-b. At the same time the shrinkage of the bodies varies from 9 to 13 % (Figure B.3.7-a), which makes a factor of nearly 3. The clarification of these phenomena lies perhaps in the quite complex densification mechanisms taking place. Especially when the inclusions intended for pores development are much larger in size than the initial grain of the matrix, the densification patterns for the both differs as suggested by Slamovich and Lange [102]. It should be however mentioned that in our case the thickness of the pores have not shrank considerably. It is also to be expected that during sintering, pores smaller than 1 μm were eliminated.

The minimum shrinkage for both the pores length and the dimension of bodies exactly at 0.3 volume fraction of fibres could be explained by the fact that an open porosity starts to develop at and above that point [25]. Here the effect of touching inclusions on the packing efficiency of the matrix should be considered.

The ceramic bodies were not deformed during sintering, which denotes that cracks seem to be arrested. However the emerging of pores having almost ideal round shape might be an indication that the process of slurry air evacuation has not lead to total elimination of the entrapped air, which has ultimately resulted in pore development. Two characteristic

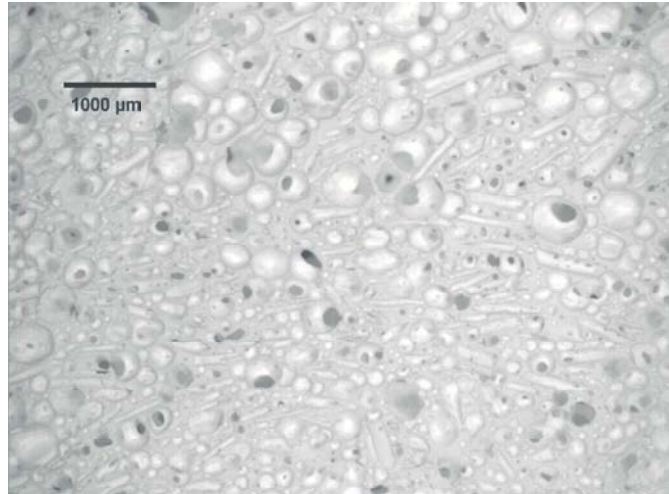
views taken during image analysis of green and sintered bodies made with 0.3 fibres fraction are indicated at Picture B.3.3.



Picture B-3.3 Image analysis view at different spots of polished sections belonging to green (left) and sintered (right) bodies developed with fibres at 0.3 fraction addition. The arrows indicate the “channel-like” pores left after fibres burnout.

B3.3.3 Increasing the connected porosity by addition of foaming agent

During the initial tests it has been observed that the viscosity of the slurries with fibres content above fraction of 0.3 is becoming relatively high which makes their casting difficult. Therefore for increasing the level of open porosity, an association of the foaming technique with fibres addition as pore developers has been pursued. The experimental findings have revealed that a “honeycomb-type” connected structure could be developed in such a way, leading to an open porosity of a more than 60 %. A characteristic view from a surface sectioning showing the pore structure inside a green body is presented at Picture B.3.4.



Picture B-3.4 Image analysis view of polished section from a green body produced by combination of fibres and foaming agent* (* - W53 Zschimmer-Schwarz, Lahnstein, Germany)

B.3.3.4 Conclusions

The main challenge in the successful application of natural fibres as pore developers lies in their dimensioning and compatibility with the slurry. During the feasibility testing of the approach, the tropical “coco” fibres have been found as the most suitable choice for pore developing phase, the developed pores resembling closely the shape of the introduced fibres. Once the pre requirement of proper fractionation (linked to the desired final porosity in the end bodies) is met, they could be used in natural state as pore developers. For overcoming the problem of higher viscosity (in volume fractions higher than 0.3) however, a **surface modification** of the fibres needs to be envisaged. Apart from providing better compatibility between the powder and the fibres, this will ease the release of air from the slurry and enable a predictable end bodies pore structure. By continuous increase of fibres addition in slurry, highly porous bodies could be developed specifically characterized by a capillary like pore structure resulting from the inherent shape of the fibres used. The niche of selective separation processes could strongly benefit from such a materials.

By combination between foaming agent and fibres, a kind of ceramics foams with induced cell connectivity could be produced. Such highly porous materials with like honeycomb structure could be used in variety of innovative applications. One application example of such ceramics could be as carriers for PCM (Phase Change Materials) where the volume of the infiltrated material varies based on ambient temperature. Another application might be the areas of particulate filtration and catalysis.

Summary and directions for further work

Handling of particulate materials in colloidal size range is an important challenge from the point of view of process engineering. An in-depth understanding of the mechanisms that govern particulate systems behaviour is required especially for achieving control over their stabilization/de-stabilisation through tailoring the particle-particle interactions. The presented work tries to give a modest contribution in answering some of the open methodological questions relative to characterization of the macro properties (like particle size and surface charge effects) of two different colloidal systems, and how these properties determine the desired behaviour of each system.

The first investigated case study has dealt with coagulation of textile dyes aiming at colour removal. Regardless that coagulation and flocculation have been studied to a larger extent worldwide and have taken with the associated research activities, in depth optimization and attempts for fundamental study of the insight chemical transformations accompanying the dye destabilization during coagulation have been done seldom. Thus the current understanding of this important area is still immature and ***break-through*** is not reached. The fact that dye removal differs significantly within a same dye class or hue groupings indicates that certain basic aspects like the influence of chemical class and chemical constitution of dyestuffs needs to be better understood as criteria for selection of specific treatment chemicals and optimum system parameters.

By means of the envisaged experimental approach it has been proved that the physico-chemical environment, type of dye and primary coagulant, pH of solution (data not presented), ***plays the most decisive role*** in promoting particular destabilization mechanism, given the shear conditions are kept constant. For the studied dyes it has been found that the predominant destabilization pattern is influenced by the intrinsic chemical structure of the dye. It was however impossible to outline any common destabilization pattern for dyes belonging to a same application class or hue. The analysis of the surface charge effects associated with dye destabilization could be however viewed as an indication about the predominant destabilization mechanism. When charge neutralization mechanism was suspected (the case of Reactive Black 5 and Acid Black 1), the point of zero charge has coincided with maximum colour removal and the developed flocs were characterized by larger size and denser structure. The Polydadmac type polyelectrolyte has led to a mosaic type non-complete charge neutralization of the Disperse Yellow 5 dye

leading to maximum colour removal. The floc structures however did not evolve considerably with varying the coagulant dose level.

The second studied case, i.e. the stabilization of aqueous suspensions of ultra fine alumina powders has been relevant to the emerging methods of colloidal processing of ceramics, which are finding increasing use in development of high-end materials needed in cutting-edge industrial niches. With the use of ultra fine or nano-sized particles, the interfacial phenomena become increasingly complex and dominating factor in determining the final properties of the intended ceramic products. A key understanding is needed therefore about the interaction between **all phases** involved in colloidal processing and about the way to control over structural evolution to eliminate unwanted heterogeneities in development of near-net-shape bodies. A first step in achieving this aim is to understand the mechanisms of interaction between the ceramic powder and the dispersants used. The correct choice of easily accessible and reliable methods for dispersant selection and dose optimization is an important milestone in delivering this objective. It has been established that the zeta potential derived from a CVI measurement could be viewed as a most reliable signal for optimizing the dispersant type and dose at an initially relative low solids loading. The degree of shift in the $\text{pH}_{(\text{i.e.p.})}$ of the powder suspensions could be considered as an indication for the pattern of interaction between the dispersant and the powder surface. The chosen optimal dose level of dispersant has been re-confirmed during gel casting at high solids loading. The streaming current measurements have occasionally suffered from fluctuations. The CST method when used for dispersant optimization has been found as strongly dependent on the mean particle size of the powder.

During the gel casting of one of the ultra fine alfa ceramic powders studied, keeping an optimal process conditions (stirring speed, air evacuation, temperature handling of the bodies, mould materials etc.) has shown to play ***an equally important role*** together with the chemical environment (dispersant dose, binder, initiator and catalyst concentrations) in providing the desired properties of the end ceramic bodies. For ceramic slips with high solids loading, it has been found out that the ultimate goal of achieving maximal high charging of the particles in the aqueous slurry does not necessary guarantee the best conditions for powder stabilization leading to the desired low viscosity. An electrosteric anionic dispersant of the Dolapix CE64 type characterized by strong adsorption at the powder surface via H-bonding has enabled to achieve solids loading of more than 54% V at a relatively low viscosities allowing casting of complex shaped bodies. The choice of

optimal binder burnout and pre-sintering regimes is crucial in providing a defect-free structure and acceptable low shrinkage of the bodies. Therefore an account on the relationship between viscoelastic properties, de-moulding (i.e. handling strength), drying behaviour and network strength of assemblies derived from the colloidal particulate gels should be taken. For full densification of the final bodies however, both the air evacuation step and the sintering regime should be further optimised.

The approach of using burnable pore developers on natural fibres basis has proved feasible in terms of development of pre-defined pore structure inside the ceramic bodies produced by gel-casting. Further attention however should be devoted especially in direction of fibres surface modification. The ultimate goal is to render fibres inert both towards the ceramic phase as well as towards the liquid vehicle in order to keep the slip viscosity low.

As a whole, it could be concluded that the characterization of surface charge related phenomena accompanying stabilization and de-stabilization processes in the tested systems has proved to be an important issue for interpretation the intrinsic mechanisms taking place. Thus the proper characterization adds to further in-depth understanding needed fro the desired manipulation of the fine particulate systems.

References

- [1] Ackler H., French R., Chianga Y., Comparisons of Hamaker constants for ceramic systems with intervening vacuum or water: From Force Laws and Physical Properties, *J. of Coll. and Interf. Sci.*, 179, 2, 1996, 460-469
- [2] Adler U., An introduction to experimental planning, Metallurgia, Moscow, 1969
- [3] Albano M., Garrido L., Processing of concentrated aqueous silicon nitride slips by slip casting, *J. Am. Ceram. Soc.*, 81, 4, 1998, 837-44
- [4] Albano M., Garrido L., Processing of Yttria-Allumina coated silicon nitride slips by slip casting, *J. of Mat. Synth. and Proc.*, 10, 4, 2002
- [5] Albano M., Garrido L., Garcia A., Surface modification and ammonium polyacrylate adsorption on Si₃N₄ powders, *Anais do 43 Congresso Brasileiro de Ceramica*
- [6] Anklekar R., Borkar S., Bhattacharjee S., Page C., Chatterjee A., Rheology of concentrated alumina suspension to improve the milling output in production of high purity alumina powder, *Colloids and Surfaces A: Physicochemical and Engineering Aspects* 133, 1998, 41-47
- [7] Araki K., Halloran J., Porous ceramic bodies with interconnected pore channels by a novel freeze casting technique, *J. Am. Ceram. Soc.*, 88, 5, 2005, 1108-1114
- [8] Babaluo A., Kokabi M., Manteghian M., Sarraf-Mamoory R., A modified model for alumina membranes formed by gel-casting followed by dip-coating, *J. Eur. Ceram. Soc.*, 24, 2004, 3779-3787
- [9] Balzer B., Hruschka M., Gauckler L., Coagulation kinetics and mechanical behavior of wet alumina green bodies produced via DCC, *J. of Coll. and Interf. Sci.*, 216, 1999, 379-386
- [10] Barthel H., Heinemann M., Stintz M., Wessely B., Particle sizes of fumed silica, *Chem. Eng. Technol.*, 21, 1998, 9
- [11] Batz-Sohn C., Zetapotential und pyrogene oxide, 6. Anwendertagung "Ladungscharakterisierung", Universität Potsdam, 21.03.2002
- [12] Batz-Sohn C., Particle sizes of fumed oxides: a new approach using PCS signals, *Part. Syst. Charact.* 20, 2003, 370-378
- [13] Bergström L., Colloidal processing of ceramics, in *Handbook of Applied Surface and Colloid Chemistry*, John-Wiley and Sons, 2001

- [14] Bhattacharjee S., Singh B., Besra L., Effect of additives on electrokinetic properties of colloidal alumina suspension, *J. of Coll. and Interf. Sci.*, 254, 2002, 95-100
- [15] Böckenhoff K, Fischer W., Determination of electrokinetic charge with a particle charge detector and its relationship to the total charge, *Fresenius J. Anal. Chem.*, 371, 2001, 670-674
- [16] Cai K., Huang Y., Yang J., Alumina gelcasting by using HEMA system, *J. Eur. Ceram. Soc.*, 25, 2005, 1089–1093
- [17] Cessarano J, Aksay I., Bleier A., Stability of α -Al₂O₃ suspensions with Poly(methacrylic acid) polyelectrolyte, *J. Am. Ceram. Soc.*, 71, 4, 1988, 250
- [18] Cesarano J., Aksay I., Processing of highly concentrated aqueous α -alumina suspensions stabilized with polyelectrolytes. *J. Am. Ceram. Soc.*, 71, 12, 1988, 1062
- [19] Chander S., Challenges in characterization of concentrated suspensions, *Colloids and surfaces A: Physicochemical and Engineering Aspects*, 133, 1998, 143-150
- [20] Colombo P., Ceramic foams: fabrication, properties and application, *Key Engineering Materials*, Vols. 206 – 213, 2002, 1913-1918
- [21] Dai J., Huang Y., Xie Z., Xu X., Yang J., Effect of acid cleaning and calcination on rheological properties of concentrated aqueous suspensions of silicon nitride powder, *J. Am. Ceram. Soc.*, 85, 2, 2002, 293–98
- [22] Dakskobler A., Kosmac T., Weakly flocculated aqueous alumina suspensions prepared by the addition of Mg(II) Ions, *J. Am. Ceram. Soc.*, 83, 3, 2000, 666–68
- [23] Degen A., Kosec M., Influence of pH and ionic impurities on the adsorption of poly(acrylic) dispersant onto a zinc oxide surface, *J. Am. Ceram. Soc.*, 86, 12, 2003, 2001–10
- [24] Deng S., Lin Y., Microwave synthesis of mesoporous and microporous alumina powders, *J. of Mat. Sci. Lett.*, 16, 1997, 1291–1294
- [25] Diaz A., Hampshire S., Characterisation of porous silicon nitride materials produced with starch, *J. Eur. Ceram. Soc.*, 24, 2004, 413–419
- [26] Dhara S., Bhargava P., Influence of nature and amount of dispersant on rheology of aged aqueous alumina gelcasting slurries, *J. Am. Ceram. Soc.*, 88, 3, 2005, 547–552

- [27] Dhara S., Kamboj R., Pradhan M., Bhargava P., Shape forming of ceramics via gelcasting of aqueous particulate slurries, Indian Academy of Sciences. *Bull. Mater. Sci.*, 25, 6, 2002, 565–568
- [28] Dukhin A., Dukhin S., Goetz P., Ultrasound for characterizing concentrated particulates at high ionic strength - particle sizing, zeta potential, adsorption, in Proceedings of Part. Systems Analysis Conference, UK, Sept. 2005
- [29] Dukhin A., Goetz P., Ultrasound for characterizing colloids – particle sizing, zeta potential, rheology, 2002, Elsevier
- [30] Dukhin A., Dukhin S., Goetz P., Electrokinetics at high ionic strength and hypothesis of the double layer with zero surface charge, *Langmuir*, 21, 2005, 9990-9997
- [31] Elimelech M., Gregory J., Jia X., Williams R., Particle deposition and aggregation – measurement, modelling and simulation, Butterworth-Heinemann, Oxford, 1995
- [32] French R., Origins and application of London dispersion forces and Hamaker constants in ceramics, *J. Amer. Ceram Soc.* 83, 9, 2000, 2117-46
- [33] Fujita H., Levi C., Zokw F., Controlling mechanical properties of porous mullite/alumina mixtures via precursor-derived alumina, *J. Am. Ceram. Soc.*, 88, 2, 2005, 367–375
- [34] Ghosal S., Emami-Naeini A., Harn Y., Draskovic B., Pollinger J., A physical model for the drying of gelcast ceramics, *J. Am. Ceram. Soc.*, 82, 3, 1999, 513–20
- [35] Greenwood R., Kendall K., Ritchie S., Snowden M., The use of poly (N-isopropylacrylamide) microgels as a multi-functional processing aid for aqueous alumina suspensions, *J. Eur. Ceram. Soc.*, 20, 2000, 1707-1716
- [36] Greenwood R., Kendall K., Effect of ionic strength on the adsorption of cationic polyelectrolytes onto alumina studied using electroacoustic measurements, *Powd. Techn.*, 113, 2000, 148-157
- [37] Greenwood R., Kendall K., Selection of suitable dispersant for aqueous suspensions of zirconia and titania powders using acoustophoresis, *J. Eur. Ceram. Soc.*, 19, 1999, 479
- [38] Gunko V., Zarko V., Leboda R., Chibowski E., Aqueous suspension of fumed oxides: particle size distribution and zeta potential, *Adv. Coll. Interf. Sci.* 91, 2001, 1-112
- [39] Günther L., Peukert W., The relevance of interactions in nanoparticle systems – application to particulate thin films, *Part. Part. Syst. Charact.* 19, 2002, 312-320

- [40] Guo X., Yang H., Investigation of compaction and sintering behavior of SiC powder after ultra-fine treatment, *Guo et al. J Zhejiang Univ SCI*, 5, **8**, 2004, 950-955
- [41] Hackley V., Colloidal processing of silicon nitride with polyacrylic acid: adsorption and electrostatic interaction, *J. Am. Ceram. Soc.*, 80, **9**, 1997, 2315-25
- [42] Hao H., Chiang P., Decolorization of waste water, *Critical Reviews in Env. Sci. and Techn.*, 30, **4**, 2000, 449-505.
- [43] Herbig R., Elektrokinetische Messungen an Suspensionen und Solen, *Mütek Workshop*
- [44] Hidber P., Graule T., Gauckler L., Influence of the dispersant structure on properties of electrostatically stabilized aqueous alumina suspensions, *J. Eur. Ceram. Soc.*, **17**, 1997, 239-249
- [45] Hiemenz P., Rajagopalan R., Principles of colloid and surface chemistry, *Marcel Decker*, 1997
- [46] Hourlier – Bahloul D., The Role of Chemistry in the Synthesis of Ceramic Materials, *Key Engineering Materials*, 206-213, 2002, 15-20
- [47] Israelachvili J., Intermolecular and surface forces, 2-nd ed., *Academic Press, London*, 1992
- [48] Izuhara S., Kawasumi K., Yasuda M., Highly porous cordierite ceramics fabricated by in situ solidification, *Ceramic Transactions*, 112, 553-558
- [49] Janney M., Nunn S., Walls C., Omatete O., Ogle R., Kirby G., McMillan A., Gelcasting, *The Handbook of Ceramic Engineering*, Mohamed N. Rahaman, *Ed.*, Marcel Dekker, 1998
- [50] Janney M., Attaining high solids in ceramic slurries, Research report under contract DE-AC05-96OR22464
- [51] Janney M., Omatete O., Walls C., Nunn S., Ogle R., Westmoreland G., Development of low-toxicity gelcasting systems, *J. Am. Ceram. Soc.* 81, **3**, 1998, 581-91
- [52] Johnson S., Scales P., Healy T., The binding of monovalent electrolyte ions on α -Alumina. 1. Electroacoustic studies at High electrolyte concentrations”, *Langmuir*, 15, 1999, 2836-2843
- [53] Jung A, Amal R., Raper J., The use of small angle light scattering to study structure of flocs, *Part. Part. Syst. Charact.* 12, 1995, 274-278

- [54] Karthikeyan J., Removal of color from textile dye wastes by chemical coagulation, *Ph.D. Thesis*, Indian Institute of Technology, Kanpur, India, 1990
- [55] Kay E., Calloway T., Koopman J., Brigmon R., Eibling R., Rheology modifiers for radioactive waste slurries, *Proceedings of ASME 2003 Fluid Engineering Division Summer Meeting July 6th-10th*, 2003
- [56] Kemper S., Kühn M., Poehnitzsch S., Koch D., Kuntz M., Grathwohl G., Developing and characterizing porous ceramic materials, *Practical Metallography*, 40, 7, 2003, 325-334
- [57] Khan A., Luckham P., Manimaaran S., Probing the mechanism by which ceramic dispersants act, *J. Mater. Chem.* 7, 9, 1849-1853, 1997
- [58] Kiminami R., Morelli M., Folz D., Clark D., Microwave synthesis of alumina powders, *Am. Ceram. Soc. Bull.*, 79, 3, 2000
- [59] Kirby G., Harris D., Qi L., Lewis J., Poly(acrylic acid)–poly(ethylene oxide) comb polymer effects on BaTiO₃ nanoparticle suspension stability, *J. Am. Ceram. Soc.*, 87, 2, 2004, 181–86
- [60] Klein S., Fisher M., Franks G., Colic M., Lange F., Effect of the interparticle pair potential on the rheological behavior of zirconia powders: I, Electrostatic double layer approach, *J. Am. Ceram. Soc.*, 83, 3, 2000, 513–17
- [61] Klimpel R., Introduction to chemicals used in particle system. In *Particle Science and Technology*; Rajagopalan R., Ed.; the NSF Engineering Research Centre for Particle Science and Technology, Florida, 1999
- [62] Koch D., Andresen L., Schmedders T., Grathwohl G., Evolution of porosity by freeze casting and sintering of sol-gel-derived ceramics, *J. of Sol-Gel Science and Technology*, 26, 2003, 149 – 152
- [63] Kosmulski M., pH-dependent surface charging and points of zero charge. III. Update, *J. of Coll. Interf. Sci.*, 298, 2006, 730–741
- [64] Kosmoc T., Near-net-shape of engineering ceramics: potentials and properties of aqueous injection molding (AIM), pp. 13-22 in *Proceedings of NATO ARW on Engineering Ceramics'96*. Edited by G. N. Batini, M. Havier, and P. Sejgalik, Kluwer Academic Publishers, New York, 1997
- [65] Krell A., Blank P., Ma H., Hutzler T., Nebelung M., Processing of high-fensity submicrometer Al₂O₃ for new applications, *J. Am. Ceram. Soc.*, 86, 4, 2003, 546–53

- [66] Kwon S., Jun Y., Hong S., Lee I., Kim H., Calcium phosphate bioceramics with various porosities and dissolution rates, *J. Am. Ceram. Soc.*, 85, **12**, 2002, 3129–31
- [67] Laarz E., Meurk A., Yanez J., Bergström L., Silicon nitride colloidal probe measurements: interparticle forces and the role of surface-segment interactions in poly(acrylic acid) adsorption from aqueous solution, *J. Am. Ceram. Soc.*, 84, **8**, 2001, 1675–82
- [68] Lange F., Powder processing science and technology for increased reliability, *J. Am. Ceram. Soc.*, 72, **1**, 1989, 3
- [69] Lewis J., Colloidal processing of ceramics, *J. Am. Ceram. Soc.*, 83, **10**, 2000, 2341–59
- [70] Li S., de Wijn J., Layrolle P., de Groot K., Novel method to manufacture porous hydroxyapatite by dual-phase mixing, *J. Am. Ceram. Soc.*, 86, **1**, 2003, 65–72
- [71] Li R., Temperature - induced direct casting of SiC, Dissertation an der Universität Stuttgart, Ber. 102, June, 2001
- [72] Lyckfeld O., Ferreira J., Processing of porous ceramics by starch consolidation, *J. Eur. Ceram. Soc.*, 18, 1998, 131-140
- [73] Lyklema J., Fundamentals in colloid and interface science, vol. 2, Academic Press, 1995
- [74] Ma J., Xie Z., Miao H., Zhou L., Huang Y., Cheng Y., Elimination of surface spallation of alumina green bodies prepared by acrylamide-based gel casting, *J. Am. Ceram. Soc.*, 89, 2, 2006
- [75] Macedo J., da Costa N., Almeida L., Vieira E., Cestari A., Gimenez I., Carreño N., Ledjane L., Kinetic and calorimetric study of the adsorption of dyes on mesoporous activated carbon prepared from coconut coir dust, *J. of Colloid and Interf. Sci.*, 298, **2**, 2006, 512-522
- [76] Marra J., Hair M., Forces between two poly(2-vinyl pyridine)-covered surfaces as a function of ionic strength and polymer charge, *J. Phys. Chem.*, **92**, 1988, 6044–51
- [77] Milling A., Mulvaney P., Larson I., Direct measurement of repulsive van der Waals interactions using an atomic force microscope, *Journal of Colloid and Interface Science* 180, 1996, 460-465

- [78] Miyagawa N., Shinohara N., Fabrication of porous alumina ceramics with unidirectionally-arranged continuous pores using a magnetic field, *J. Ceram. Soc. Jpn.* 107,1999, 673-677
- [79] Morissette S., Lewis J., Chemorheology of aqueous-based alumina–poly(vinyl alcohol) gelcasting suspensions, *J. Am. Ceram. Soc.*, 82, 3, 1999, 521–28
- [80] Morissette S., Lewis J., Solid freeform fabrication of aqueous alumina–poly(vinyl alcohol) gelcasting suspensions, *J. Am. Ceram. Soc.*, 83, 10, 2000, 2409–16
- [81] Müller R., Zetapotential und Partikelladung in der Laborpraxis, Wiss. Verlagsgesellschaft GmgH, Stuttgart, 1996
- [82] Neubrand A., Effects of ultrasound on the strength and reliability of slip-cast ceramics, *J. of Mat. Sci. Lett.*, 19, 2000, 157– 158
- [83] Niihara K., Kim B., Nakayama T., Kusunose T., Nomoto T., Hikasa A., Sekino T., Fabrication of complex-shaped alumina/nickel nanocomposites by gelcasting process, *J. Eur. Ceram. Soc.*, 24, 2004, 3419–3425
- [84] Nitzsche R., Bley L., Particle Charge Detection-eine neue Methode zur Charakterisierung und Optimierung im Kera., *Muetek Workshop*
- [85] Nitzsche R., Keramik: Bestimmung des isoelektrischen Punktes von Schlickern, *Muetek Workshop*
- [86] Padilla S., Vallet-Regi M., Concentrated suspensions of hydroxyapatite for gelcasting shaping, *Key Engineering Materials*, 254-256, 2004, 35-38
- [87] Paik U., Dispersant-binder interactions in aqueous silicon nitride suspensions, *J. Am. Ceram. Soc.*, 82, 4, 1999, 833-40
- [88] Poehnitzch S., Grathwohl G., Die Entwicklung des Zentralporenkanals in keramischen Kapillaren während des Sintern, *Prakt. Metallogr.*, 27, 11, 2001, 608 - 618
- [89] Pontin M., Lange F., Effects of porosity on the threshold strength of laminar ceramics, *J. Am. Ceram. Soc.*, 88, 2, 2005, 376–382
- [90] Premachandran R., Maglan S., Dispersion characteristics of ceramic powders in the application of cationic and anionic polyelectrolytes, *Powd. Techn.* 79, 2004, 53-60
- [91] Pretto M., Costa A., Landi E., Tampieri A., Galass C., Dispersing behavior of hydroxyapatite powders produced by wet-chemical synthesis, *J. Am. Ceram. Soc.*, 86, 9, 2003, 1534–39

- [92] Robinson T., McMullan G., Marchant R., Nigam P., Remediation of dyes in textile effluent: a critical review on current treatment technologies with proposed alternative, *Biores. Techn.*, 77, 3, 2001, 247-255
- [93] Santacruz I., Baudin C., Moreno R., Nieto M., Improved green strength of ceramics through aqueous gelcasting, *Advanced Engineering Materials*
- [94] Scott D., Characterizing particle characterisation, *Part. Part. Syst. Charact.*, 20, 2003, 305 – 310
- [95] Sigmund W., Novel powder processing methods for advanced Ceramics, *J. Am. Ceram. Soc.*, 83, 7, 2000, 1557–74
- [96] Singh B., Bhattacharjee S., Electrokinetic and adsorption studies of alumina suspensions using Darvan C as dispersant., *J. Coll. and Interf. Sci.*, 289, 2005, 592-596
- [97] Singh B., Besra L., Bhattacharjee S., Factorial design of experiments on the effect of surface charge on stability of aqueous colloidal ceramic suspension, *Colloids and Surfaces A: Physicochemical and engineering Aspects*, 204, 2002, 175-181
- [98] Singh B., Bhattacharjee S., Besra L., Influence of surface charge on maximizing solids loading in colloidal processing of alumina, *Materials Letters*, 56, 2002, 475-480
- [99] Singh B., Bhattacharjee S., Besra L., Sengupta D., Evaluation of dispersibility of aqueous alumina suspension in presence of Darvan C, *Ceramics International*, 30, 2004, 939-946
- [100] Singh B., Bhattacharjee S., Besra L., Sengupta D., Comparison between techniques based on charge characterisation and capillary suction time for assessing the dispersion characteristics of concentrated slurry, *Journal of Materials science*, 38, 2003, 1-6
- [101] Singh B., Bhattacharjee S., Besra L., Optimisation of performance of dispersants in aqueous plasma dissociated zircon suspension, *Ceramics International*, 28, 2002, 413-417
- [102] Slamovich E., Lange F., Densification of large pores: I, Experiments, *J. Am. Ceram. Soc.*, 75, 9, 1992, 2948 – 2508
- [103] Spriggs R., Effect of open and closed pores on elastic moduli of polycrystalline alumina, *J. Am. Ceram. Soc.*, 1962

- [104] Stampfl J., Fouad H., Seidler S., Liska R., Schwager F., Woesz A., Fratzl P., Fabrication and moulding of cellular materials by rapid prototyping, *Int. J. Materials and Product Technology*, 21, 4, 2004, 285
- [105] Steinborn G., Waesche R., Charakterisierung elektrokinetischer Eigenschaften in Al₂O₃-Suspensionen .met dem Partikelladungsdetektor PCD03, *Malvern-Mütek Workshop*, 5. Anwendertagung, Potsdam 2000
- [106] Stenger F., Götzinger M., Jakob P., Peukert W., Mechano-chemical changes of nano sized alfa-Al₂O₃ during wet dispersion in stirred ball mills, *Part. Part. Syst. Charact.*, 21, 2004, 31-38
- [107] Tang F., Fudouzi H., Sakka Y., Fabrication of macroporous alumina with tailored porosity, *J. Am. Ceram. Soc.*, 86, 12, 2003, 2050–54
- [108] Tang F., Fudouzi H., Uchikoshi T., Sakka Y., Preparation of porous materials with controlled pore size and porosity, *J. Eur. Ceram. Soc.*, 24, 2004, 341–344
- [109] Tari G., Advances in colloidal processing of alumina, PhD Thesis – Abstract, Universidade de Aveiro, 1999
- [110] Tari G., Ferreira J., Influence of solid loading on drying-shrinkage behavior of slip cast bodies, *J. Eu. Ceram. Soc.*, 18, 1998, 487-493
- [111] Tari G., Ferreira J., Lyckfeldt O., Influence of the stabilising mechanism and solid loading on slip casting of alumina particle suspensions: stabilization and characterization, *J. Eu. Ceram. Soc.*, 18, 1998, 479-486
- [112] Tari G., An overview of direct consolidation forming techniques, their comparison with traditional wet- or paste-processing forming techniques and selection criteria, *American Ceramic Society Bulletin*, 82, 4
- [113] Thijs I., Luyten J., Mullens S., Producing ceramic foams with hollow spheres, *J. Am. Ceram. Soc.*, 87, 1, 2003, 170–72
- [114] Tseng W., Wu C., Sedimentation, rheology and particle-packing structure of aqueous Al₂O₃ suspensions, *Ceramics International*, 29, 7, 2003, 821-828
- [115] Tuck C., Evans J., Porous ceramics prepared from aqueous foams, *J. of Mat. Sci. Lett.*, 18, 1999, 1003–1005

- [116] Vandevivere P, Bianchi R., Werstaete W, Treatment and reuse of waste water from the textile wet-processing industry: Review of emerging technologies *J. Chem. Technol. Biotechnol.*, 72, 1998, 289-302.
- [117] Vasilyeva E., Morozova L., Lapshin A., Konakov V., Ceramic materials with controlled porosity, *Mater.Phys.Mech.*, 5, 2002, 43-48
- [118] Wäsche R., Naito M., Hackley V., Experimental study on zeta potential and streaming potential of advanced ceramic powders, *Powd. Techn.*, 123, 2002, 275–281
- [119] Weh L., Gemeinert M., Dispersibility optimisation of ceramic particles for ML-LTCC production, *PARTEC – Nuernberg*
- [120] Yalamanchili M., Veeramasuneni S., Azevedo M., Miller J., Use of atomic force microscopy in particle science and technology research, *Coll. and Surf. A: Physicochemical and Engineering Aspects*, 133, 1998, 77-88
- [121] Zhang G., Yang J., Ohji T., Porous ceramics with fine uni-directionally-aligned continuous pores, *Ceramic Engineering and Science Proceedings*, 22, 4, 2001, 183-190
- [122] Zhang G., Yang J., Ohji T., Fabrication of porous ceramics with unidirectionally aligned continuous pores, *J. Am. Ceram. Soc.*, 84, 6, 2001, 1395-1397
- [123] Zhang W., Wang H., Zhang Y., Jin Z., Preparation of porous Si₃N₄ nanocomposites by gelcasting, *Fuhe Cailiao Xuebao/Acta Materiae Compositae Sinica*, 21, 5, 2004, 83-87
- [124] Zürcher S., Graule T., Influence of dispersant structure on the rheological properties of highly-concentrated zirconia dispersions, *J. Eu. Ceram. Soc.*, 25, 2005, 863-873

List of related publications

- [1] Gaydardzhiev S., Ay P. Removal of dyes from effluents by chemical coagulation - surface charge and particle size aspects, Proceedings of the Xth Balkan Mineral Processing Congress, Varna, Bulgaria, 15-20 June 2003, pp. 403 – 408
- [2] Gaydardzhiev S., Ay P. Surface charge and size characterization of coagulated dye and its implication to color removal from effluents by chemical coagulation, In CD Proceedings from “Particulate Systems Analysis” Conference, Harrogate, UK, 10 – 12 IX, 2003
- [3] Gaydardzhiev S., Ay P., 2003, Surface charge studies - an important approach for investigation of color removal from textile wastewaters by chemical coagulation, in Rao and Misra (eds), MPT 2004 Conference Proceedings, Allied Publishers, pp 741-748
- [4] Gaydardzhiev S., Ay P., Implication of surface charge effects in color removal from effluents by chemical coagulation the case of CI Reactive Blue 4 dye, In CD Proceedings PARTEC2004 Conference, March 16-18, 2004 Nürnberg
- [5] Gaydardzhiev S., Karthikeyan J., Ay P., 2005, Progression of surface charge and floc characterisation during colour removal from model solutions by coagulation, *Journal of Environmental Technology*- Vol. 27 (2006), pp. 193-199
- [6] Janeczko, M., Gaydardzhiev S, Size and structure characterization of dye flocs during chemical coagulation of Reactive Black 5 dye, *Part. Part. Syst. Charact.* 23, 210–214.
- [7] Gaydardzhiev S., Ay P., Janeczko, M, Comparative studies of dispersant optimisation techniques for evaluating the stability of concentrated alumina slurries, *Part. Part. Syst. Charact.* 23, 205–209.
- [8] Singh, B.P. Gaydardzhiev S., Ay P. Stabilization of Aqueous Silicon Nitride Suspension with Dolapix A 88, *Journal of Dispersion Science and Technology*, Vol. 27, 1 (2006), pp. 91-97
- [9] Gaydardzhiev S., Ay P., 2005 Characterisation of aqueous suspensions of fumed aluminium oxide in presence of two Dolapix dispersants, *J. of Materials Science*, vol. 41, 5257-5262
- [10] Gaydardzhiev S., Ay P. Evaluation of Dispersant Efficiency for Aqueous Alumina Slurries by Concurrent Techniques, *Journal of Dispersion Science and Technology*, Vol. 27, 3 (2006), pp. 413-417
- [11] Janeczko, M., Gaydardzhiev S, Ay P., Removal of selected azo dyes from textile wastewater by chemical coagulation/flocculation: implication of dye destabilization mechanism, in Fecko P. (ed) Proceedings of 10-th Conference on Environment and Mineral Processing, VSB Ostrava, Czech Republic, 22 - 24.06.2006, 153-159
- [12] Janeczko, M., Georgiev P., Nicolova M., Gaydarjiev S, Spassova I., Ay P., Groudev S., Colour removal from wastewater by means of microbial treatment, in Fecko P. (ed) Proceedings of 10-th Conference on Environment and Mineral Processing, VSB Ostrava, Czech Republic, 22 - 24.06.2006, 287-292
- [13] **Gaydardzhiev S.**, Ay P., (2006). Characterisation of stability behaviour of ultra fine alumina powder in view its colloidal processing by gel-casting. In Önal G. et al. (eds.), Proceedings of the XXIII IMPC, 3-8 September 2006, Istanbul, 464-467.
- [14] Janeczko, M., **Gaydardzhiev S.**, (2006). Removal of dyes from textile wastewater by chemical coagulation. In Önal G. et al. (eds.), Proceedings of the XXIII IMPC, 3-8 September 2006, Istanbul, 2163-2167.

Acknowledgment

The appearance of the habilitation work will not be possible without the kind help and contributions of the following people for which my deep thankfulness goes.

First of all I would like to thank my advisor and Head of Chair of Mineral Processing Prof. Dr. – Ing. habil Peter Ay for the work guidance, useful discussions and for the continuous encouragement received from him as well as for providing lab space and equipment for smoothly work running. Special thanks go to my colleagues and members of the Chair of Mineral Processing, namely Grit, Hans, Wiktorja, Christian, Uwe, Sigi, Claudia and Sven for their help in any matter regardless of scientific or social character and for their friendly attitude.

It is particularly important to distinguish those people with whom we actually started at the Chair of Mineral Processing the initial work in the field of charge characterizations for understanding the stabilization/destabilization phenomena in dye solutions and ceramic powder suspensions. For this I am tremendously indebted to Prof. Dr. J. Karthikeyan and Dr Bimal Singh. I highly appreciate the helpful contribution during cooperation with other colleagues. It's a pleasure to express my gratitude to Dr. Manfred Nagel (Degussa AG, Hanau) for providing various samples of Aerosil powder, to Dr. Wilker and Dipl. –Ing. Olschewski (LS Anorganische Chemie) for the DLA and sintering investigations and to Dr. Wiehe (ZAL) for the REM photographs. I am particularly indebted to my PhD student Mrs Marta Janeczko for her deep engagement within the experimental work in dyes removal from effluents and for the very fruitful discussions. Thanks should go to my graduate students (Igljka, Pilar, Emilio and Maria-Louisa) who have contributed with their dedicated work especially for the time-consuming experiments in gel-casting.

Last, but not least, I am very grateful to my loving family – my wife and children and to my mother whose support had actually made my work possible. I devote this work in memory of father who has provided me with an initial stimulus in the inspiring field of physico-chemical processing of fine particles.

Abstract

The work is dedicated to the aspects of characterization of surface charge phenomena in two colloidal systems: synthetic mixtures of textile dyes and aqueous suspension of ceramic powders. An implication to the areas of physicochemical colour removal from textile effluents and gel-casting of ceramics is made. A model for dye-coagulant interaction has been developed based on surface charge density and floc size investigations. Various dispersant optimization techniques have been compared in stabilizing aqueous slurries of ultra-fine alumina particles, the zeta potential derived from CVI measurements being viewed as a most reliable one. The chemical environment of the ceramic slurry together with maintaining an optimal process conditions in gel-casting plays an equally important role in providing a desired properties of complex shaped ceramic bodies. Development of porous ceramic by gel-casting using burnable pore developers is shown to be a feasible approach, however fibres modification and dimensioning requires further attention.

Zusammenfassung

Die Arbeit beschäftigt sich vor allem mit den Aspekten der Charakterisierung von Ladungsphänomenen hinsichtlich der Stabilisierung und Destabilisierung von zwei kolloidalen Systemen: synthetischen Mischungen aus reinen Farbstoffen und wässrigen Suspensionen von Keramikpulvern. Daher hat die Forschungsarbeit eine Relevanz zur chemischen Behandlung von Textilabwässern und zum kolloidalen Keramikformgebungsverfahren. Anhand des Ladungszustand- und Flockenformcharakterisierungen ist ein Model zur einfachen Beschreibung der Wechselwirkungen zwischen dem Farbstoffsubstrat und dem Koagulant entwickelt worden. Zur Auswahl des optimalen Dispergierungsmittels für die keramischen Suspensionen sind verschiedene Methoden ausgesucht und evaluiert worden. Die Ermittlung von Zeta Potential (CVI-Messungen) hat sich jedoch als die meist geeignete Methode etabliert. Es hat sich ergeben, dass die chemische Umgebung der wässrigen Suspensionen (z.B. Art und Konzentration der organische Additive) und die optimalen Prozessparameter des Gel-casting (z.B. Art und Dauer der Mischung), der Schlüssel zur Herstellung von geometrisch komplizierten und defektfreien Endkörpern sind. Es ist bewiesen worden, dass die Zugabe von ausbrennbaren Porenentwickler, ein ausführbarer Ansatz zur Herstellung von poröser Keramik ist. Darüber hinaus müsste weiter geprüft werden inwieweit eine optimale Dimensionierung und Oberflächenmodifizierung der Fasern, günstige Auswirkungen auf die Viskosität des Schlickers haben können.

Annex



Photos of dense ceramic bodies produced by Gel-casting

**Upon the characterization of destabilization and stabilization
phenomena in fine particulate systems – implications to
physicochemical removal of colour from effluents and colloidal
processing of ceramics**

Beitrag zur Charakterisierung von Destabilisierungs- und
Stabilisierungsphänomenen in Feinpartikelsystemen – die Relevanz zum physiko-
chemischen Farbstoffabbau und zum kolloidalen Keramikformgebungsverfahren

Band II

Publikationen

Publikationen in Richtung Farbstoffabbau und Flockencharakterisierung

- [1] Gaydardzhiev S., Ay P., Removal of dyes from effluents by chemical coagulation - surface charge and particle size aspects, Proceedings of the Xth Balkan Mineral Processing Congress, Varna, Bulgaria, 15-20 June 2003, pp. 403 – 408
- [2] Gaydardzhiev S., Ay P., Surface charge studies - an important approach for investigation of color removal from textile wastewaters by chemical coagulation, in Rao and Misra (eds), MPT 2004 Conference Proceedings, Allied Publishers, pp 741-748
- [3] Gaydardzhiev S., Ay P., Implication of surface charge effects in color removal from effluents by chemical coagulation the case of CI Reactive Blue 4 dye, In Proceedings of PARTEC2004 International Conference on particle technology, Nürnberg, 16-18 March 2004
- [4] Gaydardzhiev S., Karthikeyan J., Ay P., Colour removal from model solutions by coagulation – surface charge and floc characterisation aspects, *Journal of Environmental Technology*, Vol. 27 (2006), pp. 193-199
- [5] Janeczko, M., Gaydardzhiev S, Size and structure characterization of dye flocs during chemical coagulation of Reactive Black 5 dye, *Part. Part. Syst. Charact.* 23 (2006) 210–214, DOI: 10.1002/ppsc.200601032
- [6] Janeczko, M., Gaydardzhiev S, Ay P., Removal of selected azo dyes from textile wastewater by chemical coagulation/flocculation: implication of dye destabilization mechanism, in Fecko P. (ed) Proceedings of 10-th Conference on Environment and Mineral Processing, VSB Ostrava, Czech Republic, 22 – 24 June 2006, 153-159
- [7] Janeczko, M., Georgiev P., Nicolova M., Gaydarjiev S, Spassova I., Ay P., Groudev S., Colour removal from wastewater by means of microbial treatment, in Fecko P. (ed) Proceedings of 10-th Conference on Environment and Mineral Processing, VSB Ostrava, Czech Republic, 22 – 24 June 2006, 287-292

Publikationen in Richtung Partikelcharakterisierung und Keramikpulververarbeitung

- [8] Lilkov V., Dimitrova, E. and Gaidardzhiev St. Microscopic and laser granulometric analyses of hydrating cement suspensions, *Cement and Concrete Research*, 29, (1999), pp 3-8
- [9] Singh, B.P. Gaydardzhiev S., Ay P. Stabilization of Aqueous Silicon Nitride Suspension with Dolapix A 88, *Journal of Dispersion Science and Technology*, Vol. 27, 1 (2006), pp. 91-97
- [10] Gaydardzhiev S., Ay P., 2006 Characterisation of aqueous suspensions of fumed aluminium oxide in presence of two Dolapix dispersants, *Journal of Materials Science* , 41:5257-5262
- [11] Gaydardzhiev S., Ay P. Evaluation of Dispersant Efficiency for Aqueous Alumina Slurries by Concurrent Techniques, *Journal of Dispersion Science and Technology*, Vol. 27, 3 (2006), pp. 413-417
- [12] Gaydardzhiev S., Ay P., Janeczko, M, Comparative studies of dispersant optimisation techniques for evaluating the stability of concentrated alumina slurries, *Part. Part. Syst. Charact.* 23 (2006) 205–209, DOI: 10.1002/ppsc.200601033

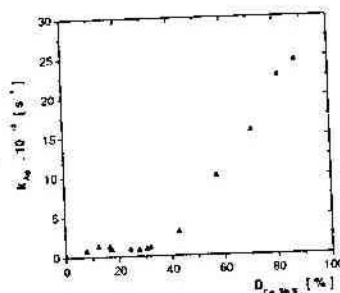


Figure 5. Rate constant (k_{AK}) for silver leaching versus degree of mechanochemical destruction (D) of tetrahedrite.

4. CONCLUSIONS

Mechanochemical alkaline pretreatment of complex sulphide concentrate has a positive influence on silver leaching from tetrahedrite. An optimum recovery of silver over 90 % was achieved from the mechanochemically treated samples after only five minutes of thiourea leaching. The leaching of as-received (non-treated) concentrate resulted in only 5 % Ag dissolution. The thiourea leaching of silver from tetrahedrite is a structurally sensitive solid-liquid reaction and the increase in D values is appreciable only when more than 30% of the tetrahedrite has been destroyed.

ACKNOWLEDGEMENTS

This work was supported by the Slovak Grant Agency for Science (grant No. 2/2103/22).

REFERENCES

Baláz, P., Kammel, R., Achimovičová, M. (1994). Mechanochemical treatment of tetrahedrite as

- a new ecologically non-polluting way of metals recovery. *Metall*, 48, pp 217-220.
- Baláz, P., Ficeriová, J., Šepelák, V., Kammel, R. (1996). Thiourea leaching of silver from mechanically activated tetrahedrite. *Hydrometallurgy*, 43, pp 367-377.
- Baláz, P., Kammel, R. (1996). Application of attritors in hydrometallurgy of complex sulphide ores. *Metall*, 50, pp 345-347.
- Baláz, P., Kammel, R., Sekula, F., Jakabský, Š. (1997). Mechanochemical leaching: the possibility to influence the rate of metals extraction from refractory ores. In: Hoberg, H., Von Blotnitz, H. (Eds.), *Proc. XXth Int. Miner. Proc. Congr.*, Vol. 4 Aachen, pp 149-159.
- Baláz, P., Achimovičová, M., Ficeriová, J., Kammel, R., Šepelák, V. (1998). Leaching of antimony and mercury from mechanically activated $Cu_{12}Sb_4S_{13}$. *Hydrometallurgy*, 47, pp 297-307.
- Baláz, P. (2000). *Extractive Metallurgy of Activated Minerals*. Elsevier, Amsterdam, pp 290.
- Baláz, P., Ficeriová, J., Villachica, C. (2003). Silver leaching from a mechanochemically pretreated complex sulphide concentrate. *Hydrometallurgy* - in press.
- Bruckard, W. J., Sparrow, G.J., Woodcock, J. T. (1993). Gold and silver extraction from Hellyer lead-zinc flotation middlings using pressure oxidation and thiourea leaching. *Hydrometallurgy*, 33, pp 17-41.
- Ficeriová, J., Baláz, P., Boldižárová, E. (1998). Structural sensitivity of leaching of silver from tetrahedrite by ammonium thiosulphate. *Acta Metallurgica Slovaca*, 4, pp 65-69.
- Heegn, H. (1986). ScD. Thesis, Research Institute of Mineral Processing of the Academy of Sciences of the GDR, Freiberg (German).
- Križani, I. (1999). Separation of gold from ores and mineral waste by ultrasonic treatment (in Slovak). *Miner. Slov.* 31, pp 341-346.
- La Brooy, S. R., Lange, H. G., Walker, G. S. (1994). Review of gold extraction from ores. *Miner. Eng.* 7, pp 1213-1241.

REMOVAL OF DYES FROM EFFLUENTS BY CHEMICAL COAGULATION: SURFACE CHARGE AND PARTICLE SIZE ASPECTS

Stoyan Gaydardzhiev, Peter Ay

Chair of Mineral Processing, Brandenburgische Technische Universität Cottbus, Theodor-Neubauer Straße 4-b,
03046 Cottbus, Germany, e-mail: gaydar@tu-cottbus.de

ABSTRACT:

Particle size and surface charge characterization of coagulated dye sludge could be used as a reliable tool for evaluating the responsible mechanism taking place during textile effluent treatment by chemical coagulation. The present paper is dealing with a similar characterization studies, however aimed for assessing the efficiency of a common solid/liquid separation approaches like centrifugation, gravity and membrane filtration when applied for post-treatment of the coagulated dye slurry. A simple model system comprising commercially used dye "Acid Blue 113" and iron chloride as inorganic coagulant was chosen. It has been established that the different solid/liquid separation modes used have a pronounced effect upon the surface charge of resultant filtrates/supernatant and on the degree of color removal as well. Particle size characteristics both of the flocs generated under different coagulant dose rates and of the resultant filtrates could also be used as a criteria for evaluating the most likely coagulation mechanism taking place.

Keywords: color removal from effluents, chemical coagulation, surface charge, particle size.

1. INTRODUCTION

The problem of color removal from dye house effluents is an important challenge for waste-water treatment technology. Widely used in this area are large spectra of techniques: chemical (neutralization, oxidation), physicochemical (coagulation and flocculation, adsorption, ion exchange) and biological processes. However, despite the significant number of research and academic studies performed in direction of color removal from effluents, there is by far lack of a unified view towards a single technologically feasible and economically acceptable method (Robinson *et al.*, 2001). One reason for this is the huge variety of chemical compounds and color-bearing components met in the liquid wastes associated with the textile industry, which necessitates development of targeted source-specific approaches for every single case most often involving a combination of two or more treatment steps. Whilst it is acknowledged fact

that coagulation with metal salts plays an important role for dye-house effluent treatment, being practiced either as pre-, post- or main method, its large-scale application is often hampered by the large amount of sludge generated which requires further disposal. This problem is further aggravated by the limited knowledge about the predominant mechanisms responsible for color removal by coagulation. One of the accepted believe adopted for mechanism explanation, is that neutral surface charge is required for disperse systems destabilization and for filtration processes enhancing also (Besra *et al.*, 2002). However, in the case of color removal by coagulation, the picture might be viewed as a more complicated and difficult to generalize one (Marmagne *et al.*, 1996; Tünay *et al.*, 1996). It is clear that intensive studies in this direction are needed and that the results anticipated from them could have relevance for the broader areas of dispersed particle systems manipulation as well.

On the background of the above, a research was initiated with the aim to provide scope on the above issues. In our previous work (Gaydardzhiev *et al.*) we have reported about correlation between the surface charge of coagulated dye slurry and the coagulant dose level and color removal for the case of two dyes, i.e. "Disperse Blue 26" and "Acid Blue 113" coagulated with ferric chloride. However, such correlation was apparently not documented when aluminum salts were used as coagulants. Hence we have assumed, that charge neutralization could be suspected as a predominant mechanism responsible for dye coagulation in the first case. Once this was established, a further objective could be set further in direction optimization both slurry/filtrate separation as well as coagulant dosage. In order to accomplish this task, it seems worthy to study what kind of charge effects accompany the different solid/liquid separation methods usually practiced and how this information could be used as a feedback for maintaining optimal coagulation conditions leading to satisfactory color removal with limited amount of sludge generation.

2. MATERIALS AND METHODS

2.1. Synthetic dye bath effluents

A commercially available disazo based dye with a CI "Acid Blue 113" manufactured by Atic Industries, India was used as received. A known amount from the dye powder was dissolved in distilled water for obtaining model effluents with concentration 100 mg/l.

2.2 Chemicals

Iron chloride $FeCl_3$ (a.g.) from Merck was used as coagulant. Respective stock coagulant solution was prepared in concentration 10 g/L. Concentrated hydrochloric acid and sodium hydroxide were used as pH regulators where needed.

2.3 Coagulation/flocculation and filtration

A 100 mL of the ready-made dye solution was transferred in a 200 mL beaker and placed on a flocculation jar-rig consisting of a 3-cm six-blade stirrer from Janke & Kunkel. Then,

the known quantity of coagulant was added to the dye solution and pH was adjusted to a pre-determined value by a pH-meter model 540 GLP, from WTW, Germany. The solution was mixed by stirring at 200 rpm for two minutes. After elapsing of the required time, a 10 mL aliquot from the solution was taken for surface charge determination. In the case of gravity filtration, part of the suspension was transferred to a glass funnel fitted with 5 μm "Osmonics" nylon filter and allowed to filtrate by gravity without disturbance for 24 h. In the case of membrane filtration, a laboratory syringes fitted with "Sartorius-Minisart" membrane filters 0.2 and 5 μm were employed. Following filtration, the collected supernatant volume was used for color removal degree evaluation and again for surface charge and particle size measurement. Centrifugation of coagulated dye was performed for 20 mL aliquots at 3500 rpm for 5 minutes by means of Megafuge 2.0 centrifuge from Heraeus. In all the experiments, temperature was kept constant in order to exclude its effect on dye coagulation and filterability.

2.4 Surface charge determination

Surface charge measurements were performed by means of a particle charge detector PCD-O3-pH from Mutek, Germany. It consists of a cylindrical test cell with fitted displacement piston which moves back and forth at constant frequency, forcing a relative motion of liquid and particles, thus inducing development of streaming potential of either positive or negative sign. The exact charge quantity was estimated by sample titration with oppositely charged standard polyelectrolyte titrant until neutralization of the streaming potential to zero value. The unit was coupled to "SM Titrimo 702" Metrohm titrator and interfaced to a PC enabling on-line monitoring of titration and results printout in table or graphical forms, potential or pH vs. spent titrant volume. The cationic standard titrant was 0.001 normal polydiallyldimethylammonium chloride solution (Poly-Dadmac), while the anionic one was 0.001 normal sodium polyethylene sulphate solution (Na-PES). Titrant volume increment was adjusted to 0.01 mL. Titrant and

dye suspension concentrations were so chosen that the spent titrant volume until zero charge in mL, was directly equivalent to the suspension specific charge in eq/g. Suspension pH was also recorded in course of titration, but its shift was found negligible.

2.5. Particle size determination

Particle size distribution (PSD) measurements of coagulated dye slurry and supernatants were done by means of CIS-100 GALAI system, a laser based size analyser which employs the time-off-transition principle. Volume ranges were recorded for non-filtered dyes, while number ranges - for filtered and centrifugated supernatants.

2.6. Color removal degree determination

A photometer MPM 3000 from WTW, Germany was used. The wavelength of the dye that gave the highest extinction factor (EF) at the photometer was adopted. Calibration curves were constructed then, linking the EF and dye concentration. The residual color concentration in the respective sample was estimated by reading from the EF-color concentration calibration curve. Color removal degree was calculated based on the difference between color concentration in the original dye-bath solution and the measured one in the supernatant after filtration/centrifugation.

3. RESULTS

The presented study has been adhered to the previously established optimal coagulation conditions regarding pH and $FeCl_3$ dosage, so pH 4 and coagulant dose level from 25 to 100 mg/L were maintained. The present focus was however placed on particle size and charge aspects observed when the coagulated dye slurry was subjected to a different solid/liquid separation modes. The results obtained in these directions are commented in details separately, with an attempt to bridge the findings in a summarising part following.

3.1 Effect of solid/liquid separation type used upon particle size characteristics of coagulated dyes

Each of the obtained slurries at the chosen coagulant dosages of 25, 50, 75 and 100 mg/l were subjected to centrifugation and membrane filtration with filters having 5 and 0.2 μm pore openings. When the dye was coagulated with 25 mg/L iron chloride, a negligible amount of extreme fine slurry was generated which precluded PSD measurements both for the slurry and the filtrates. Hence the respective curves were not obtained. The cumulative particle size distribution curves for the dye slurries and for the resultant filtrates are plotted at Figures 1 to 3 respectively for each coagulant dosage of 50, 75 and 100 mg/L. Additionally, Figure 4 compares the PSD curves for the slurries obtained within the whole dosage range, while Figure 5 compares the effect of filtration mode envisaged, i.e. 5 μm gravity or 5 μm membrane for a dye coagulated at 100 mg/L.

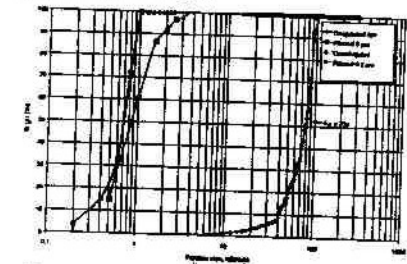


Figure 1. Cumulative PSD curves - effect of S/L separation mode for dye coagulated at 50 mg/L $FeCl_3$

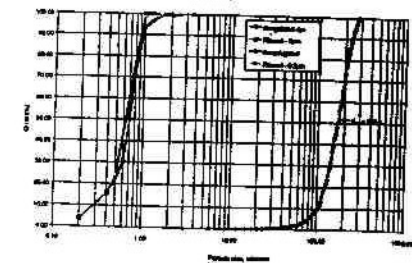


Figure 2. Cumulative PSD curves - effect of S/L separation mode for dye coagulated at 75 mg/L $FeCl_3$

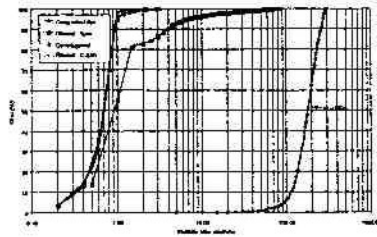


Figure 3. Cumulative PSD curves - effect of S/L separation mode for dye coagulated at 100 mg/L $FeCl_3$

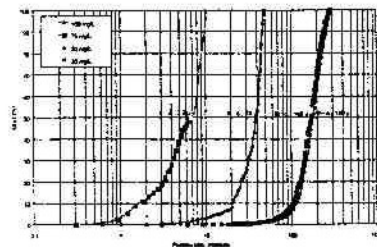


Figure 4. Comparative PSD (volume) curves for coagulated dyes at different $FeCl_3$ dosages

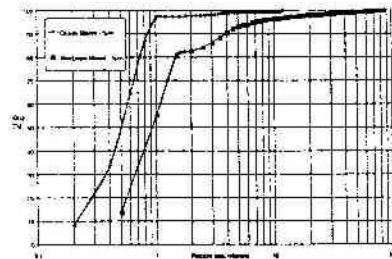


Figure 5. Comparative PSD curves for filtrates obtained from 5 µm filter - gravity and membrane mode of coagulated dye at 100 mg/L $FeCl_3$

The results from the particle size studies indicate the growth of dye flocs size with a concomitant increase in coagulant addition. Mean particle diameter rises from 7,2 to 180 micrometers with increase of $FeCl_3$ dosage from 25 to 100 mg/L - Figure 4. Logically, the

three different S/L separation modes applied are ensuring nearly identical particle size distribution characteristics of the supernatant regardless the initial dosage of coagulant. For the case of 100 mg/L, a slight increase in mean particle size for dye passed through 5 µm filter could be observed in comparison to the two filtrated samples, respectively 0.9 and 0,7 µm, Figure 3. The observations provide a good basis for commenting further the degree of color removal achievable with the different S/L separation methods tested. It should be noted, that slight post flocculation inside the CIS-100 measuring cuvette could not be excluded to occur during particle size measurements. This could explain the occurrence of particles bigger than 0.2 µm in all the filtrates coming after 0,2 µm membrane filtration and also the occurrence of particles larger than 5 µm in the filtrate which has been passed through the 5 µm membrane - Figure 4.

3.2 Membrane filtration and centrifugation of coagulated dyes - effects on streaming current potential

Generally the titration curves obtainable by PCD devices, apart from yielding directly the actual charge content of a sample, based on its cationic/anionic demand, are also a convenient way for illustration colloidal systems response towards stabilization/destabilization. Streaming current methods are widely used in wet-end industrial operations optimization. We believe such studies will be also useful in revealing the effects which accompany dye effluents coagulation. Figures 6 - 9 below present the dye slurries titration curves obtained for each coagulant dose level used.

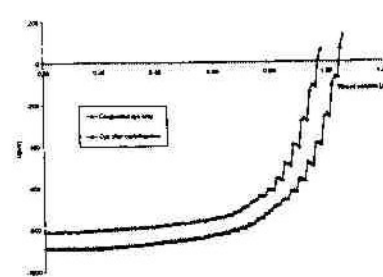


Figure 6. PCD titration curves for coagulated dye before and after centrifugation ($FeCl_3$ - 25 mg/L)

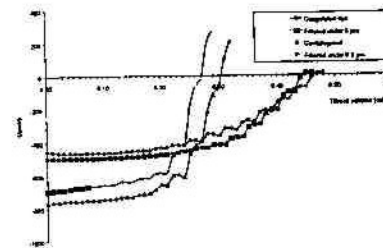


Figure 7. PCD titration curves for coagulated dye before and after solid/liquid separation ($FeCl_3$ - 50 mg/L)

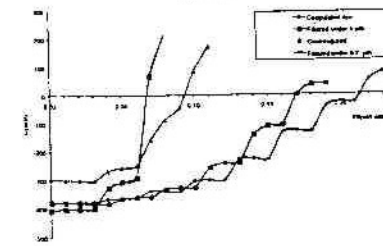


Figure 8. PCD titration curves for coagulated dye before and after solid/liquid separation ($FeCl_3$ - 75 mg/L)

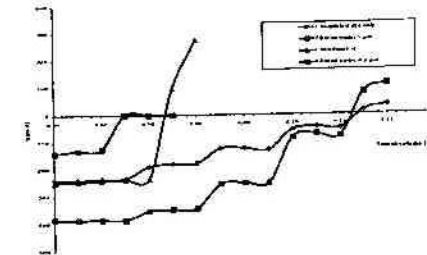


Figure 9. PCD titration curves for coagulated dye before and after solid/liquid separation ($FeCl_3$ - 100 mg/L)

3.3 Surface charge and color removal after membrane filtration and centrifugation

In order to link the findings obtained from the charge characterization with the color removal achievable under membrane filtration and centrifugation, a summarizing plot has been drawn at Figure 10 below.

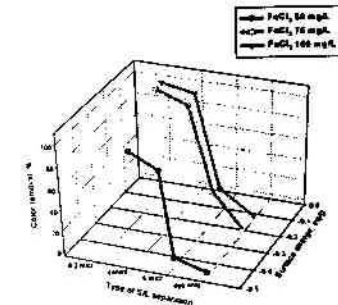


Figure 10. Color removal and surface charge as function of S/L separation type applied for dye coagulated at different $FeCl_3$ dosages

4. DISCUSSION

The results shown at Figures 6 to 9 indicate a trend for decreasing of titrant amount required for reaching the Point of Zero Charge as function of sludge separation approach chosen. This means that surface charge is shifted to positive values as coagulant dosage

is increased, Figure 10. The observation is valid for all the studied ranges of coagulant dosages and is especially pronounced when the dye sludge was subjected to 0,2 microns membrane filtration and centrifugation.

Additionally, when correlating the results at Figures 1 to 3 with those shown at Figure 10, an interesting notion about the effect of the different solid/liquid separation modes applied could be figured out. The degree of color removal is different in the filtrate after 5 micron membrane filtration and in the clear supernatant after centrifugation, regardless of the similar particle size characteristics which both liquors possess, especially at dosages below 100 mg/L. When coagulant dosage is increased to 75 mg/L and above, it is observed that both centrifugation and membrane filtration via 0,2 µm guarantee color removal above 90 %, Figure 10. This is not the case when 5 µm membrane filtration is used. From other side, lower color removal, around 60 % was achieved for 50 mg/L coagulant with centrifugation. This could be explained by the fact that perhaps at 50 mg/L dose level, the size and density of the generated flocs are relatively small, hence centrifugation is not in position to pack them sufficiently at the bottom of the centrifugation burette and accordingly fails to reach sufficiently clear supernatant.

The results shown at Figure 5 also provide an interesting standing point for interpretation regarding the role which solid/liquid separation mode plays. When dye coagulated with 100 mg/L has been filtrated through 5 micrometers membrane under pressure and 5 micrometers filter under gravity, a completely different surface charge and color removal are observed, although the later data are not presented in this paper. An implication is that regardless of the equal pore openings of the filtration media used, the manner under which filtration itself is practiced has an influence upon surface charge and color removal, moreover taking into consideration the relatively similar particle size characteristics of both supernatants - Figure 5. One possible explanation could be found in eventual dye flocs erosion and dissemination by the forces occurring during membrane filtration, thus releasing color back in filtrate. Such a phenomena could not be anticipated during the "calm" gravity filtration.

5. CONCLUSIONS

Charge neutralization seems to be the predominant mechanism for coagulation/color removal for the investigated combination dye - inorganic coagulant. In the other cases investigated elsewhere, the lack of correlation between surface charge and degree of color removal is supporting a mixed removal mechanism involving also enmeshment and specific chemical interaction.

The way by which filtration is practiced, under gravity or pressure, has an influence upon surface charge of suspension/supernatant and color removal. Although the results not shown, we have established that a gravity filtration through 5 µm filter could prove a preferable option for sludge retaining, since it ensures "calm" conditions for slurry drainage and clear filtrate with almost total color removal when 100 mg/L FeCl₃ was used. The chosen system dye-coagulant provides a reliable model for further insights and interpretations in direction of the effects which particle characteristics (size and charge) could have on coagulation and flocculation in general.

The presented study although initial, provides an interesting view in direction dye coagulation mechanisms investigation and by no means warrants further research with other dye classes, as well as such in direction of more detail floc characterizations encompassing morphology, shape and density.

REFERENCES

- Besra, L., Sengupta, D., Roy, S., Ay, P. (2002). *Int. J. of Min. Proc.*, 66 (1-4), 183-202.
- Gaydardzhiev, S., Karthikeyan, J., Ay, P. (2003). Progression of surface charge during textile dye color removal by chemical coagulation, paper submitted for publication in JSDC "Coloration technology".
- Marmagne, O., Coste, C. (1996). *American Dyestuff Reporter*, April, 15-21.
- Robinson, T., McMullan, G., Marchant, R., Nigam, P. (2001). *Bioresource Technology*, 77 (3), 247-255.
- Tünay, O., Kabdasi, I., Eremektar, G., Orhon, D. (1996). *Wat. Sci. Tech.*, 34 (11) 9-16.

THE MODERN ION-EXCHANGE TECHNOLOGY FROM VARIOUS VIEWS OF RAW MATERIALS

A.A.Kopyrin, A.A.Blohin, M.H.Ekzekov
*International academy of sciences of ecology and Saint-Petersburg, Institute per., 5;
Saint-Petersburg State Institute of Technology (T
Moskovskiy pr., 26; E-mail: Kopyrin@tu.spb.ru*

ABSTRACT:

Data on ion-exchange technologies of associated extraction of rhenium from molybdenite concentrates, which are given. Materials, are given.

Keywords: rhenium, extraction, ion exchange, molybdenite

1. INTRODUCTION

Rhenium is one of the elements least widespread in an earth's crust and has no natural deposits. It is extracted in passing at processing molybdenic, copper and some other ores on the base ingredients, and also at salvaging the secondary and some kinds of man-caused raw material. The most perspective method of extraction of rhenium from water solutions alongside with liquid-liquid extraction is ion exchange. In the present work the data received by development of ion-exchange technologies of associated extraction of rhenium from two objects are given: from molybdenic concentrates at their processing on nitric acid schema and from copper-nickel ores.

2. GENERAL

2.1. Extraction of rhenium at processing molybdenites concentrates

Molybdenites are the most affluent raw sources of rhenium. The content of rhenium in molybdenites concentrates can attain the tenth fractions of percent. The first stage of processing molybdenite concentrates always is their oxidizing. In practice for achievement of this purpose resort to oxidizing roasting more often. The alternate in relation to oxidizing roasting are only hydrometallurgical methods, founded on processing of concentrates by solutions of oxidizing agents, in particular, of hydrogen nitrate. Advantages of a method, which is

International Seminar
on
**Mineral Processing Technology
(MPT-2004)**

19-21 February 2004

Edited by

**G.V. Rao
Vibhuti N Misra**

Jointly Organised by

Regional Research Laboratory
(Council of Scientific & Industrial Research)
Bhubaneswar

&

Indian Institute of Mineral Engineers



ALLIED PUBLISHERS PRIVATE LIMITED

*New Delhi • Mumbai • Kolkata • Lucknow • Chennai
Nagpur • Bangalore • Hyderabad • Ahmedabad*

Surface Charge Studies - An Important Approach for Investigation of Colour Removal from Textile Wastewaters by Chemical Coagulation

S. Gaydardzhiev and P. Ay

Chair of Mineral Processing,
Branddenburg Technical University,
Cottbus 03046,
Cottbus,
Germany
e-mail: gaydar@tu-cottbus.de

Abstract

Surface charge measurements of coagulated dye sludge aimed to establish a correlation between its sign and progression and the degree of colour removal by chemical coagulation are presented. A model wastewater comprising of commercially used dye with a CI "Reactive Red 2" was used. The effect of the combination coagulant/flocculant on colour removal in case of sludge filtration and sedimentation is evaluated. Measurements of mean floc size and fractal dimension were performed on selected sludge samples. An implication about the predominant colour removal mechanisms has been drawn.

Keywords: coagulation, flocculation, colour removal, surface charge, particle characterisation.

Introduction

Colour removal from spent dye house effluents is an important issue facing both academic and industrial communities. An increasing concern is the fact that regardless the type of wastewater treatment plant utilised, large amount of colour finds its way through and possibly further which is leading to appreciable environmental load. As a response to the much more stringent regulations which are continuing to be imposed, the development of more efficient treatment approaches seems a challenging task. Many techniques have been tried in this context with a various level of effectiveness ranging from moderate to higher. Regardless the number of research and academic studies performed by far, they have not led to a desired breakthrough developments which could provide consensus for a technologically feasible and economically acceptable method to be used on a single basis (Robinson et al. 2001). Emerging technologies have been found effective on a singular basis imparting a certain degree of colour removal, but a combination of two or more methods appears to be a preferred practice (Hatton and Simson 1986, Kang and Chang 1997). Among others, coagulation and flocculation remain as a mostly employed methods for treatment of dye waste effluents. However, in order to assess more realistic the potential which the physicochemical methods have for the area of colour removal, a systematic studies attempting to reveal the responsible mechanisms taking place are required. It is hoped that such an approach will help also to combat the problems originating in the large amount of sludge generated which sill requires disposal.

In trying to tackle these problems, a study program was initiated encompassing both characterisation of surface charge of coagulated sludge and measurement of flocs in terms of size and shape. We have previously reported (Gaydardzhiev, Karthikeyan and Ay 2003) about correlation between the surface charge of coagulated dye sludge, the dose level of inorganic

coagulant supplied and the colour removal degree achievable for two dyes belonging to Disperse and Acid classes. The present work is a further continuation in this direction dealing with the effect from a complementary addition of flocculant to the primary coagulant, i.e. investigating the so-called Chemically Assisted Sedimentation (CAS) mode. The aim of the later approach is to produce flocs with compact structure and improved settling ability which could ultimately lead to a reduced sludge volume.

Materials and Methods

Test dye solution

The dye used in the course of the study had a generic name CI Reactive Red 2, a monoazo dye produced by Atic Industries, India. The test solution was prepared by dissolving 100 mg dye powder in 1 L distilled water.

Chemicals

A ZETAG 7103 polyelectrolyte produced by CIBA was used as a primary coagulant for destabilisation the colloidal dye suspension. It bears high charge and relatively low molecular weight (MW). A C-573 cationic polyamine flocculant (high charge, middle MW) and N300 - a non-ionic one, both from Cytec were used in combination with the primary coagulant. All chemicals were prepared as 0.01 % solutions and applied following manufacturers guidelines.

Coagulation/flocculation, filtration and sedimentation

A 100 mL from the test dye solution was transferred in a 200 mL beaker and placed on a flat 3-cm six-blade paddle from Janke & Kunkel, Germany. A predetermined quantity of the primary coagulant was added to the dye solution. The pH of reaction solution was quickly adjusted to 6 and mixed by stirring at 200 rpm for two minutes, after that stirring speed was increased to 500 rpm and kept at this level for one minute meantime introducing the flocculant. The flocculation was then carried out for further 5 minutes at a reduced speed of 40 rpm. Immediately after, a 10 mL aliquot was taken for surface charge determination. The rest suspension was further transferred into a funnel fitted with paper filter having ca 6 μm pore openings and filtered by gravity. An identical test was carried out parallel, however instead being filtered the coagulated dye solution was allowed to stand for 90 minutes without disturbance. In the first case, an aliquot from the filtrate and in the second case, a sample from the clear supernatant were collected and analysed for residual colour concentration. For the comparative case of coagulation used alone, the flocculation step was skipped.

Determination of surface charge

Surface charge density determination for the coagulated dye sludges was carried out by means of a particle charge detector PCD-03-pH from Mutek, Germany. It consists from cylindrical test cell fitted with a displacement piston, which moves back and forth at constant frequency, forcing a relative motion between liquid and particles inducing development of a streaming potential of either positive or negative sign. The exact magnitude of charge density was estimated by titration with oppositely charged standard polyelectrolyte titrant until neutralization of the streaming potential to zero value. The unit was coupled to a "SM Titrino 702" Metrohm titrator and interfaced to a PC, which enables on-line monitoring of titration and results printout in table or graphical forms.

Meas:

Colour Spectro calcula

Partic

Particle by mea range, i to obta dimens the adv porosity structur structur Jung, A measure transfor and a st taken as used, in: mL syria shear flo

When no being qu of the M

Results

The pres reagent d higher ra mg/L. Th delineate alone and

In our rec only from are unlik polymeric generate l. measurem study.

Figures 1 charge pro flocc diame

Measurement of colour removal

Colour concentration was estimated by means of a VIS spectral photometry (Genesys 10, Thermo Spectronic) at 525 nm, i.e. the wavelength giving maximum absorbance. The removal degree was calculated based on the colour concentration difference between initial and treated samples.

Particle size distribution and fractal dimension measurement

Particle size measurement of the sludge flocs coming from the cationic flocculant case was done by means of a Malvern Mastersizer X laser scattering instrument. Owing to the expected size range, a focal lens of 300 mm was used. The particle sizing software of the Mastersizer was used to obtain data about mean particle diameter, while raw light energy data were used for fractal dimension estimation using the LALS (Low Angle Light Scattering) technique. This method has the advantage in avoiding the difficulties encountered by other methods needing to consider floc porosity. The fractal dimension provides estimation about the compactness of an aggregate structure and lies between 1 and 3, with loose structures having low fractal dimension and compact structures, a higher one. The LALS technique is described in details elsewhere (Bushel et al. 2002, Jung, Amal and Raper 1995) and basically consists on recording raw light energy data after each measurement and pasting it into an Excel spreadsheet supplied by Malvern which further transforms the data into light intensity. The light intensity data were plotted versus scattering angle and a straight line was fitted to the linear section of the relationship. The fractal dimension was taken as equal to the gradient of the fitted line. The normal sample cell of the Mastersizer was not used, instead the dye sludge was drawn from the beaker to the measuring cell by means of a 150 ml. syringe fitted with a 8 mm Typhon tubing. The setup was so designed as to allow very low shear flow avoiding flocs disruption and an easy cell emptying.

When non-ionic flocculant was used however, the flocs produced have been visually detected as being quite larger, reaching nearly 2 micrometers in size thus exceeding the upper detection limit of the Mastersizer. Therefore floc size measurement was omitted in this case.

Results and Discussion

The present study has been adhered to an optimum coagulation conditions regarding pH and reagent dose level established from initial screening tests. Thus, in order to cover both lower and higher ranges, the dose levels for the primary coagulant have been chosen as 75, 250 and 300 mg/l. The supplementary addition of flocculant has been varied at two levels: 15 and 25 mg/L. To delineate the effect from flocculant addition, two treatments were compared: primary coagulant alone and coagulant/flocculant combination.

In our recent work (Gaydardzhiev and Ay), we have established that sludge floc samples resulting only from primary coagulant addition consist of aggregates which owing to their size and shape are unlikely to settle rapidly although filtration removal was quite sufficient. An addition of polymeric flocculants parallel to effecting the surface charge in case of cationic flocculant, could generate larger and tear-resistant flocs with improved settling properties. Therefore, when possible measurements of mean diameter and fractal dimension of sludge flocs have been integrated in the study.

Figures 1 to 3 bellow, summarise the results about the effect of the cationic flocculant on surface charge progression and on colour removal by filtration and sedimentation. Additionally, the mean floc diameter obtained by the Mastersizer was plotted and the fractal dimension data derived from

the LALS technique were presented inside the graph as well. The results from the non-ionic flocculant case are shown at Figures 4 to 6 respectively.

CAS with cationic flocculant

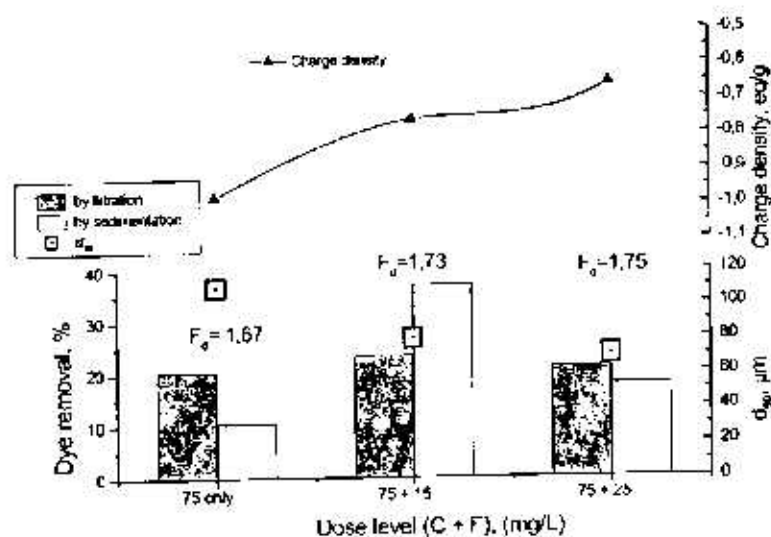


Figure
sludge

CAS

Figure 1. Effect of cationic flocculant addition on surface charge density, colour removal and sludge floc characteristics (75 mg/l primary coagulant)

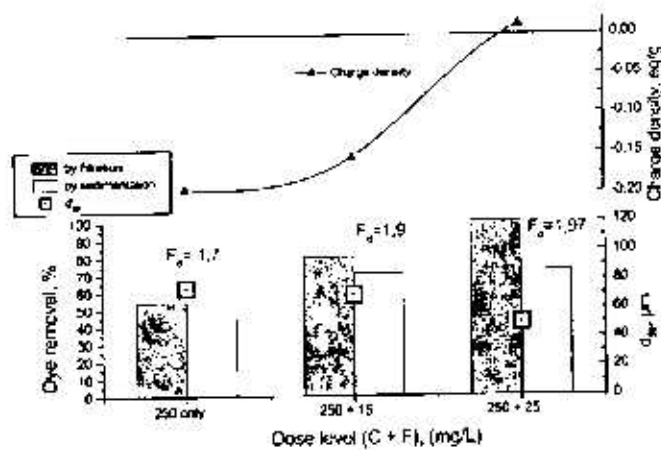


Figure
remt

Figure 2. Effect of cationic flocculant addition on surface charge density, colour removal and sludge floc characteristics (250 mg/l primary coagulant)

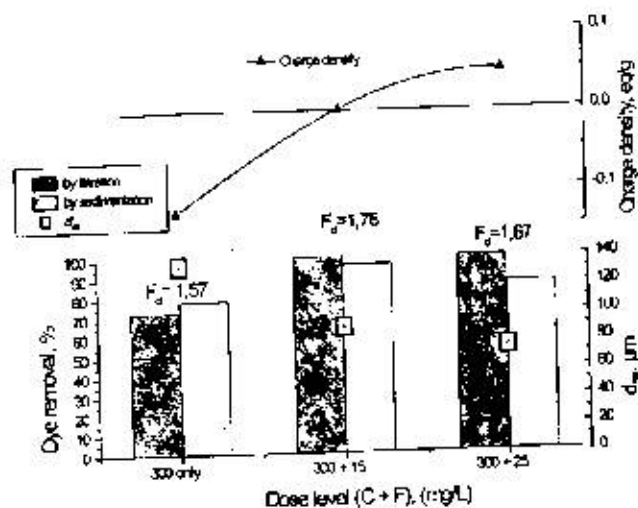


Figure 3. Effect of cationic flocculant addition on surface charge density, colour removal and sludge floc characteristics (300 mg/L primary coagulant)

CAS with non-ionic flocculant

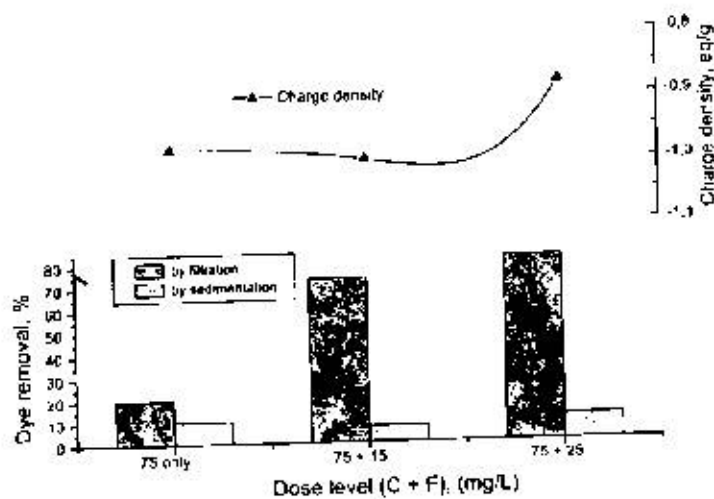


Figure 4. Effect of non-ionic flocculant addition on surface charge density and colour removal (75 mg/L primary coagulant)

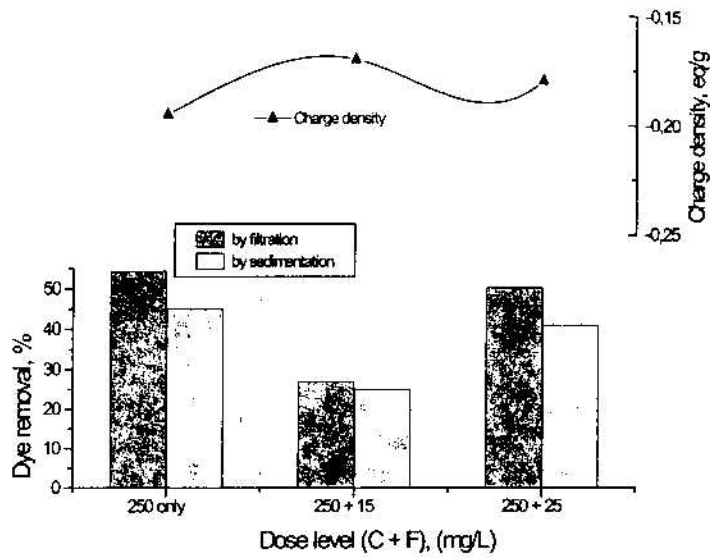


Figure 5. Effect of non-ionic flocculant addition on surface charge density and colour removal (250 mg/L primary coagulant)

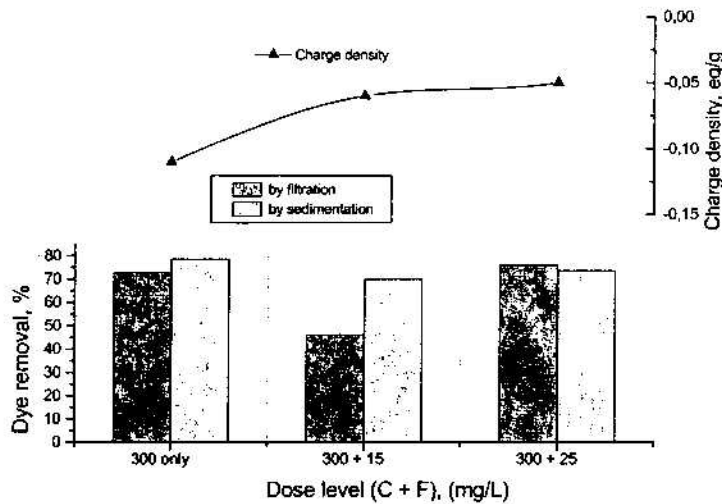


Figure 6. Effect of non-ionic flocculant addition on surface charge density and colour removal (300 mg/L primary coagulant)

The perusal of the results about mean floc size shown at Figures 1 to 3 indicate, that the progressive addition of cationic flocculant has led to reduction in mean size of sludge flocs. For

the 75 mg/L primary coagulant base level, the mean floc diameter drops from ca 120 μm without flocculant addition to 70 μm with 25 mg/L flocculant addition. Similar trend is observed for the cases of 250 and 300 mg/L primary coagulant base level. The floc fractal dimensions does not differ significantly, with the exception of the 250 mg/L primary coagulant dose level case - Figure 2, where the flocculant addition is producing more compact aggregates reaching fractal dimension of 1.96. The better compacted flocs from the 250+25 case however, have not lead to an improved removal by sedimentation perhaps due to their relatively small size. The best sedimentation removal of 96 % was reached for the 300+15 combination case, where the floc was characterised by mean size of 90 μm and a fractal dimension of 1.76 and the PZC of coagulated sludge has been reached - Figure 3, the middle graph. For this case, the good correlation between PZC and colour removal provides assumption that the adsorption of positive primary coagulant species onto dye colloids surface is leading to their charge neutralisation and subsequent aggregation via electrostatic forces. With further increase in flocculant dose to 25 mg/L the charge increases, the floc size slightly decreases and the fractal dimension also, which logically is leading to decrease in sedimentation removal from 96 to 85 %. Here, since filtration removal doesn't drop as a result from the observed surface charge sign reversal through an inflex point, suspension re-stabilization could not be expected. Hence the removal could be due to enmeshment of colour colloids within the bulky flocs formed by the primary coagulant similar to sweep flocculation. For the case of combination primary coagulant at 75 mg/L and cationic flocculant we could see that regardless flocs have reached similar size and fractal dimension like in the case of 250 and 300 mg/L base level, the removal neither by sedimentation nor by filtration was satisfactory. Perhaps this is due to the fact that the supplied amount of coagulant and flocculant does not suffice to destabilise the dye suspension to a sufficient extent, supported also by the moderate surface charge shift towards PZC.

For the case of non-ionic flocculant addition, it is interesting to note that when it has been added to a primary coagulant dose of 75 mg/L, far better removal by filtration reaching 75 and 85 % respectively for 15 and 25 mg/L dose levels could be achieved in comparison to the 22 % removal when cationic flocculant was used. This phenomena could be explained by the fact that the non-ionic flocculant addition generates tear resistive aggregates. Accordingly, those aggregates are well retained by the filter entrapping also the primary destabilised dye particles during suspension filtration. In the case of gravity settling however, part of the dye flocs which initially have not being taken by the non-ionic flocculant cluster are not in position to settle as a single particles for the given time of 90 minutes, explaining the low sedimentation removal. Since the sludge surface charge is well below the PZC, bridging flocculation could be suspected to take place in the above discussed case. The addition of non-ionic flocculant to primary coagulant dose level of 250 and 300 mg/L has not led to colour removal improvement neither by sedimentation nor by filtration. Even slight worsening of removal results could be noted - Figures 5 and 6. It is difficult to explain the reasons behind these phenomena moreover taking into account the lack of particle size data for that case. Perhaps, a mixed removal mechanism encompassing both charge neutralisation and particle bridging or enmeshment could be presumed for the cases of 250 and 300 mg/L coagulant level.

Conclusions

Being preliminary, the results from the presented study certainly do not permit a conclusion of fundamental validity to be drawn, but are believed to be useful both from colour removal and particle characterisation perspectives. The usefulness of surface charge measurement in coagulation and flocculation is demonstrated as a tool for mechanism investigation. Chemically assisted sedimentation (CAS) involving combination of either minute addition of cationic

polyamine or non-ionic flocculant to a primary coagulant initially supplied produces floc aggregates with different size and shape, bearing different filterability and settling behaviour. The fractal dimension derived from the LALS studies, should be treated with care and validated by other methods capable of yielding shape parameters or density relevant information.

References

1. Bushel et al. 2002. On techniques for the measurement of the mass fractal dimension of aggregates, *Adv. in Coll. and Interf. Sc.* 95:1-50.
2. Gaydardzhiev, S., Ay, P., 2003. Removal of dyes from effluents by chemical coagulation - surface charge and particle size aspects, in *Proceedings of the Xth Balkan Mineral Processing Congress*, Varna, Bulgaria, 15-20 VI 2003, p. 403 – 408.
3. Gaydardzhiev, S., Karthikeyan, J., Ay, P. 2003. Progression of surface charge during textile dye colour removal by chemical coagulation, submitted in *JSDC Coloration technology*.
4. Hatton, W., Simpson, A., 1986, Enhanced colour removal from sewage effluents using chemically flocculants. *Env. Techn. Letters.* 7:413-424.
5. Jung, S., Amal, R., Raper J. 1995. The use of small angle light scattering to study structure of flocs, *Part. Part. Syst. Charact.* 12:274-278.
6. Kang, S., Chang, H., 1997, Coagulation of textile secondary effluents with Fenton' reagent. *Wat. Sci. Techn.* 36:215-222.
7. Robinson, T., McMullan, G., Marchant, R., Nigam, P. 2001. Remediation of dyes in textile effluent: a critical review on current treatment technologies with a proposed alternatives, *Bioresource Techn.* 77:247-255.
8. Tang P., Raper J. 2002. Modelling of settling behaviour of aggregates – a review. *Powder Technology.* 123:114-125.

<p>P902 Imaging based optical sensors for ultrafine particle characterisation through a 2D fractal approach: "On-line" architecture set-up</p> <p><u>Bonifazi</u>, Greco (<i>U. Roma, Italy</i>)</p>	<p>P910 Optimizing the bipolar coagulation reactor</p> <p><u>Verdoold</u>, Marijnissen (<i>TU Delft, Netherlands</i>)</p>	<p>P918 Dispersion of fine powders by a jet superheated of a multicomponent liquid</p> <p><u>Stroutchayev</u>, Kopyt, Karelin (<i>Odessa Nat.U., Ukraine</i>)</p>
<p>P903 Simultaneous calculation of absorption and aerosol behaviour in a 2-stage HCl scrubber</p> <p><u>Brosig</u>, Luckas, Schmidt (<i>U. Duisburg-Essen, Germany</i>), Bittig, Haep (<i>IUTA e.V., Germany</i>)</p>	<p>P911 Mix-Technology of creation of standards of difficultly reproduced aerosol media with physical analogs and mathematical models</p> <p><u>Fertman</u>, Rizin (<i>SNIIP, Moscow, Russia</i>)</p>	<p>P919 Modeling of micronic Y(NO₃)₃ particles formation by spray pyrolysis</p> <p><u>Reuge</u>, Caussat (<i>ENSIACET, Toulouse, France</i>), Joffin, Dexpert, Verelst (<i>CEMES, France</i>)</p>
<p>P904 Powder nano-coating by atomic layer deposition in fluidized beds</p> <p>Hakim, Wank, Ferguson, Buechler, George, <u>Weimer</u> (<i>U. Colorado, USA</i>)</p>	<p>P912 Technology of disperse control for particular aerosols. Principles of optimization</p> <p><u>Rizin</u>, Fertman (<i>SNIIP, Moscow, Russia</i>)</p>	<p>P920 Controlled Particle Deposition by Design of an Electrochemical Adsorption Cell</p> <p><u>Bakhshi</u>, Taghikhani (<i>Tehran U., Iran</i>)</p>
<p>P905 Implication of surface charge effects in color removal from effluents by chemical coagulation the case of Cl Reactive Blue 4 dye</p> <p><u>Gaydardzhiev</u>, Ay (<i>BTU Cottbus, Germany</i>)</p>	<p>P913 Kinetics of thermal and diffusional processes at hydrogen dissolving in dispersed titanium</p> <p><u>Kopyt</u>, Sadli A., Sadli T., Milova (<i>Odessa Nat.U., Ukraine</i>)</p>	<p>P921 Plasma Treatment of Polymer Powders</p> <p><u>Arpagaus</u>, Von Rohr (<i>ETH Zurich, Switzerland</i>)</p>
<p>P906 Experiments and simulation of charged particle sprays</p> <p><u>Mueller</u>, Winkels, Geerse, Marijnissen, Schmidt-Ott, Luding (<i>TU Delft, Netherlands</i>)</p>	<p>P914 The temperature factor in the process of nitrogen dissolution in dispersed titanium</p> <p>Kopyt, Sadli A., <u>Sadli T.</u>, Milova (<i>Odessa Nat.U., Ukraine</i>)</p>	
<p>P907 Simulation of the powder coating process</p> <p><u>Domnick</u>, Ye (<i>Fraunhofer-IPA, Stuttgart, Germany</i>)</p>	<p>P915 Coating of aluminum particles with titanium deposits by magnetron DC sputtering</p> <p><u>Sonoda</u>, Watazu, Katou, Yamada, Asahina (<i>AIST, Japan</i>)</p>	
<p>P908 A short-cut model for free-molecular aggregation with continuous addition</p> <p><u>Wynn</u> (<i>U. Birmingham, United Kingdom</i>)</p>	<p>P916 Influence of particle and coating suspension characteristics on the coating process in spouted bed</p> <p><u>Donida</u>, Rocha (<i>State U. Campinas, Brazil</i>)</p>	
<p>P909 Statistical modelling of the spouted bed coating process using Positron Emission Particle Tracking (PEPT) data</p> <p><u>Seiler</u>, Fryer, Seville (<i>U. Birmingham, United Kingdom</i>)</p>	<p>P917 Size dependence of macroparticles electric charge in heterogeneous plasma</p> <p><u>Marenkov</u>, Naboka (<i>Odessa Nat.U., Ukraine</i>)</p>	

Implication of surface charge effects in colour removal from effluents by chemical coagulation – the case of CI “Reactive Blue 4” dye

Stoyan Gaydardzhiev, Peter Ay

Chair of Mineral Processing, Brandenburgische Technische Universität Cottbus, Th. Neubauer Straße 4-b, 03046 Cottbus, Germany

ABSTRACT

Characterizations of coagulated dye sludge in terms of surface charge and floc size and shape are presented with an aim to evaluate the colloidal destabilization mechanism, which takes place during colour removal by chemical coagulation. A simple system comprising of commercially used dye with a CI “Reactive Blue 4” and ferric chloride as primary coagulant was chosen. A supplementary addition of polymeric flocculant to the primary coagulant was tried with a twofold purpose: to reduce coagulant dose level and to generate flocs with improved settling properties. It was established that colour removal could be predominately governed by charge neutralization or by bridging mechanism when different coagulant-flocculant combinations were tested. These presumptions are based on the measured surface charge of sludge and on the different characteristics of flocs as well.

1 INTRODUCTION

The presence and necessity for removal of colour from waste effluents is by no doubts a major challenge both for the scientific community and for the dyes manufacturing companies. A fact is that widely used in this area are bright spectra of techniques like chemical, physicochemical and biological processes. However, despite the significant number of research and academic studies performed, there is by far a lack of agreed view towards technologically feasible and economically acceptable single method [1]. Emerging technologies have been found effective on a singular basis imparting a certain degree of colour removal, but a combination of two or more methods appears to be a preferred practice [2, 3]. Chemical coagulation is foremost among the methods employed for treatment of dye house effluents, being practiced as pre-, post- or main process. The peculiarity however is, that while certain application classes of dyes respond favourably to chemical treatment, others, notably acid, developed and basic fail to respond at all. As a whole, it may be reckoned that coagulation and flocculation go rarely with process optimisation together and are practiced more like an art, rather than like science without attempting to reveal the responsible mechanisms. The problem is further aggregated by the large amount of sludge generated which still requires disposal. In trying to approach these problems, a two-component research program was initiated, the first stage directed towards charge measurement only and the second towards floc characterisation. In our previous work [4], we have reported about the anticipated colour removal mechanism based upon correlation between surface charge of dye sludge and coagulant dose level and colour removal degree for two dyes belonging to Disperse and Acid classes. The present study is a continuation in this direction dealing with the effect from a

complementary addition of flocculant to a significantly reduced dose of coagulant. The aim is to improve sludge settling ability by involving the so-called Chemically Assisted Sedimentation (CAS) with a parallel size and shape analysis of sludge flocs.

2 MATERIALS AND METHODS

2.1 Test dye solution

The dye used in the course of the study had a generic name Reactive Blue 4, an anthraquinone based dye produced by Atic Industries, India. Test dye solutions were prepared by dissolving 100 mg dye powder in 1 L distilled water.

2.2 Chemicals

As a primary coagulant, ferric chloride - FeCl_3 (a.g.) supplied by Merck was used in concentration of 10 g/L, prepared fresh before each test run. A C-573 polyamine cationic flocculant (high charge, middle MW) and N300 a non-ionic one, both produced by Cytec were used. They were prepared as 0.01 % solutions and applied following manufacturer guidelines.

2.2 Coagulation/flocculation, filtration and sedimentation

A 100 mL of the test dye solution was transferred in a 200 mL beaker and placed on a flat 3-cm six-blade paddle from Janke & Kunkel, Germany, A predetermined quantity of coagulant was added to the dye solution. The pH of reaction solution was quickly adjusted to 6 and mixed by stirring at 200 rpm for two minutes, after that stirring speed was increased to 500 rpm and kept at this level for one minute meantime introducing the flocculant. The flocculation was then carried out for further 5 minutes at a reduced speed of 40 rpm. Immediately after, a 10 mL aliquot was taken for surface charge determination. The rest suspension was further

transferred into a funnel fitted with yellow band filter paper having ca. 6 μm pore openings and filtered by gravity. An identical test was carried out parallel, however instead being filtrated, the coagulated dye solution was allowed to stand for 90 minutes without disturbance. In the first case, an aliquot from the filtrate and in the second case, a sample from the clear supernatant were collected and analysed for surface charge and residual colour concentration. In case of coagulation only, the flocculation step was skipped.

2.3 Determination of surface charge

Determination of surface charge for the coagulated suspensions, filtrates and supernatants was carried out by means of a particle charge detector PCD-03-pH from Müttek, Germany. It consists of cylindrical test cell fitted with a displacement piston, which moves back and forth at constant frequency, forcing a relative motion between liquid and particles inducing development of a streaming potential of either positive or negative sign. The exact magnitude of the charge was estimated by titration with oppositely charged standard polyelectrolyte titrant until neutralization of the streaming potential to zero value. The unit was coupled to a "SM Titrino 702" Metrohm titrator and interfaced to a PC, which enables on-line monitoring of titration and results printout in table or graphical forms.

2.4 Measurement of colour removal

Colour concentration was estimated by means of VIS spectral photometry (Genesys 10, Thermo Spectronic) at 598 nm, i.e. the wavelength giving maximum absorbance.

2.5 Particle size distribution and image analysis

Particle size measurements of dye flocs for the cationic flocculant case were done by a CIS-100 GALAI system, a laser based particle counter employing a "time-off-transition" principle, providing as primary output the number size distribution, which then is used to yield volume size distribution. Magnetic stirrer speed inside the measuring cuvette was set to low in order to keep flocs in motion without disruption. Image analysis of the flocculated sludge was carried out by means of a "Leica - Q600" system giving "Roundness" and "Aspect Ratio" as shape factors. Image analysis was used also for measuring floc size for the non-ionic flocculant case, since the flocs produced at this case were exceeding the upper limit of the CIS-100 system. A wide mouth pipette was used to sample sludge volume and to transfer the flocs from the beaker after flocculation into the observation glass. Before being examined, the sample was diluted with bi-distilled water. A constant light level was maintained in all measurements and a special care was taken during sample observation in order to ensure that single floc aggregates were examined. Each

measurement encompassed about 100 individual objects being detected and measured. The values given for "Roundness" and "Aspect Ratio" are an average from five measurements of each sample.

3 RESULTS AND DISCUSSION

The present study has been adhered to a previously established optimal coagulation conditions for pH and FeCl_3 dosage. The optimum found coagulant dose level was however reduced to 30, 40 and 50 mg/L, since here the focus was on investigating the progression of sludge charge resulting from a supplementary addition of a minute amounts of flocculant (5, 10 and 15 mg/L) to a reduced coagulant dose and on correlation of this data with the colour removal degree achievable by filtration and by sedimentation. In our previous studies we have observed that sludge floc samples resulting only from primary coagulant addition are consisting of aggregates, which owing to their size and shape are unlikely to settle rapidly although filtration removal was quite sufficient. An addition of charged polymeric flocculant parallel to effecting surface charge could certainly provide a larger and tear-resistant flocs with improved sedimentation properties, therefore measurement of size and shape of the flocs deriving from flocculant addition was also set as objective. Various ways have been tried in literature to describe the sphericity of aggregates, from equivalent volume diameter to projected surface area, but none of them being sufficiently accurate to provide information on their shape irregularity and settling ability [5]. In the present study, roundness and aspect ratio have been chosen as shape parameters. The estimation for "Roundness" is given as a ratio between the squared perimeter and the projected area of an object and as such it could be viewed at first approximation as fractal dimension. The later one characterizes the compactness of an aggregate structure and lies between 1 and 3, with loose structures having low fractal dimension and compact structures, a higher one. Due to difficulties in describing irregular shapes and varying porosity of flocs, it is hard to obtain a single value to evaluate the sedimentation behaviour of floc aggregates. However it was hoped that the shape factors chosen would provide estimation about it. Since the study envisaged was a preliminary one and moreover owing to the complexity of phenomena, which need to be considered in settling behaviour studies, no attempt was made to evaluate the effect of floc porosity on their size and settling ability.

In order to delineate the effect of flocculant addition, the results obtained when flocculant was used (i.e. CAS case) are compared with those when ferric chloride alone was tested. Figs. 1 to 3 bellow, summarise results about the effect from the cationic

floculant on surface charge progression and on colour removal by filtration and sedimentation.

3.1 CAS with cationic flocculant

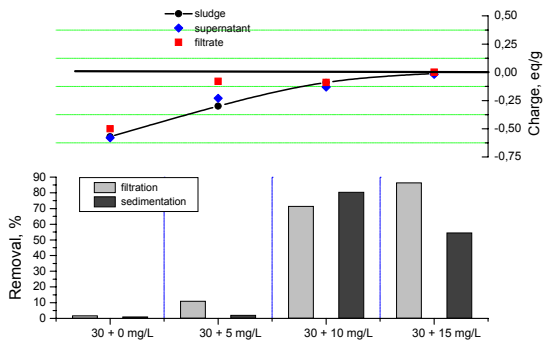


Figure 1: Effect of C573 flocculant addition on surface charge and colour removal (FeCl_3 at 30 mg/L basis)

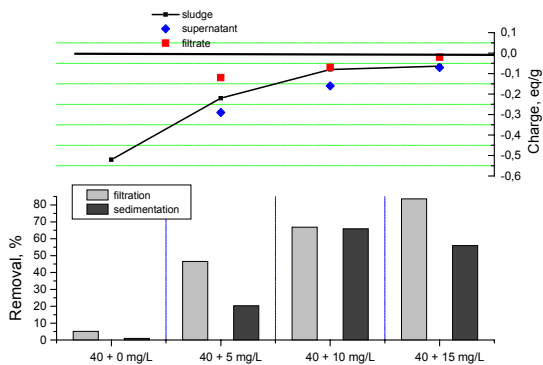


Figure 2: Effect of C573 flocculant addition on surface charge and colour removal (FeCl_3 at 40 mg/L basis)

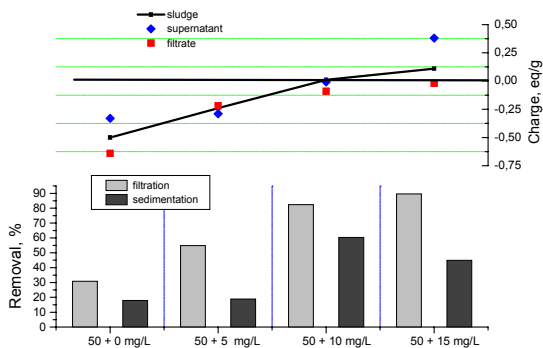


Figure 3: Effect of C573 flocculant addition on surface charge and colour removal (FeCl_3 at 50 mg/L basis)

Data shown at Figs. 1 to 3 indicate, that as the dose level of cationic flocculant increases, colour removal by filtration also increases reaching nearly 90 %, with a concomitant decrease in the negative surface charge magnitude – an indication of charge neutralization mechanism. For the sedimentation case however, the maximum removal point

corresponds close to the PZC of coagulated sludge. For sedimentation we have an optimum flocculant dose of 10 mg/L for all the three ferric chloride base level doses. The best removal by sedimentation (ca 80 %) was achieved for the case coagulant-flocculant combination of 30 + 10 mg/L. For the instance of 40 mg/L ferric chloride baseline dose, complete charge neutralisation of dye colloids has not taken place even when 15 mg/L flocculant was added. On the other hand, at 50 mg/L ferric chloride the progressive increase in flocculant dose resulted not only in maximum colour removal by filtration accompanied by a reduction in surface charge, but also has led to charge reversal at 15 mg/L flocculant addition. However, the fact that the observed charge reversal is accompanied by decrease in colour removal by sedimentation, is an implication that particle re-stabilisation might have occur, which from its side suggests again charge neutralisation as a main removal mechanism. It is interesting to compare and comment on the surface charge pertinent to filtrates and supernatants. Generally, the surface charge of filtered samples follows a trend similar to that of the sludge with nearly neutral values for the cases of flocculant co-addition irrespective from initial ferric chloride dose. The effect of the filter could not be overlooked in this context. In all CAS cases surface charge of supernatants was nearly similar to that of sludge, which could mean that different species in suspension bear charge and colour.

3.2 CAS with non-ionic flocculant

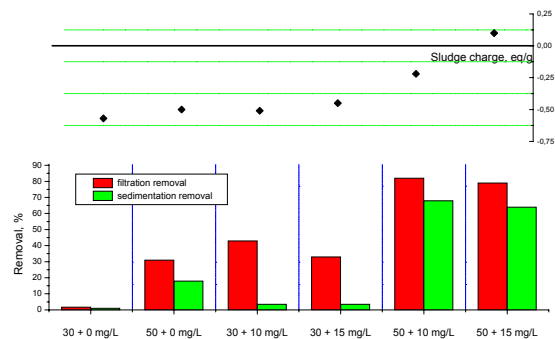


Figure 4: Effect of 10 and 15 mg/L N300 flocculant addition on surface charge and colour removal (FeCl_3 at 30 and 50 mg/L basis)

For the N300 case, two dose levels of 10 and 15 mg/L flocculant were chosen and only charge of sludge was measured. The results from Fig. 4 indicate a marked improvement in colour removal attributable to flocculant addition to 50 mg/L of FeCl_3 . Most likely, the non-ionic polymer stimulates generation of larger viscous flocs, which are easily filterable and settle better. Worth here to note is however, that sludge surface charge shifts to positive values as a result from flocculant addition. This is somehow unexpected owing to the non-ionic

character of the flocculant and the reasons for this should be investigated. Bridging flocculation could be suspected as a predominant one for the non-ionic flocculant case.

3.3 Floc characteristics

Size and shape measurements of sludge flocs were carried out in order to supplement the statements derived from surface charge studies. During the image analysis observations it was found out, that the non-ionic flocculant stimulates development of flocs with nearly bi-modal size distribution. Therefore, flocs characteristics deriving from C573 flocculant addition are presented in Table 1, while Table 2 illustrates the floc characteristics for 50+10 sample from the N300 addition, where the flocs are grouped roughly into two size categories.

Table 1. Size and shape characteristics of sludge flocs resulting from C573 flocculant addition

C+F, mg/L	Median, μm	Roundness	AR
30 only	no measurable floc	-	-
30 + 5	no measurable floc	-	-
30 + 10	160	2.2	1.9
30 + 15	180	1.7	1.8
40 only	no measurable floc	-	-
40 + 5	12	-	-
40 + 10	170	1.9	1.7
40 + 15	196	1.75	1.8
50 only	22	-	-
50 + 5	32	1.9	2.3
50 + 10	136	1.55	1.6
50 + 15	190	1.8	1.7

Table 2. Image analysis characteristics for "bimodal" sludge flocs derived from 50+10 FeCl_3 - N300 combination

Floc population	Size, μm			Roundness	AR
	d_{10}	d_{50}	d_{90}		
"fine"	55	146	212	1.7	1.8
"large"	500	1100	1800	1.8	2.1

A perusal of floc characteristics data for the case of C573 flocculant – Table 1, suggests that the dye sludge consists from flocs, which mean size increases with concomitant increase in amount of flocculant added to the primary coagulant. Sharp size increase is observed when flocculant dose was raised from 5 to 10 mg/L, after that floc size does not grow appreciably. It is interesting to note that for the case of FeCl_3 dose of 30 and 40 mg/L, the roundness value could be linked to sludge flocs settling ability. The maximum colour removal achieved by sedimentation corresponds to floc roundness of 2.2, which implies denser floc structure - the case of 30+10 combination. As noted above, the N300 flocculant stimulates development of flocs which could be grouped into two distinctly different size categories: a "larger" aggregates reaching nearly 2 mm and a "finer" ones similar in size to that produced by the cationic flocculant. At

the present stage of work it is difficult to evaluate the reasons behind this phenomena. The lack of improvement in the settling behaviour is obvious which is perhaps due to the fact that the "finer" aggregates settle under "single" rather than under "zone" settling mode. A micrograph of a typical sample from N300 (50 + 10) case is given at Fig. 5.

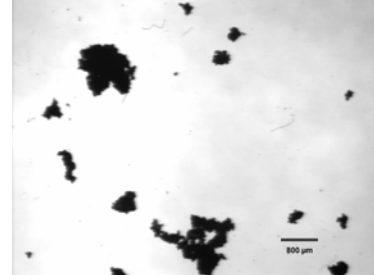


Figure 5: Image of coagulated dye aggregates (50 mg/L FeCl_3 + 10 mg/L N300)

Since the measured aspect ratios do not differ significantly, they could provide limited additional information about floc compactness, but could be used for interpreting particle size distribution data.

4 CONCLUSIONS

Being preliminary, the results from the presented study certainly do not permit a conclusion of fundamental validity to be drawn, but are believed to be useful both from colour removal and particle characterisation perspectives. CAS involving small amount cationic polyamine flocculant addition to a low dose of primary coagulant initially supplied, produces floc aggregates with median size of 140-190 μm which possess different settling behaviour. Larger and viscous in appearance aggregates could be achieved with addition of non-ionic flocculant, stimulating "bridging" mechanism. Image analysis of dye flocs seems tedious (sample preparation) and time consuming. Shape characteristics expressed as "Roundness" should be treated with care and should be validated by other methods capable of fractal dimension estimation.

REFERENCES

- [1] Robinson, T., McMullan, G., Marchant, R., Nigam, P.: *Bioresource Techn.* 77 (2001) 247-255.
- [2] W Hatton and A Simpson, *Env. Techn. Letters*, 7, (1986), 413-424
- [3] Kang, S., Chang, H.: *Wat. Sci. Tech.* 36 (1997) 215-212
- [4] Gaydardzhiev, S., Karthikeyan, J., Ay, P: Progression of surface charge during textile dye colour removal by chemical coagulation, submitted in JSDC "Coloration technology"
- [5] Tang P., Raper J.: Modelling of settling behaviour of aggregates – a review, *Powder Technology*. 123 (2002) 114-125

COLOUR REMOVAL FROM MODEL SOLUTIONS BY COAGULATION - SURFACE CHARGE AND FLOC CHARACTERISATION ASPECTS

S. GAYDARDZHIEV^{1*}, J. KARTHIKEYAN² AND P. AY¹

¹Lehrstuhl Aufbereitungstechnik, Brandenburg Technical University, Siemens-Halske-Ring 8, 03046 Cottbus, Germany
²College of Engineering, Sri Venkateswara University, 517 502 Tirupati, Andhra Pradesh, India

(Received 8 February 2005; Accepted 26 September 2005)

ABSTRACT

Chemical coagulation applied for colour removal from dye bearing solutions has been investigated from the point of view of surface charge progression. Two commercially used dyes, i.e. CI Acid Blue 113 and CI Disperse Blue 26 have been tested, employing three common coagulants: alum, aluminium chloride and ferric chloride. Coagulant type and dose level and pH of the dye solution have been studied as process parameters affecting surface charge and degree of colour removal after filtration of coagulated dye. It has been found, that both dyes could be almost completely removed with the tested coagulants, when supplied however at different dosages. From one side, the correlation between surface charge and colour removal suggests that destabilization of colour colloids occurs as a result of charge neutralization followed by removal by filtration. From other side, the lack of re-stabilization and continued high colour removal even at increased coagulant dosages implies enmeshment of destabilized dye colloids into the hydroxy flocs/precipitates of metal coagulant by "sweep coagulation". Finally, flocs from selected sludge samples have been examined for particle size and shape by image analysis and their key characteristics summarised.

Keywords: Coagulation, floc characterization, colour removal, surface charge

INTRODUCTION

The occurrence and consequent removal of colour from effluents and associated environmental problems pose a major challenge to dye stuff manufacturers, textile finishing industries, pulp and paper and leather industries, water companies, etc. In spite of several physicochemical, chemical and biological processes being investigated for removal of colour from a variety of effluents, there is no consensus regarding a reliable method(s) which is/are technically feasible and economically attractive. This is especially valid in the case of textile industries which employ a spectrum of fibers, chemicals, dyes and finishing agents and whose wastes are continually changing in chemical composition and colour [1, 2, 3].

Chemical coagulation is foremost among the methods employed for treatment of dye house effluents, being practiced either as pre-, post- or main process. Treatment with chemicals like alum, ferrous and ferric sulphate, ferric chloride, calcium chloride, copper sulphate, aluminium chloride, sulphuric and hydrochloric acid etc., for the removal of colour from a variety of industrial dye wastes, composite

mill wastes and sewage combined wastes has been investigated and summed up in excellent reviews [2, 4]. The peculiarity with coagulation however is, that while certain application classes of dyes respond favourably to chemical treatment, certain other (notably acid and basic) fail to respond at all. The reasons behind these discrepancies are still unclear [5, 6] and therefore it is difficult to outline the mechanism of colour removal by coagulation [5]. A general belief is that particle destabilization followed by aggregation takes place, however specific chemical interactions involving chelation/ complexation, precipitation and salting-out may also occur [7]. On the whole, it may be reckoned that whatever the application niche, coagulation and flocculation are seldom accompanied by process optimisation, being mostly practiced like an art rather than as science. Similar difficulties arise also in trying to formulate a common test protocol linking the molecular structure of dyes with their affinity towards bio-elimination [8]. Other technologies like membrane filtration, electrolysis, ozonation etc., have been found also to be effective on a singular basis imparting a certain degree of colour removal, but the combination of two or more methods appears to be a preferred practice [9, 10].

Whilst, measurement of electrophoretic mobility and surface charge is being used as a tool for monitoring of colloidal systems dispersion/aggregation relevant to coagulation and flocculation and some researchers have even attempted to explore its role in activated sludge flocculation and bio-flocculation control [11], there is little information regarding surface charge measurement during colour removal by chemical coagulation.

The presented results originate from a first phase research with the objective of evaluating the feasibility of surface charge measurement approach using model solutions of one acid and one disperse textile dye, coagulated with three common inorganic coagulants. The aim was to examine the influence of coagulant type and dosage on surface charge of dye colloids and if possible to correlate those with the degree of colour removal.

MATERIALS AND METHODS

Dyes and Coagulants

Two commercially available dyes namely, CI Acid Blue 113 and CI Disperse Blue 26, produced by Atic Industries, India, were used, and their principal characteristics are summarised in Table 1. Test dye solutions were prepared by dissolving 100 mg dye powder in 1 l distilled water. When the disperse dye was tested, a dispersing agent "Vernamol-S" from Atic Industries was supplied at 1 g l⁻¹ as prescribed by the dye manufacturer. Three metal salts supplied by Merck, Germany have been used as coagulants: ferric chloride anhydrous - FeCl₃ (a.g.); aluminium chloride - AlCl₃.6H₂O (a.g.) and alum - Al₂(SO₄)₃.18H₂O (extra pure). Working

solutions with a molar concentration of 0.06, 0.04 and 0.015, were prepared fresh before each test. Hydrochloric acid and sodium hydroxide were used as pH regulators.

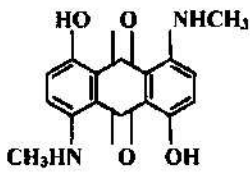
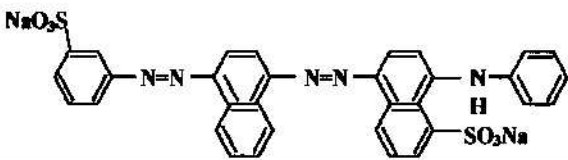
Coagulation and Filtration

100 ml of the model dye solution were transferred to a 200 ml beaker and placed on a flat 3-cm six-blade paddle, resembling a jar-test rig. Then, a predetermined quantity of coagulant was added to the dye solution and pH was quickly adjusted to the desired value by addition of an appropriate (pre-determined) quantity of acid/alkali. The suspension was mixed in a single step by stirring at 200 rpm for two minutes, which was considered sufficient to destabilize the dye colloidal solution. Immediately after, two samples were taken: 10 ml for determination of the surface charge and 5 ml for image analysis. The remaining suspension was further transferred into a funnel fitted with an "Osmonics" nylon filter having 5 μm pore openings and filtered by gravity. An aliquot from the filtrate was collected and analysed for residual colour concentration and for surface charge.

Determination of Surface Charge and Colour Concentration

Surface charge density for the coagulated dye suspensions (unfiltered sludge sample) and the filtrates after filtration was determined by means of a particle charge detector PCD-03-pH from Müttek, Germany, working on a streaming potential principle. The exact magnitude of the charge was estimated by titration with oppositely charged titrant until neutralization of the streaming potential

Table 1. Characteristics of the dyes used.

Dye	Chromophore	MW g M ⁻¹	Structure
Disperse Blue 26	Anthraquinone	298.16	
Acid Blue 113	Diazo	681.4	

to zero. Based on the amount of spent titrant until zero charge, the specific surface charge of suspension expressed in meq g^{-1} , was calculated. Colour concentration was calculated based on extinction factor, using an MPM 3000 photometer from WTW, Germany. The highest extinction factor (EF) for the both dyes was found at 585 nm and accordingly this wavelength was used for construction of calibration curves. The degree of colour removal was estimated based on the difference between colour concentration in the original dye solution and the one detected in the filtrate.

Image Analysis of Coagulated Dye Floes

Image analysis was undertaken using a "Leica Q600" system. The mean volume diameter of floes and their roundness and aspect ratio were recorded. The estimation for "Roundness" is given as the ratio between the squared perimeter and the projected area of the object and could be viewed on a first approximation as the fractal dimension. The compactness of an aggregate structure could be evaluated on that basis, with loose structures having a low fractal dimension and compact structures - a higher one. The aspect ratio is defined as a ratio between length and breadth of the object. A wide mouth pipette was used to transfer the floes from the beaker after coagulation into the observation glass. Before being examined, the sample was carefully diluted with double distilled water in the ratio 1:10 to ensure that single floc aggregates are examined. For each measurement about

100 objects were accounted by the system. The presented values are an average from ten measurements.

RESULTS AND DISCUSSION

Since system pH plays an important role in coagulation processes, initial tests were conducted to find the influence of final pH of dye solution on colour removal employing a constant coagulant dose of 0.5 mM l^{-1} . The pH of the dye solutions varied between 4 and 12. The results from these tests are not presented, but they revealed slightly differing trends in colour removal, which could be attributed to the intrinsic differences in the nature of the dye suspensions. The disperse dyes are water insoluble and are fine colloidal dispersions, whereas acid dyes form ionogenic micro colloids or macromolecules. Based on the screening, the following pH values of the dye solution have been chosen for further investigation: pH 11 for the aluminium based coagulants, and pH 4 and pH 11 for the ferric chloride.

Change in Surface Charge for CI Acid Blue 113

Figures 1 and 2 present the progressive change in surface charge due to incremental addition of coagulant and the respective colour removal for the case of CI Acid Blue 113. The charge measured at zero coagulant dosage is the charge of the pure dye solution.

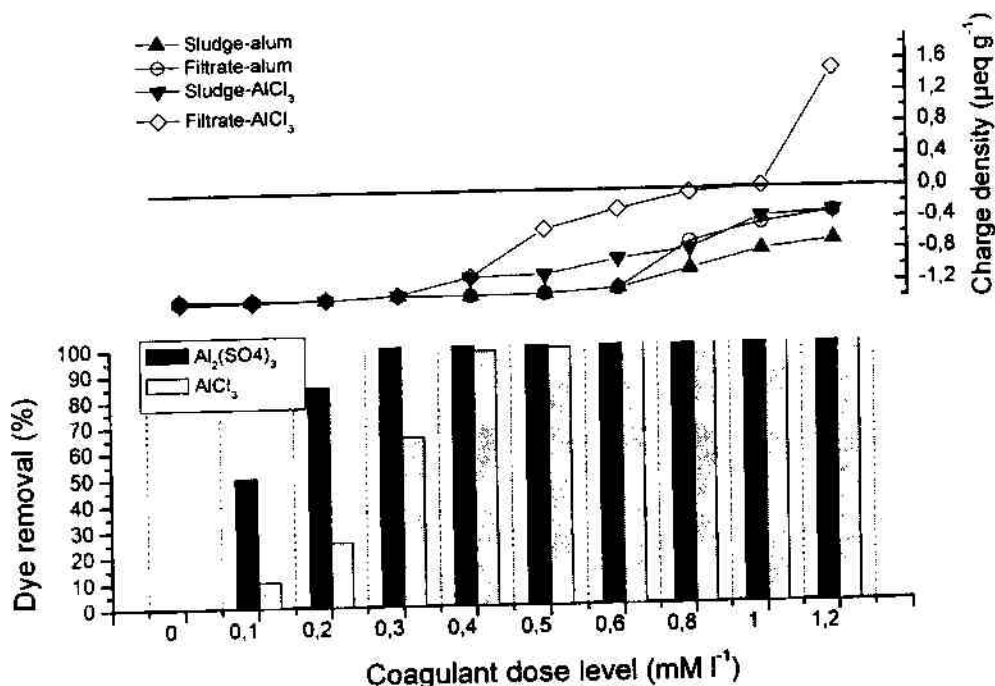


Figure 1. Coagulated dye sludge charge and colour removal using alum and aluminium chloride at pH 11 (the case of CI Acid Blue 113 dye).

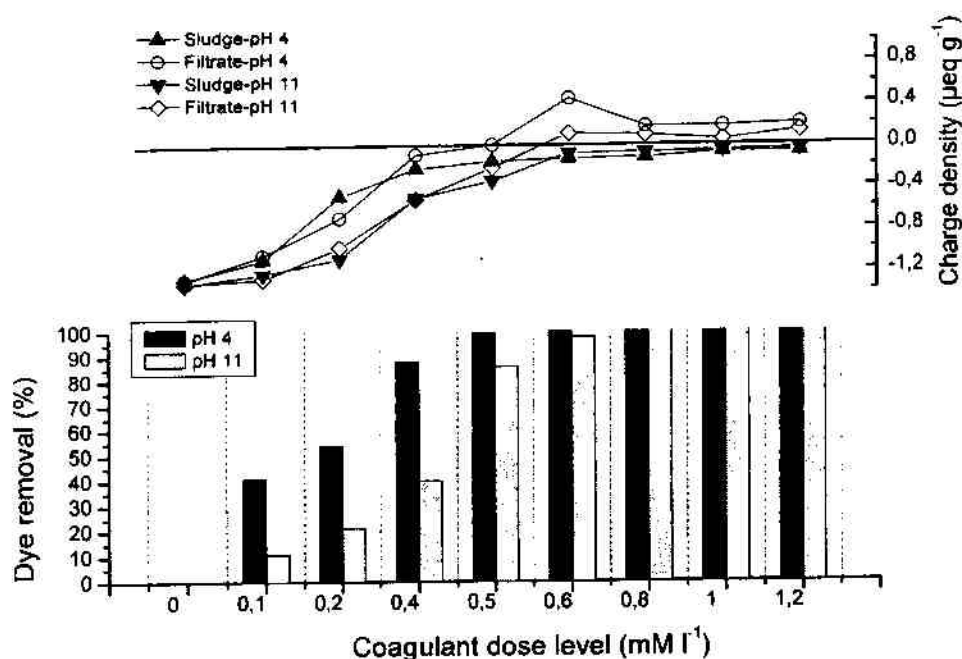


Figure 2. Coagulated dye sludge charge and colour removal using ferric chloride at pH 4 and pH 11 (the case of CI Acid Blue 113 dye).

It can be seen from the figures that the magnitude of surface charge density of the dye colloids gradually decreased as the coagulant dose increased. All three coagulants produced nearly 100% colour removal but at differing dose levels.

The relationships shown in Figure 1 suggest that as alum dosage was increased, colour removal also increased approaching 100%, however this was not accompanied with a concomitant decrease in the negative surface charge of the suspension. It may therefore be inferred, that alum does not promote predominately charge neutralization mechanism although loss of stability is present. Even at higher dosages of alum, complete charge neutralization has not occurred and there exists a small residual charge, though colour removal was nearly complete. At low dose levels, the surface charge of filtered and unfiltered suspensions was equal and at alum dosages above 0.6 mM l⁻¹ the charge for the filtrate was less negative than that for the sludge. This observation could indicate that the dye colloids might be entrapped/enmeshed into the gelatinous aluminium flocs, which are aggregated products from hydrolyzation of Al³⁺ ions, and then removed by what is known as "sweep coagulation".

For the case of aluminium chloride, the progressive increase in coagulant dosage resulted in maximum colour removal accompanied by a slight reduction in surface charge and led to charge reversal in the filtrate at higher than 1 mM l⁻¹ dose levels. The occurrence of a positive charged species in the filtrate after all colour was removed, could be due either to positive species originating from dyestuff fillers/impurities or

to emergence of polyvalent cationic coagulant species, like aluminium hydroxide sols [12].

The results shown in Figure 2 indicate that for the dye solution coagulated with ferric chloride at pH 11, the trend in colour removal was similar to the one observed for the aluminium chloride, however higher ferric chloride dosage was required to reach total colour removal. Here, the charge reversal in filtrate occurred at 0.6 mM l⁻¹, where the maximum colour removal was noticed. The charge of coagulated sludge approached zero at coagulant dosages above 0.6 mM l⁻¹. At pH 4, both charge curves were characterised by a more or less similar trend. For both pH ranges no drop in colour removal was observed at higher coagulant dosages, even after reaching charge reversal in the filtrate.

Change in Surface Charge for CI Disperse Blue 26

Figures 3 and 4 show that for the disperse dye higher dosages of coagulant are required to attain the same colour removal as that for the acid dye. Again, alum appears to be the best candidate in terms of dose requirement. A more pronounced correlation between charge progression and colour removal could be delineated.

The perusal of the results shown in Figure 3 indicates that at pH 11, both aluminium-based coagulants do not reverse the charge of dye sludge and filtrate to positive. Worthy of note is the good agreement between charge progression and colour removal in the case of aluminium chloride.

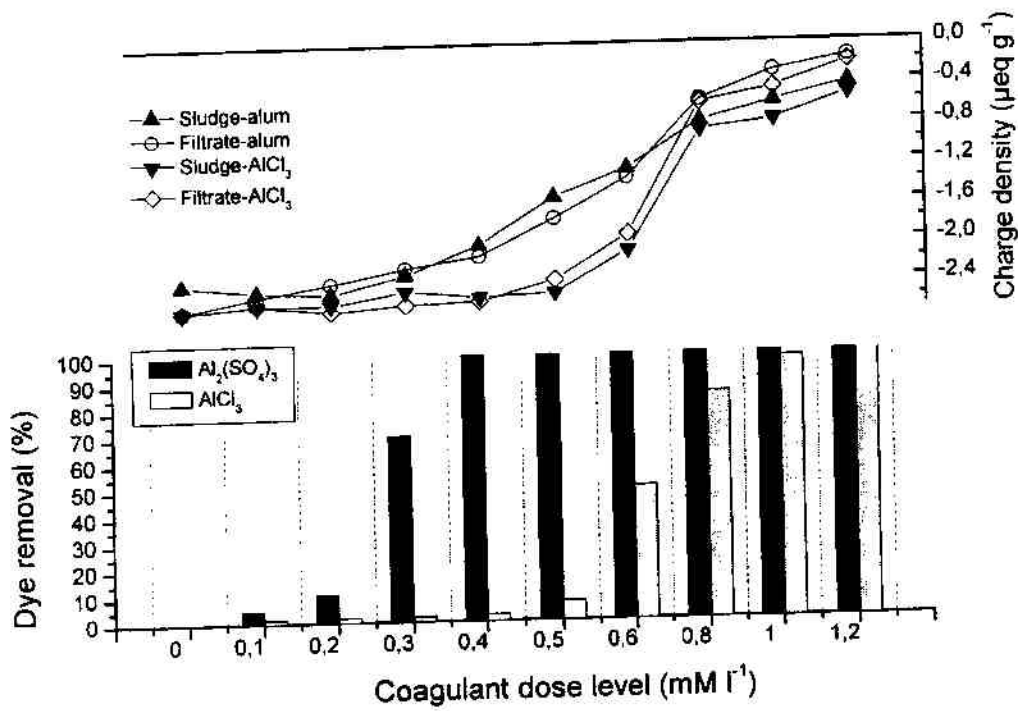


Figure 3. Coagulated dye sludge charge and colour removal using alum and aluminium chloride at pH 11 (the case of CI Disperse Blue 26 dye).

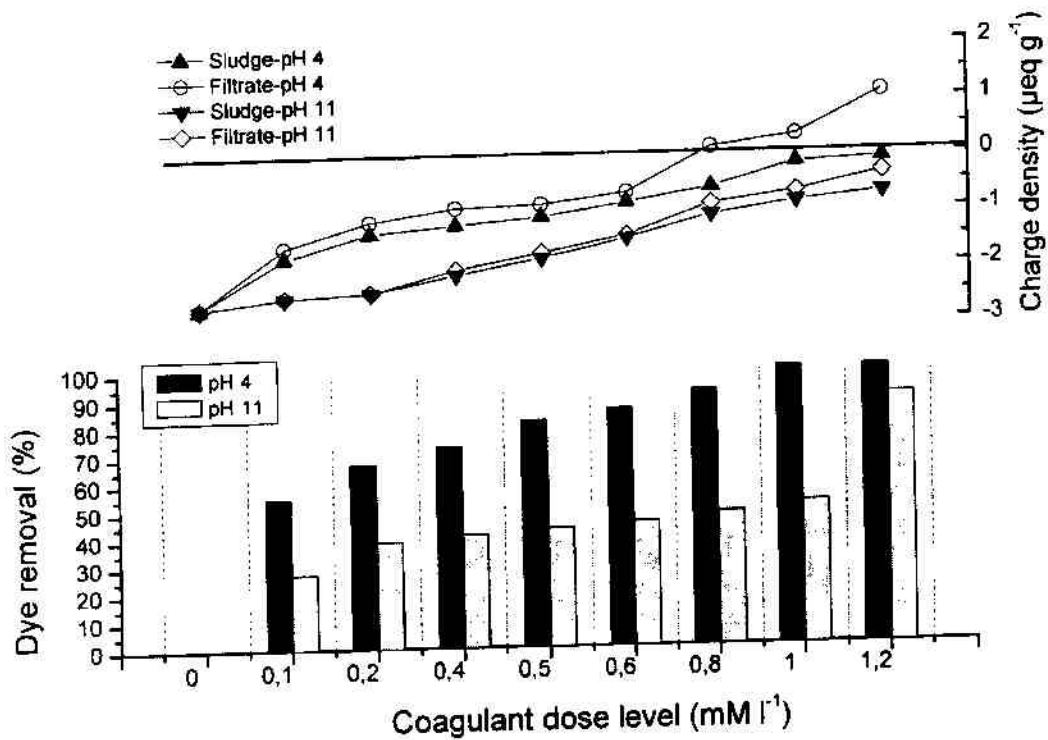


Figure 4. Coagulated dye sludge charge and colour removal using ferric chloride at pH 4 and pH 11 (the case of CI Disperse Blue 26 dye).

Figure 4 indicates that in contrast to the CI Acid Blue 113 where the role of solution pH was found to be of minor importance, the pH effect on coagulation of CI Disperse Blue 26 was more pronounced. The acidic range clearly stimulated more efficient colour removal. At pH 4, nearly double the removal of that achieved at pH 11 was observed for coagulant dose levels from 0.2 to 0.8 mM l⁻¹. Sludge charge has approached zero at dose level of 1 mM l⁻¹ and above, and a close coincidence between point of zero charge and maximum colour removal could be noted. Therefore for the ferric chloride, a charge neutralization mechanism could be attributed at pH 4, while at pH 11 the dye sludge remained negatively charged.

Floc Characterization

Four samples from coagulation of CI Acid Blue 113 at pH 11 with alum and ferric chloride, each one supplied at two optimal dosages, were examined and their floc characteristics summarized in Table 2. It could be noted that with increasing ferric chloride dosage from 0.5 to 0.6 mM l⁻¹, the mean floc diameter rose slightly from 250 to 280 μm, while roundness increased from 1.6 to 1.9, suggesting development of more compact floc structures. This was accompanied by nearly zero charge at 0.6 mM l⁻¹, leading to almost complete colour removal - Fig. 2. However, the alum supplied at half the maximum concentration generated larger and open structured floc aggregates, which are more likely to promote dye colloids removal by sweep coagulation. With a minute increase in alum dosage from 0.2 to 0.3 mM l⁻¹, flocs increased in diameter from 350 to 410 μm, while roundness dropped from 1.7 to 1.5. The aspect ratios, giving an idea about elongation of flocs, did not differ significantly. All four samples consisted of aggregates, which owing to their size and shape are unlikely to settle rapidly. The sludge arising from the FeCl₃ addition was characterised by the highest amount of fine-sized aggregates. An addition of polymeric flocculant could certainly stimulate development of larger and tear-resistant flocs with improved sedimentation properties and work in this direction is in progress.

CONCLUSIONS

The results from the presented studies do not permit a conclusion of fundamental validity to be drawn, but are believed to have theoretical implication in revealing some aspects of dye coagulation mechanism. From a practical point of view, they could be of use in the case of implementation of an on-site PCD measurement for coagulants dose rate control, likewise practiced at some municipal wastewater or paper mill treatment plants.

The approach of surface charge density measurement has proved useful, nevertheless further data evaluation should be pursued, involving statistical error analysis as well. The incremental addition of coagulant reduced the negative surface charge of the colloidal dye species and eventually rendered them positive. Except for alum, a good agreement between coagulant dosage and surface charge of the dye colloids was noted. Alum could be recommended as the most promising coagulant on a cost/dosing basis. In the alkaline region, which is mostly the case in dye houses, it promotes predominately sweep coagulation for the both dyes, in contrast to ferric chloride, which stimulates coagulation by charge neutralisation.

Detailed floc characterization studies to complement the presented findings are underway. The results from these studies which involve the use of synthetic primary coagulants as well, are in compilation. However, since image analysis of dye flocs is tedious (in terms of sample preparation) and time consuming, a LALS method was adapted, with the ultimate goal of obtaining information of practical value to sludge down-stream treatment [13].

ACKNOWLEDGMENT

One of the authors (JK) wishes to acknowledge the German Council for Academic Exchange (DAAD) in providing financial support for a three-month placement at BTU-Cottbus.

Table 2. Floc characteristics of selected coagulated dye samples (CI Acid Blue 113).

Sample No	Coagulant (dosage, final pH)	Floc mean size (μm)	Roundness	Aspect Ratio
1	Alum (0.2 mM l ⁻¹ , pH 11)	350	1.7	1.6
2	Alum (0.3 mM l ⁻¹ , pH 11)	400	1.5	1.7
3	FeCl ₃ (0.5 mM l ⁻¹ , pH 11)	250	1.6	1.9
4	FeCl ₃ (0.6 mM l ⁻¹ , pH 11)	280	1.9	1.8

REFERENCES

1. Vandevivere, P., Bianchi, R., Werstaete, W., Treatment and reuse of waste water from the textile wet-processing industry: Review of emerging technologies, *J. Chem. Technol. Biotechnol.*, **72**, 289-302 (1998).

2. Hao, O., Kim, H. and Chiang, P., Decolorization of wastewater, *Crit. Rev. Environ. Sci. Technol.*, **30**, 449-505 (2000).
3. Robinson, T., McMullan, G., Marchant, R. and Nigam, P., Remediation of dyes in textile effluent: a critical review on current treatment technologies with a proposed alternative, *Biores. Technol.*, **77**, 247-255 (2001).
4. Marmagne, O. and Coste, C., Color removal from textile plant effluents, *Am. Dyest. Rep.*, **4**, 15-21 (1996).
5. Venkata-Mohan, S., Srimurali, S., Sailaja, P. and Karthikeyan, J., Removal of a monoazo acid dye from aqueous solution by adsorption and chemical coagulation, *Environ. Eng. Pollut.*, **1** 149-154 (1999).
6. Venkata-Mohan, S. and Karthikeyan, J., Removal of colour from acid and direct dyes by adsorption onto silica fumes, *Fres. Environ. Bull.*, **7**, 51-53 (1998).
7. Karthikeyan, J., Removal of colour from textile dye wastes by chemical coagulation, Ph.D. Thesis, Indian Institute of Technology, Kanpur, India (1990).
8. Greaves, A., Philips, D. and Taylor, J., Correlation between the bioelimination of anionic dyes by an activated sewage sludge with molecular structure, *J. Soc. Dyers Col.*, **115**, 363-365 (1999).
9. Hatton, W. and Simpson, A., Color removal from sewage effluents using chemical flocculants, *Environ. Technol. Lett.*, **7** 413-424 (1986).
10. Kang, S. and Chang, C., Coagulation of textile secondary effluents with Fenton's reagent, *Water Sci. Technol.*, **36**, 115-212 (1997).
11. Liao, B., Allen, D., Dreppo, I., Leprard, G. and Liss, S., Surface properties of sludge and their role in bioflocculation and settleability, *Water Res.*, **35**, 339-350 (2001).
12. Licsko, L., Realistic coagulation mechanisms in the use of aluminium and iron (III) salts, *Water Sci. Technol.*, **36**, 103-110 (1997).
13. Bushel, G., Yan, Y., Woodfield, D., Raper J. and Amal, R., On the techniques for measurement of the mass fractal dimension of aggregates. *Adv. Coll. Interf. Sci.*, **95**, 1-50 (2002).

Size and Structure Characterization of Dye Flocs during Coagulation of Reactive Black 5 Dye

Marta Janeczko, Stoyan Gaydardzhiev*

(Received: 10 February 2006; accepted: 10 April 2006)

DOI: 10.1002/ppsc.200601032

Abstract

This paper deals with results from laboratory scale experiments with model dye effluents comprising of the commercially used textile diazo dye, CI “Reactive Black 5”, coagulated with ZETAG type primary coagulants. Size and structure analysis of flocs in coagulated dye sludge was undertaken in order to evaluate their separation abilities. The particle size distribution was estimated by use of a Galai CIS-100 particle counting system working on a time-of-transition principle, while their fractal dimension was obtained from laser scattering instrument in LALS mode. An image analysis of the flocculated dye-sludge has also been carried out. In parallel to the flocs characterization, the measurement

of surface charge density of coagulated dye sludge was performed with the aim of linking surface charge data with the floc characteristics, and on this basis, to outline the predominant mechanism of color removal. It was found that flocs produced at optimal dosage are characterized by large sizes and a high value of fractal dimension, which is manifested in a very good level of color removal by sedimentation. The evident correlation between the surface charge density progression of coagulated dye flocs and color removal, suggests adsorption and charge neutralization as the predominant mechanism of dye destabilization.

Keywords: chemical coagulation, color removal, particles, surface charge

1 Introduction

Although the textile industry is one of the most environmentally sensible activities, it presents a substantial source of water pollution, considering both the composition of effluents and the volume of waste generated. Effluents discharged without appropriate treatment have a pronounced harmful impact on recipient streams, not only due to aesthetical problems, but also by reducing light transmittance, which can lead to adverse effects on aquatic plant growth and fish life. The removal of color from textile effluents is still a challenge, both for the scientific and industrial communities.

There are a large variety of well established conventional methods for effluent decolorization involving physico-chemical, chemical and biological processes, as well as some new emerging techniques including sonochemical or advanced oxidation processes. This does not alter the fact that there is not any single economically or technically viable method, and usually two or three methods have to be combined in order to guarantee an adequate level of color removal, as reported by Hatton [1], Kang [2] and Robinson et al. [3]. Research on chemical coagulation has a long history, being performed in a variety of ways and at different scales by established research centers. It is one of the most widely practiced processes and although having some disadvantages, e.g., the considerable amount of sludge generated, it is still used as a pre-, main- and post-treatment process, both in developed and developing countries. It is an acknowledged fact that despite the significant amount of work performed both on a laboratory and on larger scales, the exact mechanism of coagulation

* Dipl.-Ing. M. Janeczko, Dr. St. Gaydardzhiev, Lehrstuhl Aufbereitungstechnik, Institut für Verfahrenstechnik, Brandenburgische Technische Universität Cottbus, Siemens-Halske-Ring 8, 03046 Cottbus (Germany).
E-mail: janecmar@tu-cottbus.de

applied to decolorize waste water is still not fully understood. This is because color removal from textile effluents by coagulation/flocculation was found to be very effective in some cases, but in other cases did not work. The literature survey shows examples of using surface charge density in controlling the stability of fine particles and its role in activated sludge floc formation. However, there has not been any investigation to explore the role of surface charge density in destabilization of compounds with a complex and aromatic structure such as dye colloids. Recent studies have shown that although the characterization of sludge floc size distributions and the measurement of their structure by a laser light scattering technique are also well established, there have only been a few efforts made to use these methods to characterize flocculated dye aggregates. This paper describes a study towards the evaluation of surface charge density effects upon the predominant color removal pattern during chemical coagulation, with an additional aim to also investigate the dye floc features including size and structure.

2 Materials and Methods

2.1 Synthetic Dye Bath and Chemicals Used

A commercially used textile disazo dye “Cibacron Marine W-B” with a CI “Reactive Black 5” supplied by CIBA, was used in this study. Synthetic solutions with concentration of 100 mg/L, simulating spent dye-bath effluent, were prepared by dissolving 100 mg of dye powder in 1.0 L of distilled water. Table 1 illustrates the main characteristics of the primary cationic coagulants used in the study. These were used as stock solutions with a concentration of 0.5 % active matter and were freshly prepared daily.

Table 1: Main characteristics of the coagulants used.

Coagulant index	Type	Active substance (%)
7101	Polyamine	50
7102	Polyamine	55
7103	Polyamine	55

2.2 Method of Coagulation

For each experimental trial, two parallel tests were carried out. 100 mL of the prepared dye solution was transferred to a 250 mL beaker and placed on a jar-rig assembly consisting of a 3 cm six-blade stirrer. Before the start of solution agitation, the surface charge density of

the pure dye solution was determined. Then, a predetermined amount of coagulant was added and the sample was mixed rapidly by stirring at 200 rpm for 2 min and then at 25 rpm for a further 5 min. After stirring was complete, the pH was recorded. Immediately following this, 10 ml of the sample was removed for determination of the surface charge density, with the remainder of the sample being utilized for color removal estimation following filtration and centrifugation. Filtration under gravity was carried out using a Whatman “blue” and “yellow” paper filter with pore openings below 2 μm and between 4–7 μm, respectively. Centrifugation was performed at a speed of 3000 rpm for 3 min. After the solid/liquid separation stage had taken place, a required amount from the filtrates or the centrates was delivered for determination of residual color concentration. The second sample coagulated in parallel, was left for 2 h of plain sedimentation, and the degree of color removal was determined in a similar manner based on supernatant analysis.

2.3 Surface Charge Density Determination

Surface charge density measurements were performed using a particle charge detector, PCD-O3-pH, Müttek, Herrsching, Germany. The instrument consists of a cylindrical test cell with a fitted displacement piston which moves back and forth at a constant frequency, forcing a relative motion of liquid and particles, thus inducing development of a streaming potential of either positive or negative sign. The cationic standard titrant was 0.001 N polydiallyldimethylammonium chloride solution (Poly-Dadmac), while the anionic titrant was 0.001 N sodium polyethylene sulphate solution (Na-PES). The exact amount of charge was estimated by titration of the sample with the oppositely charged polyelectrolyte until neutralization of the streaming potential to zero value, and was expressed as the surface charge density in [meq/g], as follows:

$$q = \frac{V \cdot c}{W} \quad (1)$$

where,

V is the volume of spent titrant until neutralization point in mL, c is the normality of the titrant (0.001 N) and W is the mass of the active substance in grams.

2.4 Color Removal Determination

The color concentration was estimated by means of VIS spectral photometry (spectrophotometer model

Genesys 10, Thermo Spectronics, UK) at the wavelength giving maximum absorbance, in this case 598 nm. The degree of color removal was calculated based on the difference between the color concentration in the original dye-bath solution and that remaining after the sludge/liquid separation.

2.5 Dye Floccs Characterization

Median Diameter

The measurement of the particle size distribution (PSD) of coagulated dye sludge was performed by employing a GALAI CIS-100 system, Ankersmid, the Netherlands, which is a laser based particle counter and size analyzer for both spherical and non-spherical particles, employing the time-off-transition principle. The system provides the number size distribution as a primary output, which is further used to yield the volume size distribution. During measurement, the dye floccs were kept in motion inside the glass cuvette by means of a magnetic stirrer rotating at a slow speed without disturbing the flocc structures. The measurement results are characterized by a high confidence value reaching more than 99.5 %.

Fractal Dimension

The fractal dimension of the floccs was estimated by measurement using a Mastersizer X, Malvern, UK, laser scattering instrument, working in Low Angle Light Scattering (LALS) mode. The LALS technique as described by recent studies [4,5], consists of recording raw light energy data after each measurement and plotting it versus scattering angle. The fractal dimension is taken as equal to the slope fitted to the linear section of the relationship trend line. In order to avoid disturbing floccs during measurement, the dye sludge was transferred from the beaker to the measuring cell by means of a 150 ml syringe fitted with tubing instead of using the normal sample cell. Considering the anticipated floccs size range, a 300 mm lens was used.

In general terms, finding the fractal value from scattering theories relies upon the power law which is based on Rayleigh-Gans-Debye (RGD) scattering theory. The fractal objects follow the power law when: 1) the RGD approximation is valid, 2) the power law region are distinct from the Guinier and Porod regions $1/R_g \ll q \ll 1/r_o$,

The RGD approximation is valid when $|m-1| \ll 1$ and $(2\pi d/\lambda)|m-1| \ll 1$, where, m is the material refractive index and d is the size of the scattered body. For the present case, it can be assumed that the refractive index of

the dye used lies between 1.33 (RI of the pigments) and 2 (RI of the Azo dyes).

Due to the fact that the size of primary particles were in the colloidal range, the second requirement of the power law region, $1/R_g \ll q \ll 1/r_o$, where R_g is the radius of gyration of the aggregate and r_o is the primary particle radius, was satisfied (assuming R_g to be about 209 μm and r_o to less than 1 μm).

For all of the samples measured, only one linear part of the plot was noted (detector number 20 and above), from which the respective slopes were taken.

Image Analysis

Image analysis of aggregates in flocculated dye sludge was carried out by means of a Kappa CF 8/1 color camera mounted on a Q600 HRSYS system, Leica, Germany. A small volume of sludge was transferred onto the observation glass by means of a wide mouth pipette and was subsequently diluted with distilled water. During all measurements, a constant light level was maintained for each captured image. Between 50 and 100 objects were counted by the system.

3 Results and Discussion

The results discussed below, relate only to the case when the coagulant 7101 was used. This is due to the fact that all of the other coagulants tested, were found to behave in a similar manner in terms of color removal efficiency and surface charge progression trend.

Figure 1 summarizes the results concerning the effect of coagulant dose level on surface charge density and color removal after filtration, sedimentation and centrifugation, while Figure 2 shows the effect of coagulant dose

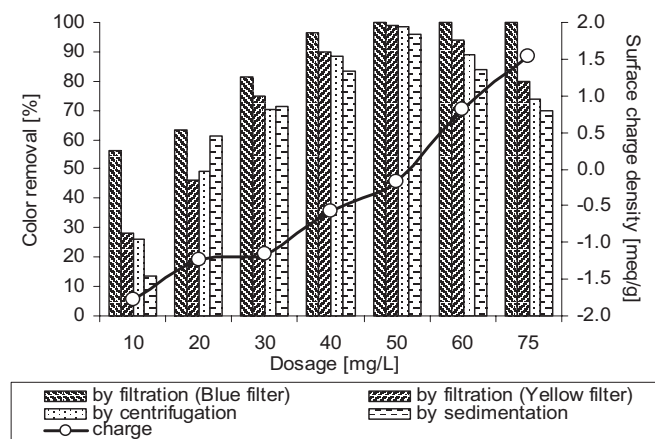


Fig. 1: Relationship between the surface charge density of the sludge and color removal.

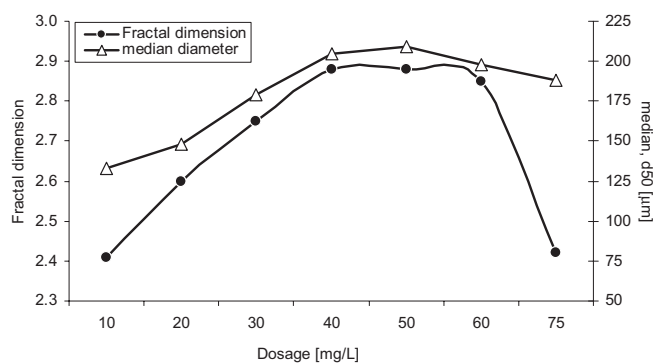


Fig. 2: Relationship between floc median and fractal dimension at different dose levels of coagulant.

level on floc median and on the dye flocs fractal dimension, as determined by the LALS method.

The results shown in Figure 1 present an obvious correlation between surface charge density and color removal efficiency. With increasing coagulant dose, the negative surface charge density of coagulated dye sludge decreases and reaches a zero point around 50 mg/L, where the best color removal was achieved. Any further increase in coagulant dose above this optimal dose, up to levels of 60 and 75 mg/L, renders the surface charge density positive, which is manifested by a decrease in color removal by filtration (yellow filter), centrifugation and sedimentation. This evident correlation between surface charge density and color removal provides an assumption that the adsorption of the positive coagulant species onto the dye colloid surface is leading to their charge neutralization and their subsequent aggregation by electrostatic forces. As can be seen from Figure 1, at the optimal dose level of 50 mg/L, the color removal by filtration, sedimentation and centrifugation has reached more than 95 %. Filtration of the dye sludge by a blue filter provided continuous high level of color removal, even when the coagulant dose was increased above the optimal level. This may be attributed to the very small pore openings of the applied paper filter, which are able to retain the restabilized dye flocs. The sedimentation and centrifugation of dye sludge have shown comparable color removal abilities, in the supernatants and concentrates, respectively. Table 2 summarizes some key data about floc characteristics and color removal achieved by plain sedimentation at the different dose levels of coagulant. The perusal of these results indicates a correlation between floc characteristics and color removal by sedimentation. As can be seen from Figure 2, both floc size and fractal dimension increase with a concomitant increase in the amount of coagulant added. The largest floc size and the highest value of fractal

Table 2: Color removal by sedimentation and floc characteristics at different coagulant dose levels.

Coagulant dosage (mg/L)	Color removal (%)	Floc median (µm)	Floc fractal dimension
10	14	133	2.41
20	62	148	2.60
30	71	179	2.75
40	84	205	2.88
50	96	209	2.88
60	84	198	2.85
75	70	188	2.42

dimension correspond to the best level of color removal obtained. At lower dose levels of coagulant, the flocs exist as small primary aggregates. However, at the optimal dose level, they can be seen as larger flocs having a median size of around 209 µm and a fractal dimension reaching 2.88. The above observation suggests that the flocs produced at the optimal coagulant dose are characterized by a dense structure and improved settling behavior. With a further increase in coagulant dose levels to 60 mg/L, the flocs' median diameter and fractal dimension decrease and the level of removal by sedimentation also drops slightly. At a dose level of 75 mg/L, the color removal was only 70 %, with the corresponding floc median of 188 µm and fractal dimension of 2.42.

The left hand side of Figure 3 below illustrates an image analysis view of typical floc clusters resulting from coagulation undertaken at 20 mg/L ZETAG 7101. It is worth mentioning that there are relatively large amounts of fine particles seen. In contrast, when the coagulant was supplied at the optimal dose level of 50 mg/L, fairly compacted aggregate structures were observed (right hand view). These characteristics are to some extent, supportive of the floc settling behavior, discussed above.

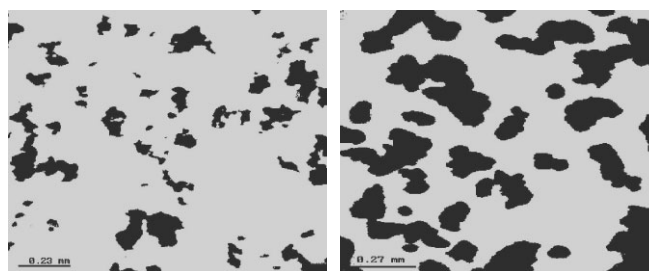


Fig. 3: Image analysis micrographs of dye aggregates (coagulant at 20 mg/L – left and 50 mg/L – right).

4 Conclusions

The results from the current study indicate, that the coagulation of CI Reactive Black 5 dye from synthetic dye effluents using a ZETAG type primary coagulants, takes place predominately under a charge neutralization pattern. At the optimally established dose level of coagulant, an efficient destabilization of dye colloids occurs, leading to the development of flocs with improved settling properties, a fact that is further corroborated by their size and fractal dimension. This approach for characterization of coagulated dye sludge in terms of surface charge density, and of the dye flocs in terms of size and shape could be expanded to other coagulated sludges derived from textile dyes commonly encountered in effluents from dyeing mills. Thus, the findings presented have implications for several areas of waste water treatment and could also be useful for application to characterization of fractal bodies.

5 Nomenclature

d_{50}	μm	median particle size
Fd	–	fractal dimension
q	meq/g	surface charge density
c	N	titrant normality
V	mL	volume of spent titrant until charge neutralization
W	g	mass of active substance

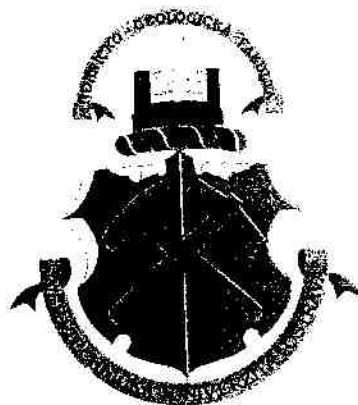
Abbreviations

CI	Chemical Index
LALS	Low Angle Light Scattering
PCD	Particle Charge Detector

6 References

- [1] W. Hatton, A. Simpson, Enhanced Color Removal from Sewage Effluents using Chemically Flocculants, *Env. Technol. Lett.*, **1986**, 7, 413–424.
- [2] S. Kang, H. Chang, Coagulation of Textile Secondary Effluents with Fenton's Reagent, *Wat. Sci. Technol.*, **1997**, 36, 215–222.
- [3] T. Robinson, G. McMullan, R. Marchant, P. Nigam, Remediation of Dyes in Textile Effluent: a Critical Review on Current Treatment Technologies with Proposed Alternatives, *Biores. Technol.* **2001**, 77, 247–255.
- [4] A. Jung, R. Amal, J. Raper, The Use of Small Angle Light Scattering to Study Structure of Flocs, *Part. Part. Syst. Charact.* **1995**, 12, 274–278.
- [5] G. Bushel, D. Yan, D. Woodfield, J. Raper, R. Amal, On Techniques for the Measurement of the Mass Fractal Dimension of Aggregates, *Adv. in Coll. & Interf. Sc.* **2002**, 95, 1–50.

**VŠB – TECHNICAL UNIVERSITY OF OSTRAVA
FACULTY OF MINING AND GEOLOGY
INSTITUT OF ENVIRONMENTAL ENGINEERING**



10th Conference on Environment and Mineral Processing

Part I



**22.6. – 24.6. 2006
VŠB-TU OSTRAVA
Czech Republic**

REMOVAL OF SELECTED AZO DYES FROM TEXTILE WASTEWATER BY CHEMICAL COAGULATION/FLOCCULATION: IMPLICATION OF THE DYE DESTABILISATION MECHANISM

Marta JANECKO, Stoyan GAYDARDZHIEV, Peter AY

Chair of Mineral Processing, Brandenburg University of Technology,
Siemens-Halske-Ring 8, 03046 Cottbus, Germany
janecmar@tu-cottbus.de

Abstract

The results of the coagulation/flocculation of six commercially used textile azo dyes coagulated with synthetic primary coagulants are discussed in the paper. Surface charge measurement of coagulated dye-flocs was employed to find a correlation between its sign and the level of colour removal. Additionally, flocs characterization was done with the aim to link data with surface charge and on this basis to outline the predominant mechanism of colour removal. Based on the results obtained, an evident correlation between surface charge density progression of coagulated dye flocs and colour removal after different solid/liquid separation methods was observed. Thus, it was concluded that the charge neutralization was the predominant mechanism responsible for dye destabilisation. It was found out also that flocs produced at optimal dosage are characterized by large median size and high value of fractal dimension.

Key words: coagulation, azo dyes, floc characterisation, wastewater

1. Introduction

Azo dyes belong to the most important type of colorants used in textile industry and considering both the number and the production volume, they represent the largest group of all synthetic dyes. Generally, the chromospheres of azo dyes consist of the one or more azo group (-N=N-) coupled with the aromatic system what make them to be very stable to biodegradation. About 10-15 % of the azo dyes can be lost in effluent during the technological process (Zollinger 2003). Thus, discharge of highly coloured textile wastewater containing unfixed dyes and other auxiliaries chemicals can result in serious environmental damages. Colour removal technologies which are reported in the literature include conventional decolourization methods like physicochemical, chemical and biological processes, as well as new emerging techniques like sonochemical or advanced oxidation processes. Application of biological processes in treatment of textile effluents has been found mostly as ineffective. Chemical methods are still unattractive mainly due to the high costs and disposal problems.

Currently there is no any single economically and technically viable method and usually two or three methods have to be combined in order to guarantee adequate level of colour removal (Hatton 1986; Kang 1997; Robinson 2001). The results from the literature review indicate that chemical coagulation is one of the most practised processes and regardless of the generation of considerable amount of sludge, it is still used in many countries. The knowledge about coagulation of dyes is at present due to the complexity of the process still very limited. Colour removal by coagulation is found in some cases very effective, in another cases however, it does not bring any positive results.

The objective of this study was to evaluate the surface charge density effects upon the predominant colour removal pattern during chemical coagulation with an additional aim to investigate the dye floc features like size and structure as well.

2. Materials and Methods

The selected textile azo dyes chosen in this study (Table 1) were delivered by CIBA, Boruta-Color and Polfa- Pabianice/Poland in the form of dye powders. All synthetic dye solutions at concentration of 100 mg/L, simulating spent dye-bath effluent were prepared by dissolving a 100 mg of dye powder in 1.0 L of distilled water.

Table 1. The characteristic of six azo dyes studied in this work

Trade Name	Chemical Index	Chromophore	Wavelength [nm]
Cibacron Marine W-B	Reactive Black 5	disazo	593
Helaktyn Red F5B 100%	Reactive Red 2	monoazo	536
Acid Black Boruta A 212%	Acid Black 1	disazo	616
-	Acid Orange 7	monoazo	481
Synten Yellow P5G 100%	Disperse Yellow 5	azo	392
Fast Scarlet 4BS 125%	Direct Red 23	disazo	501

The primary coagulants (Table 2) used in our study are characterised by high cationic charge and low molecular weight and were supplied by CIBA. The stock solutions were prepared daily as fresh batches with concentration of 0.5 % active matter.

Table 2. The characteristic of five primary coagulants used in this work

"ZETAG" Coagulants	Type	Activity [%]
ZETAG - 7101	Polyamine	50
ZETAG - 7102	Polyamine	55
ZETAG - 7103	Polyamine	55
ZETAG - 7197	Polyamine	50
ZETAG - 7125	Polydadmac	40

Procedure of coagulation test

A 100 mL of the prepared dye solution was transferred inside a two 250 mL beakers and placed on a jar-rig assembly consisting of 3-cm six-blade stirrer. Then, a pre-determined amount of coagulant was added and the sample was mixed rapidly by stirring at 200 rpm for 2 minutes and further at 25 rpm for 5 minutes. Immediately after, 10ml of the sample was taken for surface charge density determination; the rest from the first sample was being utilized for colour removal estimation following filtration and centrifugation. Filtration under gravity was carried out using a Schleicher & Schuller "blue" and "yellow" paper filter with pore openings below 2 μm and between 4 – 7 μm respectively. Centrifugation was performed at speed of 3000 rpm with duration of 3 minutes. The second coagulated sample was left for plain sedimentation for 2 hours. After solid/liquid separation, the filtrates, centrates and supernatants were delivered for determination of residual colour concentration.

Surface charge density and colour removal determination

Surface charge density measurements were performed by means of a particle charge detector PCD-O3-pH from Müttek, Germany. The cationic standard titrant was 0.001 normal polydiallyldimethylammonium chloride solutions (Poly-Dadmac), while the anionic one was 0.001 normal sodium polyethylene sulphate solutions (Na-PES). The exact amount of charge was estimated by titration of the sample with oppositely

charged polyelectrolyte until neutralization of the streaming potential to zero value and was expressed as surface charge density as follows:

$$q = \frac{V \cdot c}{W} [\text{meq/g}]$$

where: V – volume of spent titrant until neutralization point [mL];
 c – normality of titrant - 0,001;
 W – mass of active substance [g]

Colour concentration was estimated by means of a VIS spectral photometry (spectrophotometer model Genesys 10, Thermo Spectronics) at the wavelength giving maximum absorbance. Colour removal degree was calculated based on the difference between colour concentration in the original dye-bath solution and the one after sludge/liquid separation.

Dye Flocs Characterization

- I. Flocs size distribution was done by employing CIS-100 GALAI system, which is a laser based particle counter. The system is providing the number size distribution as a primary output, which is used further to yield volume size distribution. During measurement, the dye flocs were kept in motion inside the glass cuvette by means of magnetic stirrer rotating at slow speed without disturbing floc structures.
- II. Flocs fractal dimension was estimated by measurement using a Malvern Mastersizer X laser scattering instrument, working in Low Angle Light Scattering (LALS) mode. The LALS technique as described by recent studies (Jung 1995; Bushel 2002) consists of recording raw light energy data after each measurement and plotting it versus scattering angle. The fractal dimension is taken as equal to the slope of the fitted to the linear section of the relationship trend line. In order to avoid flocs disruption during measurement, the dye sludge was transferred from the beaker to the measuring cell by means of a 150 ml syringe fitted with tubing instead of using the normal sample cell. Considering the anticipated flocs size range, a 300 mm lens range was used.
- III. Image analysis of aggregates in flocculated dye sludge was carried out by means of a colour camera mounted on a Q600 HRSYS, Leica System. Small volume of sludge was transferred onto the observation glass by means of a wide mouth pipette and was subsequently diluted with distilled water. During all measurements, a constant light level was maintained and for each captured image. Between 50 and 100 objects were accounted by the system.

3. Results and discussion

Results from coagulation of Acid Black 1 with coagulant 7103

Table 3. Surface charge density and colour removal as a function of coagulant dosage

Dosage of coagulant 7103, mg/L	Surface charge density, meq/g	% of Colour Removal by			
		Filtration		Sedimentation	Centrifugation
		Blue filter	Yellow filter		
20	-1.490	89	47	48	37
30	-0.799	94	70	63	62
40	-0.426	97	90	86	88
50	-0.082	100	100	98	99
55	0.471	99	86	57	68

As shown in the Table 3, surface charge density of coagulated dye sludge increases with the increase in cationic polyelectrolyte dosage and reaches a zero point (PZC) at the dose 50 mg/L where the best

colour removal was achieved. It suggests also a good correlation between surface charge density and colour removal. At the optimal dose level of 50 mg/L the colour removal by filtration, sedimentation and centrifugation has reached more than 98 %. The further increase in coagulant dose up to 55 mg/L above this optimal dose renders the surface charge density positive, what is manifested by colour removal decrease to 68 % by centrifugation and 57 % by sedimentation. The evident correlation between surface charge density and colour removal observed in this case provides assumption that the adsorption of the positive coagulant species onto dye colloid surface is leading to their charge neutralization and their subsequent aggregation by electrostatic forces.

The results obtained from floc characteristic indicate a correlation between flocs size, fractal dimension and colour removal by sedimentation. Both parameters increase with increase in coagulant dosage. The largest floc size and the highest value of fractal dimension correspond to the best colour removal obtained. At lower dose of coagulant, the flocs exist as small primary flocs, at the optimal dose level however they could be seen as larger aggregates having a median size of around 192 μm and fractal dimension reaching 2.87. It can be concluded that the flocs produced at optimal coagulant dose are characterised by dense structure and improved settling behaviour. With further increase in coagulant dose levels, flocs median and fractal dimension decrease and the removal by sedimentation drops as well.

Table 4. Flocs characteristic and its relationship to colour removal by sedimentation

Parameters	Dosage of coagulant 7103 [mg/L]				
	20	30	40	50	55
Colour removal by sedimentation [%]	48	63	86	98	57
Median diameter, d50 [μm]	121	149	170	192	138
Fractal dimension	2.26	2.60	2.79	2.87	2.17

The figure below present an image analysis view of flocs produced at 20, 50 and 55mg/L dosages. The first photo shows a typical floc clusters coming from coagulation done at 50 mg/L. At the optimal dose (middle picture) one can observe dense and compacted floc aggregates while at dosage higher than optimal (55 mg/L) flocs can be seen as small and fragile structures.

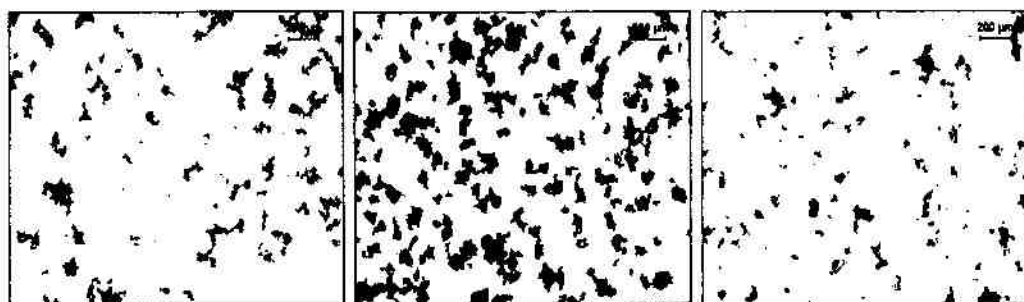


Figure 1. The flocs view from an image analysis

Results from coagulation of Disperse Yellow 5 with coagulant 7125

Table 5. Surface charge density and colour removal as a function of coagulant dosage

Dosage of coagulant 7125, mg/L	Surface charge density, meq/g	% of Colour Removal by			
		Filtration		Sedimentation	Centrifugation
		Blue filter	Yellow filter		
35	-1.117	96	93	79	85
40	-0.673	98	96	98	90
45	1.541	92	37	16	33

The results shown at Table 5, suggest lack of correlation between charge density and colour removal. At the optimal dose level of 40 mg/L, surface charge density still has a negative value -0.673 meq/g, but the colour removal reached more than 95 % by filtration and sedimentation. The removal by centrifugation was the only one appearing as lower (90%). Due to the not uniform charge neutralisation, the electrostatic patch could be viewed as the mechanism responsible for dye destabilisation. The high charged polyelectrolyte adsorbed onto dye colloid surfaces creates a "mosaic" structure consisting from positive areas surrounded by a negative ones. The oppositely charged areas of the different particles can thus enter into contact and create larger aggregates.

The results from the flocs characteristics (Table 6) present a similar like those observed at the previous case correlation. At the optimal dosage of 40 mg/L, the observed large and compacted flocs aggregates are characterized by median size 288 μm and fractal dimension 2.50. Both parameters drop with increase in coagulant dosage up to 45 mg/L. Selected flocs view are shown at Figure 2.

Table 6. Flocs characteristics and their influence on colour removal by sedimentation

Parameters	Dosage of coagulant 7125 [mg/L]		
	35	40	45
Colour removal by sedimentation [%]	79	98	16
Median diameter, d50 [μm]	282	288	52
Fractal dimension	2.40	2.50	2.09

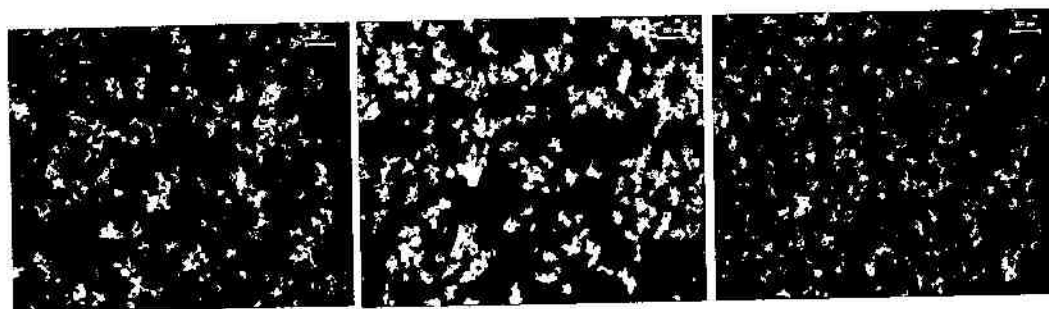


Figure 2. The flocs view from an image analysis

Summary

The main destabilization mechanisms observed after analysis of the coagulation behaviour of six azo dyes could be summarized in the table below.

Table 7. Predominant mechanisms responsible for dye destabilisation

Dye	Reactive Black 5	Reactive Red 2	Acid Black 1	Acid Orange 7	Disperse Yellow 5	Direct Red 23
Coagulant						
7101	++	++	++	++	++	++
7102	++	++	++	++	+ -	++
7103	++	++	++	++	++	++
7197	nr	nr	++	+ -	++	nr
7125	nr	nr	+ -	++	+ -	nr

Where: ++ - uniform charge neutralisation pattern; + - "mosaic" charge neutralisation; nr - no reaction

4. Conclusions

Based on the observed phenomena and their analysis the following conclusions can be drawn:

- Chemical coagulation/flocculation appears a viable technique to decrease the colour in synthetic solutions to more than 90 % by the investigated solid-liquid separation methods. Dye colloids were effectively coagulated by a cationic polymer with low molecular weight and high charge density.
- Charge neutralization pattern was the predominant mechanism responsible for destabilisation of the studied azo dyes using primary coagulants. The prove of charge patch mechanism requires more investigation.
- At the optimal dose of coagulant, an efficient destabilization of dye colloids occurs, leading to development of flocs with improved settling properties, a fact further supported by their size and fractal dimension.

5. References

- Bushel, G., Yan, D., Woodfield, D., Raper, J., Amal, R., On Techniques for the Measurement of the Mass Fractal Dimension of Aggregates, *Adv. in Coll. & Interf. Sc.*, 95, 1-50, 2002
- Elimelech, M., Gregory, J., Jia, X., Williams, R.A., "Particle deposition and aggregation. Measurement, Modeling and Simulation", Butterworth- Henemann, 1995
- Hatton, H., Simpson, A., Enhanced Colour Removal from Sewage Effluents using Chemically Flocculants. *Env. Technol, Lett.* 7, 413-424, 1986
- Jung, A., Amal, R., Raper, J., The Use of Small Angle Light Scattering to Study Structure of Flocs, *Part. Syst. Charact.* 12, 274-278, 1995
- Kang, S., Chang, H., Coagulation of Textile Secondary Effluents with Fenton's Reagent, *Wat. Sci. Technol.*, 36, 215-222, 1997
- Robinson, T., McMullan, G., Marchant, R., Nigham, P., Remediation of Dyes in Textile Effluent: a Critical Review on Current Treatment Technologies with Proposed Alternatives, *Biores. Technol.* 77, 247-255, 2001
- Zollinger, H., *Color Chemistry: Synthesis, Propertis, And Applications of Organic Dyes And Pigments*, VHCA & WILEY – VCH, Switzerland, 2003

COLOUR REMOVAL FROM WASTEWATER BY MEANS OF MICROBIAL TREATMENT

Marta JANECKO¹, Plamen GEORGIEV², Marina NICOLOVA²,
Stoyan GAYDARJIEV¹, Irena SPASOVA², Peter AY¹, Stoyan GROUDEV²

¹ Brandenburg Technical University, Cottbus, Germany

² University of Mining and Geology, Sofia, Bulgaria

Abstract

Water solutions of different dyes used in the textile industry (Reactive Black 5, Acid Orange 7 and Disperse Yellow 5) were treated under laboratory conditions by means of different microorganisms and/or their metabolites. The following microorganisms were used in this study: *Bacillus megatherium*, *B.subtilis*, *B.circulans*, activated sludge from an industrial wastewater treatment plant and a mixed enrichment culture of flocculating bacteria. It was found that the microbial effect towards the dyes was quite specific and the extent of the colour removal varied in a broad range (from 0 to 99 %). These experiments were performed in agitated reactors under batch conditions. Very good results were achieved also by means of permeable reactive barriers inhabited by flocculating bacteria and other metabolically interdependent microorganisms and operating under continuous-flow conditions. The colour removal in these cases varied in the range of about 80-90 % and was similar to that achieved by the well known chemical reagents used in the textile industry.

Key words: wastewater, *Bacillus megatherium*, *B.subtilis*, *B.circulans*

Introduction

The treatment of wastewaters from the textile industry is an important technological problem. In most cases the visible effect from the treatment is the decolourization of the polluted waters [1 - 4]. It must be noted that very often the decolourization is connected with a decrease of the toxicity of the respective wastewaters. This is due to the fact that in some cases the decolourization is a result of the degradation of the dyes present in the polluted waters to non-toxic or, at least, to less toxic products, and in some other cases - of the removal of the dyes from the water phase.

The decolourization of textile dyes has been widely studied and different chemical (oxidation, reduction), physical and physico-chemical (sedimentation, adsorption, ionexchange, membrane filtration) and biological processes have been used to solve this problem. The biological processes are quite varied and involve degradation of the dyes by means of oxidation or reduction of their functional groups, bioflocculation and biosorption [5 - 8]. It must be noted that at present the interest towards these biological processes is steadily increasing.

The present paper contains some data about laboratory studies on the microbial decolourization of water solutions of three different dyes which are used in the textile industry.

Materials and Methods

Water solutions of three different dyes used in the textile industry were used in this study (Table 1). The solutions were prepared by dissolving 100 mg of the respective dye into 1000 ml distilled water.

Table 1. Characterization of the dyes used in this study

Commercial name	Producer	Chemical index	Chemical group	Wave length, λ_{max} [nm]
Cibacron Marine	CIBA	Reactive Black 5	disazo	593
-	POLFA Pabianice, Polnad	Acid Orange 7	monoazo	481
Synten Yellow PSG 100 %	BORUTA COLOR Zgierz, Poland	Disperse Yellow 5	azo	392

Various microorganisms were used in the experiments for colour removal of the abovementioned water solutions:

- Different species of the genus *Bacillus* (*B. megatherium*, *B. subtilis*, *B. circulans*). These bacteria were grown on a nutrient medium with the following composition: glucose 20 g, peptone 4 g, yeast extract 0.35 g, K_2HPO_4 0.5 g, NH_4Cl 0.02 g, $MgSO_4 \cdot 7H_2O$ 0.35 g, distilled H_2O 1000 ml. The cultivation was carried out in 500 ml Erlenmeyer flasks containing 180 ml nutrient medium and 20 ml late-log-phase bacterial inoculum. The flasks were agitated on an orbital shaker at 180 rpm and 35°C for 72 hours.

The microbial treatment of the coloured water solutions was performed by two different means: by spent nutrient media containing bacterial cells, secreted bacterial metabolites and residual amounts of nutrients and by washed cell suspensions.

The treatment by the spent nutrient media was carried out in agitated Erlenmeyer flasks containing 30 ml water solution of the respective dye and 30 ml of the spent nutrient medium. The mixing of these two components was carried out for 2 min at 200 rpm, and then for 6 min at 80 rpm. The mixture was then filtered through Whatman paper filter "bleu band" and the colour of the filtrate was measured spectrophotometrically at the respective wave length shown in Table 1, and then was compared with the initial colour of the water solution of the respective dye.

For obtaining bacterial cell suspensions the spent nutrient media were centrifugated at 10 000 rpm for 10 min, the obtained cell precipitates were washed with distilled water and were subjected again to centrifugation. This procedure was repeated to obtain washed cells free of secreted metabolites and nutrients. The precipitated cells were suspended in 30 ml distilled water, the pH of this suspension was adjusted to 3.2 by addition of ice acetic acid. Such washed cell suspensions were mixed with 30 ml of water dye solution and the further treatment follows the procedures described above for the treatment by means of spent nutrient media:

- Microorganisms present in activated sludge from wastewater treatment plant.

The treatment was carried out by means of crude activated sludge containing a varied biocenose as well as by means of enriched mixed culture of flocculating bacteria isolated from the activated sludge. The nutrient medium mentioned above for the growth of *Bacillus spp.* was used for obtaining the enrichment culture. The treatment of the water dye solutions was carried out using the procedures described for the *Bacillus spp.*

The treatment by means of the crude activated sludge was carried out using water suspensions with pH of 3.4 containing ~ 30 wt % activated sludge. 30 ml of such suspensions were mixed with different volumes of water dye suspensions containing 100 mg/l of the respective dye. The mixtures were agitated for 2 min at 200 rpm, and then for 6 min at 80 rpm. The mixtures were then centrifugated for 10 min at 10000 rpm and the supernatants were filtered through Whatman paper filter "bleu band" before the determination of colour intensity.

- Treatment of water solutions of dyes by means of permeable reactive barriers inoculated with activated sludge

The permeable reactive barriers were cylindrical glass columns with a volume of 1600 ml each filled with a mixture consisting of (in wt %): cow manure 75, hay 20, quartz sand 5. Drain zones consisting of gravel lumps (with a particle size of + 15 - 25 mm) and glass cotton were located in the bottom and top zones of the columns. The total water volume of the individual barrier was 880 ml, and its porosity was 68.0 %. The barriers were inoculated by activated sludge containing viable microbial population at density $\sim 10^{10}$ cells/g. The water solutions of dyes were directed to the barriers by means of peristaltic pumps at rates reflecting residence times from 120 to 24 hours. The quality of water was monitored at least once per day at the inlet and outlet of the barriers.

Results and Discussion

It was found that the decolourization of the water solutions of dyes by means of bacteria related to the genus *Bacillus* was much more efficient in the cases when these bacteria were used in the form of washed cell suspensions (Table 2). The effect strongly depended on the pH of the reaction mixture (dye + bacteria) and much better results were achieved at acidic pH. This was due to the fact that the charge of the surface of the bacterial cells at pH higher than 4.5 was negative, like the charge of the dyes used in this study. However, the charge of the bacterial surface at acidic pH was changed to positive and this made the flocculation of dyes and the subsequent decolourization much more efficient.

Table 2. Treatment of water solutions of textile dyes by means of *Bacillus* spp. at pH -3.3

Microorganisms	Reactive Black 5		Acid Orange 7		Disperse Yellow 5	
	I	II	I	II	I	II
	Colour removal, %					
<i>Bacillus megatherium</i>	21.4	74.2	53.2	83.7	0	60.2
<i>Bacillus subtilis</i>	21.7	79.0	44.8	81.8	0	66.2
<i>Bacillus circulans</i>	58.1	64.4	75.0	83.7	65.3	80.6

Note: I - Treatment by means of spent nutrient media;
 II - Treatment by means of washed cell suspensions.

The amount of biomass in the reaction mixture was also very important for an efficient decolourization of the water solutions of dyes. The data shown in Table 2 were achieved by means of mixtures containing ~ 750 mg/l bacterial biomass and 100 mg/l dye, i.e. ~ 7.5 mg per mg dye. An increase of the biomass/dye ratio from 7.5 to 15 increased the colour removal of the dyes by means of washed cell suspensions to over 90 %. The individual *Bacillus* spp. differed considerably from each other with respect to their efficiency towards the different dyes. The best results were achieved by means of *B. circulans* which produced large amounts of exopolysaccharides. These exopolysaccharides formed the large mucilaginous capsules of these bacteria and partially dissolved in the nutrient medium. This explained the good results obtained by the spent nutrient medium formed after the cultivation of these bacteria.

The different dyes differed from each other with respect to their amenability to decolourization by means of bacterial treatment. The Disperse Yellow 5 was the most refractory to such treatment.

Apart from the flocculation, the sorption of dyes by bacterial biomass was also a mechanism involved in the decolourization of their water solutions. This was shown by the decolourization, although at a lower extent, achieved at pH close to the neutral point, as well as by experiments in which Mg^{2+} cations were added to the reaction mixture. These ions acted as desorbents towards ions, mainly bivalent, adsorbed on the bacterial surface and in this way increased the sorption capacity of this surface for the dyes. It must be noted also that different inorganic sorbents such as zeolite, bentonite and activated carbon were also active in the decolourization of dyes.

The decolourization of water dye solutions by means of an enriched mixed culture of flocculating bacteria was even more efficient than the decolourization achieved by means of the bacteria related to the genus *Bacillus* (Table 3). Very good results were obtained by means of spent nutrient media containing bacterial cells and secreted metabolites. This was connected with the large amount of biomass in these media (over 5 g/l). However, the best results were achieved by means of activated sludge used at high concentrations (> 3%) and a high biomass/dye ratio (Table 4).

Table 3. Treatment of water solutions of textile dyes by means of enriched mixed culture of flocculating bacteria

Dye	Way of treatment			
	By spent nutrient medium		By means of washed cell suspension	
	Initial pH of the system			
	3.2	6.5	3.7	5.3
	Colour removal, %			
Reactive Black 5	97.3	53.0	80.7	15.4
Acid Orange 7	97.2	86.8	79.6	52.5
Disperse Yellow 5	90.1	46.4	86.0	0

Table 4. Treatment of water solutions of dyes by means of activated sludge

Water solution of dye added to the activated sludge, ml	Reactive Black 5	Acid Orange 7	Disperse Yellow 5
30	98.0	98.0	90.5
50	95.2	96.1	90.3
80	99.1	96.3	91.23
100	97.0	97.4	92.5
150	99.1	96.1	87.3
300	99.5	95.0	84.4

The treatment of the dye solutions by means of permeable reactive barriers was very efficient (Table 5). It was found that the microbial cenoses which developed in the barriers contained mainly anaerobic and facultatively anaerobic bacteria. The pH during the treatment was stabilized around the neutral point and the redox potentials were slightly positive.

Table 5. Treatment of water solutions of dyes by means of permeable reactive barriers inoculated by activated sludge from wastewater treatment plant

Parameters	Reactive Black 5	Acid Orange 7	Disperse Yellow 5
pH	7.21-7.38	7.25-7.81	7.30-7.94
Eh, mV	(+8)-(+28)	(-35)-(+125)	(+5)-(+86)
Total dissolved solids, mg/l	91-125	95-442	1112-1175
Dissolved oxygen, mg/l	4.6-5.6	5.3-6.4	5.0-5.4
Dissolved organic carbon, mg/l	23-48	35-55	80-91
Heterotrophic aerobic bacteria, cells/ml	10 ⁵ -10 ⁷	10 ⁴ -10 ⁷	10 ⁴ -10 ⁶
Heterotrophic anaerobic bacteria, cells/ml	10 ⁴ -10 ⁶	10 ⁴ -10 ⁶	10 ⁴ -10 ⁶
Colour removal, %	80-88	86-91	78-84

The results obtained by means of the microbial treatment as a whole were similar to those obtained by means of coagulants, which are used in commercial-scale operations (Zetang 7101, 7102, 7103, 7197, 7125 which were supplied by CIBA Specialty Chemicals).

The decolourization of the dye solutions used in this study was stable and no coloration appeared again even after long periods of time (several weeks). This may be an indication for almost complete removal or degradation of the dyes. However, further studies are needed to establish the exact mechanisms involved in the solution decolourization. It is necessary to perform studies on the toxicity of the treated solutions to establish whether the colour removal is connected with a decrease of their toxicity.

Acknowledgements

This work was financially supported in the frame of the project N DAAD44 entitled "Mechanisms of bioflocculation and nature of the floccules and their industrial applications" in connection with the scientific cooperation between Germany and Bulgaria.

References

1. Gehrke, T., Telegdi, J., Thierry, D. and Sand, W., *Appl. Environ. Microbiol.*, 64(7), 2743-2747, 1998.
2. Vandevivere, P.C., Bianchi, R. and Verstraete, W., *J. Chem. Technol. Biotechnol.*, 7, 289-302, 1998.
3. Marmagne, D. and Coste, C., *Am. Dyest. Rep.*, 85(4), 15-21, 1996.
4. Pala, A. and Tokat, E., *Water Research*, 36, 2920-2925, 2002.
5. Blaquez, P., Casas, N., Font, X., Gabarrell, X., Sarra, M., Caminal, G. and Vicent, T., *Water Research*, 38, 2166-2172, 2004.
6. Forster, C.F., *Water Research*, 5, 861-870, 1971.
7. Eriksson, L. and Alm, B., *Water Sci. Technol.*, 24(7), 21-28, 1991.
8. Houghton, J.I. and Quarmby, J., *Curr. Opin. Biotechnol.*, 10, 259-262, 1999.



Microscopic and laser granulometric analyses of hydrating cement suspensions

Vili Lilkov^a, Ekaterina Dimitrova^b, Stoyan Gaidardzhiev^a

^aUniversity of Mining and Geology, Department of Physics, Darvenitsa 1100, Sofia, Bulgaria

^bCentral Laboratory of Physico-Chemical Mechanics, Bulgarian Academy of Sciences, Sofia, Bulgaria

Manuscript received 26 January 1998; accepted manuscript 23 September 1998

Abstract

The results from microscopic and laser granulometric analyses of hydrating cement suspensions, containing active mineral additives (silica fume, fly ash, and a mixture of both called Pozzolit) are presented. Conclusions are drawn about the specific hydration processes of the cements investigated, as well as the applicability of the laser granulometry method for the study of cement and its hydration products. The investigation is part of a program studying the combined effect of silica fume and fly ash on the hydration process and the physical and mechanical properties of cement mortars and concretes. © 1999 Elsevier Science Ltd. All rights reserved.

Keywords: Laser granulometry; Microscopy; Mineral additives; Cement suspensions; Hydration; Particle size distribution

Laser granulometric analysis has been used in cement research for the study of particle size distribution of unhydrated cements and the assessment of their quality. The scope of the method has been extended to the study of cement clinker mineral activity in contact with water. It has been evaluated according to the variation of particle concentration with time [1], the time dependence of particle size variation for suspensions and cement pastes with different inorganic admixtures [2,3], as well as the specific surface determination of various pozzolanic additives [4] and the effect of chemical admixtures on the dispersity and specific surface of cement particles [5].

The microscopic methods used in their different versions have proved to be universal for the study of various microscopic objects. They provide extremely valuable information based on direct observation of the investigated objects.

This work presents the results obtained from microscopic and laser granulometric research of cements containing active mineral additives (silica fume, fly ash, and a mixture of both) hydrating in the form of suspensions.

1. Materials and methods

Portland cement PC45 (C), silica fume (SF) (a by-product material of the production of ferro-silicon steel in the "Kremikovtsi" Metallurgical Plant, Bulgaria, with a content

of about 93% of amorphous silica), classified fly ash (FA) from the "Bobov Dol" Thermal Power Generation Plant, Bulgaria, and a Pozzolit (Pz) mineral additive [6] based on a 50:50 mixture of silica fume and fly ash were used in the present investigation. Four different cement compositions, without and with mineral additives, were studied. In three the cement was replaced by 10% silica fume, fly ash, or Pozzolit.

The microscopic analysis was performed using an Image Analyzer developed at the Technical University, Sofia. The device is used to determine the disperse composition of emulsions and suspensions. It includes a Jena 2-Carl Zeiss optical microscope equipped with a CCTV-SSC-8001 video camera and a computer. The average dimension L_{av} and the $\alpha = L_1/L_2$ ratio between the maximal (L_1) and the minimal (L_2) linear dimensions of each of the observed particles had been determined. The program provides the graphic image and calculation of the effective diameter D_{eff} for the whole group of analyzed particles. The advantage of the method is that the sizes of the particles are obtained directly and that it is possible to work individually with the objects. The suspensions of the cement and mineral particles are investigated in 0.5-mm high glass cells. Adjustment of the device and the recording time for each measurement do not exceed 3 min.

The laser granulometer (Laser Particle Sizer Analysette-22, Fritsch) is based on an He-Ne laser wavelength of 632 nm, power of 5 mW, and a multielement 31-channel detector. The apparatus is capable of measuring particle size distribution over the range from 0.3 to 1100 μm , based on the presumption of a spherical particle. The software offers the

* Corresponding author. Tel.: (359 2) 62 581/347; E-mail: lilkov@staff.mgu.bg.

Table 1
Particle size distribution (%) of the additives and of the cements depending on the $\alpha = L_1/L_2$ ratio.

α in the interval	1-1.16	1.16-1.5	1.5-2	>2
Additives				
SF	54.2	18	17.5	10.3
FA	46.4	26.4	20	7.2
Pz	45.1	25.6	19.3	10
Cements				
C	46.5	27	14.5	12
C + SF	49.5	21.9	18.6	10
C + FA	47.7	22.9	20.2	9.1
C + Pz	47.5	26	15.7	10.8

L_1 , maximal and L_2 , minimal linear dimension of the particles.

possibility of obtaining both frequency size distribution and cumulative size distribution. At the beginning of each test the distance between the cell and the detector had been adjusted, and in all measurements beam obscuration was kept within the limits of 8% to 10%. The duration of one measurement was about 1 min.

Cement suspensions were prepared with 400 mg of cement and 100 mL of distilled water mixed in a magnetic stirrer (5 min) and subsequently stored until the moment of measurement. The suspensions were ultrasonically dispersed for 1 min immediately before measurement. The water-to-solid ratio of the suspensions investigated was determined experimentally in the range of maximum sensitivity of the laser granulometer.

The differential particle size distribution of the materials used and of the cements was investigated in a liquid medium of pure ethyl alcohol to avoid the dissociation and agglomeration of cement particles that occur upon contact with water.

2. Results and discussion

The microscopic analysis proved that about 54% of the SF particles and more than 45% of the FA, Pz, and initial cement particles are of a close to spherical form, with the α ratio being less than 1.16. Addition of the additives to the initial cement does not change significantly the form of the particles (Table 1).

The results from the microscopic and laser granulometric analyses of the initial materials (Fig. 1) are very close because the materials investigated are characterized by a greater share of the spherical particles.

When mixing fly ash and silica fume the share of particles smaller than 2 μm is decreased whereas the share of particles with an average size larger than 5 μm is increased. The effective diameters of the SF, FA, and Pz particles are 1.9, 7.9, and 9.5 μm , respectively. The graphic images and the SEM micrographs of the mineral additives particles are shown in Figs. 2 and 3, respectively.

The graphic images of the particles of the cements investigated are shown in Fig. 4. The effective diameter of the

particles is 5.4 μm for the initial cement and 5.0, 7.1, and 7.7 μm for the cements with silica fume, fly ash, and Pozzolit, respectively.

The results confirm that the silica fume and fly ash particles, as well as the cement and additive particles, are susceptible to sticking to one another, forming complexes of heterogeneous particles that exist in the mixtures together with the particles of the initial materials.

The graphic images of the particles of the cement suspensions investigated at the fourth hour of hydration are presented in Fig. 5.

In the process of hydration of all the cement suspensions, the number of particles with a close to spherical shape decreases. This is especially well expressed for the silica fume and Pozzolit containing cement suspensions (Table 2). The silica fume particles obviously serve as links between the single hydrating particles, uniting them in complexes of particles of irregular shape.

During the first hour of hydration, the average dimension of the particles in the pure cement suspensions decreases as a result of the dissolution of particles larger than 5 μm , thus increasing the share of particles with average dimension less than 1 μm (Fig. 6a). In the case of cement suspensions with mineral additives, the share of the finest and the most coarse particles is diminished during the same period,

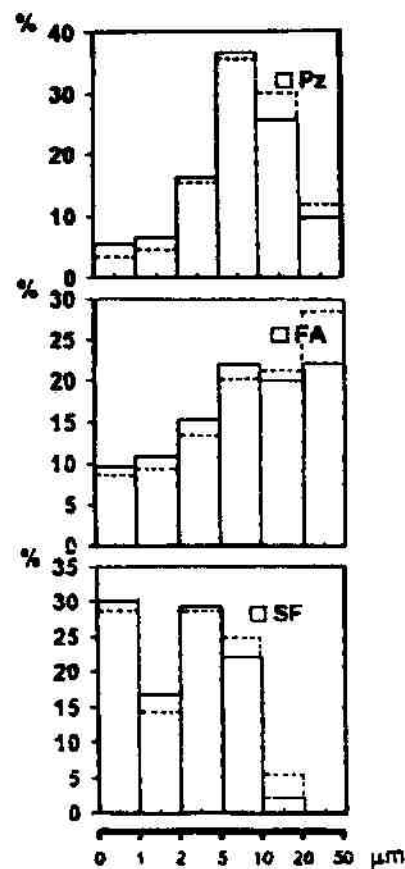


Fig. 1. Differential particle size distribution of the SF, FA, and Pz particles: (—), microscopic study; (---), laser granulometric study.

whereas
increases

At the
sions, th
 μm is de
s increa
zolit con
larger th
pense of
to 10 μm

At the
particles
taining c

Comp
the aver
analysis
ters (Fig
recordin
alteratio
hydratio
solid pa
fluid res
(turbule
tary mov
posed on

Table 2
Particle si
depending

Cements
C
C + SF
C + FA
C + PZ

L_1 , m

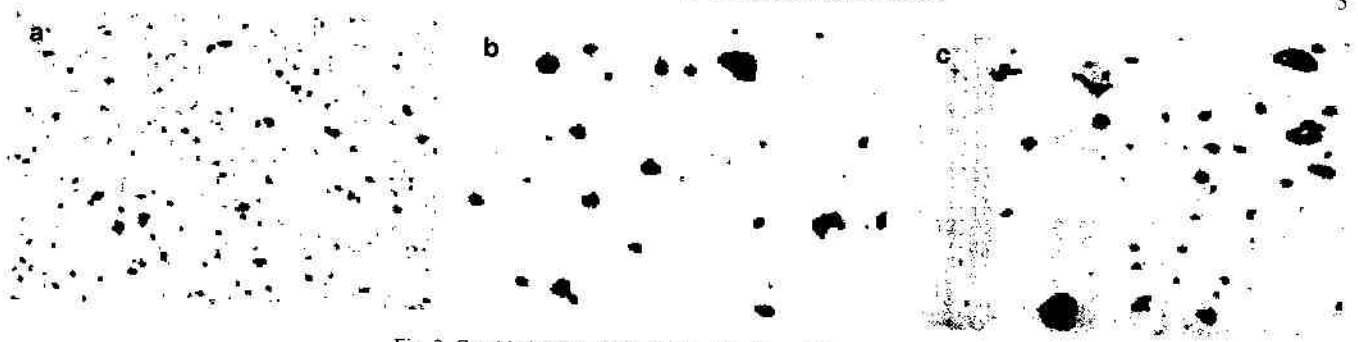


Fig. 2. Graphic images of the SF (a), FA (b), and Pz (c) particles.

whereas the share of the middle-size particles (2–10 μm) is increased (Figs. 6b–6d).

At the fourth hour of hydration of pure cement suspensions, the share of particles with an average size less than 2 μm is decreased and the share of particles larger than 5 μm is increased (Fig. 6a), whereas in the silica fume and Pozzolite containing cement suspensions the share of particles larger than 10 μm is increased more than twice at the expense of the decreased share of particles in the range from 1 to 10 μm (Figs. 6b and d).

At this stage of hydration, strong growth of the share of particles larger than 20 μm is observed for the fly ash containing cement suspensions (Fig. 6c).

Compared to the results from microscopic investigations, the average particle sizes obtained from laser granulometric analysis are shifted in the direction of larger particle diameters (Fig. 7). The reason for this difference is in the object recording principle of laser granulometry, as well as in the alterations of particle shape that occur during the course of hydration. The unequal friction forces on the surface of solid particles of irregular shape suspended in a viscous fluid result in pressure fluctuations leading to vortex drag (turbulence resistance) [7], thus causing oscillatory and rotary movement of the particles in the stream that is superposed on their oriented flow in the suspension. The record-

Table 2
Particle size distribution (%) of the hydrating cement suspensions depending on the $\alpha = L_1/L_2$ ratio

Cements	α in the interval (h)	α in the interval (h)			
		1–1.16	1.16–1.5	1.5–2	>2
C	0	46.5	27	14.5	12
	1	36.4	36.4	18.1	9.1
	4	36.0	31.2	19.5	13.3
C + SF	0	49.5	21.9	18.6	10
	1	25	35.5	22.1	17.4
	4	30.1	28.5	23	18.4
C + FA	0	47.7	22.9	20.2	9.2
	1	35.7	30.9	22.6	10.8
	4	34.8	29.8	23.2	12.2
C + PZ	0	47.5	26	15.7	10.8
	1	30.0	34.7	20.2	15.1
	4	29	30.1	23.1	17.8

L_1 , maximal and L_2 , minimal linear dimensions of the particles.



Fig. 3. SEM micrographs of the FA (a) and Pz (b,c) particles.

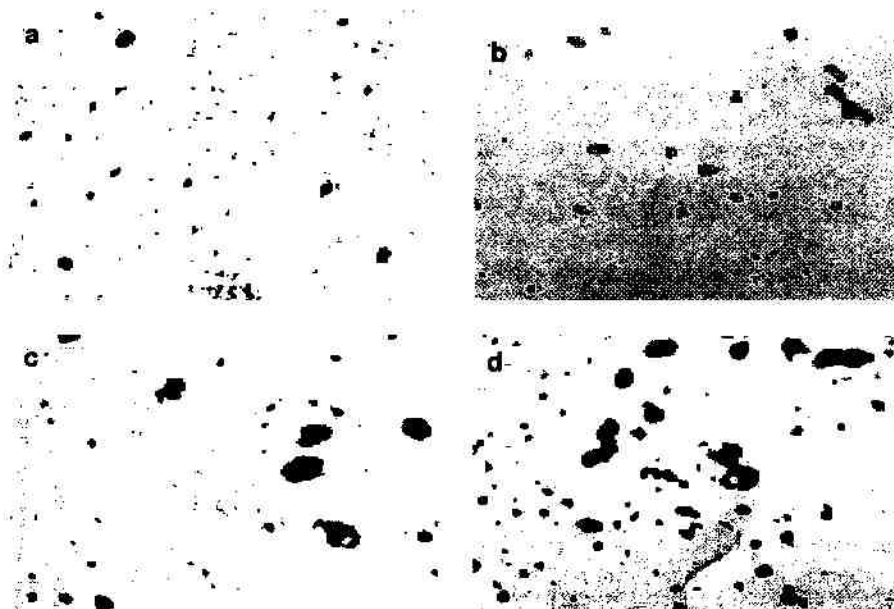


Fig. 4. Graphic images of the particles of the (a) initial cement (C) and cements with (b) SF (C + SF), (c) FA (C + FA), and (d) Pz (C + Pz).

ing principle of operation of the laser granulometer is based on the Fraunhofer diffraction of the laser beam by the suspended particles [8], when the differently oriented particles in the bulk of the suspension, varying in shape and size, can be "seen" by the detector as identical and vice versa. On the other hand, the larger particle sizes established by laser granulometry, in comparison with the real ones obtained from microscopic investigations, result from their oscillatory and rotary movement during the measuring process when they are "seen" by the detector as spheres with a di-

ameter equal to their maximal linear dimension, because the recording time is considerably longer than the period of particle oscillation in the range of the laser beam.

3. Conclusions

1. In the fly ash/silica fume mixtures the silica fume particles cover mainly the fine fly ash grains, forming stable Pozzolit grain complexes.

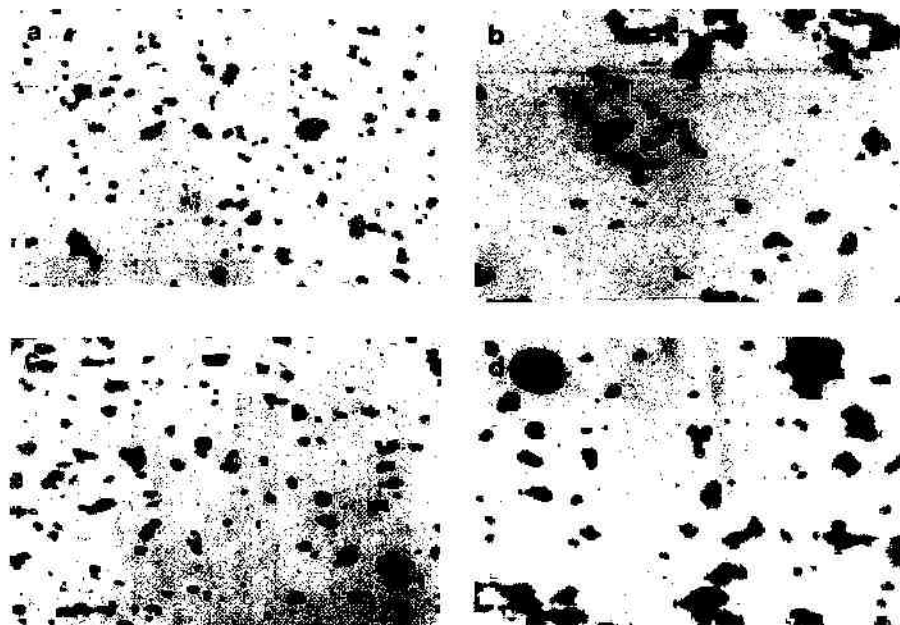


Fig. 5. Graphic images of the particles of (a) the plain cement suspension (C) and cement suspensions with (b) SF (C + SF), (c) FA (C + FA), and (d) Pz (C + Pz) at the fourth hour of hydration.

2. The
gat
par
con
sol
siz
cle
3. Ap
diti
sph
dis

Fig. 6. Dif
Microscopi

2. The first hours of hydration of the cements investigated are characterized by variations in the effective particle size and particle size distribution. Several concurrent processes proceed simultaneously: the dissolution of cement particles and diminution of their size on the one hand and aggregation of small particles on the other.
3. Approximately half of the particles of the mineral additives and of the investigated cements have a close to spherical shape. The relative share of these particles diminishes during the course of hydration of the cement suspensions at the expense of the irregularly shaped particles, this being expressed most strongly

for the silica fume and Pozzolit containing cements. The fine silica fume particles possessing a great specific surface serve as links between the single hydrating particles.

4. Laser granulometric analysis is applicable to investigation of materials with particles of nearly equal shape, which can be defined unambiguously by the so-called shape parameter of the particles. The most accurate results are obtained for materials with a spherical particle shape in an inert, for them, medium. The method is not applicable to hydrating cement suspensions, because the shape of the particles becomes irregular and is changed greatly during the hydration process.

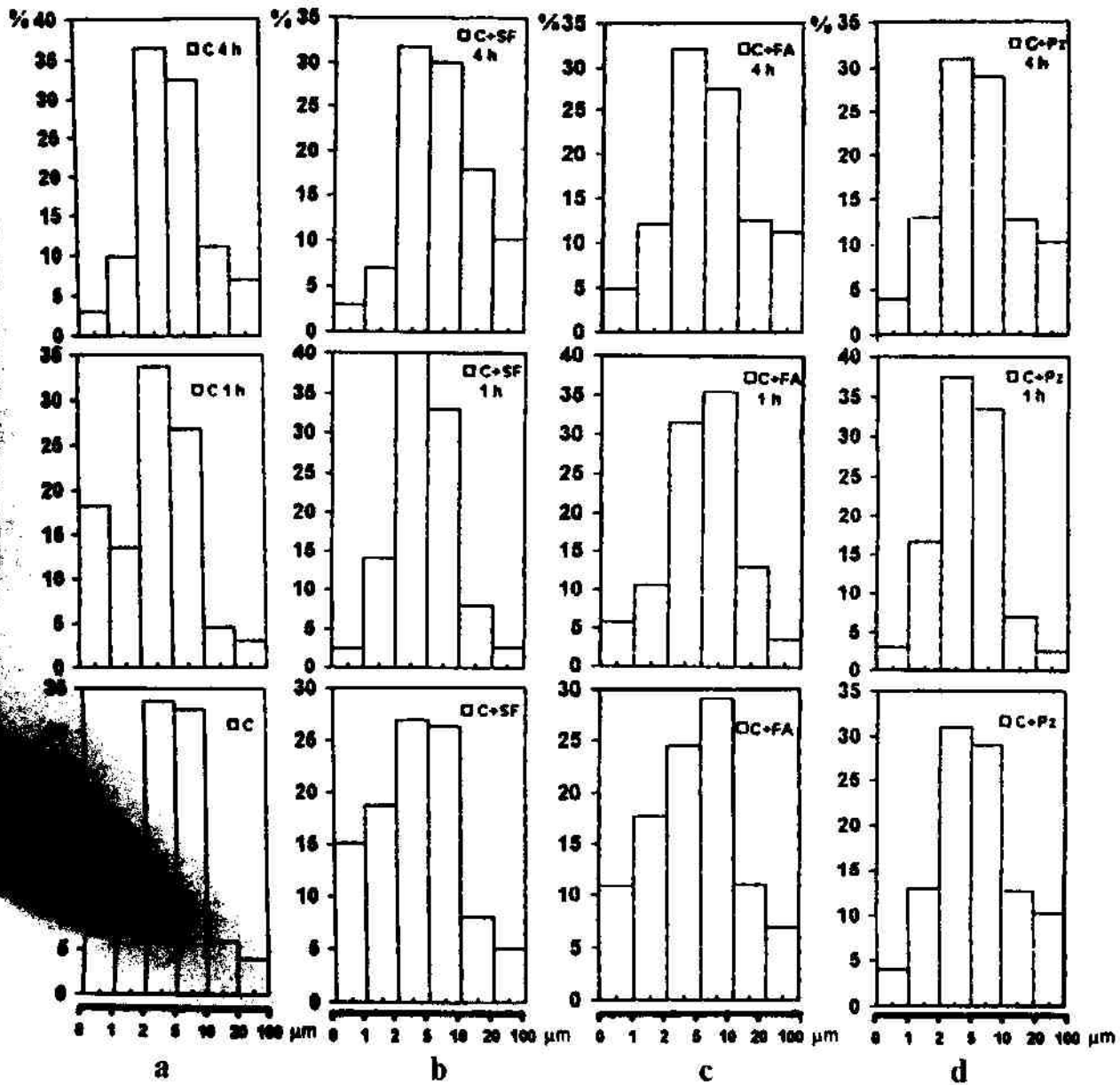


Fig. 6. Differential particle size distribution during hydration of the plain cement suspension (a) and cement suspensions with SF (b), FA (c), and Pz (d) by microscopic investigation.

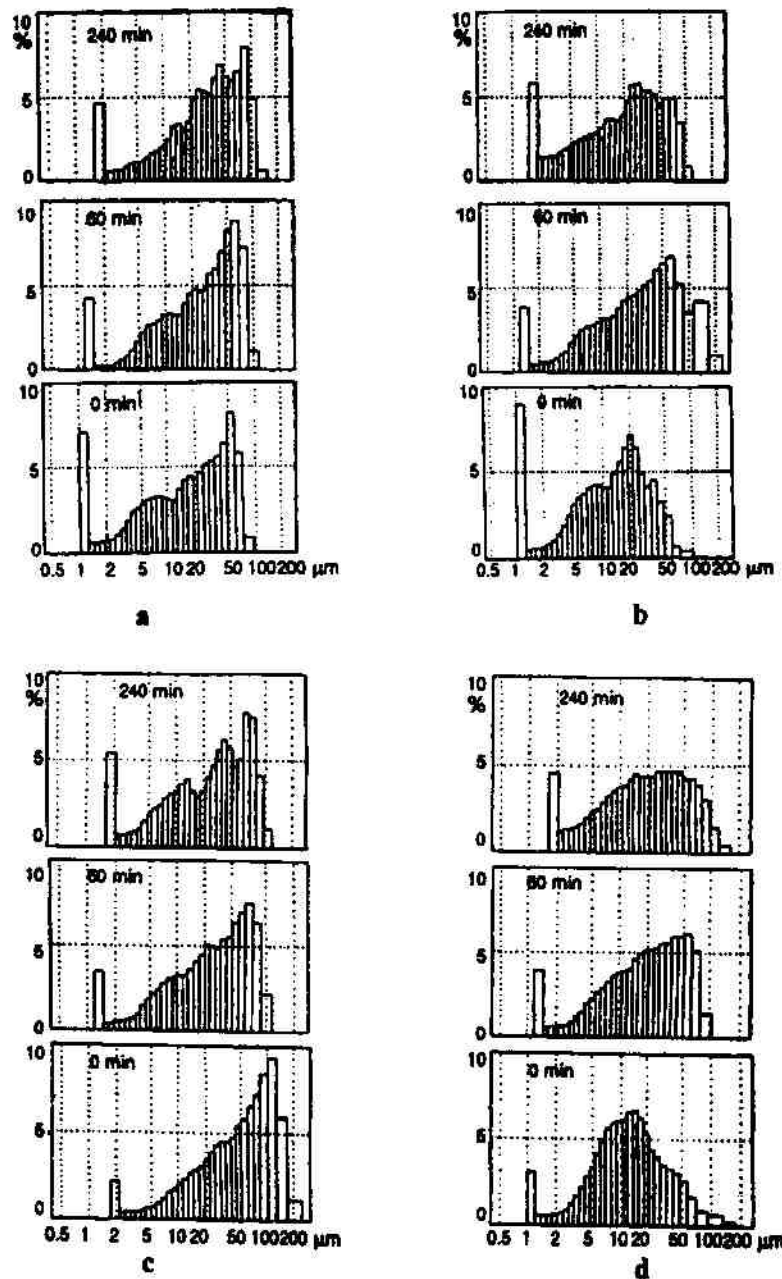


Fig. 7. Differential particle size distribution during hydration of the plain cement suspension (a) and cement suspensions with SF (b), FA (c) and Pz (d) by laser granulometric study.

Acknowledgments

The present investigation was carried out with financial support from the National Fund "Scientific Investigations" of the Bulgarian Ministry of Education and Science (Project H3-417).

References

- [1] A. Negro, L. Montanaro, A. Bachiornini, *Cem Concr Res* 15 (1985) 315.
- [2] I. Odler, T. von Borstel, *Cem Concr Res* 19 (1989) 295.
- [3] L. Montanaro, A. Bachiornini, *Il Cemento* 82 (1985) 153.
- [4] M. Frias, M.J. Sanchez de Rojas, M.P. Luxan, N. Garcia, *Cem Concr Res* 21 (1991) 709.
- [5] I. Masood, S.K. Agarwal, U.N. Sinha, *Cem Concr Res* 24 (1994) 527.
- [6] V. Lilkov, V. Stoitchkov, *Cem Concr Res* 26(7) (1996) 1073–1081.
- [7] L. Landau, E.M. Lipshitz, *Theoretical Physics, V. VI. Hydrodynamics*. Nauka, Moscow, Russia, 1998 (in Russian).
- [8] G. von Bernuth, *Laser Partikel-Sizer "Analysette 22." Ein Labor- und Betriebmessgeraet* zur Messung von Partikelgroessenverteilungen an Mineralischen und Synthetischen Rohstoffen, FRITZSCH GmbH, Laborgeraetebau D-6580 Idar-Oberstein (published in *TiZ* 5/88).

Stabilization of Aqueous Silicon Nitride Suspension with Dolapix A88

Bimal P. Singh

Regional Research Laboratory, Bhubaneswar, India

Stoyan Gaydardzhiev and Peter Ay

Chair of Mineral Processing, Brandenburg University of Technology, Cottbus, Germany

The dispersing phenomenon of silicon nitride suspension has been investigated systematically by measuring surface charge density, sediment volume, and turbidity of the suspension. Dolapix A88 has been used as dispersant to improve the stability of the suspension, and assessed through measurement of the specific surface charge of the Si_3N_4 system. The isoelectric point (IEP) of Si_3N_4 powder has been found to be at $\text{pH}_{\text{iep}} = 6.91$, and there was no shift in IEP due to the presence of dispersant, indicating that the interaction between the powder and the dispersant Dolapix A88 is purely physisorbing in nature. Good agreement has been observed among dispersion characteristics, surface charge, and streaming potential inflection. The article also describes the selection and optimization of the dispersant in controlling the stability of an aqueous suspension of Si_3N_4 . It can be concluded from this investigation that the PCD technique for measurement of specific surface charge can be conveniently used for the assessment of dispersibility of ceramic suspensions in dilute as well as in concentrated suspensions.

Keywords Silicon nitride, Dolapix A88, dispersion, stabilization, surface charge, streaming potential

INTRODUCTION

Due to its low thermal expansion coefficient and modest elastic modulus, silicon nitride is an important high-temperature structural ceramic material (Nitzsche et al. 1987). Dense silicon nitride ceramics are characterized by good high-temperature stability, resistance to thermal shock, and relatively high ability to withstand oxidation (Wang et al. 2000). The comparatively low density of silicon nitride (3.2 g/cm^3) offers the possibility for production of much lighter components than would otherwise be possible (Ziegler et al. 1987). However, due to low reliability and reproducibility of its properties the application niche for this material is still limited. Colloidal processing routes offer the possibilities for overcoming the above limitations by controlling material/slurry properties. Recent studies (Cesarano and Aksay 1988; Jean and Wang 1990; Hackley 1997) and suggestions (Pugh 1994) that engineered ceramics based on physicochemical

routes are more valuable for high-temperature applications have generated a revival of interest in understanding the physicochemical properties of these materials.

Colloidal processing of ceramic powders requires precise control of homogeneity, rheology, and dispersion ability of the slurry. Homogeneity and rheology of highly concentrated ceramic suspensions are key control factors for the processing of ceramic components via wet routes. A homogeneous mixture of solid, liquid, and additive components is necessary to provide good sintering characteristics. In practice, the dispersion of silicon nitride is a critical step in the colloidal processing of powders, affecting both rheology and homogeneity. Therefore, it is important to understand the physicochemical properties of all components in the suspension phase.

There are mainly two approaches for achieving stable dispersions of submicron-sized silicon nitride powder described by (Wang et al. 2000). In one approach, the Si_3N_4 powder is coated by an oxide layer such as SiO_2 or Al_2O_3 ; therefore, the powder behaves in a manner similar to such oxides, for which dispersion behavior is well investigated and documented (Han et al. 1996; Wang and Riley 1992; Kulig et al. 1989). In the other approach, Si_3N_4 powder is stabilized by selective dispersants. It has been reported that chemical additives like

Received 6 April 2005; Accepted 9 April 2005.

Address correspondence to Bimal P. Singh, Regional Research Laboratory, Bhubaneswar 751013, India. E-mail: bpsingh99@yahoo.com

amino alkanol seem to have good dispersion abilities for aqueous Si_3N_4 suspensions (Schwelm 1992). Lange and co-workers (Luther et al. 1994, 1995) reported salts or grafting small molecules onto the Si_3N_4 surface for better suspension. Similarly, some additives known as coupling agents have attracted interest as dispersants for Si_3N_4 , as they can be strongly attracted to the particle surface due to the formation of chemical bonds (Porter 1994). It has also been reported that the interaction of surface probe molecules with the Si_3N_4 surface indicates that the absorbing moiety of the dispersants for Si_3N_4 should contain amine or alcohol groups because of their high affinity to the powder surface (Wang et al. 1996). Therefore, in the present investigation, a dispersant (Dolapix A88) with an amino head group has been chosen.

This article reports on findings derived from systematic study of the dispersion behavior of silicon nitride suspensions with Dolapix A88 dispersant and discusses the stability of the aqueous suspensions in terms of charge characteristics, slurry sedimentation, turbidity, and solids loading.

EXPERIMENTAL

Material

An α -type silicon nitride powder of high purity obtained from Alfa Aesar (Germany) has been used in all experiments. It is characterized by a mean particle size (d_{50}) below $1\ \mu\text{m}$ and a specific surface area (BET) of $2.5\ \text{m}^2/\text{g}$. The main powder characteristics are summarized in Table 1. The dispersant used was 2-amino-2 methyl propanol (Dolapix A88, Zschimmer & Schwarz, Germany) as 10% solution. Its characteristic properties are shown in Table 2. The reagents (NaOH and HCl) used to adjust the pH were of analytical grade, supplied by Merck (Germany). Bi-distilled water with conductivity below $0.01\ \mu\text{S}/\text{cm}$ and pH 6.7 has been used unless otherwise stated.

Method

Surface Charge Measurement

Surface chemical properties of the silicon nitride powder were assessed by measurement of their specific surface charge using a particle charge detector (PCD-O3-pH) from Müttek (Germany). Its operational and measuring principles

TABLE 1
Properties of silicon nitride powder

Powder characteristics	Typical values
Molecular weight	140.28
Size	$< 1\ \mu\text{m}$
Crystallographic phase	α (99.9 %)
Surface area (BET)	$2.5\ \text{m}^2/\text{g}$
Density	$3.44\ \text{g}/\text{cm}^3$

TABLE 2
Some characteristic properties of Dolapix A88

Properties	Typical values
Active matter	90%
Density (20°C)	$0.95\ \text{g}/\text{cm}^3$
pH (1% solution)	11
Solubility	Water soluble
Dissociation	Complete in alkaline solution

are reported elsewhere (Singh et al. 2002a, b; Nitzsche and Bley 1997).

Determination of Optimum Dispersant Dosages

The optimum dosage level of Dolapix A88 dispersant required for obtaining maximum dispersion of the silicon nitride suspension was estimated by means of streaming potential measurement with the help of Particle Charge Detector (PCD-O3-pH). For this purpose, 5 wt% of silicon nitride suspension has been used and the streaming potential was measured in the presence of various dosage levels of dispersant Dolapix A88. The inflection point in the plot between dosage level and PCD potential indicated the optimum dispersant dosage, leading to maximum dispersion (Singh et al. 2002b).

Sedimentation Tests

Sedimentation tests were performed using 25 mL calibrated glass cylinders by dispersing 1.25 g of silicon nitride powder in 25 mL of water containing predetermined amounts of dispersant. The suspensions were vigorously shaken and allowed to stand undisturbed for 24 h. The sediment heights were then read directly from the graduated cylinder. The higher the sediment, the more stable is the suspension.

Turbidity Measurement

The stability of a silicon nitride suspension under different pH conditions in the presence and absence of dispersant was additionally evaluated by means of a turbidity technique, employing the 'Turbiquant 3000 IR' turbidity meter from Merck (Germany). It measures the amount of light scattered from a focussed IR light source by a solution. High turbidity values indicate a larger incident light scattering, which in turn indicates stable suspension presence.

RESULTS AND DISCUSSION

Surface Charge Effects in Silicon Nitride Powder Processing

The measurement of surface charge could be viewed as a reliable predictive parameter for aqueous dispersion behavior. The amount of charge on the surface is an important

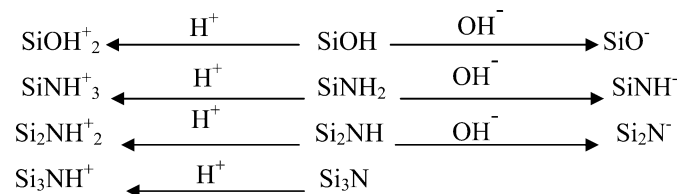
TABLE 3
Test results of specific surface charge density of Si₃N₄ (5% w/v)

pH	Specific surface charge (C/g)	Streaming potential (mV)	Observation
1.8	+0.0041	+450	
3.6	+0.0028	+483	Natural pH, (5 % w/v)
5.2	+0.0013	+330	
6.4	-0.00012	-29	Near p <i>H</i> _{iep}
7.0	-0.0011	-200	
8.9	-0.00354	-180	
10.5	-0.012	-350	

particle characteristic, as it governs many suspension properties. In this investigation, the 5% w/v Si₃N₄ slurry has shown a natural pH of 3.65 in double-distilled water. The results from the potentiometric titration, linking the surface charge variation of the silicon nitride with suspension pH, are presented in Table 3. It is evident from the data that under the prevailing experimental conditions of natural pH the Si₃N₄ particles exhibit a slightly positive surface charge.

The stability of a Si₃N₄ suspension is closely related to its interfacial properties in aqueous solution. It has been established earlier that the silicon nitride surface contains amphoteric silanol (Si-OH), as well as basic primary, secondary, and tertiary amine groups (SiNH₂, Si₂NH, Si₃N) (Busca et al. 1986). The measurement of surface charge up to pH 6.9 has outlined the dominating influence of the basic surface groups. These groups act as proton acceptors due to the free lone pair of electrons on the nitrogen atom and acquire positive surface charges as per Scheme 1 (Nitzsche et al. 1987).

The equilibrium p*H*_{iep} for Si₃N₄ in aqueous suspension has been reported to be 6.8 ± 0.3 (Bergstrom and Pugh 1989). A mean theoretical p*H*_{iep} value of approximately 7 has been reported for 1:1 ratio of acidic silanol and basic secondary amine by Kulig and Greil (Nitzsche et al. 1987). In the present investigation the p*H*_{iep} was determined by the PCD technique and was found to be 6.91. This value agrees well with the earlier reported ones (Nitzsche et al. 1987).



SCH. 1.

Surface Chemical Properties of Silicon Nitride

The isoelectric point (IEP) of the silicon nitride suspension was estimated on the basis of streaming potential. Figure 1 depicts the variation of PCD potential (mV) as function of pH in the presence and absence of dispersant. The natural pH of 5% silicon nitride suspension has been observed as 3.6, the suspension being positively charged. Without addition of dispersant, the p*H*_{iep} of the system has been estimated as 6.91, the Si₃N₄ suspension being positively charged at pH below 6.91 and negatively charged above that point. The magnitude of the negative PCD potential increased with concomitant pH increase. These findings suggest that the Si₃N₄ suspensions should experience progressive deflocculation with increase in pH. An almost similar trend of potential variation with pH has been observed for the case when dispersant was added. It is interesting to note that the dispersant addition did not shift p*H*_{iep}, which was also found as 6.9. This coincidence clearly indicates that the interaction between Si₃N₄ and dispersant is physical in nature (Pradip 1988). The physical sorption is usually characterized as weak and reversible, involving negligible energy change, about 20–40 kJ/mol. Electrostatic and van der Waals forces are mainly responsible for physical adsorption (Pradip 1988). The PCD potential decreased at higher pH values. This might be explained owing to the fact that at the alkaline region, the increased requirement for NaOH to buffer the pH leads to a higher ionic strength in the suspension and subsequent compression in the double layer thickness, and hence results in a decrease in surface charge/PCD potential at the interface of the particles and in dispersion stability as well. The surface charge tends to decrease under both extreme acidic and basic environments due to increased ionic strength leading to double layer compression (Singh et al. 2004).

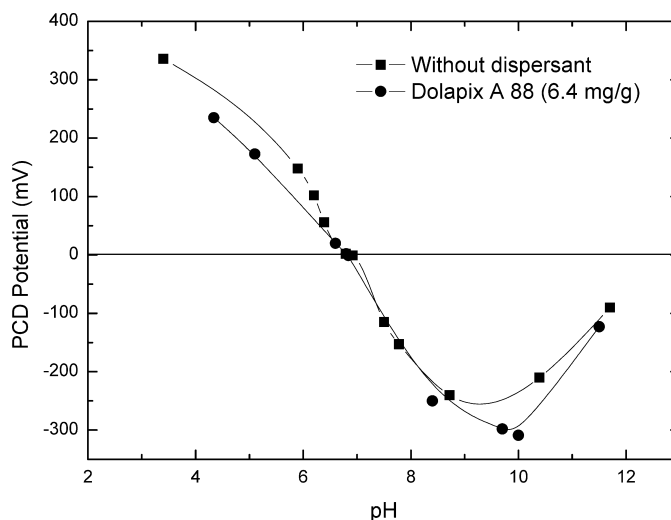


FIG. 1. Determination of streaming potential from PCD measurements as a function of pH at a particle concentration of 5%.

Determination of Optimum Dispersant Dosages

Figure 2 shows the variation of PCD potential as a function of different dosages of dispersant. The relationship shown clearly indicates that the addition of a minute amount of Dolapix A88 completely neutralized the initial positive charge, and a steep increase in negative PCD potential was observed with increase in dispersant concentration. After reaching the plateau value of approximately -699 mV, it remains almost constant. Therefore, 6.4 mg/g dispersant has been chosen as an optimum dose for the Si_3N_4 powder under study, which is in good agreement with the optimal dose determined by the sedimentation study. Any amount of dispersant supplied above optimum dosage could remain in the suspension, thus affecting its viscosity. From this experimental trial it is evident that the potential characteristics derived from the PCD measurement could be viewed as a very accurate and easy tool for determination of the optimum amount of dispersant, and it is also worth noting the possible implications of this technique for practice.

Sedimentation Studies

Figure 3 shows the results of sedimentation test for the suspension of silicon nitride with different amounts of Dolapix A88 at room temperature 18°C . One could note that, at the beginning, with increase in Dolapix A88 concentration up to 6.4 mg/g, a steep rise in the dispersion volume can be observed, and after that a plateau was reached after which no further increase in dispersion volume was observed. Therefore, the dispersion concentration of 6.4 mg/g was reconfirmed as an optimal one, providing a stable suspension. The results are in good agreement with those from the PCD technique.

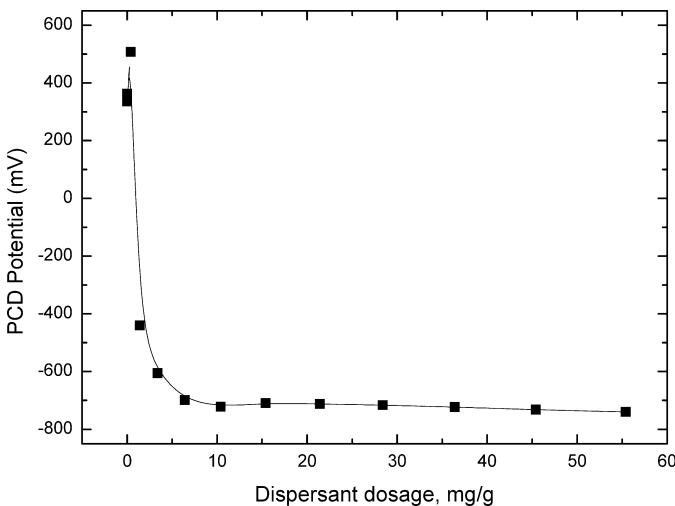


FIG. 2. Determination of optimum dispersant dosage by PCD method.

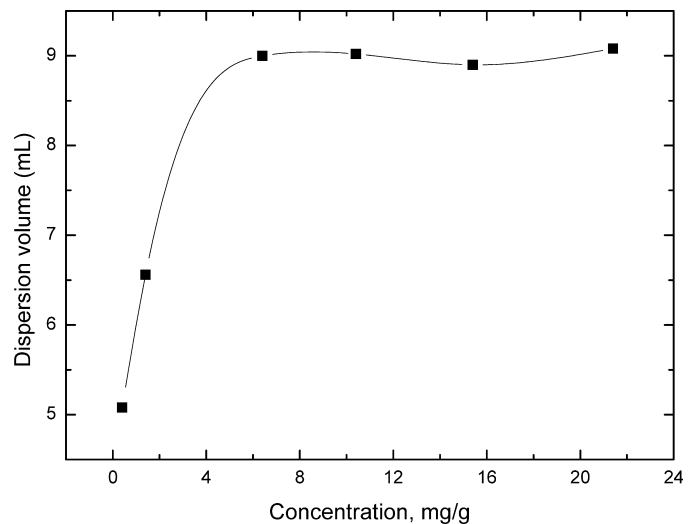


FIG. 3. Sedimentation tests of silicon nitride particles in aqueous suspensions for 24 h in the presence of Dolapix A88.

Effect of pH on Dispersion Volume

Figure 4 shows the dispersion characteristics of silicon nitride suspension at pH ranging from 2 to 12 in the presence and absence of dispersant. The results suggest that without dispersant addition, sufficient dispersion (expressed as sediment height) could be maintained both at low and high alkaline pH ranges, which could be due to the highly positive surface charge in acidic and the highly negative surface charge in basic environments. There was a very sharp fall in the dispersion volume as the surface charge approached the point of zero charge, which is found to be pH 6.91. As the point of zero charge for the Si_3N_4 powder has been found at pH 6.91,

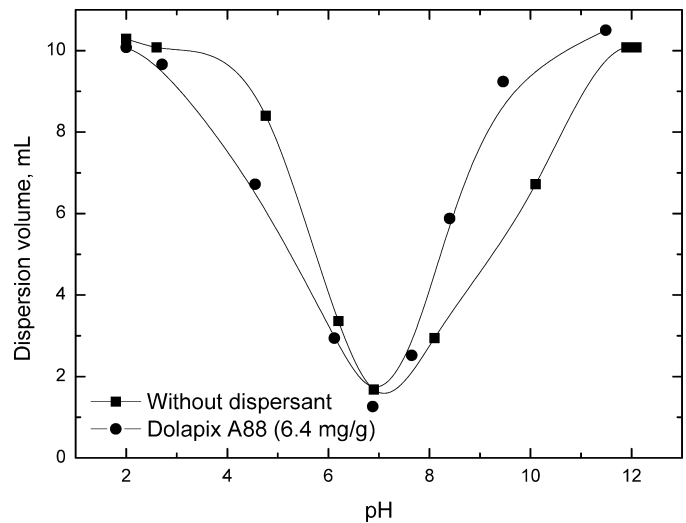


FIG. 4. Effect of slurry pH on dispersion characteristics of 5% (w/v) Si_3N_4 with and without dispersant Dolapix A88 after 24 h.

the particles close to this pH region are characterized by minimal charge. Therefore, all particles possess a natural tendency of agglomeration and settle very fast. With pH rising towards the alkaline range, the dispersion volume increased, which could be attributed to the increased particle charge. Therefore, without addition of dispersant, a purely electrostatic stabilization could be presumed. Further, when the dispersant has been present at an optimum amount of 6.4 mg/g, it is worth noting that the stabilization pattern is more or less similar to the one without dispersant. It could be presumed, however, that the mutual interactions between particle surfaces and dispersant are leading to predominately steric stabilization.

Turbidity Measurement

In order to verify further the results from the sedimentation studies, suspension turbidity tests at different pH with and without dispersant were performed, and the results are presented in Figure 5. An underlying assumption behind this study lies in the fact that a well-dispersed suspension should maintain high turbidity and with suspension de-stabilization the turbidity should decrease. The relationships obtained suggest that without dispersant, the turbidity was quite high within the acidic pH ranges from 2.3 to 4, after which it decreased very rapidly between pH 4 and 6.8 and then again rose sharply in the alkaline pH range from pH 6.8 to 10.5. In the presence of the optimum dosage of dispersant (6.4 mg/g), a more or less similar trend was observed. The minimum turbidity was detected at pH 6.8, which is very close to the pH IEP of 6.91. Such behavior is to be expected in the light of the classical DLVO theory, taking into account the surface charge data shown Table 1. The particles are positively charged within the acidic pH range, and the suspension is well dispersed, resulting in high turbidity. At pH_{IEP} , as the surface charge is minimum, the particles tend to aggregate,

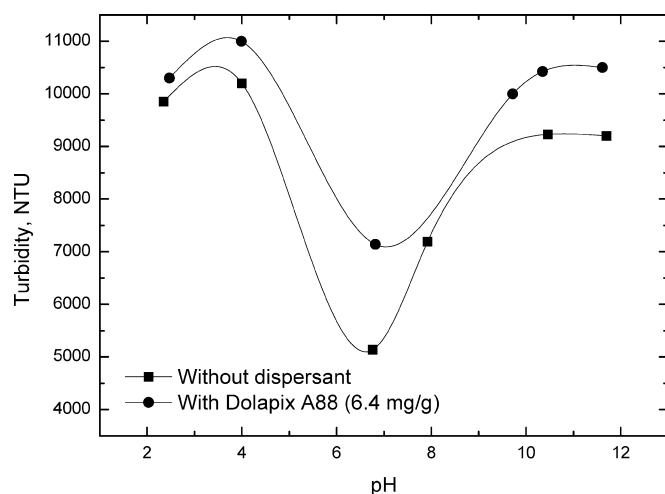


FIG. 5. Turbidity of silicon nitride particle suspension as a function of pH.

leading to minimum turbidity. Within the alkaline pH region, the particles are characterized by negative charge below pH_{IEP} , which is reflected in high turbidity in the presence of dispersant. The high turbidity implies larger scattering of the incident light, which in turn indicates a stable suspension. This observation could be viewed as another way to express sedimentation phenomena, the turbidity measurements being most reliable when used on non-settling and translucent slurry.

Polyelectrolyte Dose Level versus Suspension Surface Charge

The variation of specific surface charge for the silicon nitride suspension at different dispersant dosage levels for two marginal pH regions of 3.5 (i.e., the natural pH of 5% w/v dispersion) and 9.0 is depicted in Figure 6. It could be observed that the addition of an almost minute amount of dispersant, 0.4 mg/g, shifts system pH from 3.6 to nearly 9 and reverses the surface charge from +0.00294 to -0.00526 C/g. Both with and without dispersant, the surface charge remained almost constant, possessing either negative or positive charge within the whole range of dispersant concentrations investigated. As the most favorable conditions for the dispersion of the silicon nitride powder, one could choose the case when the pH has not been lowered but left at the alkaline region only as a result of dispersant addition/dissociation.

Solid Loading Vis-à-Vis Surface Charge

Figure 7 shows the variation of suspension specific surface charge with solids loading in the presence and absence of dispersant. Throughout the whole solids loading range from 1 to 60% w/v tested, the specific surface charge remained positive and virtually constant with no addition of dispersant. Due to system limitations it was not possible to measure surface charge beyond 60% w/v. However, in the presence

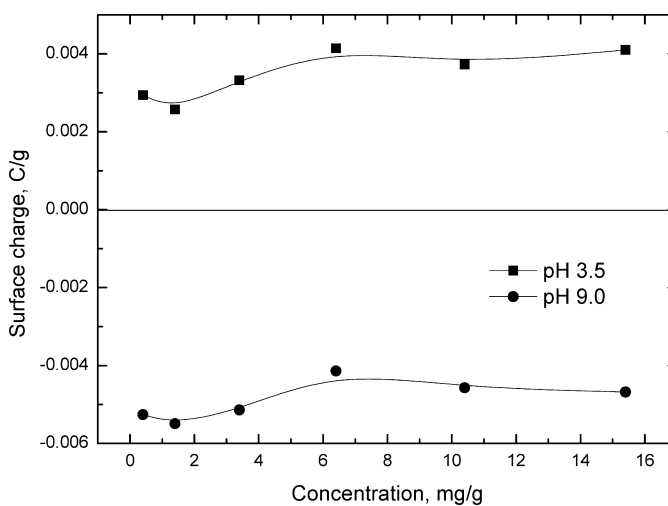


FIG. 6. Effect of polyelectrolyte concentration on the surface charge of Si_3N_4 powder at two different constant pH.

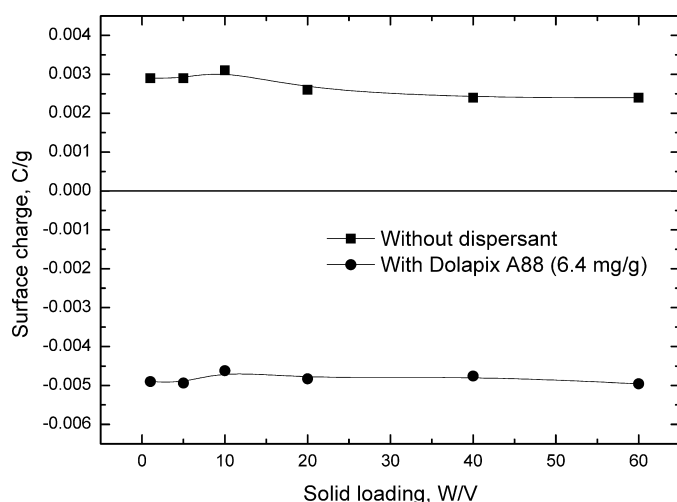


FIG. 7. Effect of solids loading on the specific surface charge of Si_3N_4 with and without dispersant.

of dispersant at the optimum dosage level of 6.4 mg/g, despite an increase in solids loading, there has been again no variation in the specific surface charge, and the positive surface charge has been shifted substantially towards the negative range. It could be inferred that the solids loading does not influence the specific surface charge of the system and that quite good dispersion at higher solids loading could be anticipated, which is a prerequisite for all slurry-based forming processes. As also expected, a notably better suspension fluidity was observed with dispersant addition. The dispersant screening process usually starts at low solids loading, using either sedimentation or light scattering for determination the degree of dispersion of the particles inside the solvent. The results emanating from this investigation suggest no variation of surface charge even at higher solids loading, which could prove highly favorable in view of achieving the required solids loading needed for gel-casting applications. Therefore, for the system under investigation one could obtain reliable information about system behavior at lower solids loading, which could be relevant at higher solids loading as well. Nevertheless, to prove this statement further studies at high solids loading should be pursued, since it has been shown that a dispersant providing efficient distensibility at low solids loading may not necessarily demonstrate the same properties at higher solids loading (Janney 2001; Singh et al. 2002c).

CONCLUSIONS

The following conclusions can be drawn from the above discussion:

1. The PCD technique provides one of the most reliable methods for determination of dispersion conditions and of optimum concentration of dispersant. It is reproducible and in good agreement with conventional sedimentation techniques.

2. The specific surface charge remained almost invariant at different solids loading. Therefore, the optimization of dispersant concentration done at lower levels solids loading could be expected to be highly relevant for higher solids loading as well.
3. Qualitative estimation of the dispersion abilities for the different dispersants could be accomplished by means of a streaming current technique. The optimal dose level chosen has been verified independently by alternative methods.
4. The pH_{iep} of 6.91 was found for the silicon nitride powder under study, which is in good agreement with the published data, pH 6.8–7. The fact that no shift in pH_{iep} in the presence of the studied dispersant was observed could lead to the assumption that the nature of the interaction between the dispersant and the powder is physical sorption.

ACKNOWLEDGMENTS

One of the authors, Dr. Bimal P. Singh, is thankful to Dr. Vibhuti N. Misra, Director, Regional Research Laboratory, Bhubaneswar, for his kind permission to publish this article. Dr. Singh is also equally thankful to the authority of DAAD, Bonn, Germany for providing a senior DAAD fellowship under the exchange program, enabling him to spend three months at BTU-Cottbus.

REFERENCES

- Bergstrom, L. and Pugh, R.J. (1989) *J. Am. Ceram. Soc.*, 72 (6): 103.
- Busca, G., Lorenzelli, V., Pocile, G., Baraton, M.I., Quintard, P., and Marchand, R. (1986) *Mat. Chem. Phys.*, 14 (3): 123.
- Cesarano III, J. and Aksay, I. (1988) *J. Am. Ceram. Soc.*, 71 (7): 250.
- Hackley, V.A. (1997) *J. Am. Ceram. Soc.*, 80 (9): 2315.
- Han, K.R., Lim, C.S., Hong, M.J., Choi, S.K., and Kwon, S.H. (1996) *J. Am. Ceram. Soc.*, 79 (2): 574.
- Janney, M.J. (2001) Attaining high solids in ceramics slurries. Available at: <http://www.ms.ornl.gov/researchgroups/process/cpg/gelcasting.html>, 6/8/01.
- Jean, J. and Wang, J. (1990) *J. Am. Ceram. Soc.*, 81 (6): 1589.
- Kulig, M., Orosehin, W., and Griel, P. (1989) *J. Eur. Ceram. Soc.*, 5 (6): 209.
- Luther, E.P., Kramer, T.M., Lange, F.F., and Pearson, D.S. (1994) *J. Am. Ceram. Soc.*, 77 (4): 1047.
- Luther, E.P., Lang, F.F., and Person, D.S. (1995) *J. Am. Ceram. Soc.*, 78 (8): 2009.
- Nitzsche, R. and Bley, L. (1997) Particle charge detector—a new method to characterize and optimise the processing of ceramics. In *Operating Manual*; Herrsching Müttek: Germany.
- Nitzsche, R., Friedrich, H., Boden, G., and Hermel, W. (1987) Electrochemical surface investigation: an important technique for ceramic powder processing, Academy of Sciences, Institute of Solid State Physics and Material Research, Dresden, AN 6012, 280–291.
- Porter, M.R. (1994) Speciality surfactant. In *Handbook of Surfactants*, 2nd ed.; Blackie Academic and Professional: New York, 277–291.
- Pradip (1988) *Trans. Indian Ins. Met.*, 41 (3): 15.

- Pugh, R.J. (1994) Dispersion and stability of ceramic powders in liquids. In *Surface and Colloid Chemistry in Advanced Ceramics Processing*; Pugh, R.J. and Bergstrom, L., eds.; Marcel Dekker: New York, 127–191.
- Schwelm, M. (1992) Dispersion of Si_3N_4 with $\text{Y}_2\text{O}_3\text{-Al}_2\text{O}_3$ Sintering Additive in Pressure Casting, Ph.D. Diss, University of Stuttgart.
- Singh, B.P., Besra, L., and Bhattacharjee, S. (2002a) *Colloids Surf A. Physicochem. Eng. Asp.*, 204 (1): 175.
- Singh, B.P., Bhattacharjee, S., and Besra, L. (2002b) *Ceram. Int.*, 28 (4): 413.
- Singh, B.P., Bhattacharjee, S., and Besra, L. (2002c) *Mater. Lett.*, 56 (5): 475.
- Singh, B.P., Bhattacharjee, S., Besra, L., and Sengupta, D.K. (2004) *Ceramic Int.*, 30 (4): 496.
- Wang, C. and Riley, F.L. (1992) *J. Eur. Ceram. Soc.*, 10 (3): 83.
- Wang, L., Bindal, I., Sigmund, W.M., and Aldinger, F. (1996) Colloidal processing on non-oxide ceramics. In *Proceedings of Werkstoffwoche '96, Symposium*, 611–616.
- Wang, L., Sigmund, W.M., and Aldinger, F. (2000) *J. Am. Ceram. Soc.*, 83 (4): 697.
- Ziegler, G., Henrich, J., and Wotting, G. (1987) *J. Mater. Sci.*, 22 (4): 3717.

Characterisation of aqueous suspensions of fumed aluminium oxide in presence of two Dolapix dispersants

S. Gaydardzhiev · P. Ay

Received: 28 December 2004 / Accepted: 30 September 2005
© Springer Science+Business Media, LLC 2006

Abstract The stability of a fumed aluminium oxide nano powder suspended in water has been assessed through measurement of zeta potential and streaming current, using the fact that the particles exhibit maximum repulsion at high magnitude of charge. Two commercial dispersants belonging to a Dolapix series have been tested. Dolapix CE 64 has shown a better deflocculating action than Dolapix A 88. The iso electric point of the powder suspension has been found close to pH 9. A notable shift in the pH of iso electric point when Dolapix CE 64 was present, indicating that the interaction between particles and dispersant has involved chemical sorption. It has been found out, that at the relative low solids loading studied and within the limits of the pH measurement accuracy, a dispersant supplied in dose levels from 12 to 24 mg/g, has confined the pH of iso electric point to a relatively narrow range. A capillary suction time technique has been tried for evaluation of suspension fluidity as function of dispersant concentration and pH. For the dispersant stabilised suspensions, a correlation between their capillary suction time and pH of iso electric point has been documented.

Introduction

Flame synthesized nano-scaled oxides find wide use in many innovative applications. The aluminium oxide,

among them, is mainly designed for improving the flowability of powder products (e.g. powdered lacquers), for thickening of liquids, for rheology maintaining and as antiblocking agent in PET films production. As a rule, most of the commercial products formulated on fumed oxides basis are used as aqueous dispersions, therefore their characterisation in terms of surface and interfacial properties, parallel to size, shape and morphology is mandatory. This is because any change in powders composition and characteristics directly influences their processing (rheology, dust generation, mixing, segregation etc.), and product performance. These challenges have motivated a large number of investigations devoted to structure–effect correlation, for enabling sound control over important product properties relevant to their engineering applications [1]. For a particular application, given properties of the powder in aqueous medium might be beneficial, while for other niches, the same properties might be undesirable and detrimental. For instance, the generic principle of gel casting, which is one of the emerging direct consolidation methods for colloidal processing of ceramics, is to ensure well-dispersed powder suspension and to prevent agglomeration before slurry casting in moulds. After slurries casting, they are transformed into rigid bodies without removal of water. Mainly two approaches have been followed here: in the first category, the generic principle is to encourage polymers (or monomer reacted to form polymers) to create a 3-D gel network keeping the particle suspension stable, while in the second category, particle coagulation is encouraged via colloidal based consolidation (i.e. by changing external conditions such as pH, ionicity, temperature etc.).

The aluminium oxide presented here, was characterised by high specific area, nano size and γ phase presence [2, 3], which determines its unique characteristics. The aim of the

S. Gaydardzhiev (✉) · P. Ay
Department of Mineral Processing, Brandenburg Technical
University – Cottbus, Siemens-Halske-Ring 8, 03046 Cottbus,
Germany
e-mail: gaydar@tu-cottbus.de

present study was, by involvement of an established approach for dispersant optimisation in colloidal processing of ceramics, to compare two common dispersants towards stabilisation of aqueous powder suspension and to discuss its behaviour in terms of fluidity.

Experimental

Materials

An aluminium oxide powder of high purity obtained from Degussa AG, Germany, has been used. Its main characteristics, as reported by the product specification sheet, are summarised in Table 1.

The two dispersants used, have been Dolapix A 88 (2-amino 2-methyl propanol) and Dolapix CE 64 (carbonic acid based polyelectrolyte), supplied by Zschimmer & Schwarz, Germany. According to product information data, the A 88 is a pseudo cationic in nature and its deflocculating effect on the ceramic particles surface is expressed by generation of charges of same polarity, which cause the particles to repel each other. The CE 64 possesses bivalent functional groups and is characterised by adsorption on the particle surfaces and complete dissociation at pH above 8.5 [4]. De-ionised water from ‘‘Modulab’’ purification system with conductivity in the range 0.1–0.2 $\mu\text{S}/\text{cm}$ has been used. NaOH and HCl from Merck (1 M) have been chosen for pH adjustment. Unless otherwise stated, suspensions with solids fraction of 4.76% w/v have been tested through all the studies.

Particle size distribution, zeta potential and streaming current measurement

A DT 1200 spectrometer from Dispersion Technology, USA has been used in acoustic attenuation mode to measure particle size distribution and in electro acoustic mode for zeta potential, calculated on the basis of colloidal vibration current. The instrument precision in obtaining particle size distribution is determined by the error in the attenuation spectra, the later normally being very low for suspensions with good density contrast. The zeta potential probe has been calibrated against a standard Silica–Ludox suspension. For the titration tests, 5 g of the powder have been added to 100 ml water, containing a predetermined

amount of dispersant, calculated on solid mass. The suspensions have been agitated for 2 min with magnetic stirrer, followed by 20 s with an ultrasonic disintegrator model UP 400 S, Dr. Hilscher, Germany. Immediately after, they have been transferred into the spectrometer measurement chamber, where were kept in circulation by the built-in magnetic stirrer. Their natural pH denotes the starting pH before titration. In case of volumetric titration, one of the integrated micro burettes has been filled with dispersant solution, which exact amounts dispensing inside suspension volume has been enabled by software control. Streaming current has been measured by means of a particle charge detector, PCD-03-pH from Müttek, Germany. It consists of cylindrical cell fitted with a displacement piston, which moves back and forth at constant frequency forcing a relative motion between the liquid and particles, thus inducing development of a streaming potential of either positive or negative sign. The powder–liquid mixing has been realised directly inside the 10 ml cell for 2 min, a duration which has been considered sufficient, as indicated by establishment of a stable steaming current. A small pH electrode has been fitted to the cell, enabling on-line pH monitoring. Upon requirement, the exact magnitude of the charge could be estimated by titration with oppositely charged standard polyelectrolyte until neutralization of the streaming potential to zero value.

Capillary suction time measurement

In order to evaluate fluidity of the powder suspensions, capillary suction time experiments have been envisaged. They have been realised with a ‘‘CST 100/A’’ device from HeGo Biotech Germany, equipped with a hollow cylinder capable of handling 5 ml suspension, standing on a filter paper similar to a Whatman 17 type. Two successive measurements have been carried out and their mean value taken. The suspensions for the CST tests have been prepared under the same mixing procedure like the samples measured by the DT 1200 system.

Determination of optimum dispersant dosages

The optimum dose level of polyelectrolyte required for obtaining maximum powder dispersion in water has been estimated by two means: by the zeta potential obtained by the DT 1200 spectrometer and from the streaming current readings of the particle charge detector. The inflection point in the plots between the dispersant dose level vs. zeta potential and streaming current should indicate the optimum dispersant dosage, leading to a maximum dispersion [5, 6]. Settling tests, linking sediment height with dispersant dosage, are also commonly used as a tool for selection of dispersant type and its optimal concentration. For the

Table 1 Main characteristics of the Aeroxide Alu–C powder

Average primary particle size (nm)	Specific surface area (BET) (m^2/g)	Density (g/cm^3)	pH as 4% w/v suspension
13	100	2.9	4.5–5.5

case of the studied powder however, such tests were found not suitable, since the suspensions did not settle even after long time.

Results and discussion

Powder characterisation

A microphotograph of the powder taken by a raster electronic microscope (model Zeiss DSM 962) is shown at Fig. 1. Large clusters consisting of particles with irregular shape could be seen. It was impossible to visualise single particles, since they agglomerate possibly due to the high surface area pertinent to this nano powder. It should be noted, that previous studies of fumed silica powder, have also reported that isolated primary particles did not exist [2, 7].

A typical particle size distribution of the powder suspension, as measured by the acoustic spectrometer, is shown at Fig. 2. The mean and median particle size was determined respectively as 50 and 39 nm with standard deviation of 0.27 and at 2.6% fitting error. Since the producer specifies an average particle size for the dry powder about 13 nm—Table 1, it could be presumed that the powder agglomerates when suspended in water.

Dispersant selection and dose level optimisation

The dispersants efficiency towards keeping the particles in suspension has been evaluated by zeta potential and streaming current characteristics of suspension. The results obtained in this direction are shown at the Fig. 3 in form of a

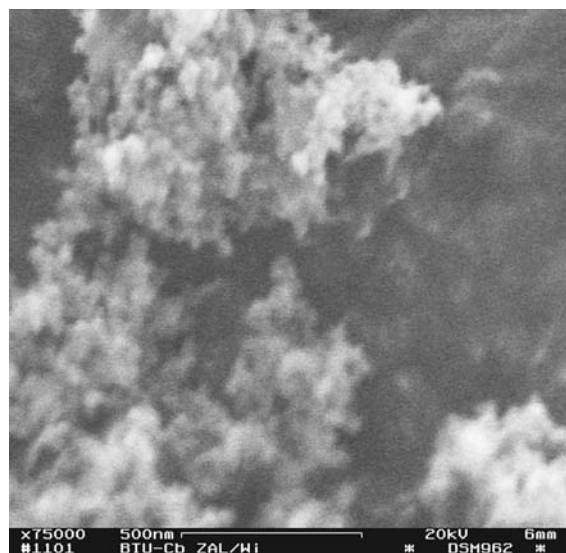


Fig. 1 REM image of an agglomerated Alu-C powder

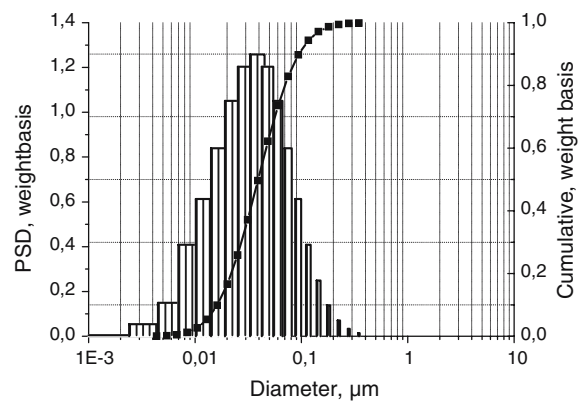


Fig. 2 Particle size distribution of powder suspension at natural pH

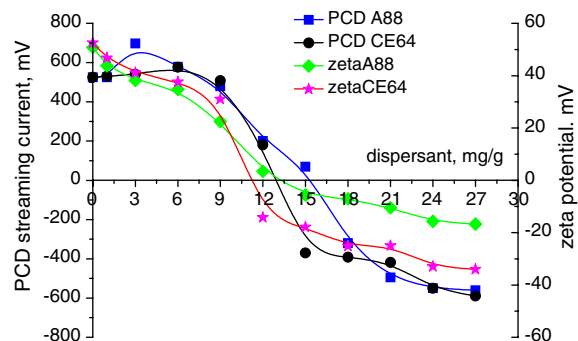


Fig. 3 Effect of dispersant concentration on zeta potential and streaming current

volumetric titration curves performed by progressive supply of the tested dispersants in dose levels up to 27 mg/g.

As could be seen from the figure, all curves are characterised by a similar trend, decreasing monotonically parallel to dispersant addition. While the streaming current curves for the both dispersants nearly overlap, the zeta potential curves differ at higher dosages of dispersants. Both dispersants have completely neutralised the initial positive charge, but the Dolapix CE 64 has provided higher charge loading compared to Dolapix A 88. It is worth to note the slight deviation in the dose levels leading to exact zero charge, gained independently from the zeta potential and from the streaming current curves for a same dispersant. The both methods are viewed as identical regarding determination of $\text{pH}_{(\text{iep})}$ by potentiometric titration [8]. In case of the volumetric titration however, the observed shift could be attributed to the different mode of dispersant addition adapted for the DT 1200 spectrometer and for the particle charge detector. In case of the DT 1200 system, the plotted curve originates from measurement of one and a same sample of suspension, treated with step-addition of dispersant, the amount of which has been exactly calculated for each point. Each zeta potential value has been taken after 2 min elapsing required for mixing/equilibration. It should

be noted, that owing to the minute amounts of supplied dispersant, any dilution effects were viewed negligible regarding the measured zeta potential. In case of the particle charge detector however, each streaming current value relates to a single sample, prepared and measured separately. Therefore, mixing effects could be responsible for the observed deviation, considering also the high specific area of the powder and the fact that the measurement accuracy has been found within the acceptable limits.

It is evident, that without addition of dispersant, the suspension system acquires high positive charge, as result of surface hydroxyl groups, which dissociate in water or act as proton acceptors. Thus, the natural stabilisation without dispersant, could be due to electrostatic repulsion forces, which are known as weak and short ranged ones, and as such could lead to less stable powder suspensions. Additionally, hydration forces could be suspected to exist. Their origin is debatable and for SiO_2 sols could be linked to hydration effects due to presence of silanol groups [9].

With the addition of dispersants, both the zeta potential and the streaming current are reduced. At 15 mg/g, the suspension could be still partially stabilised by electrostatic and steric forces. At 18 and 21 mg/g dose levels, the zeta potential has almost approached -30 mV, a level considered as a minimum for full steric stabilisation. It has appeared from the CE 64 curve (star symbols), that an inflection point is poor for description. Nevertheless, after 24 mg/g, a curve flattening could be distinguished, the potentials remaining almost constant thereafter. Based on this, a dose level of 24 mg/g has been viewed as an optimal one for maximum powder dispersion. As a rule, any amount of dispersant supplied above that optimum, will remain unbounded in suspension and lead to unwanted high viscosity.

In order to evaluate any pH effects resulting from dispersant dissociation, it was important to follow the pH variation after dispersant addition, since any significant shift in suspension pH resulting from dispersant addition above the optimal dosage, could lead to higher ionic strength in the suspension and subsequently affect its colloidal stability. This relationship is plotted at Fig. 4, where it could be noted that the both dispersants when supplied above 12 mg/g, have shifted the pH towards alkaline region. However, above this dose level and further passing through the optimal one, the CE 64 maintains a steady milder level of pH compared to that of A 88, an added argument for choosing the former dispersant for more detailed study further.

Shift in $\text{pH}_{(\text{iep})}$ resulting from dispersants addition

The pH of iso electric point is an important characteristic when considering the stabilisation/destabilisation

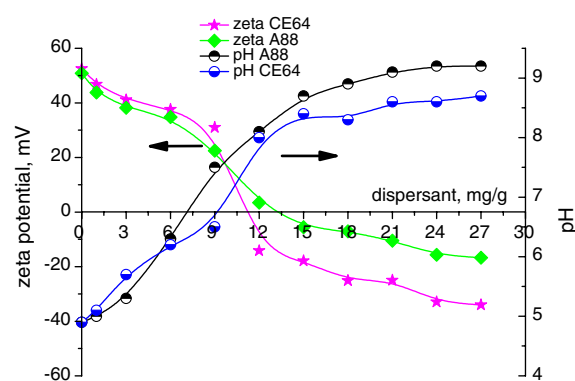


Fig. 4 Zeta potential and pH of suspension as function of dispersant concentration

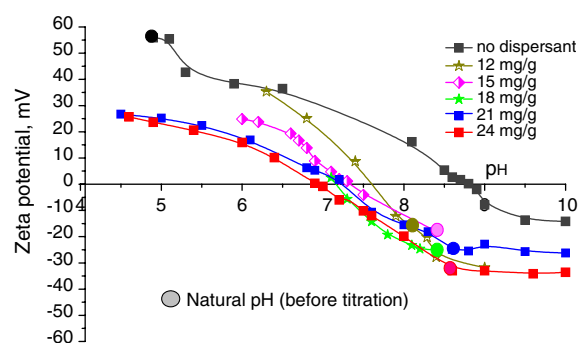


Fig. 5 Determination of zeta potential as function of suspension pH, with and without addition of Dolapix CE64

phenomena in colloidal systems. According to the DLVO theory, rendering the pH to the respective iso electric point, should lead to repulsive forces weakening and to fast agglomeration. Therefore, for evaluating the shift in the $\text{pH}_{(\text{iep})}$ and the effect of dispersant addition on the same, a potentiometric titration has been carried out. Since during the volumetric titration, CE 64 has shown better performance in comparison to A88, its effect upon the shift in $\text{pH}_{(\text{iep})}$ has been studied within a broader dose level range, i.e. from 12 to 24 mg/g. This range has been intentionally chosen, since after 12 mg/g, a reversal in the zeta potential sign has been documented—Fig. 3. The titration results for CE64 are depicted at Fig. 5 and the respective shift in $\text{pH}_{(\text{iep})}$ are summarised at Fig. 6.

Figure 5 indicates, that without dispersant, the $\text{pH}_{(\text{iep})}$ of the suspension is around 8.9. This value is lower than the one of 9.9 reported for a similar powder [2]. Upon addition of dispersant in concentration from 12 to 24 mg/g, the $\text{pH}_{(\text{iep})}$ is shifted towards neutral region. From other side, the natural pH of the suspension is shifted from an acidic range of pH 4.9, towards an alkaline pH region of 8–8.5 where the dispersant should be nearly 100 % dissociated [4], according to the reaction:

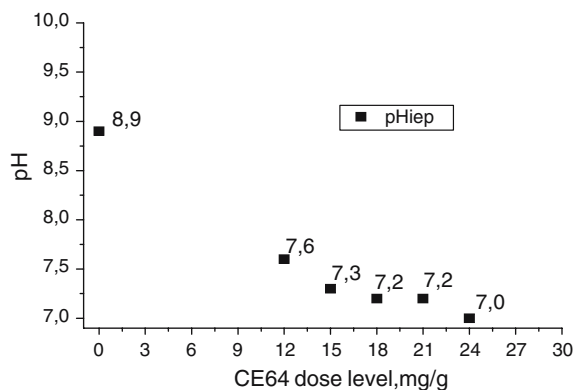


Fig. 6 Effect of CE 64 dose level on $pH_{(iep)}$ shift



The $pH_{(iep)}$ shift resulting from dispersant addition (Fig. 6), could be an indication that the dispersant is well fixed on the powder by formation of H-bond between its dissociated $RCOO^-$ group and the OH^- group on the alumina surface. It should be noted also, that the natural pH of the suspension after addition of dispersant found in the range of 8–8.5, is relatively apart from the range of the respective $pH_{(iep)}$ being between 7 and 7.5.

Potentiometric titrations of suspensions treated with A88 supplied at 15 and 18 mg/g have been done in a similar manner as well. It has been found out, that in contrast to the CE64 case, the addition of A88 did not shift markedly the $pH_{(iep)}$. The iso electric points for both 15 and 18 mg/g dose levels have been found at pH 8.7, which is a negligible shift from the value of pH 8.9 established for the non-treated dispersion. This nearly coincidence in the $pH_{(iep)}$, with and without dispersant, clearly indicates that the interaction between the powder and the A88 is a physical in nature, which additionally favours CE64 as a better dispersant.

Evaluation of suspension fluidity by CST

The rheological properties and fluidity of suspensions are affected by the surface structures of the particles, which often are determined by the powder manufacturing history. For the case of the studied fumed oxide powder, it was important to find out, if a correlation between the suspension fluidity and the optimal level of dispersant determined by the volumetric titration exists. At this point, only CE 64 dispersant has been considered. Figure 7 displays the CST evolution for the suspension treated with increasing concentration of dispersant. The respective pH values are plotted as well.

A perusal of the relationship shown at Fig. 7 indicates a pronounced maximum for 15 mg/g dispersant dose, after

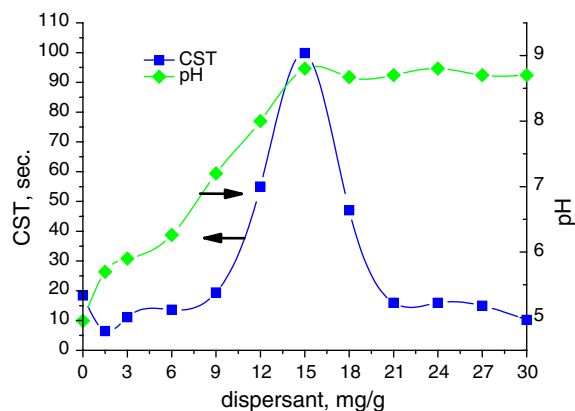


Fig. 7 CST and pH of suspension as function of dispersant concentration

which point, the CST has dropped. At the optimum level of 24 mg/g suggested by the volumetric titration, the suspension is characterised by low CST and at the same time has been visually appearing quite fluid.

In a separate group of experiments, the CST variation with pH has been evaluated, for suspensions without dispersant and for such treated with 12, 15, 18 and 24 mg/g. The relationships shown at Fig. 8 indicate, that without addition of dispersant, the suspension CST rises continuously with pH increase. This trend is not affected, even when the suspension has been adjusted to the respective $pH_{(iep)}$ of 8.9. A maximum CST value is observed at pH above 10. From other side, the CST curves for the dispersant treated suspensions always have passed through a peak. It is interesting to note, that for 12, 18 and 21 mg/g, the maximum CST lies within the region of $pH_{(iep)}$ found for the respective dose level, i.e. between 7 and 7.5. Effectively, the more the pH of suspensions has been buffered towards $pH_{(iep)}$, the more they have been structured to gel. For 15 mg/g however, the maximum CST has been found at pH 8.5, coinciding with the natural pH of the suspension and being higher than the $pH_{(iep)}$ for this dose level.

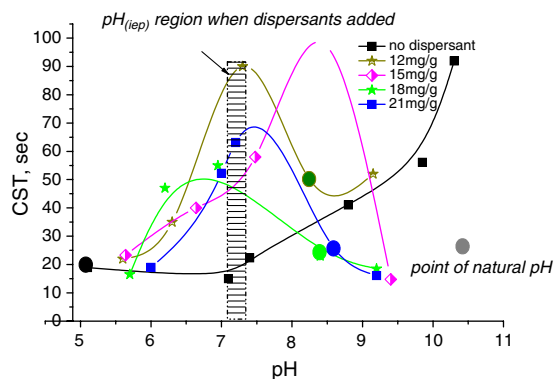


Fig. 8 CST as function of pH at different dispersant dose level

The above observations are quite intriguing and a possible explanation could be found in the CST measuring principle. Whilst the exact pore size of the CST filter paper is not known, it is for sure much larger than the primary particle size of the suspended powder. An assumption could be launched, that when the suspension has been treated with optimal dispersant dose and when its pH has been maintained away from the IEP, the suspended particles will go through the pores and the suspension will flow like water giving short suction time. On the other hand, at pH close to IEP, particles agglomerate and tend to block the pores, thus yielding high CST values—Fig. 8. For the non-treated suspensions, the lack of pronounced peak around the IEP could be due to a continuous particles agglomeration, which is irreversible and is unaffected by driving the pH towards alkaline region. Therefore, the CST value, which normally characterise sludge water holding capacities, in case of the studied powder suspension, could not be directly related to its structure and rheology, rather to its fluidity.

Conclusions

Experimental data about zeta potential and streaming current of water suspension containing aluminium oxide nano powder are reported. Being from an initial study phase, the presented results do not lead to fundamental conclusions. They are believed to have implication on revealing some properties of the powder in water dispersion (stability, durability) and the role, which common deflocculants could play in maintaining the characteristics of the suspension. The results could be relevant to other fumed oxides as well. Due to the pyrogenic method of synthesis they possess some common properties.

The studied nano powder has its main application as filler, rheology maintainer etc., but one could find its use in quite diverse fields also. For example, the same gamma aluminium oxide has been used among others as a model colloidal system, for investigation of aggregate structures relevant to flocculation and dewatering processes [10].

Whichever the application niche is, it is conceivable that its dispersion stability is of primary importance.

The anionic deflocculant CE64 has shown better effect in terms of electrosteric stability and suspension pH, than the cationic A88. The electroacoustic method used for measuring particle size distribution and zeta potential of the nano powder has shown good results at the moderate solid concentrations. The zeta potential and streaming current techniques have provided comparable data for determination of pH of iso electric point for the studied gamma alumina nano powder, likewise it has been established for alpha alumina powders [11]. The CST method has an advantage being simple and rapid, but in our case, it has yielded limited information about suspension structure and rheology. The studied nano powder belongs to the fumed oxides family and undoubtedly possesses indigenous characteristics and a liquid media such as water and its composition, could markedly change its state and accordingly the particle–particle interactions and the properties of the entire suspension. For further elucidation of the presented findings, more studies, encompassing rheology as well should be pursuit.

Acknowledgement We thank the Degussa AG for the powder samples and Dr. W. Wiehe for the raster electron microscopy.

References

1. Batz-Sohn C (2003) *Part Part Syst Charact* 20:370
2. Gunko VM, Zarko VI, Lebeda R, Chibowski E (2001) *Adv Coll Interf Sci* 91:1
3. Waite TD (1999) *Coll Surf A: Physicochem Eng Asp* 151:27
4. Albano M, Garrido L (2002) *J Mater Synth Proc* 10(4):211
5. Singh BP, Bhattacharjee S, Besra L (2002) *Ceram Intern* 28:413
6. Pretto M, Costa A, Landi E, Tampieri A, Galassi C (2003) *J Am Ceram Soc* 86:1534
7. Barthel H, Heinemann M, Stintz M, Wessely B (1998) *Chem Eng Tech* 21:745
8. Wäsche R, Haito M, Hackley V (2002) *Powd Techn* 123:275
9. Günther L, Peukert W (2002) *Part Part Syst Charact* 19:312
10. Waite TD (1999) *Coll Surf A: Phys Chem Asp* 151:27
11. Steinborn G, Wäsche R (2000) In: *Proceedings of Mütke-Malvern Workshop*. Potsdam, Germany, March 2000

Evaluation of Dispersant Efficiency for Aqueous Alumina Slurries by Concurrent Techniques

Stoyan Gaydardzhiev and Peter Ay

Mineral Processing, Brandenburg University of Technology, Cottbus, Germany

This article reports on results from a comparative study assessing a suitable method for dispersant efficiency evaluation in the case of water-based suspensions of ultrafine alumina stabilized by a commonly used dispersant, Dolapix CE64. The following measurements were evaluated: zeta potential, specific surface charge, sedimentation behavior, and capillary suction time. The suitability of each of the tested techniques is discussed. A good agreement between the zeta potential and the specific surface charge as a way to determine the optimal dose of dispersant is documented.

Keywords Alumina powder, suspension, dispersant, electrokinetic phenomena

INTRODUCTION

Direct consolidation techniques, gel casting being one of them, based on colloidal processing and claiming to yield complex near-net shape bodies with consistent properties and minimal defects have been recently taking a place as viable alternatives to conventional routes of ceramics manufacturing. The common element among all of them is that they make use of well-dispersed suspensions with high solids loading. However, regardless of their acknowledged advantages, many of them have not succeeded in leaving the laboratory level or pilot plants of ceramic companies, with only few small-scale installations running for some complicated parts. One main challenge is the low production rate, which still cannot compete with dry pressing. The gel-casting process is based on the development of an aqueous or nonaqueous slurry of colloidal-size ceramic particles, together with predetermined amounts of dispersant, gelling reagents, initiators, and catalysts. Since the optimal dispersion of the particles and the stability of powder suspension is a key factor for the development of desirable end products, the appropriate choice of dispersant type and its dose level is of paramount importance for realizing a successful gel-casting process. Often it is imperative to reach as high a solids loading as possible in the slurry. This is because high solids loading reduces the drying and firing shrinkage with a parallel increase in the green strength.

Usually dispersants are selected on an empirical basis, which involves a time-consuming screening procedure to evaluate

their performance. The conventional technique employed most often is to assess the macroscopic properties of the suspension, such as sedimentation behavior and viscosity, which, however, does not provide information about the interfacial phenomena taking place during particle-dispersant interaction. Therefore, it is desirable to choose a method capable of evaluating the dispersant-powder compatibility, that is uncomplicated, fast, and reliable as well able provide information about the surface behavior of the dispersant. With entering the colloidal size range in particulate systems, the control over particle dispersibility becomes increasingly difficult, since surface properties of particles and associated interfacial phenomena determine to large extent their behaviour. Hence, to control particle aggregation one should possess sound knowledge about surface and interfacial properties. Dispersibility could be viewed as the ease with which particles are distributed in a continuous phase, so that each one of them is completely surrounded by the liquid phase and there is no permanent contact with any particles so that they do not subsequently agglomerate (Klimpel, 1999). As a rule, the process of dispersant screening begins at low solids loading by using straightforward methods like sedimentation or light scattering for evaluation of the degree of particle dispersibility. Nevertheless, it has been documented that not every dispersant that demonstrates efficient dispersibility at lower solids loadings will maintain good dispersion at high solids loading (Singh et al., 2002). The present article reports on results from a systematic evaluation of the dispersive behavior of ultrafine alumina suspension stabilized by means of a commonly used dispersant, Dolapix CE64. The suspension stability has been assessed through the following parameters: zeta potential, surface charge density, capillary suction time, and sedimentation behavior.

Received 8 August 2005; Accepted 9 August 2005.

Address correspondence to Stoyan Gaydardzhiev, Mineral Processing, Brandenburg University of Technology, Siemens-Halske-Ring 8, 03046, Cottbus, Germany. E-mail: gaydar@tu-cottbus.de

EXPERIMENTAL SECTION

Materials

An α -type calcined alumina powder, CR6, obtained from Baikowski-Chemie (France) was used. According to the producer's data, it is characterized by a mean particle size of $0.53\ \mu\text{m}$ and specific surface area (BET) of $5.8\ \text{m}^2/\text{g}$. For verification purposes, the powder suspended in water was subjected to particle size distribution measurement by the means of a DT1200 spectrometer in acoustic attenuation mode, the results of which are shown in Figure 1. One can see very good agreement between the measurement and the data coming from producer. The dispersant used was Dolapix CE64, an anionic ammonium polyacrylate, supplied by Zschimmer & Schwarz (Germany). Its deflocculating effect is attributed to the interaction between the bivalent functional groups of the additive and the surface-charged ceramic particles. It was used as a 10% solution and was applied in a concentration range between 0.25 and 6 mg/g for the sedimentation tests and between 1 and 24 mg/g for the rest of the studies. Unless stated otherwise, bidistilled and deionized water from a Modulab purification system with conductivity under $0.2\ \mu\text{S}/\text{cm}$ and a pH of 6.7 was used.

Measurement of Zeta Potential and Specific Surface Charge

The electrokinetic properties of the alumina powder in suspension have been expressed two ways: as a zeta potential coming from measurement of colloid vibration current (CVI) by an acoustic and electroacoustic spectrometer DT1200 and as a specific surface charge coming from streaming current measured by a particle charge detector PCD-O3-pH from Müttek (Germany). The operational and measurement principles of both systems are reported elsewhere (Dukhin and Goetz, 2002; Wäsche et al., 2002). For the CVI tests, 5.5 g of powder were added to 110 mL water, giving solids loading of 4.36% W. The suspensions were agitated for 2 min by magnetic stirrer, followed by 20 s with an ultrasonic disintegrator model UP 400 S, Dr Hilscher (Germany). Immediately after, they were transferred inside the measuring chamber, where they were kept in circulation by the built-in magnetic stirrer.

For estimation of the optimal dose of dispersant, two separate volumetric titrations were performed. First, the titration was done using the CVI instrument, where a predetermined amount of dispersant calculated on solid mass was added inside the chamber by means of an integrated burette and thoroughly mixed before zeta potential values were taken. In the second approach, using the PCD, the powder-liquid mixing was realized by the piston movement directly inside the 10 mL sample cell for 2 min, a duration considered sufficient as indicated by establishment of stable streaming current. A small pH electrode was fitted to the cell, enabling on-line pH monitoring. The exact magnitude of the charge,

expressed as specific surface charge or charge density, was estimated by titration with oppositely charged standard polyelectrolyte until neutralization of the streaming potential to zero value.

Thus, the optimum dispersant dose level leading to maximum powder dispersion was considered to be the one coinciding with the inflection point of the plots between dispersant dose level and zeta potential and between dispersant dose level and surface charge density, derived respectively from CVI and streaming current measurement.

Sedimentation Studies

Sedimentation tests were performed using 25 mL calibrated glass cylinders. For each test, 1.25 g of alumina powder was mixed with 25 mL water containing a predetermined amount of dispersant: 0.25, 0.5, 0.75, 1, 3, and 6 mg/g. The suspension was vigorously shaken and allowed to stand undisturbed for 21 days. The sediment heights were read directly from the graduated cylinders. The higher the sediment height, the more stable the suspension.

Capillary Suction Time

Additionally, the optimal dose level of dispersant was evaluated by subjecting the powder suspensions to a capillary suction time (CST) measurement. This was realized with a CST 100/A device from HeGo Biotech (Germany), equipped with a hollow cylinder standing on a filter paper similar to Whatman 17 type. The operation of the CST instrument is based on the principle of capillary suction pressure of porous medium and could be viewed as a means for evaluation of the water-holding capacity of sludge or suspension and to some extent of its viscosity. The suspensions for the CST tests were prepared at a solids loading of 4.36% W under the same mixing procedure used for the samples measured in the CVI instrument. Two successive measurements, each one involving 5 mL suspension, were carried out and the mean from both values taken. The optimal dispersant dose level was chosen as the one yielding maximum capillary suction time or longer drainage rate, similar to the proposed method by Singh et al. (2003).

RESULTS AND DISCUSSION

The results from the volumetric titration of the suspensions are summarized in Figure 2. For the CVI case, the dispersant was progressively dosed in a step-by-step mode inside the same sample and accordingly each zeta potential value relates to measurement of the same sample. Each single point taken for the surface charge density however, was derived from measurement of an individual sample.

As can be seen from Figure 2, without addition of dispersant the alumina-water suspension is positively charged, as a result of the surface hydroxyl groups, which dissociate in water or act as proton acceptors. Without dispersant addition, the suspension was characterized by a pH of around 7 and appeared to

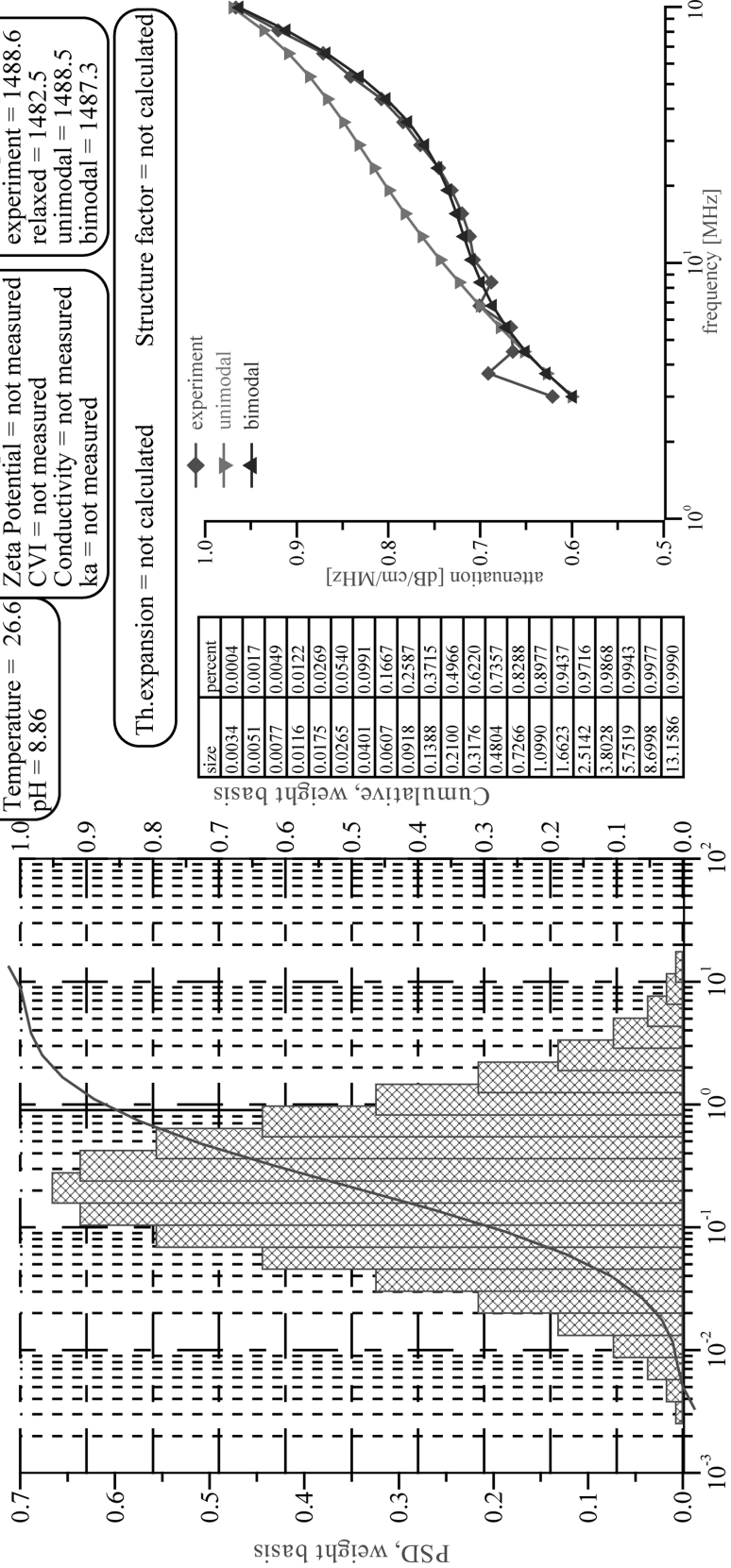
Dispersion Technology Acoustic and Electroacoustic Spectrometer DT-1200

Sample Content: 4.8%wt of aluminaalpha in water
File Name: c:\dataaco\Excel\11171315P.csv
Sample ID: CR6 new without disp psd
Measured: 17-Nov-04 1:15:40 PM

General Data
 Temperature = 26.6
 pH = 8.86
Electric Properties
 Zeta Potential = not measured
 CVI = not measured
 Conductivity = not measured
 ka = not measured

Sound Speed [m/sec]
 experiment = 1488.6
 relaxed = 1482.5
 unimodal = 1488.5
 bimodal = 1487.3

Th.expansion = not calculated Structure factor = not calculated



Median size = 0.2100 Diameter [micron]
 Mean size = 0.2618 D16% = 0.0587
 St.deviation = 0.599 D84% = 0.7877

Attenuation Data Fitting Error Unimodal = 5.4
 Frequency range: 3-99.5[MHz] Fitting Error Bimodal = 1.4

FIG. 1. Particle size distribution of powder suspension in water at 4.8% W solids loading.

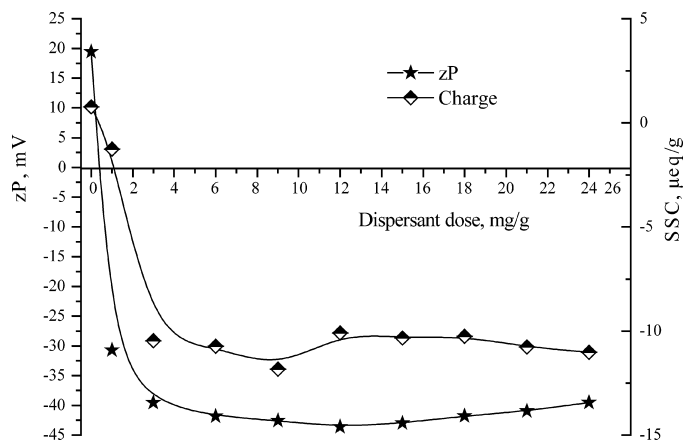


FIG. 2. Zeta potential and specific surface charge of powder suspension as function of dispersant dose level.

be naturally stabilized by electrostatic repulsion forces, which are known to be weak and short ranged. With increase in the amount of supplied dispersant, the positive zeta potential dropped, and after passing through the zero charge, the powder acquired negative charge. After 3 mg/g dispersant dose level, an inflection point could be noticed, and above that point, both the zeta potential and the surface charge density curves flattened. As a rule, any amount of dispersant supplied above the optimum will remain unbounded in suspension, leading to unwanted high viscosity. Hence the optimum dispersant dose level lies between 3 and 6 mg/g. Within this range, the zeta potential approached -40 mV, which implies stronger stabilization involving electrosteric mechanism. It has to be noted that the progressive addition of dispersant within the envisaged range did not shift the suspension pH

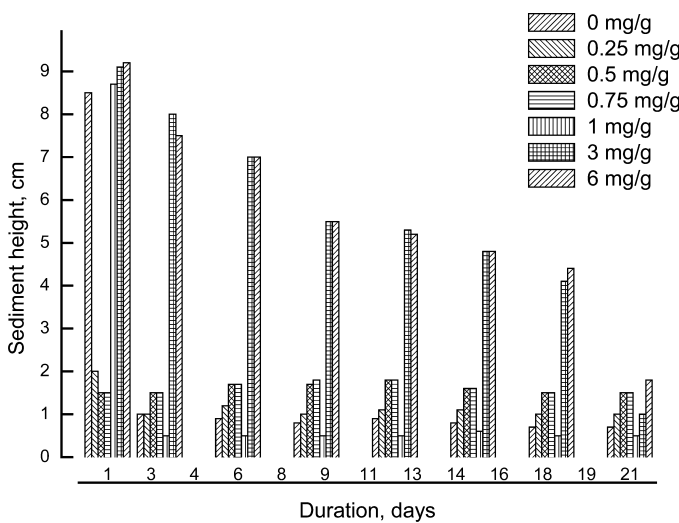


FIG. 3. Time variation of sedimentation heights at various dispersant concentrations.

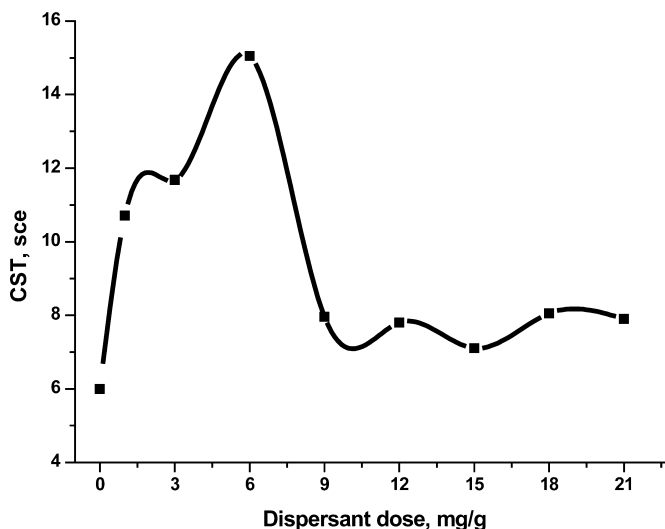


FIG. 4. CST of suspension as function of dispersant dose level.

dramatically. The pH was found to slightly decrease from 8.9 at 1 mg/g, to about 8.2 at 24 mg/g dose level.

Further, it was interesting to investigate if the optimal dispersant dose suggested by the zeta potential and the specific surface charge would be reconfirmed by sedimentation and CST tests. Figure 3 summarizes the results from the plain sedimentation of powder suspensions with and without addition of dispersant. A perusal of these results indicates that without addition of dispersant the sediment height was maintained high within the first 24 hours, implying, as already noted, a naturally stabilized suspension. After that period, the suspension stability collapsed. Similarly, the addition of dispersant in dosages up to 1 mg/g has not led to notable stabilization, since after 24 hours the powder settled out of suspension. The supply of dispersant at concentration levels of 3 and 6 mg/g contributed to a relatively stable suspension in the long term. After 18 days, the sediments of the suspensions treated with 3 and 6 mg/g dispersant were characterized by a nearly double decrease in height, i.e. from 9 to 4.5 cm. However, after three weeks of settling under quiescent conditions, the powder from these two suspensions almost settled out in a packed bed, leaving a relatively high cloudy/clear interface height. According to Janney et al., behavior like this suggests, that Dolapix CE64 supplied between 3 and 6 mg/g is a quite appropriate choice for stabilization of the powder under study. Obviously, the suggestions regarding the optimal dose level of dispersant from the sedimentation study are in good agreement with those obtained from the CVI and PCD tests.

In Figure 4, the results derived from the CST experiments are shown. It should be noted that parallel to the increase in dispersant concentration up to 6 mg/g, capillary suction time rose as well. After that point, the CST dropped sharply. Since the CST reached its maximum value at 6 mg/g, this dose level

can be again viewed as an optimal one. Under this condition, a full stabilization leading to the highest water holding capacity of the suspension could be expected. On the other hand, the short suction times imply particle agglomeration and accordingly faster water drainage rate.

When comparing the results from the electrokinetic studies, the sedimentation and CST tests, it is clear that for the studied suspensions a dispersant dose level of 6 mg/g could be finally chosen as the optimal one. Regardless of the different modes used for dispersant introduction inside the slurry during the CVI and streaming current determination, the trend of the zeta potential and specific surface charge curves was similar.

CONCLUSIONS

The following conclusions could be drawn based on the presented results:

- Each of the investigated techniques possesses advantages and drawbacks.
- Good agreement between the optimum dose level of dispersant required to stabilize the suspension was noted, as indicated by the zeta potential from the CVI and the specific surface charge derived from the streaming current measurements. This is in line with results reported by Wäsche et al. (2002), where during determination of pH_{iep} for suspensions of alumina, silicon carbide, and silicon nitride at different solids loadings, a linear correlation between the zeta and streaming potentials was established.
- For the powder under consideration, the CST technique has proven a fast and simple way for evaluation of the dispersion stability and for checking the optimal dispersant dose level. However, how

CST relates to suspension rheology should be further studied.

- The use of plain sedimentation, although time consuming, has appeared as a relatively accurate approach for optimization of dispersant dosage, provided secondary effects like temperature and physical disturbances are eliminated. Additionally, the sediment volume could provide information about the nature of dispersed particles.
- It remains to be proven whether the current optimal dose level of dispersant will maintain similarly stable dispersions at the much higher solids loading of powder usually employed in gel casting.

REFERENCES

- Dukhin, A. and Goetz, P. (2002) *Ultrasound for Characterizing Colloids*; Elsevier: Boston.
- Janney, M., Omatete, O., Walls, C., Nunn, S., Ogle, R., and Westmorland, G. (1988) Development of low-toxicity gelcasting systems. *J. Am. Ceram. Soc.*, 81: 581–591.
- Klimpel, R. (1999) Introduction to chemicals used in particle system. In *Particle Science and Technology*; Rajagopalan, R., ed.; NSF Engineering Research Centre for Particle Science and Technology: Gainesville, FLa.
- Singh, B., Bhattacharjee, S., and Besra, L. (2002) Influence of surface charge on maximising solids loading in colloidal processing of alumina. *J. Mater. Lett.*, 56: 475–480.
- Singh, B., Bhattacharjee, S., Besra, L., and Sengupta, D. (2003) Comparison between techniques based on charge characterisation and capillary suction time for assessing the dispersion characteristics of concentrated slurry. *J. Mater. Sci.*, 38: 1–6.
- Wäsche, R., Naito, M., and Hackley, V. (2002) Experimental study on zeta potential and steaming potential of advanced ceramic powders. *Powder Technol.*, 123: 275–281.

Comparative Studies of Dispersant Optimization Techniques for Evaluating Stability of Alumina Slurries

Stoyan Gaydardzhiev, Peter Ay, Marta Janeczko*

(Received: 10 February 2006; accepted: 10 April 2006)

DOI: 10.1002/ppsc.200601033

Abstract

The choice of a reliable method for the testing of dispersant efficiency is an important issue in ceramics processing by emerging near net shape methods. The present paper presents the comparison of four methods for evaluation of the dispersibility properties of a commercial deflocculant Dolapix CE64, towards stabilization of sub-micron alumina powder suspended in water. The following techniques have been investigated for this purpose:

zeta potential obtained from CVI measurement, specific surface charge based on streaming current, sedimentation and capillary suction time. A good correlation between the zeta potential and the streaming current as a means for determining the optimal dispersant dose and improved understanding of the dispersion mechanisms were obtained.

Keywords: alumina powder, dispersants, electrokinetic properties, suspension

1 Introduction

Direct consolidation techniques, e.g., gel casting, based on colloidal processing and proposing the formation of complex near net shape bodies with consistent properties and minimal defects, have recently emerged as viable alternatives to the conventional routes for developing ceramics materials. These techniques make use of well dispersed suspensions with relatively high levels of solids loading. Although their advantages are known, most of them remain under development either in laboratories or in the pilot plants of ceramic companies, with a few small scale installations in operation for some complex shaped parts. One main problem to overcome is the low production rate, which at present cannot compete with dry pressing. The gel-casting process encompasses the development of aqueous or non-aqueous slur-

ries of colloidal sized ceramic particles, with the addition of predetermined amounts of dispersant, gelling reagents, initiators and catalysts. Since the dispersion of the particles and the stability of the powder suspension is a key factor for the development of desirable end products, the appropriate choice of dispersant type and dose level, are of major importance for realizing a successful gel casting process. It is often imperative to achieve the highest possible solids loading in the slurry, since the high solids loading guarantees low shrinkage during drying and firing, and accordingly increases the green strength. Commonly, the selection of dispersants is carried out on an empirical basis, involving screening of various products to achieve acceptable performance, which is time consuming. The conventional techniques most often employed, assess the macroscopic properties of the suspension such as sedimentation behavior and viscosity, which provide little information about the interfacial phenomena taking place during the particle-dispersant interaction. Therefore, it is desirable to search for a method which has the ability to evaluate an appropriate dispersant for a given powder dispersion, and which is easily accessible, fast and reliable, while having the ability to elucidate the surface-active behavior of the dispersant. When entering the colloidal size

* Dr. St. Gaydardzhiev, Prof. Dr.-Ing. habil. P. Ay, Dipl.-Ing. M. Janeczko, Lehrstuhl Aufbereitungstechnik, Institut für Verfahrenstechnik, Brandenburgische Technische Universität Cottbus, Siemens-Halske Ring 8, 03046 Cottbus (Germany). E-mail: gaydar@tu-cottbus.de

range in particulate systems, maintaining control over their dispersion behavior becomes increasingly difficult. Surface properties and interfacial phenomena determine the state of particle dispersion and knowledge of these parameters is of critical importance for controlling particle aggregation. Dispersibility is defined as the ease with which particles are distributed in a continuous phase, so that each particle is completely surrounded by the liquid phase and no permanent contact exists with any other particles, thus preventing subsequent agglomeration, [1]. As a rule, the dispersant screening process starts at low solids loading, using either sedimentation or light scattering to evaluate the degree of particle dispersibility. It has been shown by Singh et al. [2], that not every dispersant which demonstrates efficient dispersion at lower solids loading, maintains good dispersion at high solids concentration. The present paper presents results from a systematic evaluation of the dispersive behavior of a colloidal alumina suspension stabilized by the commercially available dispersant, Dolapix CE64. The following parameters have been chosen as a means of assessing the stability of suspension: zeta potential, surface charge density, capillary suction time and sedimentation.

2 Experimental

2.1 Materials

The powder employed in this study was an α -type calcined alumina with brand name CR6, produced by Baikowski-Chemie, France. The producer reports a median particle size (d_{50}) of 0.53 μm and a specific surface area (A) of 5.8 m^2/g . A microphotograph of the powder taken by a raster electronic microscope, model DSM 962 (Carl Zeiss, Oberkochen Germany) is shown at Figure 1. Both agglomerates (which predominate) and single powder

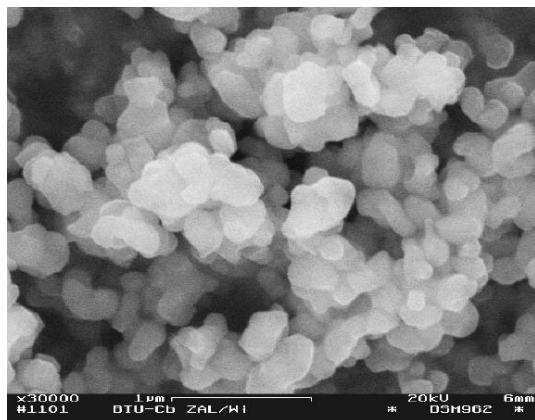


Fig. 1: REM image of a CR 6 alumina powder.

particles with irregular shape, can be distinguished. The dispersant used, was Dolapix CE 64, an ammonium polyacrylate type free from alkalis, supplied by Zschimmer & Schwarz, Lahnstein, Germany. The interaction between the functional groups of the additive and the surface charged ceramic particles is responsible for its deflocculating effect. The dispersant was used as a 10 % solution and its efficiency has been tested in concentration ranges between 0.25 and 6 mg/g in the sedimentation studies, and between 1 and 24 mg/g in the rest studies. Unless otherwise stated, bi-distilled and deionized water from a purification system, model Modulab (U.S. Filter, Lowell, USA), with a conductivity (σ) below 0.2 $\mu\text{S}/\text{cm}$ and pH of 6.7, has been used.

2.2 Zeta Potential and Specific Surface Charge

The electrokinetic properties of the aqueous powder suspension have been expressed in two ways: as the zeta potential coming from measurement of colloid vibration current (CVI) by means of an acoustic and electroacoustic spectrometer, model DT1200 (Dispersion Technology Inc., Mount Kisco, USA), and as the specific surface charge derived from the streaming current, as measured by a particle charge detector PCD-O3-pH (Mütek Analytic GmbH, Herrsching, Germany). The working and measurement principles of the both systems are reported elsewhere, Dukhin [3] and Wäsche [4]. For the CVI tests, 5.5 g of powder were added to 110 mL water, giving a solids loading of 4.76 weight %. The suspensions were agitated for 2 min with a magnetic stirrer, followed by 20 s using an ultrasonic disintegrator model UP 400 S (Topas GmbH, Dresden, Germany). Immediately following agitation, the suspensions were transferred to the inside of the measuring chamber of the spectrometer, where they were circulated by means of a built-in magnetic stirrer. For the volumetric titration performed with the CVI instrument, a predetermined amount of dispersant calculated on solid mass was added to the inside the sample chamber by means of the integrated burette and thoroughly mixed before the zeta potential value was recorded. For the same titration in the PCD case, the powder and liquid were directly mixed inside the 10 mL sample cell for 2 min by the piston movement. The 2 min agitation was considered sufficient as indicated by establishment of a stable streaming current. A small pH electrode was fitted to the cell, enabling on-line pH monitoring. The exact magnitude of the charge, expressed as a specific surface charge or charge density, was estimated by titration with oppositely charged standard polyelectrolyte, until neutralization of the streaming potential to zero value. The optimum dispersant dose level leading to maximal dispersion of powder has

been considered as that coinciding with the inflection point of the plots between dispersant dose level and zeta potential, and between dispersant dose level and surface charge density derived respectively, from the CVI and PCD measurements.

2.3 Sedimentation

Sedimentation tests were performed using calibrated glass cylinders with 25 mL volume. For each test, 1.25 g of alumina powder was mixed with 25 mL water, containing a predetermined amount of dispersant of concentrations 0.25, 0.5, 0.75, 1, 3 and 6 mg/g, respectively. The suspension was vigorously shaken and further allowed to stand undisturbed for a period of 21 days. The sediment heights were read directly from the graduated cylinders. The higher the sediment height, the more stable the suspension.

2.4 Capillary Suction Time

The optimal dispersant dose level has been likewise evaluated by measuring the capillary suction time (CST) of the powder suspensions. This has been realized by the use of a CST device, model 100/A (HeGo Biotech, Tetlow-Seehof, Germany), equipped with a hollow cylinder standing on a Whatman 17 type filter paper. The operation of the CST instrument is based on the principle of capillary suction pressure of a porous medium and could be viewed at first approximation as a means for evaluation of the water holding capacity of sludge or suspensions, and to some extent of their viscosity. The suspensions tested for CST were prepared under the same mixing procedures used for the samples measured by the CVI instrument, with the same solids loading of 4.36%. Two successive measurements, each involving 5 mL of suspension were carried out and the mean from the two values recorded. Following the findings obtained by Singh et al. [5], a dose level of dispersant which had yielded maximum capillary suction time was chosen as optimal, i.e., it has secured the longest drainage rate of suspension.

3 Results and Discussion

3.1 Selection of Optimum Dispersant Dose

Figure 2 summarizes the results from the volumetric titration of suspensions, aimed at the determination of the optimum dispersant concentration. When the CVI instrument was used, the dispersant was progressively

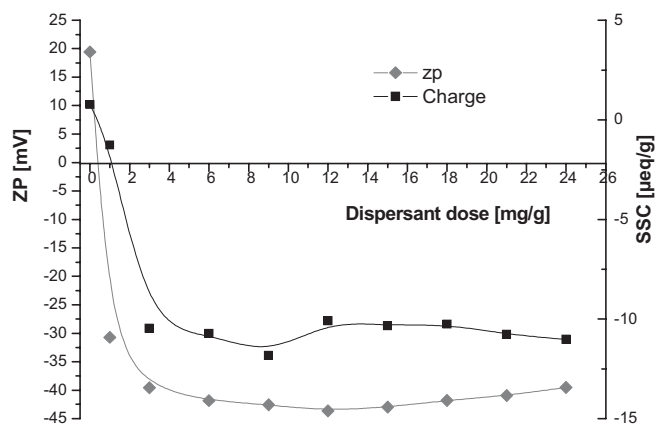


Fig. 2: Graph showing variation of zeta potential and specific surface charge of suspension at different dose levels of dispersant.

dosed in a step-by-step manner inside a similar sample of suspension and accordingly, each zeta potential value relates to the measurement of this sample. Each single point taken for the specific surface charge however, corresponds to the measurement of individual sample.

As can be seen from Figure 2, in the absence of dispersant, the aqueous suspension of alumina is positively charged, as a result of the surface hydroxyl groups, which dissociate in water or act as proton acceptors. Without dispersant, the suspension was characterized by a pH of ca. 7 and appeared to be naturally stabilized by electrostatic repulsion forces, known as weak and short range forces. With an increase in the amount of added dispersant, the positive zeta potential is seen to drop and pass through the zero charge point, and the powder acquires a negative charge. An inflection point is observed following a dispersant dosage of 3 mg/g. Hence, the optimum dispersant dose level should be found between 3 and 6 mg/g. Within this range, the zeta potential approached -40 mV, which implies a stronger electrostatic stabilization. Further from that point, both the zeta potential and surface charge density curves are seen to flatten. It is expected that any amount of dispersant supplied above that optimum level, will remain unbound to the particles in suspension and will lead to an unwanted high viscosity. It should be noted that the suspension pH was not shifted considerably, as results from the progressive addition of dispersant within the envisaged range. At 1 mg/g of dispersant, the pH was 8.9 and at a 24 mg/g dose level, the pH had only decreased slightly to ca. 8.2. It is interesting to evaluate whether the optimal dosage suggested by the zeta potential and specific surface charge, will be reconfirmed by the sedimentation and CST tests. The results from the plain sedimentation tests of the powder suspensions, with and without, addition of dispersant are presented in Figure 3. A perusal of the results indicates that, without addition of dispersant the

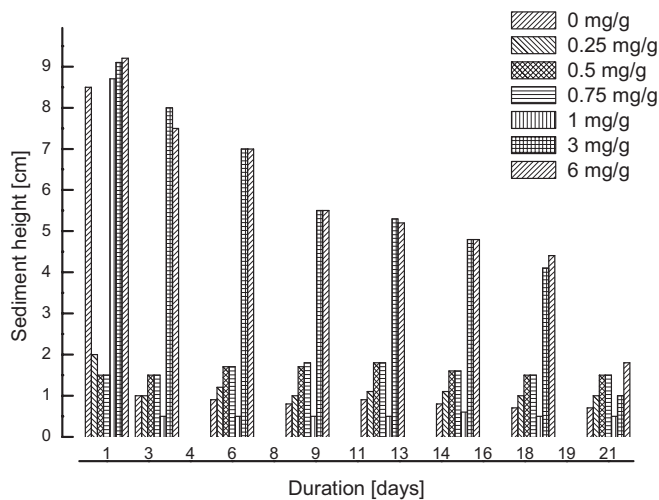


Fig. 3: Sedimentation behaviour at various concentration of dispersant.

sediment height has stayed high during the first 24 h, suggesting a naturally stabilized suspension. After this time, the suspension stability collapses. Similarly, the addition of dispersant in doses up to 1 mg/g does not lead to notable stabilization, since the powder settles out of the suspension after 24 h. The supply of dispersant at concentration levels of 3 and 6 mg/g has contributed to a relatively stable suspension in the longer term. After 18 days, the sediment height for suspensions treated with 3 and 6 mg/g have decreased almost twofold, from 9 cm to 4.5 cm. The powder from both these suspensions had almost entirely settled out in a packed bed after 3 weeks of settling under quiescent conditions, leaving a relatively high cloudy/clear water interface. Such behavior, according to results published by Janney et al. [6], suggests that the dispersant under consideration could be a quite good choice for the powder, when supplied between 3 and 6 mg/g. Consequently, the findings concerning the optimal dose level of dispersant from the sedimentation study are in good agreement with those derived from the CVI and PCD tests.

The results from the CST experiments are presented in Figure 4. It should be noted, that capillary suction time rises, accompanying increases in dispersant concentration up to 6 mg/g. After that point, the CST drops off sharply. Since the CST reaches its maximum value at 6 mg/g, this dose level could be viewed as the optimal one. At this dose level, complete powder stabilization leading to high water holding capacity of the suspension is expected. In contrast, the short suction times imply particle agglomeration and accordingly, a faster water drainage rate.

On comparison of the results from the electrokinetic studies, the sedimentation and CST tests, it becomes clear that for the suspension studied, a dispersant dose

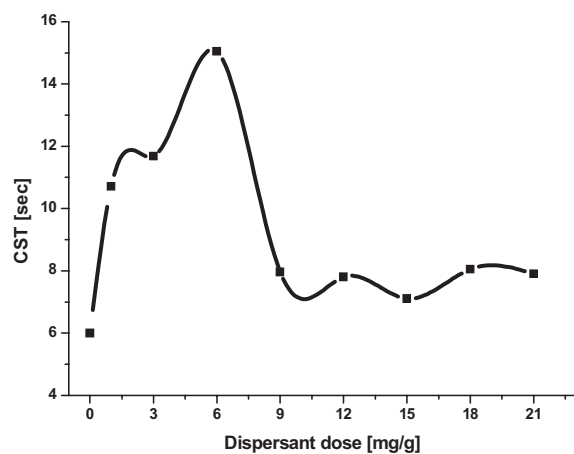


Fig. 4: Relationship between CST and dispersant dose level.

level of 6 mg/g could be viewed as optimal. Regardless of the different modes of dispersant introduction during the CVI and the streaming current measurements, the trends for the suspensions were similar in the zeta potential and specific surface charge curves.

4 Conclusions

This paper provided a description of four methods used to evaluate the efficiency of dispersants in stabilizing water dispersions of fine alumina slurries. The presented results allow the following conclusions to be drawn:

- Each of the measuring techniques investigated possess specific advantages and weaknesses;
- There was a good agreement between the optimum dose level of dispersant required to stabilize the suspension, as indicated by the zeta potential from the CVI measurement, and the specific surface charge derived from the streaming current. This finding is in line with the results reported by Wäsche [4], where during determination of the pH_{iep} of water suspensions of alumina, silicon carbide and silicon nitride at different solids loadings, a linear correlation between the zeta and streaming potentials has been established;
- For the powder under consideration, the CST technique has proved to be a fast and simple way of evaluating dispersion stability and for checking the optimal dispersant dose level. However, further studies as to how CST values relate to suspension rheology, are required;
- The use of plain sedimentation, although time consuming, was shown to be a relatively accurate approach for optimization of dispersant dosage, provided secondary effects such as temperature and physical disturbances are eliminated. Additionally,

the sediment volume could provide information on the nature of the dispersed particles.

The findings from this study have potential application, for example, in designing gel-casting schemes. However, it remains to be proven, whether the current optimal dose level of dispersant will maintain stable dispersions at the much higher solids loading of powder usually required in gel-casting processes.

5 Nomenclature

A	m ² /g	specific surface area (BET)
d ₅₀	μm	mean particle size
s	μS/cm	conductivity

Abbreviations

CST	Capillary Suction Time
CVI	Colloidal Vibration Current
PCD	Particle Charge Detector
SSC	Specific Surface Charge

6 References

- [1] R. Klimpel, Introduction to Chemicals used in Particle System, in *Particle Science and Technology* (Ed.: R. Rajagopalan), the NSF Engineering Research Centre for Particle Science and Technology, Florida, **1999**.
- [2] B. Singh, S. Bhattacharjee, L. Besra, Influence of Surface Charge on Maximising Solids Loading in Colloidal Processing of Alumina, *J. Mat. Lett.* **2002**, *56*, 475–480.
- [3] A. Dukhin, P. Goetz, *Ultrasound for Characterizing Colloids*, Elsevier, 2002.
- [4] R. Wäsche, M. Naito, V. Hackley, Experimental Study on Zeta Potential and Steaming Potential of Advanced Ceramic Powders, *Powder Technol.* **2002**, *123*, 275–281.
- [5] B. Singh, S. Bhattacharjee, L. Besra, D. Sengupta, Comparison Between Techniques Based on Charge Characterization and Capillary Suction Time for Assessing the Dispersion Characteristics of Concentrated Slurry, *J. Mat. Sci.* **2003**, *38*, 1–6.
- [6] M. Janney, O. Omatete, C. Walls, S. Nunn, R. Ogle, G. Westmorland, Development of Low-toxicity Gelcasting Systems, *J. Am. Cer. Soc.* **1988**, *81*, 581–591.